Impacts of underwater anthropogenic noise on individuals and populations

Kieran Patrick McCloskey

Submitted by **Kieran Patrick McCloskey**, to the University of Exeter as a thesis for the degree of ***Doctor of Philosophy in Biological Sciences*** in March 2022.











Bude Nippers




Acknowledgements

This thesis is the result of a long, incredible journey, for which I have many people to thank. First, thank you to Steve Simpson for your unwavering encouragement and leadership, which has guided me through the highs and lows of this PhD. Your enthusiasm and ability to make the impossible possible has taught me to dream big and to embrace adversity. None of this work would have been achieved without your belief in me, and I leave this PhD with a self-confidence and pride that I attribute to your mentorship.

Thank you also to Andy Radford for your support and tutelage in all aspects of science, big and small. Your masterful grasp of research has helped me to turn fledgling ideas into concrete science, and to consider all angles of an experiment. You are incredibly patient and kind when giving advice and feedback, and I can honestly say that I am a better scientist, writer, and person thanks to your supervision.

Thank you to my co-supervisors, collaborators, and co-authors for their invaluable contributions to each piece of work presented in this thesis. I have to give specific thanks to Rod Wilson, Darren Croft, Mark McCormick, Dan Exton, Ben Titus, Richard Sibly, Joe Watson, Rob Boyd, Kieran Hyder, Nathan Merchant, Adrian Farcas, and Nicola Walker for sharing your expertise and wisdom.

I would also like to thank my colleagues and friends at Exeter, Bristol, Lizard Island, and Operation Wallacea, of which there are too many to list. Instead, I’ve included some photos of the fun and unforgettable moments that we have shared, and for which I am incredibly grateful. I have to give a special thanks to the Swag Babes. I’m honestly blown away by each of you, and it has been a privilege and joy to have been a part of such a wonderful and inspiring research group.

Thank you to the organisations that provided funding and supported my PhD research, including the University of Exeter, the Natural Environment Research Council, and Operation Wallacea. Thank you also to the staffs at Lizard Island Research Station and at Coral View Beach Resort & Dive Center who provided logistical support during fieldwork.

Thanks to all my new friends in the UK for making me feel welcome. Thanks to Dad for the virtual cooking classes, to Uncle Brian for keeping me updated on the Caps, to the McCloskey clan for getting me through the pandemic with our Sunday calls, and to the Stuart boys for all the chats. A special thanks to Mom and Steve for encouraging me to go on a volunteer conservation trip to the Philippines six years ago; I am grateful for that and for everything you have done for me. It has not been easy to be so far from home, but I have felt your love and support from across the pond.

Finally, a very, very special thanks to Shannon Cameron for sticking with me and being there for every step of this journey. Thank you for cheering me on and celebrating the victories, for helping me through the rough patches, and for keeping me sane and grounded. It is undeniable that I would not have been able to accomplish any of this without your love and support and, for that, I am forever grateful.

Dedication

I would like to dedicate this thesis to my late grandfather, Robert McCloskey, and my late uncle, Chris Burns, who always supported me but sadly passed away before I could complete this work. I miss you both and would have loved to celebrate this accomplishment with you.

Thesis abstract

Anthropogenic noise is an established global pollutant, with mounting evidence that noise from human activities (e.g., transportation, construction, and resource extraction) can impact behaviour, physiology, and fitness in a broad range of taxa. Establishing noise as a stressor and pollutant has been an evolving process where research methods, techniques, and investigative scope continue to change and develop. However, there still exists many unanswered questions, such as impacts on local community structures and populations. Therefore, evolution within the field of anthropogenic noise research (e.g., new study systems and technology) can be used to help researchers explore logistically challenging questions.

This thesis presents an integrated body of research on the impacts of noise to aquatic life at varying levels of biological organisation: starting with impacts on individuals, moving to effects on interspecific interactions and local communities, and ending with population-level assessment. Importantly, I have strived to incorporate aspects of noise mitigation in each section.

In Chapter One, I introduce anthropogenic noise, the importance of underwater sound to taxa, and outline the evolution of noise-related research. Then, I present data showing that real motorboat noise negatively affects egg-tending and nest defence in male damselfish on the Great Barrier Reef, but also provide evidence for the potential benefits of a simple, yet effective, noise-mitigation strategy (Chapter Two). Following this, I provide evidence that playback of SCUBA noise hinders interspecific behaviour and alters community structure near ecologically important cleaning stations on the Mesoamerican Barrier Reef (Chapter Three). Moreover, by establishing acoustic disturbance as a mechanism for the negative impacts of diver presence, I am also identifying a potential avenue for mitigation. In Chapter Four, I develop and present an energetic and spatially explicit individual-based model that uses realistic projections of noise-pollution levels in the Northeast Atlantic to explore the impacts of noise to an important fish stock. Using the model, I further unpick the population-level impacts of noise to the fish stock and use findings to develop and test a targeted noise-mitigation strategy to improve population-level outputs (Chapter Five). Finally, I discuss the implications of findings, present important areas for further research, and critically discuss the management of noise in our oceans (Chapter Six).

Table of Contents

List of Figures

List of Tables

List of Abbreviations

ABC	Approximate Bayesian computation
$\mathrm{AEL}_{\mathrm{cum}}$	Particle-acceleration-exposure level (cumulative)
AICc	Akaike information criterion
ANOVA	Analysis of variance
DF	Degrees of freedom
E	Normalised root-mean-square difference
$\bar{E}$	Bias
E'	Variability
EIA	Environmental impact assessment
FDR	False discovery rate
FFT	Fast Fourier transform
GLMM	General linear mixed model
IBM	Individual-based modelling
ICES	International Council for Exploration of the Sea
NEm	Noise-energy modifier
NFm	Noise-feeding modifier
NMm	Noise-mortality modifier
nMDS	Non-metric multidimensional scaling
NRm	Noise-reproduction modifier
ODD	Overview, design concepts, details
PERMANOVA	Permutational multivariate analysis of variance
PCAD	Population consequences of acoustic disturbance
PHY	Phytoplankton density
PSD	Power spectral densities
r	Correlation coefficient
RMS	Root mean square
sAIS	Satellite automatic identification system
$\mathrm{SAL}_{\mathrm{rms}}$	Particle-acceleration level (root-mean-square)
SCUBA	Self-contained underwater breathing apparatus
SE	Standard error
$\mathrm{SEL}_{\mathrm{cum}}$	Sound-pressure-exposure level (cumulative)
SEM	Standard error of means
$\mathrm{SPL}_{\mathrm{rms}}$	Sound-pressure level (root-mean-square)
SS3	Stock synthesis 3
SSB	Spawning stock biomass
SST	Sea surface temperature
TRACE	Transparent and comprehensive ecological modelling documentation

Glossary

Accelerometer – specialised recording equipment used to measure particle acceleration

Acoustic buffer zone – a designated area used for reducing the levels of noise exposed to wildlife via speed and/or distance restrictions placed on motorboat driving

Agent – simulated individuals (or groups of individuals) that interact with each other and their environment

Anthrophony – unnatural sounds generated from human activity

Anthropogenic noise – noise generated from human activity

Beaufort scale – empirical measure for describing wind intensity based on observed sea conditions; used in Met Office forecasts

Biophony – natural, biological sounds (e.g., vocalisations, movement, and feeding) emanating from organisms within an ecosystem

Fast Fourier transform (FFT) – a mathematical operator used to transform a signal into the sum of a number of sine wave frequency components

Geophony – natural, non-biological sounds (e.g., wind, waves, and rainfall) that occur

Hydrophone – specialised recording equipment used to measure sound pressure

Individual-based modelling (IBM) – a bottom-up approach to simulate a population of discreet individuals where a combination of individual state and environmental variables change individual behaviour

Initialisation – loading of the model to a starting position/configuration

Mass-at-age – total biomass across varying ages of modelled fish

Noise – unwanted or unintended sound that is often indiscernible and can interfere with naturally occurring sound

Noise abatement – the reduction of noise entering the environment altogether, typically by removing activities that produce noise or technological changes/measures to reduce noise from sources (as opposed to redistributing noise to another time and/or location)

Noise mitigation – measures/management used to reduce the amount of noise to specific locations, time periods, or target animals; this is typically done by imposing spatiotemporal restrictions or using noise of lesser intensity as a deterrent to disperse animals before more harmful noise levels are emitted

Numbers-at-age – total abundance across varying ages of modelled fish

Overlap – reduces leakage during signal processing by overlapping samples by a designated amount

Patches – units of area in a model that have their own set of dynamic variables

Particle acceleration – a vector component resulting from the oscillation of fluid particles surrounding a vibratory source

Population consequences of acoustic disturbance (PCAD) – modelling approach that translates behavioural and physiological responses of individuals into changes in vital rates

Power spectral density (PSD) – the measure of a signal's power content versus frequency

Sound – vibratory energy that propagates through a medium (i.e., solid, liquid, or gas) as an acoustic wave, which can transmit auditory information

Soundscape – collection of biological, geophysical, and anthropogenic sounds that emanate from a landscape and which vary over space and time reflecting important ecosystem processes and human activities (Krause 2012)

Sound pressure – the resulting fluctuation of pressure during compressions and refractions of oscillating fluid particles

Spawning stock biomass – total mass of mature fish >42 cm

Spin-up – period that is used to stabilise the model before simulations can occur; stabilisation can be helped/driven by input data

Super-individual – many individuals with identical state variables (typically used in modelling to reduce run/computational time)

Weberian ossicles – anatomical structure that provides a physical connection between the inner ear and gas-filled organs to improve/broaden hearing capabilities

Window function (Hamming) – a mathematical function that is zero-valued outside of some chosen interval. Hamming is a common window function used for narrowband applications.

Window length – determines the number and length of samples used for signal processing

Chapter One – General introduction and thesis aim

1.1 Anthropogenic noise and the importance of underwater sound

Natural soundscapes are comprised of biological (biophony) and non-biological (geophony) sounds. However, a third component has now become ubiquitous in contemporary soundscapes: the anthrophony, or unnatural sounds generated from human activity (commonly referred to as anthropogenic noise) (Krause 2012). Here, I define noise as unwanted to unintended sound that is often indiscernible and can interfere with naturally occurring sounds. Over recent decades, anthropogenic noise has intensified in our oceans, causing increases in both background noise levels and peak intensity levels (Hildebrand 2009). The main sources of marine anthropogenic noise include acute noise produced by military exercises, seismic surveys, and pile-driving, as well as more chronic noise generated by recreational vessels, commercial shipping, and offshore windfarms (Francis & Barber 2013; Merchant *et al.* 2016; Carroll *et al.* 2017). Some noise is deliberately produced, such as military sonar for surveillance, fisheries sonar to detect marine organisms, and seismic exploration via air-gun arrays to locate natural resources, while other sources of anthropogenic noise are created as a by-product of human activity, including offshore construction, coastal development, and commercial and recreational vessel traffic (Hildebrand 2009). While unintentional noise might appear less nefarious, noise that is considered to be a by-product of human activity (e.g., shipping noise) is thought to be particularly pervasive across large spatiotemporal scales, and threatening, due to large acoustic overlap with biologically important, low-frequency bandwidths (Fig. 1.1: Duarte *et al.* 2021).

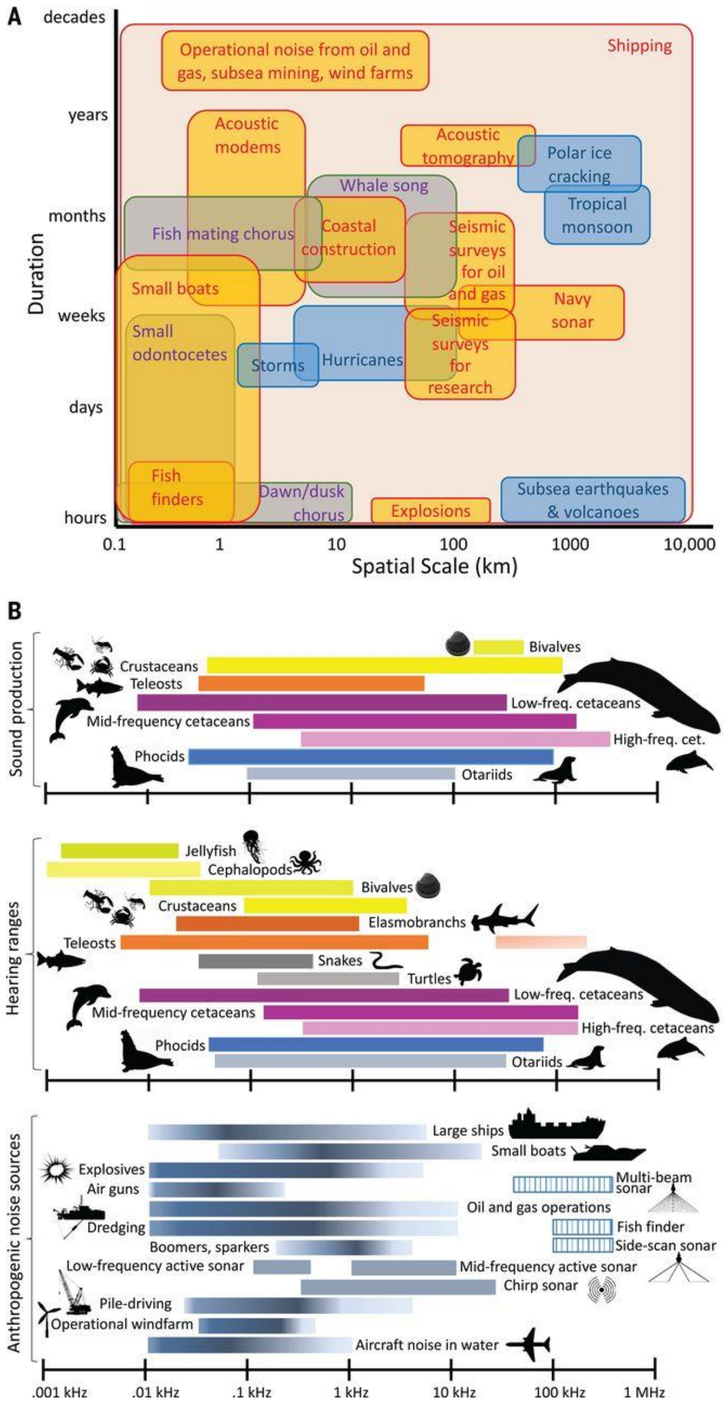

Figure 1.1. Sources and animal receivers of sound in the ocean soundscape from Duarte et al. (2021)*). A) Stommel diagram showing the spatial extent and duration of selected biophony (rounded grey squares), geophony (rounded blue squares), and anthrophony (rounded yellow squares) events. B) Approximate sound production and hearing ranges of marine taxa and frequency ranges of selected anthropogenic sound sources. These ranges represent the acoustic energy over the dominant frequency range of the sound source; colour shading roughly corresponds to the dominant energy band of each source. Dashed lines represent sonars to depict the multifrequency nature of these sounds. Sources for data displayed in the figures are provided in Duarte et al. (2021).*

Sound propagates far and fast underwater, and does so independently of hydrodynamics, making it a long-distance current-independent source of sensory information compared to visual or chemical cues (Urick 1975; Ladich & Winkler 2017). This is due to the physical properties of sound waves and of water as a fluid medium. A sound wave is comprised of two physical components: particle motion, a vector quantity resulting from the oscillation of fluid particles surrounding a vibrating sound source; and sound pressure, a scalar quantity that results from the fluctuation of pressure during compressions and rarefactions of oscillating fluid particles (Nedelec *et al.* 2016a). Because water is a relatively dense fluid medium, a sound wave can travel four to five times faster through water than air (Ladich & Winkler 2017). Many marine organisms, including fishes and invertebrates, mainly detect sound through particle motion (Fay 2009; Ladich & Schulz-Mirbach 2016; Radford *et al.* 2022). Moreover, particle motion, as a vector, is highly directional and therefore imparts the potential for determining sound source direction. In fish, this is potentially done through a combination of mechanisms, including polarized sensory hair cells of the inner ear, relative output levels of the two ears, and detection by other groups of sensory hair cells (Fay 2009; Popper & Fay 2011). Therefore, sound is a key sensory cue and information pathway for a wide range of aquatic organisms (Lema & Kelly 2002; Ladich & Winkler 2017).

Hearing in marine animals ranges from marine invertebrates, fishes, and reptiles, which tend to perceive sounds of low frequency (typically <5 kHz), to cetaceans, which can detect high-frequency sound (up to 200 kHz) (Popper & Fay 2011; Ladich & Schulz-Mirbach 2016; Erbe *et al.* 2016; Radford *et al.* 2022). Mechanosensory hair cells for hearing appeared early in the evolution of animals, evolving first in aquatic invertebrates, which detect particle motion, then in fish, capable of detecting both particle motion and sounds pressure of low-frequency sounds (<5 kHz). Moreover, fishes belonging to the superorder Ostariophysi have evolved further to develop ancillary hearing structures (Weberian apparatus) that provide a physical connection between the inner ear and gas-filled organs, such as swim bladders, subsequently improving/broadening hearing bandwidths and sensitivities (Popper & Fay 2011; Ladich & Schulz-Mirbach 2016). Lastly, marine mammals evolved from terrestrial tetrapods that returned to the ocean, and as this happened, sound perception changed further (Ladich & Winkler 2017). For example, the middle ear of cetaceans has evolved to receive sound passing through fatty tissues in the jaws, effectively increasing the upper hearing limit of some species to 200 kHz (Clack 2002).

Many aquatic animals produce sounds of biological importance. For example, all marine mammal species have been shown to produce sound (Erbe *et al.* 2016), more than 800 species of fish from over 100 families have been documented to produce sounds (Radford *et al.* 2014), and sounds produced by crustaceans, such as snapping shrimp, typically dominate acoustic signatures of tropical coastal benthic habitats (Johnson *et al.* 1947; Chitre *et al.* 2012). Biological sounds are produced for many different reasons, but they can be broadly divided into two categories: those that arise incidentally from another activity, such as feeding, movement or respiration, and those generated, often by specialised organs/structures, for specific purposes (Radford *et al.* 2014). For example, toothed whales (odontocetes) produce a variety of whistles and clicks, with main energies of a few kilohertz (thus detectable for humans) up to ultrasonic frequencies (>100 kHz), used for communication and echolocating prey (Ladich & Winkler 2017). Fish have evolved the largest diversity of sound generating organs among vertebrates (Ladich & Winkler 2017). Regardless, fishes produce sounds at a limited frequency range (typically low frequencies) for similar communicative purposes, such as to attract a mate, defend territories, communicate with offspring, and to warn of danger (Radford *et al.* 2014). Collectively, the diversity of hearing capabilities and sound production means that certain taxonomic groups will be more at risk when exposed to anthropogenic noise sources that match their respective hearing and communicative ranges (Duarte *et al.* 2021; Fig. 1.1).

Francis & Barber (2013) reviewed and outlined the impacts of noise on terrestrial wildlife, with a particular focus on avian species, and provided a conceptual framework to guide future research. They postulated that noise stimuli may be perceived as a threat or interfere with cue detection by wildlife. They further suggested that these disturbances can elicit behavioural responses that have consequences for fitness via physiological stress responses, which can also feed back to behavioural changes (Francis & Barber 2013). In this introduction chapter, I have completed the same exercise with anthropogenic noise research pertaining to aquatic organisms, particularly fishes (Fig. 1.2). Similar to the conceptual framework developed by Francis & Barber (2013), Fig. 1.2 helps to visualise links between response mechanisms and potential consequences for noise disturbance in aquatic environments. However, this exercise focuses on noise exposure at the individual level, since there exists a paucity of evidence for the impacts of anthropogenic noise to communities and populations (Slabbekoorn *et al.* 2019; Mortensen *et al.* 2021). Consequently, studies that can integrate individual behaviour, population responses among multiple species, and species interactions are critical to understanding the cumulative and community-level consequences of noise (Francis & Barber 2013).

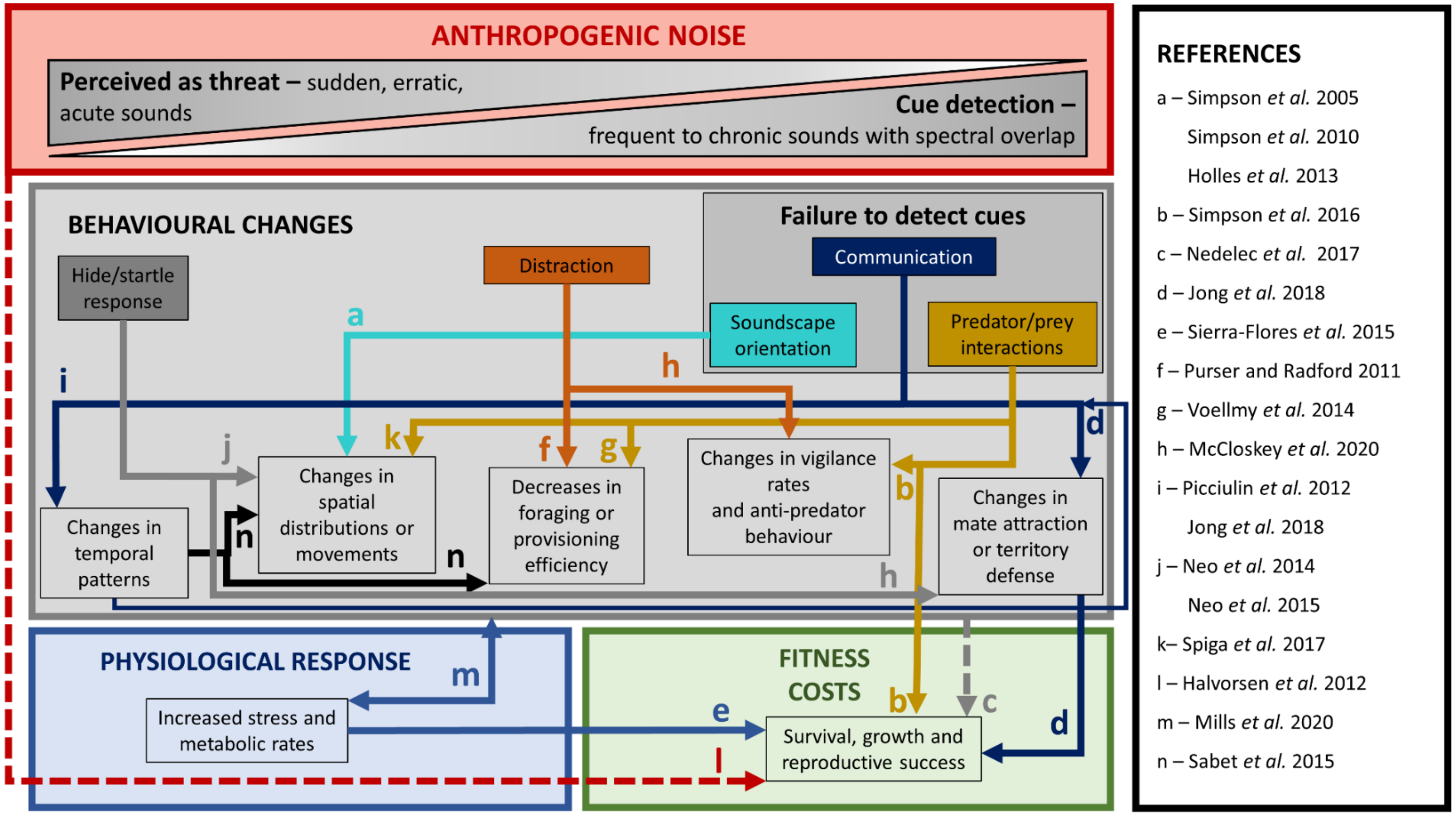

Figure 1.2. Conceptual framework for understanding the behavioural, physiological, or fitness consequences of underwater noise stimuli*. This figure has been adapted from an original conceptual framework presented by Francis & Barber (2013). Hide/startle responses occur in response to noise stimuli that are perceived as a threat; problems arising from a failure to detect cues occur when noise stimuli mask biologically relevant cues; and problems relating to distraction may occur as a result of sounds with features ranging from those that interfere with cue detection to those that are perceived as a threat* (Francis & Barber 2013)*. Lowercase letters indicate studies (listed on the right) providing evidence for the link made for each arrow. Dashed arrows signify a link that may be important but for which no current evidence exists. The studies included are given as examples to evidenced links between potential mechanisms and various biological effects; this is not an exhaustive list of relevant research.*

Compared to the established recognition of anthropogenic noise in terrestrial ecosystems, the impacts of noise on marine animals have been relatively overlooked by reviews of cumulative stressors and drivers of global ocean change, as well as scientific assessments and policy frameworks [United Nations Convention on Biological Diversity (UNCBD), UN Convention for the Law of the Sea (UNCLOS, UN Sustainable Development Goals (UN SDGs)] aimed at improving ocean conservation and sustainability (Duarte *et al.* 2021). Duarte *et al.* (2021) addressed this neglect with the largest and most comprehensive review, to date, of empirical evidence for the impacts of anthropogenic noise in our oceans. They found broad evidence demonstrating the negative impacts of noise on a wide range of aquatic taxa (e.g., marine mammals, fishes, invertebrates, marine reptiles, and birds), including effects on behaviour, presence/absence, physical health, physiology, mortality, and demography, thus corroborating preceding systematic reviews (Shannon *et al.* 2016; Cox *et al.* 2018).

1.2 Early observational research of noise impacts on marine mammals

Research interest and initial awareness of the potential impacts of anthropogenic noise began with observational data and reports of an anecdotal nature. Early collaboration between military and civilian scientists led to the discovery of echo-ranging in marine mammals and pioneered the first cataloguing of marine bioacoustics (reviewed in Au & Hastings 2008). The risks of military sonar noise to cetaceans received international attention following a highly publicised mass stranding of Cuvier's beaked whales *Ziphius cavirostris*, Blainville's beaked whales *Mesoplodon densirostris*, and northern minke whales *Balaenoptera acutorostrata*, which occurred in the Bahamas in 2000 (Balcomb & Claridge 2001). This event was considered a 'smoking gun', as it forced the US Government to determine a stranding event to be the result of active sonar use (Parsons 2017); although the link between naval exercises and live whale strandings had first been documented in the 1970s (Van Bree & Kristensen 1974). Subsequent investigation found that about 28 of the 40 mass strandings of beaked whales since 1960 occurred at the same time and place as naval manoeuvres or use of active sonar, near naval bases, or co-occurred with other noise sources, such as seismic surveys (Weilgart 2007). While the co-occurrence of noise and strandings is not enough to prove causation, the chance that these two rare events would repeatedly occur together by coincidence is extremely low. Regardless, it has taken decades of research to determine disturbance impacts on marine mammal populations and, even then, scientific evidence and analyses have not incontrovertibly established that the threat exists due to large uncertainties and variabilities in marine science (Parsons 2017). Regulation and protection have adopted a precautionary approach to avoid catastrophic declines in cetacean populations before science catches up with the problem (Parsons 2016). Parsons (2017) cautions that it may be a long time before technology and methods are easily available to answer the many still unanswered questions about the exact nature and degree of the impacts of noise on marine mammals; a warning that can be applied to all marine taxa.

More recent research has focused on the consequences of noise exposure, such as barotrauma, behavioural changes, hearing damage, and communication masking, in cetaceans and other marine mammals (Weilgart 2007). Prior to 2010, roughly 75% of anthropogenic noise studies focused on marine mammals (Duarte *et al.* 2021; Harding *et al.* 2021). However, attention after 2010 has shifted to include more taxonomic groups, resulting in a 235% increase in the number of studies dedicated to noise impacts on marine fishes and invertebrates (Duarte *et al.* 2021; Harding *et al.* 2021). Meanwhile, marine reptiles and marine birds remain the most understudied groups (Duarte *et al.* 2021; Harding *et al.* 2021). Throughout this time, our collective understanding of anthropogenic noise, and of stressors in general, has continually evolved. Methods and investigative scopes have adapted to fit model systems and study organisms. For example, the study of fishes and invertebrates through experimental lab and field studies is relatively inexpensive and more logistically feasible to manage compared to the study of marine mammals (Rosen & Trites 2007).

1.3 Acute responses in the lab

A major challenge in understanding how environmental stressors, such as anthropogenic noise, affect organisms is establishing cause and effect relationships

(Adams 2003). Consequently, only carefully designed, and controlled, experiments that account for potentially confounding factors allow for robust conclusions about the impacts of noise disturbance. Because noise-exposure experiments in free-ranging animals can be logistically difficult to conduct, tank-based experiments using recorded playback of noise have been successfully employed as an alternative (Kunc *et al.* 2016). There are important questions and contexts that are well-suited to tank-based experiments, such as situations where species cannot avoid noise-polluted areas (McLaughlin & Kunc 2015), investigating underlying mechanisms (Purser & Radford 2011), and the long-term effects of repeated exposure (Radford *et al.* 2016a).

In parallel with initial research on impacts of noise on marine mammals, concern for physical damage to hearing and internal organs in fish via acoustic trauma from noise exposure drove some of the early investigation. For example, acute exposure to noise can impair hearing in several fish species, including the Oscar *Astronotus ocellatus* (Hastings *et al.* 1996), the fathead minnow *Pimephales promelas* (Scholik & Yan 2001, 2002), catfish *Pimelodus pictus* (Amoser & Ladich 2003), and goldfish *Carassius auratus* (Amoser & Ladich 2003; Smith *et al.* 2004). However, unlike mammals, fish are capable of regenerating damaged sensory hair cells (Monroe *et al.* 2015), and full recovery of hearing loss following noise cessation is possible (Smith *et al.* 2004). With regards to physical harm and injury, exposure to anthropogenic noise, and especially impulsive sounds, can lead to barotrauma that damages sensory systems and internal organs in fishes (McCauley *et al.* 2003; Casper *et al.* 2012; Halvorsen *et al.* 2012a, b) and invertebrates (André *et al.* 2011). However, the direct impacts of noise on mortality remains inconclusive (Halvorsen *et al.* 2012a; Casper *et al.* 2013). While emphasis was previously placed on the direct impacts of anthropogenic noise on health and anatomy, more recent scientific knowledge has shown that other physiological and behavioural responses (e.g., stress-related responses) are more likely to occur and may have broad implications (Aguilar de Soto *et al.* 2016). For example, it is likely that aquatic organisms will frequently experience sub-lethal and sub-injurious levels of noise throughout their lifetime. Consequently, there exists a need to better understand the physiological and behavioural responses of aquatic organisms to anthropogenic noise because negative effects could occur at any life stage and may be cumulative (Graham & Cook 2008; Dahl 2015).

Alongside hearing and physical injury, measures of physiological stress have been employed to determine acute responses to anthropogenic noise exposure. Respiration, measured by opercular beat rate or closed/circuit-respirometry, has been studied to assess acute impacts of noise in several species of aquatic organisms, including European sea bass *Dicentrarchus labrax* (Radford *et al.* 2016a), black seabream *Spondyliosoma cantharus* (Bruintjes *et al.* 2016b), European eels *Anguilla anguilla* (Simpson *et al.* 2014; Bruintjes *et al.* 2016a), and shore crabs *Carcinus maenas* (Wale *et al.* 2013). Furthermore, acute changes to biomarkers in response to noise exposure have been well-documented. For example, plasma cortisol levels tripled after 10 minutes of exposure to white-noise playback, relative to controls in goldfish (Smith *et al.* 2004). Similarly, playback of ship noise (30 min) increased cortisol levels of three species of fish: European perch *Perca fluviatilis*, common carp *Cyprinus carpio*, and gudgeon *Gobio gobio* (Wysocki *et al.* 2006). However, signs of habituation or desensitisation to noise have also been observed for changes to both oxygen consumption (Bruintjes *et al.* 2016a; Radford *et al.* 2016a) and stress-related biomarkers (Smith *et al.* 2004). It is important to note that even well-accepted physiological indicators of acute stress do not necessarily reflect states of chronic stress (Sadoul & Geffroy 2019).

There is ongoing debate about the efficacy of both tank-based and playback experiments (Kunc *et al.* 2016). In small tanks, the ratio of sound pressure and particle motion have been shown to deviate considerably from what would be expected in theoretical far-field environments (Campbell *et al.* 2019), thus limiting extrapolation of responses to natural conditions (Slabbekoorn 2015). With regards to playback experiments, loudspeakers are generally incapable of producing very low frequencies that may be important to aquatic life (Fig. 1.1). Moreover, loudspeakers do not have a linear response, which likely changes the spectral quality of playback and also results in an imbalance of pressure and particle motion sound components (Voellmy *et al.* 2014a). Despite these limitations, tank-based, playback experiments have successfully highlighted reactions to noise in controlled settings, thus demonstrating potential consequences in natural environments. To better understand how free-ranging aquatic organisms respond to noise, alternative approaches in semi-open or controlled-field settings (Neo *et al.* 2016; Kok *et al.* 2021) that use real noise sources (Simpson *et al.* 2016; McCloskey *et al.* 2020) can and should be employed.

1.4 Experimental noise research in the field

Studying the impacts of real noise sources in natural environments is essential for testing the external validity of effects observed in the laboratory setting. Importantly, there is a distinction between experimental field studies and observational field data, as the experimental designs of the former aim to reduce the problems of confounding factors and allow for interpretations about causation (Slabbekoorn 2015). However, there are logistical challenges to studying free-ranging animals, which can limit the investigative scope. Consequently, most field research on the impacts of noise has been limited to studying behavioural responses by small, territorial benthic species in relatively shallow water (Simpson *et al.* 2016; Nedelec *et al.* 2017b; Mills *et al.* 2020).

Site-attached, benthic species provide valuable model systems for anthropogenic noise research in the field, as their static nature can facilitate the design and execution of controlled, experimental study. For example, anthropogenic noise altered vocal behaviour in two species of cryptic toadfish, the Lusitanian toadfish *Halobatrachus didactylus* (Alves *et al.* 2017) and the oyster toadfish *Opsanus tau* (Krahforst *et al.* 2016; Luczkovich *et al.* 2017). Similarly, sedentary brown meagres *Sciaena umbra* increased vocalisations, as a potential compensatory mechanism, when repeatedly exposed to motorboat passes (Picciulin *et al.* 2012). Site-attached life stages, such as spawning and reproductive periods, might offer opportunistic times for the study of anthropogenic noise impacts. For example, *in situ* motorboat noise affected parental care and nesting behaviour in two species of tropical damselfish, the spiny chromis *Acanthochromis polyacanthus* (Nedelec *et al.* 2017b) and the Ambon damselfish *Pomacentrus amboinensis* (McCloskey *et al.* 2020), and also a species of freshwater fish, the smallmouth bass *Micropterus dolomieu* (MacLean *et al.* 2020). Lastly, localised areas of activity, such as cleaning stations, might offer unique opportunities not only to observe behavioural responses of specific cleaner species, but also potentially to monitor changes in interspecific interactions. Bluestreak cleaner wrasse *Labroides dimidiatus* inspected client fishes for longer and were significantly less cooperative during exposure to noise from motorboat passes (Nedelec *et al.* 2017a).

Alternative study designs have been employed to broaden the investigative scope for anthropogenic noise impacts on animals in semi-natural conditions. For example, several papers by Neo *et al.* employed a large outdoor floating pen, equipped with cameras, to observe changes in swimming and shoaling behaviour of European sea bass *Dicentrarchus labrax* to a variety of brown-noise treatments (Neo *et al.* 2015b, 2016, 2018). Additionally, researchers might use a mix of laboratory and controlled-field experiments to infer consequences of noise disturbance. For example, Simpson *et al.* (2016) used a suite of complementary experiments to determine a negative impact of motorboat noise on antipredator behaviour and survival of *P. amboinensis*, including impacts of motorboat-noise playback on antipredator responses and prey survival in the lab, impacts of real motorboats on antipredator responses and prey survival in a controlled arena in the field, and survival of post-settlement larvae on experimental patch reefs exposed to motorboat-noise playback. While the logistics and set up of such experiments can be complex, semi-open or controlled-field studies can include natural conditions and variation, such as weather, temperature, and hydrodynamics, without abandoning experimental control to allow for better interpretations of observed behavioural changes.

Behavioural studies make up the majority of anthropogenic noise research to date with the greatest number of significant effects (Duarte *et al.* 2021). It can be argued that changes in behaviour may take place in the largest proportion of animals exposed to anthropogenic noise, as responses can occur at relatively low levels of sound (Hawkins & Popper 2017; Fig. 1.3). Changes to important behaviours may come at a cost to individuals by affecting energy and time budgeting (Read *et al.* 2014). Certain behavioural changes can have direct consequences for fitness, such as impaired courtship, survival, or reproductive success (Francis & Barber 2013). However, it is challenging to determine the long-term impact on welfare or fitness from short-term behavioural changes in response to acute anthropogenic noise (Slabbekoorn *et al.* 2019), as behaviours might return to normal when sound production ceases, and animals might desensitise, come to tolerate, or habituate to chronic noise exposure (Hawkins & Popper 2017).

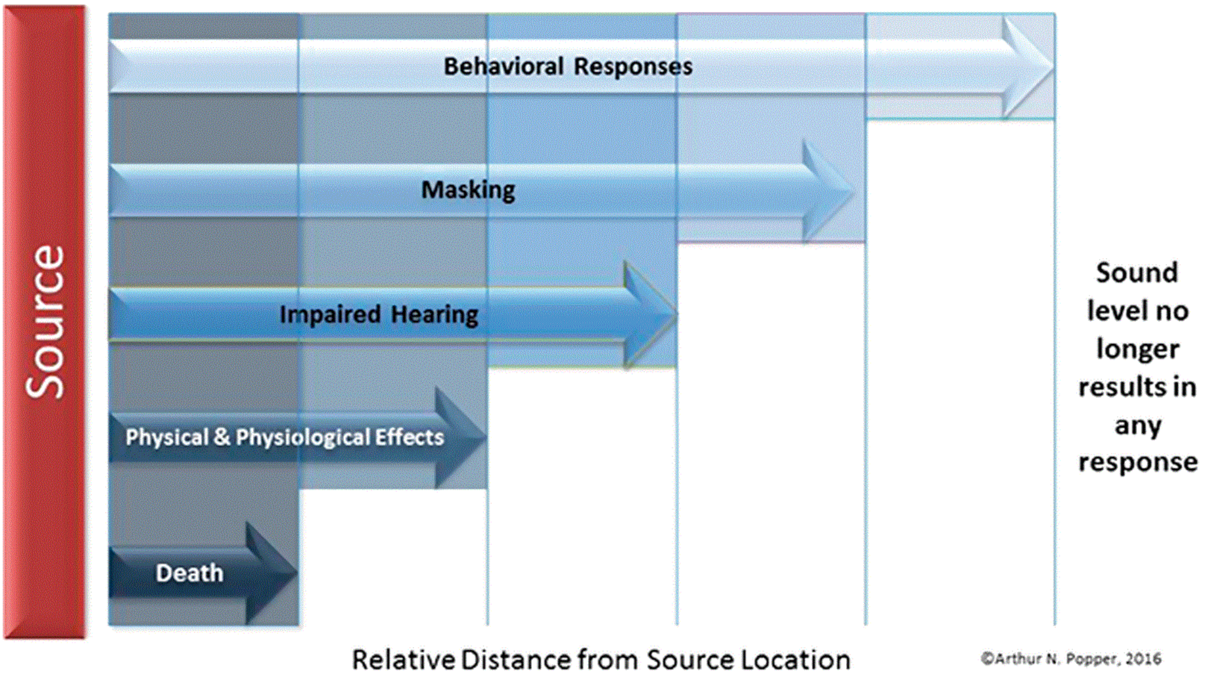

Figure 1.3. Potential effects of sound disturbance at different, relative distances from a source*; from Hawkins and Popper (2017). Actual distances will depend on the source type and level, and the distance from any given source that some effect may 'drop out' will likely vary as a result of numerous factors including the receiver species and characteristics (e.g., age, size, life-history)* (Hawkins & Popper 2017)*.*

1.5 Repeated exposure, long-term impacts, and fitness consequences

The degree to which individuals differ in sensitivity to noise due to prior experience has been underappreciated (Francis & Barber 2013). Behavioural and physiological responses may get stronger through sensitisation to acoustic disturbance, as shown in the case of hypersensitisation of startle reflexes to loud sounds in fish (Bhandiwad *et al.* 2018) and mammals (Götz & Janik 2011). Alternatively, noise-induced effects can diminish over time in animals that are repeatedly exposed, for which Kok *et al.* (2021) states there are three potential causes. First, animals living in disturbed areas may become habituated, desensitised, or tolerant to noisy conditions (Nedelec *et al.* 2016b; Harding *et al.* 2018). Second, animals unable to cope may leave disturbed areas (Bejder *et al.* 2006; Francis *et al.* 2009). Third, non-coping animals unable to leave might die sooner than coping individuals (Simpson *et al.* 2016). A combination of these factors could lead to observed decreases in the effects of short-term noise exposure, therefore recent research has shifted to consider potential effects of habituation, desensitisation, and/or tolerance to long-term exposure of individuals to noise (Kok *et al.* 2021). However, Francis & Barber (2013) warn that citing habituation in the absence of noise impacts might oversimplify the effects of noise on animals, and that acclimation to a stressor might not release an organism from costs to fitness (Romero *et al.* 2009).

Research on the ultimate fitness consequences of noise—that is, on an individual's ability to survive and reproduce—will translate to assessments of population viability and overall ecosystem functioning (Weilgart 2018). Therefore, an increasing number of studies have considered vital rates (e.g., survival, growth, and reproduction) over larger spatiotemporal scales. However, results thus far remain inconclusive and species-specific (Duarte *et al.* 2021). For example, spiny chromis *Acanthochromis polyacanthus* parents experiencing 12 days of motorboat-noise playback at *in situ* nests suffered higher juvenile mortality compared to control parents experiencing ambient-sound playback, despite increased nest defence behaviours by parents under noisier conditions (Nedelec *et al.* 2017b). In contrast, twelve weeks of repeated noise exposure did not affect growth or mortality in European sea bass *Dicentrarchus labrax* (Radford *et al.* 2016a). Furthermore, four weeks of repeated motorboat-noise playback did not affect hatching success or post-hatching larval growth in daffodil cichlids *Neolamprologus pulcher* (Bruintjes & Radford 2014). However, daily exposure to artificial noise (100–1000 Hz linear sweeps) during an entire spawning window (ca. nine months) for Atlantic cod *Gadus morhua* resulted in transient, mild cortisol elevations in parents and subsequent reductions in the total egg production, fertilisation rates, viable embryos, and cortisol content of fertilised eggs (Sierra-Flores *et al.* 2015). It is important to note that there is considerable variability of conditions and context among these studies, and that the degree to which species and individuals vary in sensitivity to noise during each life-history stage, as well as behavioural context, remains undervalued and understudied (Francis & Barber 2013; Harding *et al.* 2019). The impact of sound on animals is not often very direct or obvious, and while indirect conclusions about fitness might be drawn from changes to behaviour and/or physiology (Francis & Barber 2013), ultimately direct, long-term measures of the fitness consequences of anthropogenic noise are needed.

1.6 Communities and populations

Most of the research to date focuses on how underwater noise affects individual animals; there has been little investigation of now noise effects scale up to interspecific, population, and community-level consequences (Kunc *et al.* 2016). While there is a paucity of investigations into community-level responses to noise in aquatic ecosystems, terrestrial anthropogenic noise (e.g., traffic noise near roads) has been shown to have a range of effects on avian communities, including to abundance, species richness, and community structure (Francis *et al.* 2009; Slabbekoorn & Halfwerk 2009; Ware *et al.* 2015; McClure *et al.* 2017). Due to the density of roads and highways systems, associated traffic noise may impact individuals and communities at the national level (Cooke *et al.* 2020a; Senzaki *et al.* 2020). Comparatively, only one aquatic study to date has considered community-level demographics (Nedelec *et al.* 2017a), and only a small handful of studies have demonstrated that noise can alter interspecific relationships among fishes, such as predator–prey interactions (Simpson *et al.* 2016; Ferrari *et al.* 2018) and cooperative mutualisms (Nedelec *et al.* 2017b).

It can also be challenging to identify broader trends from response patterns at the individual level (de Jong *et al.* 2020), and to translate effects into population-level consequences (Slabbekoorn *et al.* 2019; Mortensen *et al.* 2021). This may in part be due to challenges with observing and quantifying the impacts of sublethal stressors, such as anthropogenic noise, on life-history processes (e.g., growth, survival, and reproduction). Therefore, population modelling offers a complementary approach to answering such questions. The use of population models has become more prominent in recent years due to developments of a population consequences of acoustic disturbance (PCAD) framework (National Research Council 2005). Originally developed and used for anthropogenic noise impacts on marine mammal populations, PCAD has been used successfully to simulate population-level responses to noise pollution in a variety of contexts (King *et al.* 2015; Van Beest *et al.* 2017; Nabe-Nielsen *et al.* 2018). In fish, PCAD has been implemented to show that population growth rates might be particularly sensitive to the effects of anthropogenic noise on energy expenditure and food intake (Soudijn *et al.* 2020). While PCAD models are important tools for understanding noise-driven changes to population-level dynamics, they lack spatial context that other modelling frameworks, such as individual-based modelling, can incorporate (Mortensen *et al.* 2021).

Individual-based modelling (IBM) uses a bottom-up approach to simulate a population of discreet individuals where a combination of dynamic individual state and environmental variables drive individual behaviour within a population (DeAngelis & Grimm 2014). Importantly, population dynamics are not approached from a statistical interpretation of observations but emerge from simulated interactions between individuals and adapt to context and environment (Railsback & Grimm 2019). While a handful of studies have successfully used IBM to explore the impacts of anthropogenic noise disturbance on marine organisms, only two studies are related to fish species (Rossington *et al.* 2013; Heinänen *et al.* 2018). However, these studies focus primarily on population-level changes to movement and distribution as a response to point anthropogenic noise disturbance events. To further understand the possible population-level consequences of anthropogenic noise, Mortensen *et al.* (2021) recommends the combined use of PCAD and IBM frameworks where affected life functions are translated into long-term age-specific vital rates, which has been done in marine mammals (Van Beest *et al.* 2017; Nabe-Nielsen *et al.* 2018) but not fishes (Slabbekoorn *et al.* 2019; Mortensen *et al.* 2021).

1.7 Mitigation

Duarte *et al.* (2021) describes anthropogenic noise as a pollutant that cannot be ignored and must be addressed in policies to mitigate human impacts on the oceans. However, a review of 10 major international agreements that address noise found that all but one, the European Union’s Marine Strategy Framework Directive (MSFD), are voluntary or noncommittal in nature (Lewandowski & Staaterman 2020). Currently, the most effective way of reducing the impacts of anthropogenic noise on wildlife is through noise abatement (i.e., lessening the amount of noise pollution entering the marine environment), either by reducing noise emitted at the source or by reducing the amount of noise-generating activity (Merchant 2019). However, exploitation of marine and coastal waters continues to increase, and it is highly unlikely that there will be a reduction of activity to these areas (Merchant 2019; Duarte *et al.* 2021). Therefore, the use of simple, accessible noise-mitigation measures that principally focus on reducing noise-exposure levels present important opportunities to reduce the detrimental impacts of noise on wildlife. For example, adjusting distances away from target locations containing at-risk species and/or speed to limit damaging anthropogenic noise exposure have been successfully employed to protect at-risk marine mammal populations, such as the critically endangered southern resident killer whales *Orcinus orca* (Williams *et al.* 2019). Ultimately, there is enough evidence that anthropogenic noise harms marine life to prompt action and management (Shannon *et al.* 2016; Kunc & Schmidt 2019; Duarte *et al.* 2021); however, such noise-mitigation measures require rigorous testing to ensure that potential benefits to wildlife are validated scientifically.

1.8 Thesis aim and outline

The aim of this thesis is to explore the impacts of anthropogenic noise on aquatic life at varying levels of biological organisation using a mixed-methods approach and a variety of study species (fishes and one invertebrate species). Specifically, I employed an integrated, ‘bottom-up’ approach, starting with impacts on reproductive behaviour of individuals, expanding out to interspecific interactions and localised changes in community structure, and finally investigating potential impacts on whole populations via computational modelling. Throughout, I have strived to consider and incorporate aspects of mitigation at each level of investigation.

In Chapter Two, I explore the potential impacts of real motorboat noise on reproductive behaviour of Ambon damselfish *Pomacentrus amboinensis in situ*, while also investigating the potential benefits of a novel mitigation approach. In Chapter Three, I examine the effects of SCUBA-noise playback on interspecific cooperation and community structure at ecologically important cleaning stations of the

Pederson's cleaner shrimp *Ancylomenes pedersoni*; this investigation establishes acoustic disturbance as a likely mechanism for previously documented diver-presence effects on marine animals and provides an avenue for mitigating the negative impacts associated with diver presence. In Chapter Four, I develop a combined PCAD/IBM modelling framework to simulate the effects of anthropogenic noise on a hypothetical population of European sea bass *Dicentrarchus labrax*. Subsequently, in Chapter Five, I use this population model to explore the impacts of projected noise-pollution levels in the Northeast Atlantic to the modelled population of European sea bass and explore the potential benefits of contrasting noise-abatement theories and management scenarios. In support of Chapters Four and Five, and as an Appendix to this thesis, I provide standardised documentation of the modelling process (TRACE document; Appendix B), including the model's rationale, design, and testing, which is considered a requirement of good modelling practice (Grimm *et al.* 2014). Finally, in Chapter Six, I revisit the main findings from each chapter before suggesting broader opportunities for future noise research and discussing plausible strategies for managing noise pollution, and associated negative impacts, in our oceans.

Chapter Two – Effects of anthropogenic noise on territorial behaviour of nesting coral reef fish with exploration of a potential mitigation strategy

Author contributions: K.P.M. was responsible for designing the research, including pilot data during previous field seasons for Experiments 1 and 2, and for leading with data collection in the field. K.P.M. conducted video and data analysis for Experiment 2 and took the lead with manuscript writing along with co-first author K.E.C (who conducted analysis and wrote paragraphs relating to Experiment 1). K.P.M. also independently analysed acoustic data, designed the graphical abstract, and created data figures.

Collaborator contributions: K.E.C., L.C., A.N.R., and S.D.S. assisted with designing the study with in-field advice from M.I.M.; K.E.C. and L.C. assisted with carrying out the fieldwork and collecting data; K.E.C. assisted with data extraction from videos and data analysis of Experiment 1; L.C., A.N.R., and S.D.S. advised on data analysis; L.C. and S.D.S advised on acoustic analysis; K.E.C. assisted with manuscript writing of Experiment 1; L.C., A.N.R., and S.D.S commented on drafts of the manuscript.

Sections 2.1 to 2.6 of this chapter have been published as:
McCloskey KP, Chapman KE, Chapuis L, McCormick MI, Radford AN, Simpson SD. 2020. Assessing and mitigating impacts of motorboat noise on nesting damselfish. *Environ. Pollut.* 288, 115376.

2.1 Abstract

Motorboats are a pervasive, growing source of anthropogenic noise in marine environments, with known impacts on fish physiology and behaviour. However, empirical evidence for the disruption of parental care remains scarce and stems predominantly from playback studies. Additionally, there is a paucity of experimental studies examining noise-mitigation strategies. We conducted two field experiments to investigate the effects of noise from real motorboats on the parental-care behaviours of a common coral-reef fish, the Ambon damselfish *Pomacentrus amboinensis*, which exhibits male-only egg care. When exposed to motorboat noise, we found that males exhibited vigilance behaviour 34% more often and spent 17% more time remaining vigilant, compared to an ambient-sound control. We then investigated nest defence in the presence of an introduced conspecific male intruder, incorporating a third noise treatment of altered motorboat-driving practice that was designed to mitigate noise exposure via speed and distance limitations. The males spent 22% less time interacting with the intruder and 154% more time sheltering during normal motorboat exposure compared to the ambient-sound control, with nest-defence levels in the mitigation treatment equivalent to those in ambient conditions. Our results reveal detrimental impacts of real motorboat noise on some aspects of parental care in fish, and successfully demonstrate the positive effects of an affordable, easily implemented mitigation strategy. We strongly advocate the integration of mitigation strategies into future experiments in this field, and the application of evidence-based policy in our increasingly noisy world.

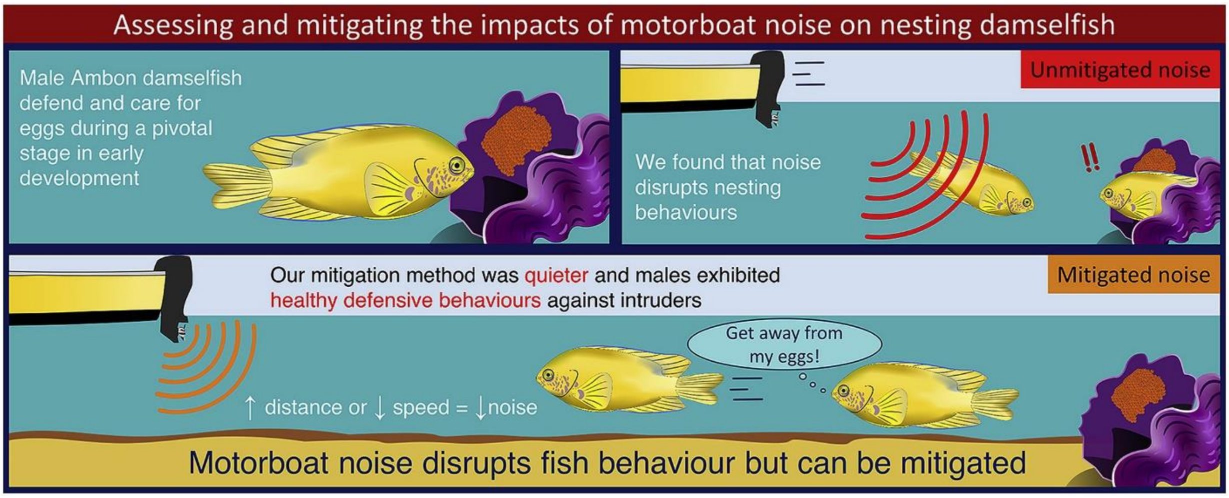

Figure 2.1. Graphical abstract of results for publication in Environmental Pollution.

2.2 Introduction

Ocean soundscapes throughout the world are increasingly altered by human-generated noise. This noise comes from a variety of sources including energy production, resource extraction, construction, and transportation (Hildebrand 2009; Slabbekoorn *et al.* 2010). Consequently, policymakers, such as the International Maritime Organization (IMO 2014), and legislation, such as the European Commission Marine Strategy Framework Directive (Tasker *et al.* 2010) and the US National Environment Policy Act, have classified anthropogenic noise as a globally pervasive pollutant, calling for scientific assessment and informed mitigation solutions (Hawkins *et al.* 2015; Buxton *et al.* 2017). There has been an increase in evidence demonstrating the negative impacts of noise on a wide range of aquatic taxa, including effects on spatial distribution, communication, foraging, homeostasis, and con- and hetero-specific interactions (see reviews: Shannon *et al.* 2016; Cox *et al.* 2018; Kunc & Schmidt 2019; Popper & Hawkins 2019). However, investigation of the impacts of noise on reproductive behaviour is needed, as successful reproduction is essential for population resilience and viability (Weilgart 2018; de Jong *et al.* 2020).

Parental care is a key aspect of reproductive behaviour in many fish species (Blumer 1982), but there are relatively few studies investigating how this may be impacted by noise pollution. Parental care in fish comprises a suite of behaviours, including nest maintenance, egg oxygenation, and defence against competitors and predators (Zoran & Ward 1983; Haley & Müller 2002; Hale & Mary 2007), which directly influence offspring survival and therefore fitness (Sabat 1994). Bruintjes and Radford (2013) found that captive male daffodil cichlids *Neolamprologus pulcher* reduced nest-digging rate and delayed initiating this behaviour during exposure to motorboat-noise playback, with a concurrent reduction in anti-predator behaviour when there were no eggs in the nest. Similarly, but at natural nests, Picciulin *et al.* (2010) found a negative effect of boat-noise playback on the time spent by Mediterranean chromis *Chromis chromis* cleaning and egg tending. More recently, Nedelec *et al.* (2017b) showed that spiny chromis *Acanthochromis polyacanthus* parents experiencing 12 days of motorboat-noise playback at natural nests increased their nest-defence behaviours, but suffered higher juvenile mortality compared to control parents experiencing ambient-sound playback. Although two of these experiments were conducted *in situ*, all used playback of recordings as a noise treatment, which does not fully replicate sound exposures that would be experienced when exposed to real noise sources (Slabbekoorn 2015).

Here, we aim to address this knowledge gap with two *in situ* experiments that examine the effects of an ecologically relevant noise source on parental care in a wild fish population, using motorboats as a direct sound source. Nearly half of the Earth's growing population of 7.6 billion people live within 60 miles of the shore, and as humans continue to cluster around coasts, use of inshore waters will continue to increase (McCormick *et al.* 2018; Wright & Nichols 2018). For example, 11.9 million recreational vessels were registered in the USA in 2017 (NMMA 2017) and 0.5 million recreational motorboats are expected to be using the Great Barrier Reef by 2040 (GBRMPA 2014). Motorboats are therefore an extensive and increasing source of anthropogenic noise, and evidence is emerging regarding impacts of motorboat noise on fish endocrine and stress responses (Mills *et al.* 2020), development (Jain-Schlaepfer *et al.* 2018; Fakan & McCormick 2019), antipredator behaviour (Ferrari *et al.* 2018), reproduction (Nedelec *et al.* 2017b), and survival (Simpson *et al.* 2016; McCormick *et al.* 2018).

While there has been recent public and political call for further mitigation of marine noise, this consideration mainly concerns impacts on marine mammals (Williams *et al.* 2019), despite the high abundance, prevalence, and socio-economic importance of fishes and invertebrates (Williams *et al.* 2015). It is conceivable that changes to guidelines for recreational motorboating can be promoted to mitigate the detrimental impacts of noise on marine ecosystems. One method which has been tested in relation to biological responses in coral reef fishes is the installation of quieter engine types onto boats (Jain-Schlaepfer *et al.* 2018; McCormick *et al.* 2018, 2019). Although this method was successful in reducing impact, it is expensive and as a result would be difficult to implement widely. There is a need for affordable mitigation options which can be integrated into policy, but can also be immediately employed by motorboat users. One such possibility is recommending the alteration of driving practice; for example, spatial management and speed restrictions could be implemented near vulnerable areas, such as coral reefs, to limit damaging noise exposure. Similar concepts are currently being promoted to protect at-risk marine mammal populations, such as the critically endangered Southern Resident killer whales *Orcinus orca* (Williams *et al.* 2019). In freshwater fish, MacLean *et al.* (2020) found that residency time in nesting smallmouth bass *Micropterus dolomieu* was adversely affected by motorboat noise playback, but only when close to the loudspeaker. However, the application of similar measures to coral reef habitats requires rigorous testing to ensure that potential benefits to wildlife are validated scientifically.

Here, we assessed the effects of motorboat noise and noise mitigation on parental care in an abundant Indo-Pacific coral-reef fish species, the Ambon damselfish *Pomacentrus amboinensis* (family Pomacentridae). This demersal-spawning species exhibits male-only parental care (McCormick 2016) and has been shown previously to be disturbed by motorboat noise, notably in assessment of risk (McCormick *et al.* 2018), predator-recognition learning (Ferrari *et al.* 2018), anti-predator behaviours (Simpson *et al.* 2016), and feeding and movement (Holmes *et al.* 2017). Specifically, we conducted two experiments on individual male *P. amboinensis* caring for clutches of eggs. The first experiment considered the effect of noise from real motorboats on behaviours occurring inside the nest in association with the eggs, to determine whether these fish are less attentive parents in noisy conditions. The second experiment considered the impact of motorboat noise on defensive behaviours triggered by the presence of a conspecific male intruder outside the nest. Having found detrimental effects of real motorboats in our first experiment, we added a mitigation-strategy treatment (altering motorboat-driving practice adjacent to the reef edge) for our second experiment to address the paucity of experimental evidence regarding noise-mitigation methods.

2.3 Methods

2.3.1 Ethics statement

This work was approved by the University of Exeter Animal Ethics Committee (Application, 2013/247), the University of Bristol Animal Welfare Ethical Review Board (University Investigator Number UB/16/057) and James Cook University Animal Ethics Committee (Application A2361), and was completed in strict accordance with the guidelines of the Australian Code of Practice for the Care and Use of Animals for Scientific Purposes (8th Edition, 2013). Permits were granted by the Great Barrier Reef Marine Park Authority and Queensland Parks and Wildlife Service (Permit G17/39752.1) and the Queensland Department of Agriculture Fisheries and Forestry (Permit 170251).

2.3.2 Experimental overview

We collected data between October and December 2018 on reefs near to Lizard Island Research Station (14°4′S 145° 28′E; Fig. A.1a), Great Barrier Reef, Australia. Two experiments were conducted on male *P. amboinensis* occupying artificial nests at six study sites along the reef edge (Fig. A.1b). We exposed nests to the following noise treatments: ambient-sound conditions (Experiments 1 and 2), motorboats being driven nearby (Exp. 1 and 2), and motorboats being driven under a mitigation regime (Exp. 2). Video cameras recorded parental-care behaviours within the nest (Exp. 1) and immediately surrounding the nest (Exp. 2) during these treatments.

2.3.3 Study species

On the Great Barrier Reef, male *P. amboinensis* exhibit parental care of demersal broods within a nest throughout the breeding season (October–January; McCormick & Meekan 2007). During the parental-care period, males aggressively guard their territory from intruders and egg predators, maintain the nest, clean the broods, and oxygenate eggs by fanning with their pectoral and dorsal fins (Moyer 1975; McCormick & Smith 2004; McCormick & Meekan 2007). Parental care in this species therefore involves costs in terms of time, energetic investment, and trade-offs with future reproductive opportunity (males continue to court females during this period; McCormick 2016), but improves offspring survival at this vulnerable stage (Gross & Sargent 1985).

2.3.4 Artificial nests

We placed a total of 120 artificial nests within six study sites, each consisting of 100 m stretches of continuous reef, with at least 200 m between neighbouring sites. Previous work has shown that *P. amboinensis* readily occupies artificial nests, including terracotta tiles (Kerrigan 1997) or PVC half-pipes (Emslie & Jones 2001). In addition to their high site-fidelity, small home ranges, and resilience to physical disturbance, this makes breeding males easy to manipulate experimentally. Our nests consisted of upturned half PVC pipes (18 cm diameter, 30 cm length) surrounded by coral rubble (approx. 0.5 m^3) (following McCormick 1998) and placed on sandflats along reef edges at depths of 2–5 m. The distance between each nest was determined by the natural proximity of males (minimum distance of 1 m); half-pipes were placed near relatively large individuals observed to exhibit territorial aggression, to increase the likelihood of settlement and successful courtship (McCormick & Meekan 2007). Following placement, each nest was readily explored and subsequently adopted within minutes of placement by an individual male *P. amboinensis,* which guarded that nest for the remainder of the breeding season, as observed in earlier studies (Kerrigan 1997; Emslie & Jones 2001).

We monitored each of the six study sites approximately every 2–3 days in rotation, and ran experimental trials within 2 days of eggs being found at a nest, as the incubation period for a single clutch in this species is ca. 4–5 days at 28 °C (Kerrigan 1997). Experimental trials were always conducted between 0800 and 1500 h. Trials were not conducted on days with uncharacteristically bad weather (>2 on the Beaufort scale) or heavy rainfall due to noisier ambient conditions associated with these natural phenomena (Putland *et al.* 2017). As spawning was asynchronous, and treatments were applied to whole sites, some individual males were exposed to our treatments before the trial in which they were recorded. However, the potential for noise-induced carry-over effects in fishes remains inconclusive (Mills *et al.* 2020), and given the short-term nature of the treatments (5–10 min), we do not believe that previous exposure would impact the response of an individual during a trial. Regardless, we endeavoured to minimise the likelihood of carry-over effects from motorboat-noise by staggering exposure to the same study site (no repeat exposures of the same type within 48 h). Furthermore, to reduce the potential for cross-contamination by noise to nests which were not currently being recorded, trials were not conducted in neighbouring study sites on the same day.

2.3.5 Experimental noise procedure

To introduce motorboat noise experimentally to study sites, motorboats (5 m long aluminium hull with 4-stroke 30-horsepower Suzuki DF30A outboard engine) were driven at varying speeds and distances, depending on treatment type. A total of five motorboats of similar size, hull type, and engine type were used in rotation throughout the study to minimise pseudoreplication. The motorboats were always driven by the same individual (K.P.M) to standardise driving style between trials.

Each experimental trial was conducted under one of three noise conditions: ambient sound (no motorboat), motorboat noise, or mitigated-motorboat noise (hereafter referred to as ambient, motorboat, and mitigation, respectively). All ambient trials which experienced unplanned boat passes within 500 m of the focal study site were discarded, however this was rare (<5 occurrences) as this location experiences minimal traffic (<5 boats a day). The motorboat treatment consisted of full-speed passes by a single motorboat parallel to the reef and 10–20 m from the reef edge. For the mitigation treatment, the motorboat was excluded from an ‘acoustic buffer zone’ within 20 m of the reef edge, and was driven parallel to the reef through two zones: 20–120 m from the reef where speed was reduced to quarter throttle, and >120 m from the reef where the motorboat was driven at full speed. Although each nest would experience a fluctuating level of noise during the treatments, they would have received the same cumulative sound exposure level at the end of the treatment (i.e., each nest experienced the same number of boat passes at one speed and distance from the reef).

2.3.6 Acoustic recordings and analysis

The acoustic properties of the ambient, motorboat, and mitigation treatments were recorded at each of the six study sites, in sea states between 0 and 2 on the Beaufort scale, and in the absence of rain. Sound pressure was recorded using an omnidirectional hydrophone with inbuilt digital recorder (SoundTrap 300 STD; Ocean Instruments NZ, Auckland, New Zealand). Particle-acceleration recordings were made using a triaxial accelerometer (M20-040; sensitivity following a curve over the frequency range 0–3 kHz; calibrated by manufacturers; Geospectrum Technologies, Dartmouth, Canada) connected to a digital 8-track recorder (F8 field recorder, sampling rate 48 kHz; Zoom Corporation, Tokyo, Japan). Recordings were made at the approximated midway point of each study site over sandy-bottom areas along the reef edge, at 1.5–2.5 m depth. At each of the six sites, we recorded ambient conditions once and motorboat and mitigation treatments three times. By recording noise from three of the five motorboats used in the experiments, we included potential acoustic variation between motorboats in our acoustic analysis.

We analysed the recordings in *MATLAB R2017b* using *PAMGuide* (sound pressure; Merchant *et al.* 2015) and *paPAM 0.9* (particle acceleration; Nedelec *et al.* 2016a), analysing across a frequency range of 1–2000 Hz; the likely hearing range relevant to pomacentrid fishes (Kenyon 1996; Wright *et al.* 2011). Power spectral densities (PSD) (Fig. 2.1a and b), root-mean-square levels (SPL_{rms} and SAL_{rms}), and cumulative sound exposure levels (SEL_{cum} and AEL_{cum}) (Table 2.1) were calculated in both the sound-pressure and particle-acceleration domains using a Hamming filter with a window length of 1024 and 50% overlap over batch-processed 1-min subsamples of the recordings (n = 6 ambient recordings; n = 18 motorboat recordings; n = 18 mitigation recordings). These subsamples were selected to represent closely the acoustic conditions of each treatment for analysis. For motorboat-treatment recordings, our subsamples included three full motorboat passes, typically at the middle of recordings to avoid acceleration and deceleration portions. Lastly, we subsampled mitigation-treatment recordings to include one full slow-driving approach and departure, towards and away from the recording equipment (usually lasting about 30 s), along with 1–2 full-speed passes farther than 120 m away from the reef.

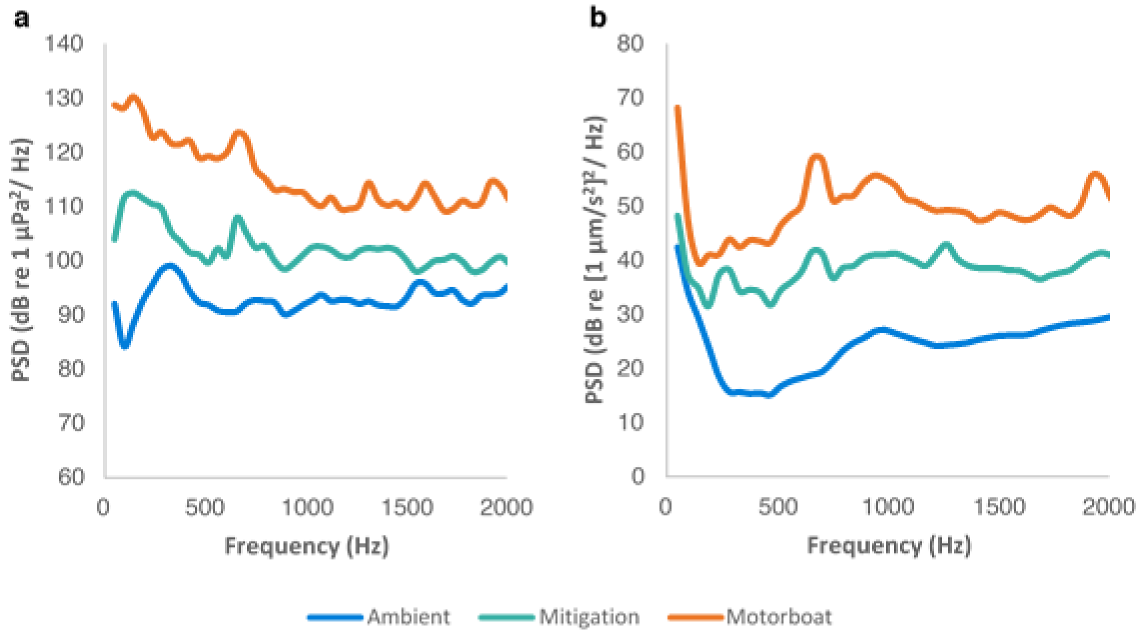

***Figure 2.2. Mean power spectral densities (PSD) of ambient, motorboat, and mitigation treatments** in both (a) sound pressure and (b) triaxial particle acceleration, giving an average sound profile for each treatment (fft length = 1024, Hamming evaluation window, 50% window overlap, 1–2000 Hz).*

***Table 2.1.Root-mean-square and cumulative sound exposure levels** in both sound pressure (SPL_{rms} and SEL_{cum}) and triaxial particle acceleration (SAL_{rms} and AEL_{cum}) for each treatment.*

Treatment	SPL_{rms} (dB re 1 µPa)	SEL_{cum} (dB re 1 µPa^2 s)	SAL_{rms} (dB re (1 µm/s^2)	AEL_{cum} (dB re (1 µm/s^2)^2 s)
Ambient	106.8	132.3	73.5	91.3
Mitigation	120.1	150.4	84.0	102.3
Motorboat	131.6	161.9	96.5	114.1

2.3.7 Experiment 1: Egg tending

To investigate the impact of motorboat-noise exposure on egg tending, data were collected on four within-nest behaviours of male *P. amboinensis*: nest visitation, egg fanning, nest maintenance, and vigilance (Table 2.2). We approximated the duration of a dorsal fanning event as 0.5 s (from a mean of 30 events) in order to give combined counts and durations for dorsal fanning and pectoral fanning together.

***Table 2.2. Ethogram for the recorded egg-tending behaviours** exhibited by male P. amboinensis within the nest (Experiment 1).*

Behaviour	Description	Variables
Nest visitation	When the male was underneath the artificial nest	Count, duration, intervals
Egg fanning	Combined scores of: (1) pectoral fanning, when the male faced the brood, fanning with its pectoral fins and often pecking at the clutch with its mouth; and (2) dorsal fanning, when the male wriggled the length of its body along the eggs with the dorsal fin in contact with the clutch	Count, duration
Nest maintenance	When the male exhibited tidying of the nest, including removing objects (e.g., shells), mouth-pecking away from the brood, and digging in the substrate	Count
Vigilance	When the male was stationary in the nest entrance, looking out	Count, duration

We recorded behaviours at each nest under each of two treatments (ambient and motorboat). Both treatments of a single nest occurred on the same day and multiple nests at the same site were treated simultaneously; the first trial was completed between 0800 and 1000 h and the second between 1300 and 1500 h. We randomly assigned which treatment would occur first each day at each study site and counterbalanced treatment order on subsequent days to avoid ordering bias at each. Within-nest behaviours were filmed using weighted GoPro Hero 5 cameras set approximately 10 cm from the entrance to the nest by a snorkeler who then left the area. In both treatments, the first 5 min was not analysed to allow the fish to resume normal behaviour following disturbance (Nedelec *et al.* 2016b), after which 10 min was recorded to determine baseline level of behaviour in ambient-sound conditions. Following this, fish were given a 10-min exposure period under either the motorboat or ambient treatment, as described above. We collected videos for both treatments at 38 nests over 11 non-consecutive days.

2.3.8 Experiment 2: Nest defence

To investigate the impact of motorboat-noise exposure and a noise-mitigation strategy on nest defence, data were collected on five defensive behaviours of male *P. amboinensis*: time in shelter, time interacting with an intruder, displaying, striking, and chasing (Table 2.3).

***Table 2.3. Ethogram for the recorded nest-defence behaviours** exhibited by male P. amboinensis when presented with a conspecific intruder (Experiment 2).*

Behaviour	Description	Variables
Time in shelter	When the male sought refuge either in the artificial nest or nearby coral/rubble	Duration
Time interacting with an intruder	When the male was within one body length of the intruder’s plastic bag	Duration
Displaying	When the male extended its dorsal and anal fins or fanned its caudal fin at the intruder	Count, duration
Striking	When the male lunged at the bag, delivering a bite	Count
Chasing	When the male rapidly swam toward the intruder	Count

Each nest received three treatments (ambient, motorboat, and mitigation). We ran trials across three consecutive days at each nest, administering one treatment at that nest per day in a Latin-square block design to counterbalance for order effects, after which no repeat trials were recorded for that nest. Multiple nests were treated simultaneously at the same site, and three sites were treated per day, between 1000 and 1200 h. For the experimental trials, we introduced one conspecific male ‘intruder’ (mean standard length 6.5 ± 0.1 cm) outside each nest. Conspecific intruders were collected from neighbouring locations outside of the study areas by divers using hand nets. To reduce the number of captured fish, intruders were used at multiple sites throughout the day and released after the last trial to their original collection locations. We transported these fish in a large container that provided physical and visual isolation, as well as shade from the sun, replacing the holding water between sites with fresh seawater to remove waste and provide oxygenation during transport. Care was taken to avoid previously used collection areas on subsequent days, so that intruders were naïve to the experiment each day. The intruder for each trial was presented in an 8-L plastic bag, which we secured in place with a steel rod within 0.5 m of the guarded nest (McCormick & Meekan 2007). Aggressive behaviours towards a presented intruder began instantly, necessitating an experimental design with no acclimation period (cf. Exp. 1) and required the noise treatment to start 5 min prior to intruder presentation. Trials lasted for 10 min and defensive behaviours were recorded with one weighted GoPro Hero 5 camera per nest, which we placed approximately 0.5 m away from the nest entrance and angled so that the nest entrance and intruder bag were fully in frame. A total of 69 videos were collected at 23 guarded nests. However, five nests were excluded from subsequent analysis due to loss of broods by either predation or hatching, resulting in an incomplete set of trials for those nests in the matched experimental design and a final sample size of 18.

2.3.9 Video analysis

All videos collected in the field were cropped using *ffmpeg 4.1.3* (ffmpeg.org). For the egg-tending experiment (Exp. 1), videos were cut to baseline and exposure periods (10 min each). Two nests were removed from analysis due to unusable camera angles, and two more were removed due to filming of non-focal species occupying the nests. For the nest-defence experiment (Exp. 2), videos were cut to 5-min clips starting approximately 30 s after the snorkeler was last visible in the camera frame.

All videos were saved with coded file names and were watched with no sound so that we (K.E.C for Exp. 1; K.P.M for Exp. 2) were blind to the noise treatment during observation. We scored behaviours from the videos using the behavioural observation software *BORIS 7.6.1* (Friard & Gamba 2016).

2.3.10 Statistical analysis

For Experiment 1, we calculated rates (for counts) and time-budget proportions (for durations) by dividing the data by the total time that the fish spent in the nest in that 10-min period. The change in behaviour from the baseline period (ambient-sound condition) to the exposure period (motorboat or ambient) was calculated for each behavioural variable. We analysed the baseline–exposure change in the ambient treatment against the baseline–exposure change in the motorboat treatment as paired data for each fish (n = 34 individuals) using paired t-tests and paired Wilcoxon signed-ranks tests, depending on whether the data met the assumptions for parametric testing. Where a significant difference between treatments was found, one-sample t-tests or one-sample Wilcoxon signed-ranks tests were used to determine whether the behavioural measure in the exposure period (motorboat or ambient) was significantly different from the baseline within each treatment. Three pairs of data were identified as outliers (using Interquartile Range) and omitted from the analysis of the mean interval between nest visits. Holm-Bonferroni corrections for multiple measures were used for nest visitation (three measures), fanning (two measures), and vigilance (two measures).

For Experiment 2, we calculated the proportion of time spent sheltering by dividing the time of observed behaviours by the total time spent on screen. To investigate the remaining responses independently of changes to the sheltering proportion, variables were calculated to include only time spent out of shelter and swimming in open water. Therefore, we calculated the proportion of time spent interacting with the conspecific intruder (duration) and all behavioural rates (counts of displaying, striking, and chasing) by dividing the data by the total time that the focal male spent on screen and out of shelter. We analysed the differences between the three treatments (ambient, motorboat, and mitigation) for each fish (n = 18 individuals) using one-way repeated measures ANOVA tests with the *ez 4.4-0* package (Fazio *et al.* 2012) or Friedman tests using the *rstatix 0.4.0* package (Kassambara 2019), depending on whether the data met assumptions for parametric testing. Holm-Bonferroni corrections were used for the analyses of strikes and displays, as these behaviours often occurred simultaneously, and displays were measured in two ways. *Post hoc* comparisons were conducted using either pairwise t-tests or pairwise Wilcoxon signed-rank tests, both with Holm-Bonferroni corrections.

All analyses were completed in *R V3.5.2* (R Core Team, 2018). Statistical significance was assumed where $p < 0.05$. We derived statistical effect sizes for significant results using the *rstatix* package: Cohen's *d* for t-tests, Wilcoxon's effect size *r* for Wilcoxon tests, and Kendall’s *W* for Friedman tests. Furthermore, we calculated absolute effect sizes for significant results as percentage difference (to the nearest whole percent) of the mean (parametric tests) or median (non-parametric tests) value, from the baseline to the exposure period in Experiment 1, and from the ambient to the motorboat treatment or from the motorboat to the mitigation treatment in Experiment 2. All other values presented in the Results are means ± standard error of the means.

2.4 Results

2.4.1 Experiment 1: Egg tending

Male *P. amboinensis* spent 159 ± 14 s (mean ± SE) in the nest in the 10-min baseline period, visiting the nest for 9 ± 1 s at a time every 30 ± 3 s. There were no significant differences between the treatments in the baseline–exposure change in: the total time spent inside the nest, hereafter *nest time* (paired *t*-test: $t_{33} = 0.483$, $p = 0.633$), the mean duration of nest visits (Wilcoxon test: $V_{33} = 386$, $p = 0.282$), or the mean interval between visits ($V_{30} = 334$, $p = 0.282$).

Egg fanning occurred at a baseline rate of 17.5 ± 1.4 events per min of nest time, taking up 38.4 ± 1.7% of total nest time. There was no significant difference between treatments in the baseline–exposure change in fanning rate (paired *t*-test: $t_{33} = -0.37$, $p = 0.711$). The change in the proportion of nest time spent on fanning was close to, but did not meet, the threshold of α (0.05) for statistical significance (Wilcoxon test $V_{33} = 421$, $p = 0.069$). Upon further evaluation of this trend, we found there was a significant decrease from the baseline in the motorboat treatment ($V_{33} = 180$, $p = 0.044$, $r = 0.35$), where males spent on average a 19% lower proportion of time fanning when exposed to motorboat noise, but no significant change from the baseline in the ambient treatment ($V_{33} = 360$, $p = 0.293$).

Males undertook nest-maintenance at a baseline rate of 0.4 ± 0.1 events per min of nest time. There was no significant difference between the treatments in the change in nest-maintenance rate (Wilcoxon test: $V_{33} = 175$, $p = 0.484$).

Males exhibited vigilance at a baseline rate of 3.3 ± 0.3 events per min of nest time, taking up 8.5 ± 0.7% of total nest time. Treatment significantly affected the baseline–exposure change in vigilance rate by the males (paired *t*-test: $t_{33} = -3.20$, $p = 0.006$, $d = 0.55$; Fig. 2.2a), which significantly increased by 34% from the baseline in the motorboat treatment (one-sample *t*-test: $t_{33} = 3.11$, $p = 0.004$, $d = 0.53$) and did not significantly differ from the baseline in the ambient treatment ($t_{33} = -1.86$, $p = 0.072$). There was also a significant effect of treatment on the change in proportion of nest time spent on vigilance (Wilcoxon test: $V_{33} = 182$, $p = 0.048$, $r = 0.34$; Fig. 2.2b). There was a significant increase of 17% from the baseline in the motorboat treatment ($V_{33} = 371$, $p = 0.046$, $r = 0.34$), compared to no significant change from the baseline in the ambient treatment ($V_{33} = 234$, $p = 0.581$).

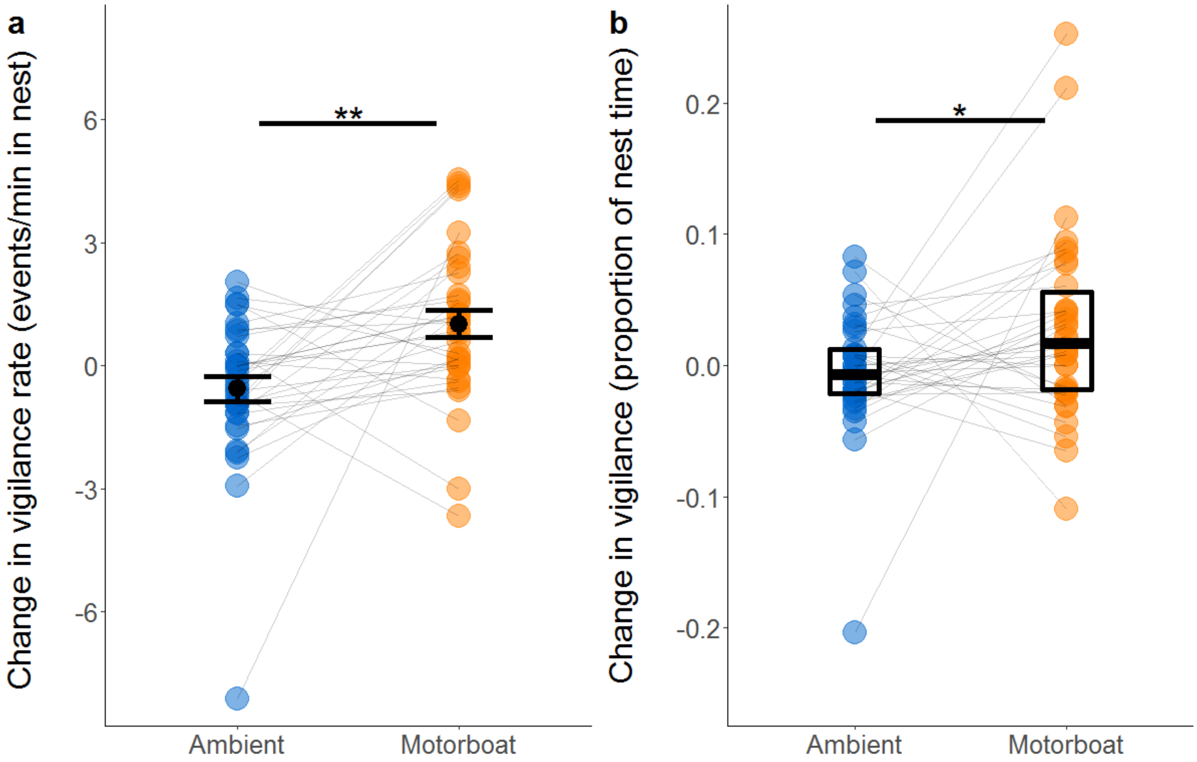

Figure 2.3. Treatment responses in (a) vigilance rate and (b) proportion of nest time spent on vigilance *by male P. amboinensis in the two treatments. Black points in (a) show mean treatment responses ± SEM error bars; boxes in (b) show median and interquartile range; coloured points show treatment responses; grey lines indicate paired data from individuals across the two treatments.* $*p < 0.05$, $**p < 0.01$. *n = 34 individuals for both response measures.*

2.4.2 Experiment 2: Nest defence

Male *P. amboinensis* spent 290 ± 3 s within the camera frame, or 97.1 ± 0.8% of the total 5-min time window. There was no significant difference in the total time spent in frame between the three treatments (ambient, motorboat, and mitigation) (one-way repeated measures ANOVA: $F_{2,34} = 0.31$, $p = 0.73$).

Sheltering occurred at a rate of 1.9 ± 0.3 events per min of time within the camera frame, taking up 16.3 ± 2.8% of total frame time. Males differed in the proportion of time spent sheltering during the three treatments (Friedman test: $X^2_2 = 6.79$, $p = 0.03$, $W = 0.19$; Fig. 2.3a). They spent a 154% higher proportion of time sheltering during motorboat-noise exposure than during the ambient treatment (Wilcoxon test: $V_{17} = 30$, $p = 0.03$, $r = 0.57$). Furthermore, the males spent an 80% lower proportion of time sheltering in the mitigation treatment compared to the motorboat treatment ($V_{17} = 158$, $p < 0.001$, $r = 0.74$). There was no significant difference between ambient and mitigation treatments ($V_{17} = 113$, $p = 0.09$).

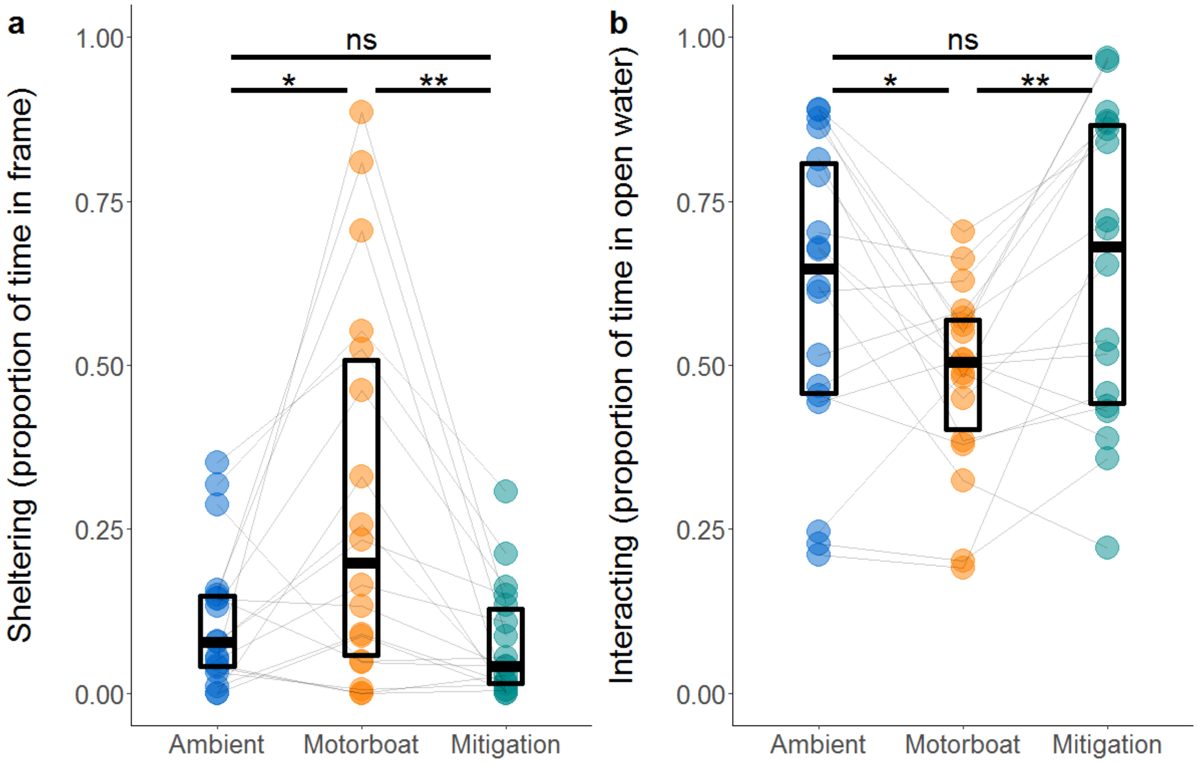

Figure 2.4. Treatment responses of male P. amboinensis in (a) proportion of frame time spent sheltering and (b) proportion of open-water time spent interacting with the intruder. *Boxes show median and interquartile range; coloured*

points show treatment responses; grey lines indicate paired data from individuals across the three treatments. Post-hoc pairwise comparisons are designated by annotated lines; 'ns' = non-significant, ∗ = p < 0.05, ∗∗ = p < 0.01. n = 18 individuals for all response measures.

Males interacted with the presented conspecific intruder at a rate of 6.5 ± 0.5 events per min of time swimming in open water, taking up 58 ± 2.9% of the total time unsheltered. Male *P. amboinensis* differed significantly in the proportion of time spent interacting with the intruding conspecific males during the three noise treatments (Friedman test: $\chi^2_2 = 10.11$, $p = 0.006$, $W = 0.28$; Fig. 2.3b). Males spent a 22% lower proportion of time interacting with the intruder during motorboat-noise exposure than in the ambient treatment (Wilcoxon test: $V_{17} = 139$, $p = 0.04$, $r = 0.55$). Additionally, they spent a 35% greater proportion of time interacting in the mitigation treatment compared to the motorboat treatment ($V_{17} = 18$, $p = 0.006$, $r = 0.69$). There was no significant difference between ambient and mitigation treatments ($V_{17} = 65$, $p = 0.39$).

Displays occurred at a rate of 6.1 ± 0.5 per min, for 20.7 ± 2.2% of total time spent swimming in open water. Males did not significantly differ between treatments in either display rates (one-way repeated-measures ANOVA: $F_{2,34} = 1.30$, $p = 0.573$) or the proportion of time spent displaying (Friedman test: $\chi^2_2 = 7$, $p = 0.091$). Strikes occurred at a rate of 11.1 ± 1.2 per min. There was no significant difference in strike rate during the three noise treatments (one-way repeated-measures ANOVA: $F_{2,34} = 0.54$, $p = 0.588$). Lastly, charges occurred at a rate of 0.93 ± 0.2 per min with no significant difference in charge rate between the three noise treatments ($F_{2,34} = 0.66$, $p = 0.52$).

2.5 Discussion

We found that motorboat noise affected some behaviours of the tropical damselfish *Pomacentrus amboinensis* both inside and outside the nest during the breeding season; a critical life-history phase. While inside the nest, egg-tending males exposed to motorboat noise significantly increased the proportion of time spent on vigilance and tended to decrease the proportion of time spent fanning eggs, compared to their behaviour in ambient conditions. Outside the nest, males exposed to motorboat noise spent proportionally more time seeking refuge and devoted proportionally less time to interacting with a conspecific intruder compared to those in ambient conditions. Employing a change in motorboat driving practice effectively lowered noise-exposure levels to nesting males, and mitigated these effects on defensive behaviours.

In Experiment 1, we found a 34% increase in the rate of vigilance events, which corresponded with a 17% increase in the proportion of nest time spent on vigilance during the motorboat-noise exposure. Therefore, male *P. amboinensis* may be investing more time in vigilance, potentially at the expense of other parental-care behaviours when exposed to noise; a trade-off which has previously been considered in ambient conditions (Lissåker & Kvarnemo 2006). Empirical studies examining the interplay of sensory modalities (e.g., vision, olfaction, and hearing; Hartman & Abrahams 2000; Manassa *et al.* 2013) have suggested that a reduction in the efficacy of hearing may lead to sensory compensation, with complementary information obtained from other senses such as vision and olfaction (Nedelec *et al.* 2017b; McCormick *et al.* 2018). Thus, by increasing vigilance, males may be attempting to compensate for the potential masking of acoustic information regarding possible threats in the nest vicinity during motorboat disturbance (Holles *et al.* 2013; Radford *et al.* 2014). While vigilant, males may also be seeking to identify the source of the noise, may perceive the noise as a threat, or may be responding to a noise-induced change in community composition; vigilance can improve the latency of response to threats, such as egg predators or conspecific competitors (Krause J. & Godin J.G.J. 1996).

We also observed a trend of a 19% lower proportion of time spent on fanning the clutch during motorboat exposure. Frequent fanning of the clutch with the pectoral, caudal, and dorsal fins ventilate the eggs, which increases oxygen consumption and promotes development and survival (Zoran & Ward 1983; Green *et al.* 2006). Additionally, fanning is often accompanied by mouth-pecking at the clutch for the removal of damaged, diseased or dead eggs (Blumer 1982). Embryonic development has been shown to be compromised by noise exposure in the spiny chromis *Acanthochromis polyacanthus* (Fakan & McCormick 2019) and the sea hare *Stylocheilus striatus* (Nedelec *et al.* 2014), although the hatching success of captive daffodil cichlids *Neolamprologus pulcher* was unaffected by noise playback (Bruintjes & Radford 2014). Further evidence would be required to determine the potential impacts on development that could result from a reduction in egg fanning during noise exposure.

In Experiment 2, nest-guarding males spent a 22% lower proportion of time interacting with a conspecific intruder during the motorboat treatment compared to the ambient treatment. For demersal-spawning fishes, vulnerability to egg predation during development can have substantial consequences for overall embryo mortality (Emslie & Jones 2001). Furthermore, cannibalism by non-parental conspecifics has been observed in *P. amboinensis* and other species when there is intense competition for limited nest space and/or mates (Gross & MacMillan 1981; Nakazono *et al.* 1989; Emslie & Jones 2001; Pereira *et al.* 2017). Therefore, the observed decrease in interaction with a conspecific intruder could result in a higher risk of egg predation and non-parental cannibalism, ultimately impacting embryo mortality and reproductive success for the noise-exposed resident male.

The proportion of time males spent under shelter, including the artificial nest as well as natural shelters such as coral covers, was 154% higher during exposure to motorboat noise compared to ambient-sound conditions in Experiment 2. Similar increases in sheltering have been found for the red-mouthed goby *Gobius cruentatus* (Picciulin *et al.* 2010) and European sea bass *Dicentrarchus labrax* (Spiga *et al.* 2017). However, no changes in nest visitation were found in Experiment 1. The difference in outcomes of our two experiments may be due to an increase in sheltering outside of the nest only in Experiment 2, or simply a contextual response to the presence of an intruder (Figueira & Lyman 2007; Bruintjes & Radford 2013). Sheltering outside of the nest would reduce the time available for egg tending (Picciulin *et al.* 2010), potentially compounding the trend of decreased fanning found in the egg-tending experiment, and an increase in sheltering outside the nest would also reduce the time available to invest in defensive behaviours against egg predators or territory competitors (Lissåker & Kvarnemo 2006). This could increase the likelihood of territory takeover by a conspecific male, which would not only result in the loss of the current clutch but also the loss of the nest site, potentially affecting future reproductive opportunity (Magnhagen & Vestergaard 1991; Smith & Wootton

1995). However, given our findings from Experiment 1, it is possible that sheltered males are also remaining vigilant outside of the nest, for surveillance and maintenance of the territory, without direct interaction with an intruder.

The impacts of motorboat noise on *P. amboinensis* behaviour found in our two experiments could have arisen via three major mechanisms. First, noise can result in physiological stress (Simpson *et al.* 2014; Celi *et al.* 2016; Vazzana *et al.* 2017; Mills *et al.* 2020), which could alter decision-making processes or reduce cognitive performance, potentially resulting in negative reproductive outcomes (e.g., males resorting to filial cannibalism as a cost-effective way to gain energy; McCormick 2016). Second, noise may be a source of distraction that causes natural behaviours (e.g., defence from intruder or parental care) to be performed with reduced efficiency and/or causes important environmental and social cues and signals to be ignored (Chan *et al.* 2010; Purser & Radford 2011). Finally, if artificial noise in an environment occurs at similar frequencies to biologically important sounds, for example from egg-predators or conspecific intruders, masking can occur, inhibiting the ability of receivers to perceive vital acoustic information effectively (Vasconcelos *et al.* 2007; Holles *et al.* 2013; Pine *et al.* 2016).

The nest-defence behaviours of *P. amboinensis* in the mitigation treatment were not significantly different from the ambient treatment, including those behaviours affected by motorboat noise, demonstrating the value of our mitigation regime, and corroborating similar results in freshwater fish (MacLean *et al.* 2020). Adherence to a noise-conscientious motoring protocol considerably lowered root-mean-square levels and frequency power spectra in both acoustic domains (RMS levels of motorboat noise were ca. 4 times higher than mitigation noise) to match ambient-sound conditions more closely, as shown in the acoustic analyses (Fig. 2.1a and b; Table 2.1). Three recent studies conducted on the Great Barrier Reef (Jain-Schlaepfer *et al.* 2018; McCormick *et al.* 2018, 2019) successfully mitigated biological responses to motorboat noise in embryonic and juvenile reef fish using 4-stroke engines instead of 2-stroke engines (the former are comparatively quieter). Due to the high cost of switching engines, and potential reluctance from motorboat owners to invest to limit their noise output, alteration of driving practice may be a more viable alternative to mitigate biological effects of traffic noise in many places.

Our mitigation treatment combined changes to the motorboat speed and distance of the driving path from the reef into a zone-based strategy, which we believe would be easy to implement, however the relative importance of these separate factors in reducing behavioural impacts warrants further study. Vitally, our strategy reduced overall noise-exposure levels at the nests. Currently, there is enough evidence that anthropogenic noise harms marine life to prompt action and management (Shannon *et al.* 2016; Kunc & Schmidt 2019), and we strongly advocate the use of simple, accessible noise-mitigation measures that principally focus on reducing noise-exposure levels, such as presented here, to reduce the detrimental impacts of noise on wildlife.

2.6 Conclusion

Our results provide *in situ* experimental evidence that nesting behaviours of wild *P. amboinensis* can be detrimentally affected when exposed to motorboat noise, and therefore have the potential to impact offspring indirectly via impairment of the behaviours of the nest carer. These findings have implications for coral-reef communities globally due to the widespread use of small motorboats for tourism, recreation, and the exploitation of marine resources in these habitats. However, our study also demonstrates that, by altering motoring practice to reduce noise, policymakers, managers, and users can make noise-conscientious decisions to help lessen the harmful impacts of motorboat noise on marine life.

Chapter Three - SCUBA noise alters communities and cooperation at coral reef cleaning stations

Author contributions: K.P.M. was primarily responsible for designing the research, carrying out the fieldwork, analysing the data, and writing the manuscript. K.P.M. also independently analysed the acoustic data, extracted behavioural data from videos, and produced the data figures.

Collaborator contributions: A.N.R., B.M.T., D.A.E. and S.D.S. assisted with designing the research; A.R., G.C., and N.L. assisted with carrying out the fieldwork; A.N.R., E.W., B.M.T., D.A.E., and S.D.S. advised on data analysis; A.N.R., B.M.T., D.A.E., and S.D.S commented on drafts of the manuscript.

Acknowledgments: We thank the Operation Wallacea staff and volunteers (especially Alec Atherton and Lydia Woods) that enabled this project to be completed; the staff at Coral View Beach Resort & Dive Center for logistical support and accommodation during fieldwork; and Harry Harding and Lucille Chapuis for assistance with statistical and acoustic analyses. This work was supported by funding from Operation Wallacea, a University of Exeter Vice-Chancellor Scholarship for Postgraduate Research (to K.P.M.), and a Natural Environment Research Council Research Grant (NE/P001572/1 to S.D.S. and A.N.R.).

3.1 Abstract

Recreational SCUBA diving is growing in popularity on coral reefs worldwide. Diving equipment is inherently noisy and, by seeking out areas of high biodiversity, divers inadvertently expose reef communities to an intrusive source of anthropogenic noise. Currently, little is known about SCUBA noise as an acoustic stressor, and there is a general lack of empirical evidence on community-level impacts of anthropogenic noise on coral reefs. Here, we conducted a playback experiment on Caribbean reefs to investigate impacts of SCUBA noise on fish communities and interspecific cooperation at ecologically important cleaning stations of the Pederson's cleaner shrimp *Ancylomenes pedersoni*. When exposed to SCUBA-noise playback, the total occurrence of fishes at the cleaning stations decreased by 7%, and the community and clientele compositions were significantly altered. Compared with ambient-sound playback, SCUBA noise resulted in clients having to wait 29% longer for cleaning initiation and receiving 43% less cleaning. Our results are the first to demonstrate experimentally the impacts of SCUBA noise on reef organisms, confirming it as a stressor and pollutant. Moreover, by establishing acoustic disturbance as a likely mechanism for impacts of diver presence on reef animals, we also pinpoint a potential avenue for mitigation in these valuable ecosystems.

3.2 Introduction

SCUBA diving is a multibillion-dollar industry and is one of the largest and fastest growing recreational sports globally, with over 28 million certified divers and one million new divers being certified annually (Lück 2016; PADI 2021). Because divers seek out areas of high biodiversity, visibility rarely exceeds 30 m and many reef organisms are small, divers often move close to habitat and site-attached animals, meaning that this popular pastime can have negative impacts on coral reefs (Davenport & Davenport 2006). SCUBA divers can cause physical damage to reef habitat (Hawkins & Roberts 1993; Zakai & Chadwick-Furman 2002), but the mere presence of divers can also elicit stress and behavioural changes in marine mammals, fishes, and invertebrates, thus affecting aquatic communities and disrupting ecosystem services (Curtin & Garrod 2008; Lindfield *et al.* 2014; Titus *et* *al.* 2015a; Giglio *et al.* 2022). However, the mechanisms underpinning these detrimental diver-presence effects have not been established. Given that recreational diving equipment is inherently noisy and potentially detectable up to 200 m away (Lobel 2005; Radford *et al.* 2005), acoustic disturbance is a plausible but untested reason for organismal responses to diver presence.

Anthropogenic noise from a wide range of sources (e.g., pile-driving, sonar, shipping, motorboats) pervades almost all aquatic ecosystems (Duarte *et al.* 2021), with increasing evidence demonstrating a suite of negative impacts across many taxa (see reviews: Shannon *et al.* 2016; Cox *et al.* 2018; Kunc & Schmidt 2019; Duarte *et al.* 2021). However, most of the research to date focuses on how underwater noise affects individual animals; there has been little investigation of how noise effects scale up to affect multiple species and interspecific interactions (Kunc & Schmidt 2019). For example, only one aquatic study that we know of has considered community-level demographics (Nedelec *et al.* 2017a), and only a small handful of studies have demonstrated that noise can alter interspecific relationships among fishes, such as predator–prey interactions (Simpson *et al.* 2016; Ferrari *et al.* 2018) and cooperative mutualisms (Nedelec *et al.* 2017a).

While there is a paucity of investigations into community-level responses to noise in aquatic ecosystems, terrestrial anthropogenic noise (e.g., traffic noise near roads) has been shown to have a range of effects on avian communities, including to abundance, species richness and community structure (Francis *et al.* 2009; Slabbekoorn & Halfwerk 2009; Herrera-Montes & Aide 2011; Cooke *et al.* 2020b). That body of work includes experimental application of traffic noise (a ‘phantom road’) to a roadless landscape, identifying noise as the principal mechanism for the negative impacts of roads on avian populations and communities (McClure *et al.* 2013, 2017; Ware *et al.* 2015). Whilst early studies suggested overall population reductions in response to road traffic (Reijnen & Foppen 1994; Reijnen *et al.* 1995), more recent investigations show that community-level changes can be complex, and that species may respond differently to noise (Cooke *et al.* 2020b; Senzaki *et al.* 2020). Applying this foundational knowledge (i.e., acoustic stressors driving community-level responses) to aquatic ecosystems, noise might underpin previously documented impacts of diver presence on coral reefs. For example, the presence of divers has been shown to affect coral reef fishes (Benevides *et al.* 2019; Branconi *et al.* 2019; Giglio *et al.* 2022) and fish communities, including species-specific changes to diversity and abundance (Lindfield *et al.* 2014; Andradi-Brown *et al.* 2018); in these studies, SCUBA noise was highlighted as a potential contributing factor but was not evaluated experimentally in isolation.

To investigate impacts of SCUBA noise on coral reefs, we focused on ecologically important cleaning stations, considering potential changes to the local community composition and disruption to cooperative interactions between cleaners and clients. Mutualistic services play an integral part in the complex web of interactions that help maintain ecosystem health and function (Grutter *et al.* 2003; Clague *et al.* 2011; Waldie *et al.* 2011). On coral reefs, cleaning symbioses are classic interspecific mutualisms between cleaners, such as gobies, wrasse and shrimp, and a diverse range of client fishes (Grutter 1999; Becker & Grutter 2004; Vaughan *et al.* 2017). These complex and highly developed associations positively impact individual fish health and community-wide diversity (McCammon *et al.* 2010; Clague *et al.* 2011; Waldie *et al.* 2011). Furthermore, cleaner species are thought to influence movement patterns, habitat choice, activity, and local diversity and abundance of reef fishes (Grutter *et al.* 2003), and may also play a role in determining the distribution of territorial fishes (Whiteman *et al.* 2002). Typically, a cleaner species will occupy discrete microhabitats that serve as cleaning stations, which are visited by clients. During cleaning interactions, client fish will pose motionless, making them vulnerable to predation while cleaners inspect, remove, and ingest ectoparasites and dead tissue. Conversely, cleaner species often service clients that would otherwise be natural predators. Because cleaning imposes cost and potential risk to participants (Cheney & Côté 2001; Chapuis & Bshary 2009), involves multiple species that are likely to differ in their sensitivity to stressors (Vaughan *et al.* 2017), and is important for ecosystem function (Losey 1972), cleaning symbioses are ideal interactions for testing hypotheses about how anthropogenic stressors, such as noise, can have impacts beyond those to just individual species.

Here, we experimentally assessed the effects of SCUBA noise on the local community structure and cooperative interactions at the cleaning stations of a well-studied cleaner shrimp species, the Pederson's cleaner shrimp *Ancylomenes pedersoni* (Titus *et al.* 2015a, b, 2019). These obligate cleaners (i.e., species that clean throughout juvenile and/or adult life) typically inhabit corkscrew sea anemones *Bartholomea annulata* to form ecologically important cleaning stations that are visited by over 20 reef fish families (Huebner & Chadwick 2012; Titus *et al.* 2015b; Gilpin & Chadwick 2017; Huebner *et al.* 2019). These established locations facilitate observation of important interspecific mutualistic behaviours and allow experimental exposure of cleaners and clients to different acoustic treatments, to test for a mechanism underpinning previously documented impacts of diver presence on coral reef organisms. We conducted a playback experiment at *A. pedersoni* cleaning stations to evaluate the impacts of SCUBA noise on: 1) community structure near the stations, 2) clientele composition, and 3) interspecific behaviour during cleaning interactions.

3.3 Methods

3.3.1 Ethics statement

Experimental protocols were approved by the University of Exeter Animal Ethics Committee (Application, eCLESBio000295). This research was conducted under a research permit (ICF-508-2019) issued to Operation Wallacea by the Honduran government.

3.3.2 Experimental overview

We conducted a playback experiment at 40 *Ancylomenes pedersoni* cleaning stations on the Coral View reef (N 16° 05' 17.87" W 86° 54' 38.56"), on the Bay Island of Utila, Honduras, which is located at the southern end of the Mesoamerican Barrier Reef. This site has been visited regularly by snorkelers and SCUBA divers for more than 20 years (Titus *et al.* 2015a). Furthermore, Coral View reef is a fringing reef on the southern coast of the island that slopes from ca. 3 to 30 m depth and is considered a typical contemporary Caribbean reef in terms of oligotrophic nutrient conditions, percentage live coral cover, fish abundance and reef community structure

(Titus *et al.* 2019). On Caribbean reefs, Pederson's cleaner shrimps *Ancylomenes pedersoni* inhabit corkscrew sea anemones *Bartholomea annulata* to form mutualistic and ecological important cleaning stations. Reef fish use the sea anemones as visual cues to locate cleaning stations and engage in cleaning interactions with resident shrimp (Huebner & Chadwick 2012b; Gilpin & Chadwick 2017). Similarly, for research purposes, seeking *B. annulata* facilitates the finding and observing of these fixed-location cleaning stations. We located and monitored 40 *B. annulata* cleaning stations occupied by *A. pedersoni* at depths of 4–18 m. To avoid duplication, we tagged and mapped each station; stations were mapped in sections based on location relative to the entrance point of Coral View reef. We monitored cleaning activity and numbers of shrimp at these sections every 5–7 days.

At each station, we administered two noise treatments: playback of local reef soundscape (ambient sound) and playback of local reef soundscape with added noise from SCUBA (SCUBA noise), presented in a counterbalanced, repeated-measures design. By comparing responses to playback of local reef soundscape alone with those to local reef soundscape and SCUBA noise, we could isolate SCUBA noise as the experimental stressor, reducing confounding influences of the acoustic playback itself and/or electromagnetic interference from the loudspeakers. To avoid disturbance by observers, and to allow analysis of replicates while blind to the treatment, video cameras recorded the local fish community and cleaning activity during each deployment.

3.3.3 Playback tracks and sound analysis

Field recordings were made using a digital recorder (H6-BLACK field recorder, sampling rate 48 kHz; Zoom Corporation, Tokyo, Japan). This was connected to an omnidirectional hydrophone (HTI-96-MIN with inbuilt preamplifier, High Tech Inc., Gulfport MS; manufacturer calibrated sensitivity -164.3 dB re 1 V μPa-1; frequency range 0.2–30 kHz) to measure sound pressure, and to a triaxial accelerometer (M20-040: sensitivity following a curve over the frequency range 0–3 kHz; calibrated by manufacturers; Geospectrum Technologies, Dartmouth, Canada) to measure particle acceleration. Recordings were taken in sea states between 0 and 2 on the Beaufort scale and in the absence of rain, with recording equipment suspended approximately 1 m above the seabed from a submerged stand.

We made three 5-min daytime recordings of ambient coral reef sound and of open-circuit SCUBA noise at coral reefs, using both a hydrophone (for sound pressure) and an accelerometer (for particle acceleration). In each SCUBA-noise recording, a pair of divers approached the recorder, remained stationary approximately 1 m from the recorder for 4 min, and then swam away from the recorder to simulate a recreational visit to inspect/observe/photograph a cleaning station. We used the original field recordings to create experimental playback tracks for each 45-min trial using *Audacity 2.2.1* (http://audacity.sourceforge.net/). Three replicate tracks per treatment were constructed and used in rotation to minimise pseudoreplication. Each replicate used a different recording of ambient sound or SCUBA noise and was played on a loop. For the SCUBA-noise treatment, this resulted in six SCUBA disturbances per trial, at randomised intervals of 4±1 min (mean±SD). We re-recorded, analysed, and compared playback tracks to original recordings.

Recordings were analysed using *PAMGuide* (sound pressure; Merchant *et al.* 2015) and *paPAM* (particle acceleration; Nedelec *et al.* 2016a) in *MATLAB R2017b* across a frequency range of 1–2000 Hz, which is the auditory range relevant to coral reef fishes (Wright *et al.* 2011; Ladich & Fay 2013) and decapods (Popper *et al.* 2001; Roberts & Elliot. 2016). We calculated spectrograms, power spectral densities (PSD), root-mean-square levels (SPLrms and SALrms), and cumulative sound exposure levels (SELcum and AELcum) in both the sound-pressure and particle-acceleration domains. Calculations were made over batch-processed 30-s subsamples of the recordings (n=3 per recording-type) for each of the four recording-types (original ambient-sound recordings, ambient-sound playback tracks, original SCUBA-noise recordings, and SCUBA-noise playback tracks; Fig. 3.1, Fig. 3.2, and Table 3.1).

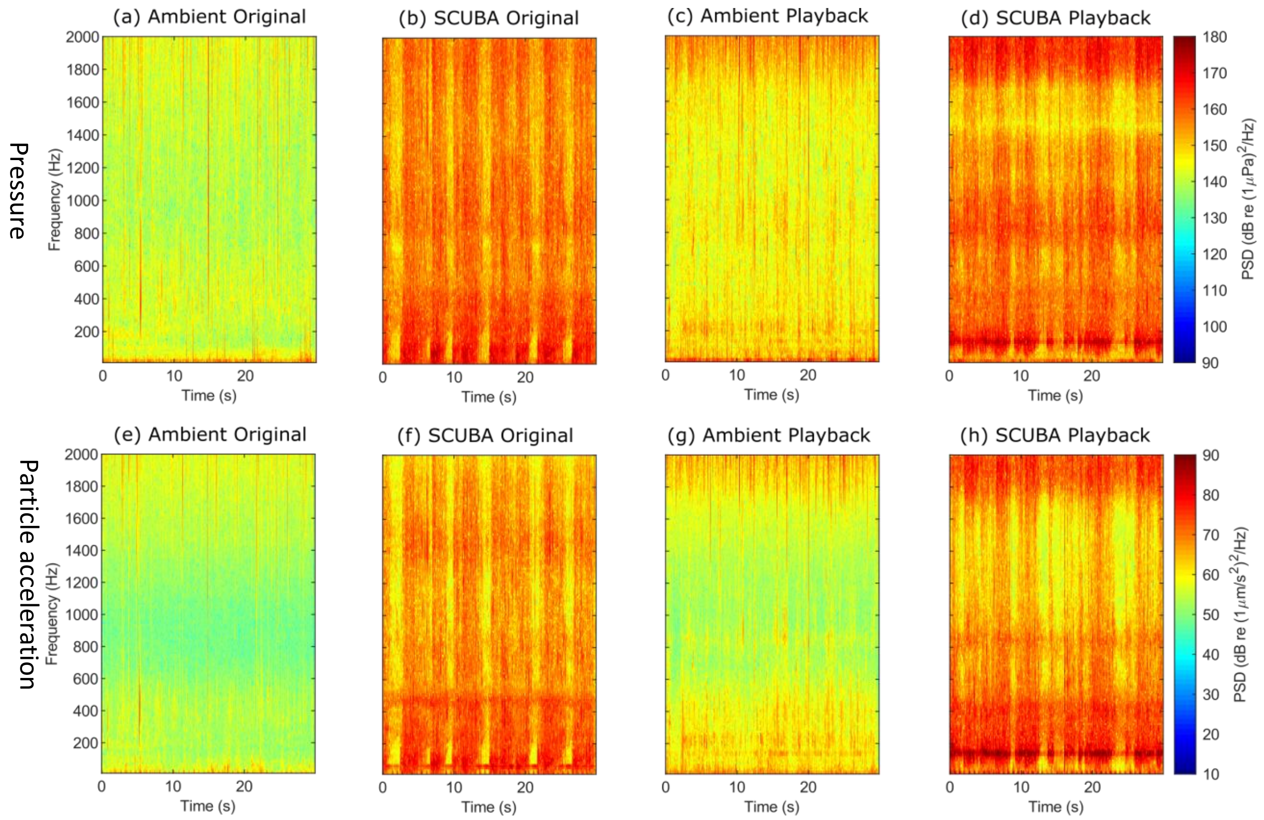

Figure 3.1. Spectrograms of sound-pressure (a–d) and triaxial particle-acceleration levels (e–h) *for original ambient-sound (a, e) and SCUBA-noise (b, f) recordings, and playback tracks for ambient-sound (c, g) and SCUBA-noise (d, h) treatments. For these comparisons, 30-s subsamples of one SCUBA-diving pair and one ambient recording were analysed (fft window length = 4048, Hamming filter, 75% overlap, 0–2 kHz).*

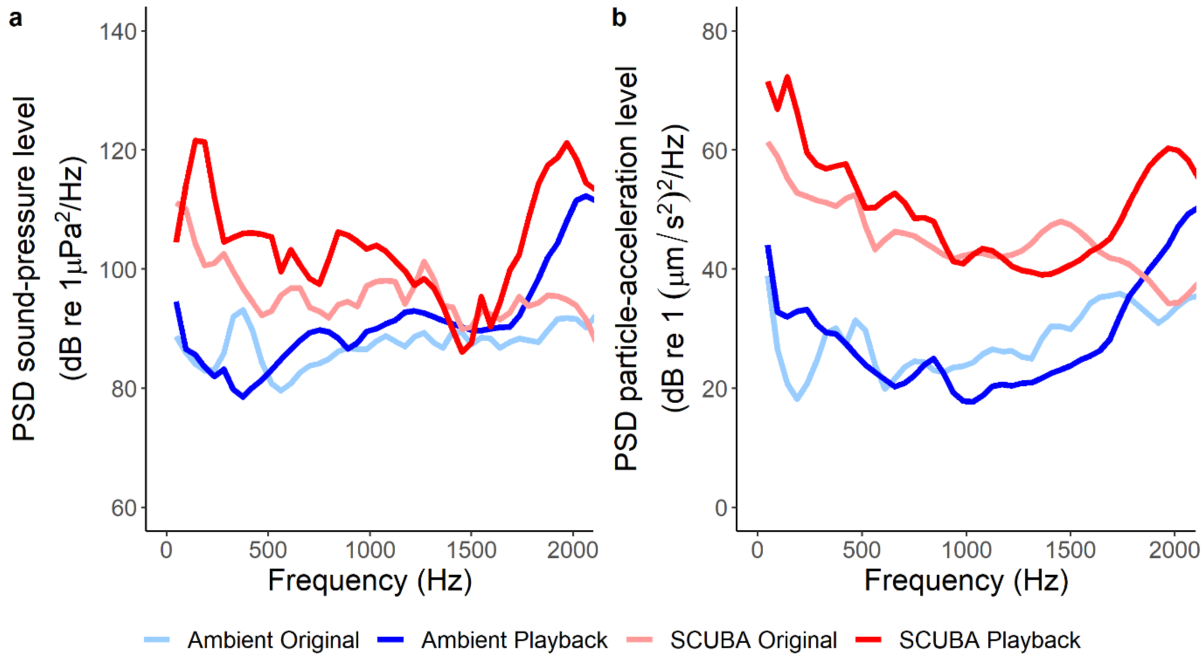

Figure 3.2. Mean power spectral densities (PSD) of the original ambient-sound recordings, ambient-sound playback tracks, original SCUBA-noise recordings and SCUBA-noise playback tracks *in terms of sound pressure (a) and particle acceleration (b), giving an average sound profile for each treatment (fft length = 1024, Hamming evaluation window, 50% window overlap, 1–2000 Hz).*

Table 3.1. Root-mean-square and cumulative sound-exposure levels *in both sound pressure (SPL_{rms} and SEL_{cum}) and triaxial particle acceleration (SAL_{rms} and AEL_{cum}) for each recording.*

Recording	**SPL_{rms} (dB re 1 μPa)**	**SEL_{cum} (dB re 1 μPa^2 s)**	**SAL_{rms} (dB re ($1 \mu m/s^2$))**	**AEL_{cum} (dB re $(1 \mu m/s^2)^2$ s)**
Ambient-sound original	100.1	119.7	94.8	110.5
Ambient-sound playback	112.4	131.9	98.5	113.8
SCUBA-noise original	115.4	135.0	105.7	118.5
SCUBA-noise playback	129.0	148.6	117.0	129.4

3.3.4 Experimental procedure

For experimental playbacks, we used underwater loudspeakers (University Sound UW-30; max output level 156 dB re 1 μPa at 1 m, frequency response 0.1–10 kHz; Lubell Labs) that were kept in position, ca. 0.5 m away and facing the focal cleaning station, using a custom-made stand (PVC piping with loudspeaker attached using elastic bungee cord). Loudspeakers were powered by an amplifier (M033N, 18 W, frequency response 0.40–20 kHz; Kemo Electronic GmbH), an MP3 player (SanDisk Clip Jam) and a battery (12v 12Ah sealed lead-acid) housed at the surface. For each trial, we also placed a GoPro Hero 5 camera at 1 m from the focal cleaning station.

Both acoustic treatments (ambient-sound and SCUBA-noise playback) were administered to a station on the same day (in counterbalanced order), and two stations were treated simultaneously (with random allocation of one station to each treatment order). Trials were completed between 0800 and 1300 h, with previous research showing that cleaning interactions at *A. pedersoni* stations on this same study reef do not change predictably throughout the day (Titus *et al.* 2015b).

Our study was designed to evaluate noise as a driving mechanism behind previously identified impacts of SCUBA diver presence on interspecific interactions at *A. pedersoni* cleaning stations, using the same study system at the same location (Titus *et al.* 2015a). The first 10 min of a trial consisted of silent playback to allow the local fish and resident *A. pedersoni* to resume normal behaviour following disturbance from placing equipment (Titus *et al.* 2015a; Nedelec *et al.* 2016b; Nanninga *et al.* 2017); this was double the acclimation period from the previous work on the study system, to ensure a return to pre-disturbance behaviour (Titus *et al.* 2015a). There followed the administration of each treatment (SCUBA noise and ambient sound) over two 45-min segments separated by a 10-min gap of silent playback between the first and second treatment. We video-recorded both treatments at 40 cleaning stations over 20 non-consecutive days.

All videos collected in the field were cropped using *ffmpeg 4.13* (ffmpeg.org). For each treatment, we cut 45-min segments and saved them with coded file names. Videos were watched with no sound so that the observer (K.P.M.) was blind to the acoustic condition. We scored community assessments and individual behaviours from the videos using the behavioural observation software *BORIS 7.6.1* (Friard & Gamba 2016).

3.3.5 Community-wide assessment and analysis

To test for impacts of SCUBA noise on the local community at *A. pedersoni* cleaning stations, we collected data on the frequency of fishes passing directly over the cleaning station and identified individual fish to species level during each trial. Analyses of the local fish communities were carried out for 39 of the possible 40 cleaning stations; one station was removed due to unintended interference by passing SCUBA divers. Similarly, we identified to species all fish cleaned by *A. pedersoni* (hereafter clientele) and limited assessment of clientele composition to stations where at least one clean was observed (n=22 stations). To analyse local community and clientele composition, we removed species with extremely low occurrences (<1% of total individuals; nine species from surrounding community: *A. Chirurgugs, A. coeruleus, C. capistratus, C. Striatus, E. diaphana, H. flavolineatum, L. jocu, S. tigrinus,* and *S. viride*; six species from clientele composition: *E. diaphana, H. flavolineatum, H. unicolor, L. Jocu, S. taeniopterus,* and *S. leucostictus*). Multivariate analyses were performed in *R V4.0.0* (R Core Team 2020) using the *Vegan 2.5-7* package (Oksanen *et al.* 2020), and univariate analyses were conducted using generalized linear mixed models (GLMMs) fitted with AICc selection using the *lme4 1.1-26* package (Bates *et al.* 2015). Levels of significance were determined for fixed effect terms via comparisons to null models without the term of interest. Test assumptions were checked by visualising and evaluating model residuals for normality, homogeneity of variance, collinearity and influence of outliers with Cook's distance.

We measured total fish occurrence, recorded as the total number of fish for each species observed in the videos. This video-based method precludes a complete assessment of abundance, because it is possible that the same fish can re-enter the frame of view and any fish out of frame cannot be counted, but it avoids disturbance caused by observers in the water. We used species ID and measures of occurrence to calculate species composition for each station, and assessed these with GLMMs using a Poisson distribution, with acoustic treatment and station as fixed and random factors respectively. Species assemblages were compared between ambient-sound and SCUBA-noise playback using unrestricted one-way nested PERMANOVA (maximum permutations=9999), with acoustic treatment as a fixed factor and cleaning station as a random factor. Variation in fish species assemblages between ambient-sound and SCUBA-noise treatments was visualised using non-metric multidimensional scaling (nMDS) based on a Bray-Curtis similarity matrix. Lastly, species-level variation between the two treatments was assessed in separate GLMMs with Poisson distributions. Our hypothesis tests were conducted across 15 species for local community analysis and eight for clientele analysis, after the removal of species with <1% occurrence, using False Discovery Rate (FDR) to correct for multiple test comparisons.

3.3.6 Cleaning behaviour assessment

To investigate the impact of SCUBA noise on interspecific interactions at cleaning stations, we collected data on several cooperative behaviours of *A. pedersoni* and their clients: time shrimp was visible within the camera view (i.e., ‘in-frame’), ‘antenna whipping’ by shrimp (hereafter signalling; Caves *et al.* 2018), fish ‘poses’ at the cleaning station (Titus *et al.* 2017; Caves *et al.* 2018), time to initiate a cleaning interaction (hereafter delay; Nedelec *et al.* 2017), cleaning rate and time, and cheating rates (Titus *et al.* 2019; Supplementary Table S2). First, we determined whether acoustic treatment (i.e., either SCUBA-noise or ambient-sound playback) affected the likelihood that each of signalling, posing, and cleaning occurred, using separate McNemar’s tests for paired binomial data from all 39 stations. For sites where cameras recorded at least one cleaning interaction in either treatment (n=22 stations; 113 cleaning interactions in total), we then determined whether acoustic treatment affects the rate (for counts) or activity-budget proportion (for durations) of each cleaning-related behaviour; paired t-tests or Wilcoxon signed-ranks tests were used, depending on whether the data met the assumptions for parametric testing. In some cases, behavioural measures are dependent on the occurrence of another behaviour and therefore only cleaning stations where the latter behaviour occurred were included in analyses. For example, cheating and cleaning delays are functions of cleaning interactions, and therefore analyses require that both treatments experienced at least one cleaning interaction (n=8). These considerations were made to ensure statistical robustness, emphasise biological context and relevance, and maintain confidence and conservativeness in the resulting conclusions.

Table 3.2. Ethogram for the recorded interspecific behaviours by A. pedersoni and client fishes.

Behaviour	Description	Variables
In-frame	Shrimp are visible within the view of the camera	Duration
Signalling	Shrimp vigorously waves or ‘whips’ antennae	Count
Poses	Client fish arrives within a body length of the station and remains motionless for a brief period; often accompanied by a flaring of the opercula and/or fins	Count, duration

Clean	Shrimp makes physical contact and begins to clean the client fish	Count, duration
Cheating	Client fish ‘jerks’ or ‘twitches’ during a clean	Count
Delay	Time between the client fish arriving and remaining motionless until the first shrimp makes visible contact	Duration

All data were analysed using *R V4.0.0 (*R Core Team 2020). Statistical significance was assumed where $p<0.05$. We also derived effect sizes for significant results using the *rstatix 0.6.0* package: Cohen’s d for t-tests and Wilcoxon’s effect size r for Wilcoxon tests (Kassambara 2020).

3.4 Results

3.4.1 Local fish community

Fishes passed over the cleaning stations at a mean±SE rate of 0.73±0.09 events per min during the 45-min trials. For the local fish community, there was no significant difference in species richness between acoustic treatments (GLMM: $X^2_1=0.24$, $p=0.62$). However, there was a 7% lower total occurrence of fishes during SCUBA-noise playback compared to the ambient-sound control ($X^2_1=4.23$, $p=0.04$; Fig. 3.1a), and the species composition of the local fish communities was significantly different between treatments (PERMANOVA: Pseudo-F=0.77, df=1, $p=0.03$, 9999 permutations; Fig. 3.1b). Three species were present significantly less during SCUBA-noise playback compared to ambient-sound playback (Fig. 3.2): 22% fewer bicolour damselfish *Stegastes partitus* (GLMM: $X^2_1=7.33$, FDR-adjusted $p=0.025$), 61% fewer cocoa damselfish *Stegastes varibilis* ($X^2_1=19.01$, FDR-adjusted $p<0.001$) and 80% fewer bluehead wrasse *Thalassoma bifasciatum* ($X^2_1=30.14$, FDR-adjusted $p<0.001$). Conversely, one species was present significantly more during SCUBA-noise playback: 259% more beaugregory *Stegastes leucostictus* ($X^2_1=26.34$, FDR-adjusted $p<0.001$; Fig. 2).

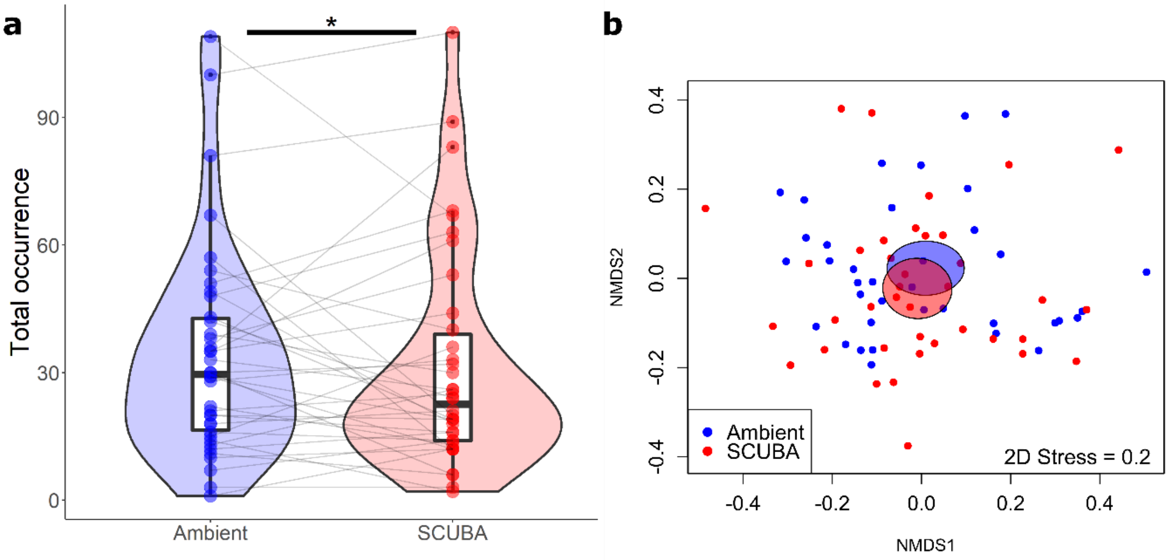

Figure 3.1. Community-level differences in total fish occurrence between the two acoustic treatments (playback of ambient sound or SCUBA noise). *(a) Total fish occurrence. Boxes show median and interquartile range; violin plots show the kernel probability density of the data at different values; coloured points show treatment responses; grey lines indicated paired data from stations across the two treatments. *p<0.05. N=39 cleaning stations. (b) Nonmetric multidimensional scaling (nMDS) ordination showing variation in fish community. Individual dots show replicates at cleaning stations (n=39); shaded ellipses represent the standard error of the weighted average for each treatment.*

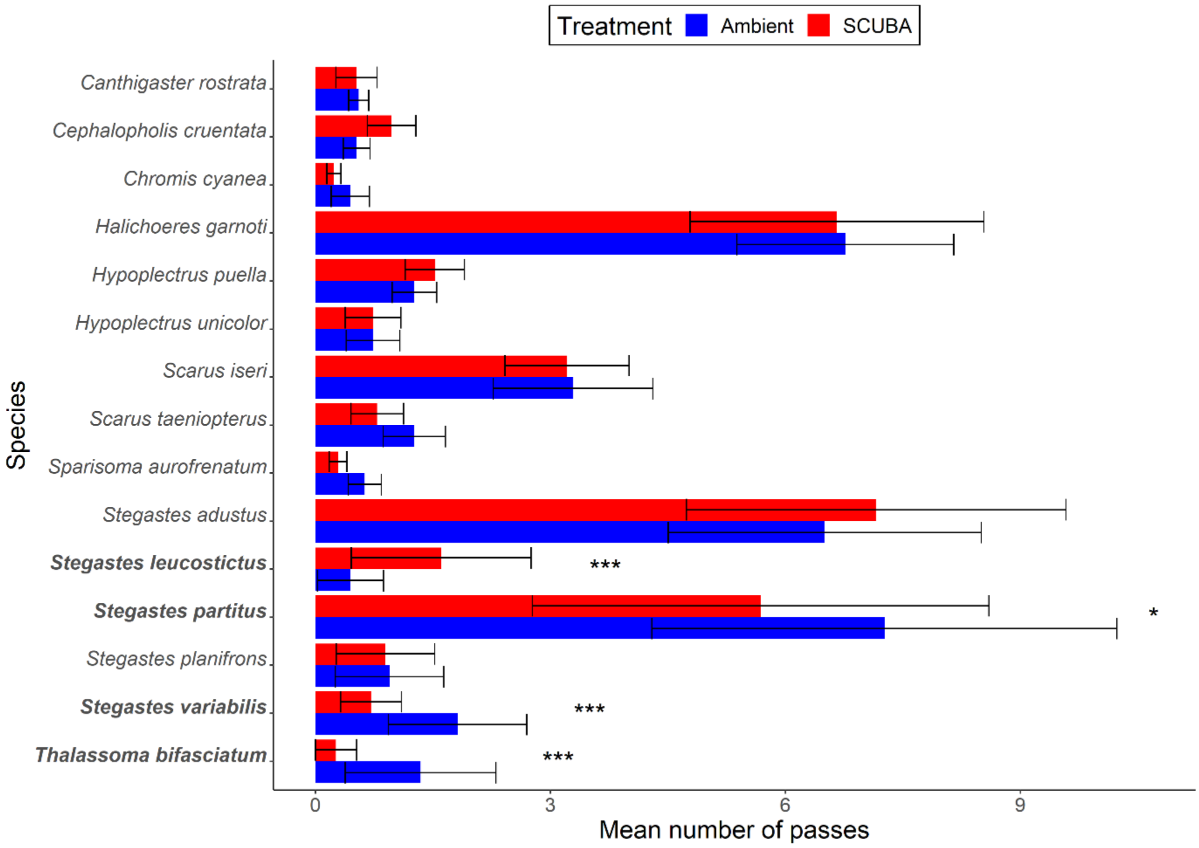

Figure 3.2. Occurrence of fish species in the surrounding community during the acoustic treatments (playback of ambient sound or SCUBA noise). *Shown are mean±SE number of passes by fishes for those species above the occurrence threshold (>1%). * p<0.05, *** p<0001. N=39 cleaning stations.*

3.4.2 Clientele community

There was no significant difference between treatments in the overall composition of clientele at cleaning stations (PERMANOVA: Pseudo-F=0.16, df=1, *p*=0.90, 9999 permutations). However, two species were present significantly less during SCUBA-noise playback compared to ambient-sound control (Fig. 3.3): 89% fewer Caribbean sharp-nose puffer *Canthigaster rostrata* (GLMM: X^2_1=7.36, FDR-adjusted *p*=0.034) and 71% fewer dusky damselfish *Stegastes adustus* (X^2_1=6.92, FDR-adjusted *p*=0.034).

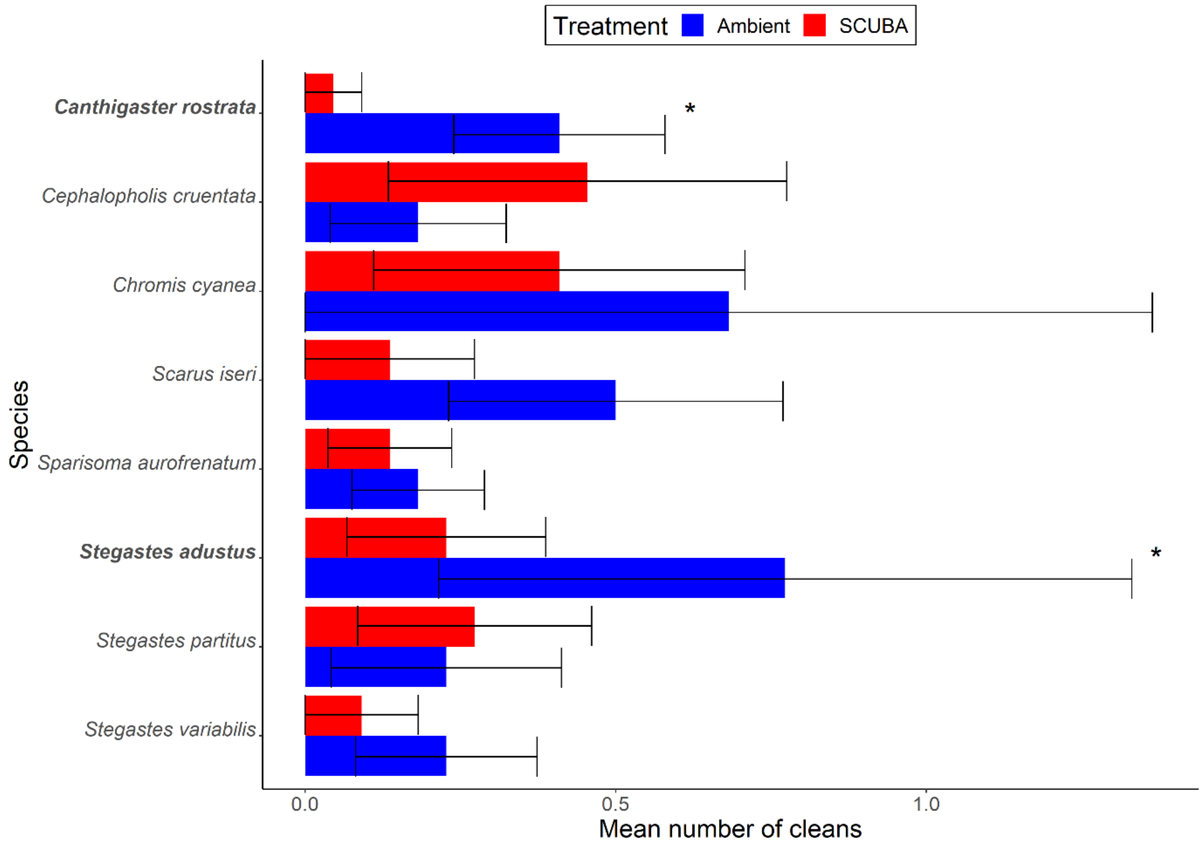

Figure 3.3. Client occurrences, identified to species level, during the two acoustic treatments (playback of ambient sound or SCUBA noise). *Shown are mean±SE number of cleans of fishes for species above the occurrence threshold (>1%). * p<0.05. N=39 cleaning stations.*

3.4.3 Cleaning behaviour

There were no significant difference between the two acoustic treatments (SCUBA-noise and ambient-sound playback) in the likelihood of the four cleaning-related behaviours to occur: signalling by *A. pedersoni* (McNemar's test: X^2_1=1.13, *p*=0.29, *n*=39 pairs), poses by client fishes (X^2_1=0, *p*=1, *n*=39 pairs), nor cleaning interactions between *A. pedersoni* and clients (X^2_1=1.79, *p*=0.18, *n*=39 pairs).

There was no significant difference between the two acoustic treatments in the total time that *A. pedersoni* spent in-frame at the focal cleaning stations (mean±SE: 43±1 min; Wilcoxon test: V_{22}=128, *p*=0.98). There was also no significant treatment difference in the signalling rate by *A. pedersoni* (23.9±0.5 events per hour for time spent within view; V_{22}=161, *p*=0.28), nor any significant difference between the two treatments in posing behaviour by client fishes: posing rate (4.9±0.1 events per hour; V_{22}=110, *p*=0.56), total posing time (60±3.8 s; $V_{22}V_{39}$=119, *p*=0.82).

Acoustic treatment did significantly affect the delay to initiate cleaning when a client fish arrived at the station (mean±SE: 1.9±0.5 s; Wilcoxon test: V_8=0, *p*=0.008, *d*=0.89); delay times were 29% greater when there was SCUBA noise compared to ambient sound (Fig. 4a). Acoustic treatment also significantly affected the cleaning rate of *A. pedersoni* (3.4±0.1 events per hour; V_{22}=151, *p*=0.02, *d*=0.52), with a 43% lower cleaning rate in the SCUBA-noise treatment compared to the ambient-sound control. There was, however, no significant treatment difference in either the average clean time (7.4±1.5 s; V_{22}=127, *p*=0.70) or the rate of cheating by *A. pedersoni* (2.92±1.06 events per min of cleaning; V_8=3, *p*=0.08).

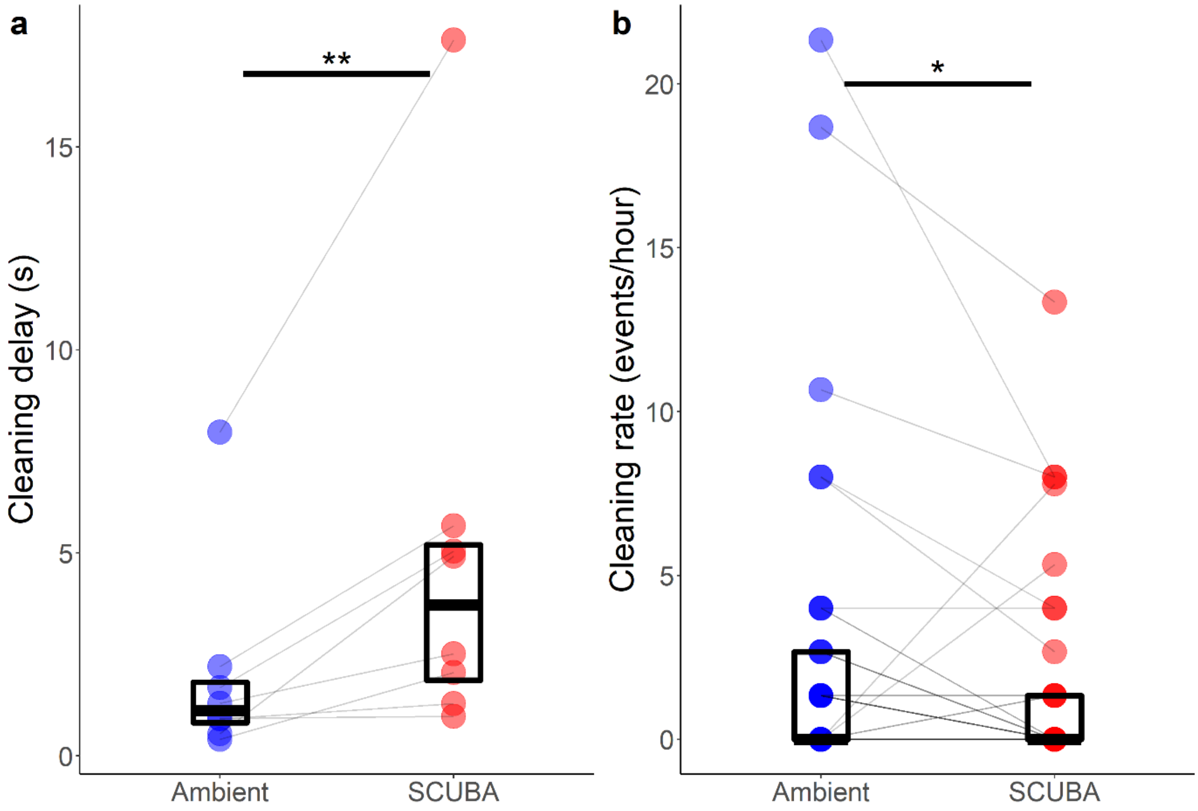

Figure 3.4. Difference in A. pedersoni (a) delay to initiate cleaning, and (b) cleaning rate between the two acoustic treatments (playback of ambient sound or SCUBA noise). *Boxes show median and interquartile range; coloured points show data from individual cleaning stations; grey lines indicate paired data from the same cleaning station in the two treatments. *p<0.05, ** p<0.01. N=8 cleaning stations for (a); and n=22 cleaning stations for (b).*

3.5 Discussion

Our findings suggest that noise generated by open-circuit SCUBA diving can negatively impact Caribbean coral reef communities. Specifically, we found that SCUBA-noise playback altered community composition around cleaning stations, and negatively affected cleaning interactions between the common Caribbean cleaner-shrimp species *Ancylomenes pedersoni* and client fishes. At the community level, the prevalence of four common Caribbean reef-fish species differed when exposed to SCUBA-noise playback compared to ambient-sound playback, with changes in the occurrence of these species driving changes in overall fish community composition between the two acoustic treatments. However, these responses were not uniform, with three species showing a reduction in occurrence during SCUBA noise, but one species showing an increase. Additionally, our results showed altered clientele composition of fishes cleaned by *A. pedersoni*, with two fish species being cleaned less during the SCUBA-noise treatment. Regarding individual cleaning behaviour, SCUBA-noise playback resulted in longer delays in cleaning initiation and reduced the number of cleaning interactions between *A. pedersoni* and client fishes. To our knowledge, this is the first demonstration of the impacts of SCUBA noise on coral reef communities and interspecific interactions, highlighting SCUBA noise as a potentially harmful stressor in coral reef ecosystems.

When exposed to SCUBA-noise playback, the occurrence of fishes near *A. pedersoni* cleaning stations was 7% lower and the overall community composition of fishes was significantly altered. These results mirror those from terrestrial studies where longer-term experimental playback of traffic noise along ‘phantom roads’ reduced overall bird abundance and altered community structures (McClure *et al.* 2013, 2017). The observed interspecific variation in noise effects is not surprising given that species differ in, for example, ecology (Kunc & Schmidt 2019), life history (de Jong *et al.* 2020), prior exposure (Harding *et al.* 2018), hearing ability (Popper & Hawkins 2019) and vocal behaviour (Radford *et al.* 2014), all of which may influence their responses to noise. For instance, noise can induce physiological stress (Wale *et al.* 2013; Celi *et al.* 2016; Mills *et al.* 2020), which may subsequently alter decision-making processes and behaviour during disturbance (Purser & Radford

2011; Voellmy *et al.* 2014a), but species differ considerably in their susceptibility to stress (Pottinger 2010). Furthermore, because anthropogenic noise has the potential to mask acoustic cues and signals, soniferous species, such as damselfish, may be particularly vulnerable to noise disturbance (Radford *et al.* 2014; Weilgart 2018). Interspecific variation in noise effects may also arise through knock-on consequences. We found that three of four species affected by SCUBA noise were members of the same damselfish genus, *Stegastes*: two species (*S. partitus* and *S. variables*) occurred less during SCUBA-noise playback, while a third species (*S. leucostictus*) occurred more. It is possible that *S. partitus* and *S. variables* moved away, sought refuge more or exhibited less territorial behaviour (Benevides *et al.* 2019) during SCUBA-noise playback, which, in turn, created an opportunity through competitor release for *S. leucostictus* to encroach on territories and resources (Robertson 1996).

Our finding that SCUBA-noise playback altered cleaning interactions between the cleaner shrimp *A. pedersoni* and its clients, with a 29% longer delay to initiate cleaning and a 43% lower cleaning rate compared to the ambient-sound control, may be due to distraction (Chan *et al.* 2010) or stress (Pottinger 2010; Wale *et al.* 2013; Mills *et al.* 2020) in cleaners and/or clients. Either way, the results establish acoustic disturbance as a potential mechanism for the previously documented impacts of diver presence on cleaning by *A. pedersoni* (Titus *et al.* 2015a), and are in line with work showing that motorboat-noise playback can disrupt mutualistic cleaning behaviour by the Indo-Pacific bluestreak cleaner wrasse *Labroides dimidiatus* (Nedelec *et al.* 2017a). A decrease in cleaning activity suggests a trade-off, with avoidance of the potential risk and/or cost associated with SCUBA noise occurring at the expense of parasite removal for client fishes and dietary intake for *A. pedersoni* (Cheney & Côté 2001). While not assessed here, noise negatively affects physiology (Wale *et al.* 2013; Filiciotto *et al.* 2014), behaviour (Nousek-McGregor & Mei 2016; Solan *et al.* 2016; Filiciotto *et al.* 2014, 2016), and stress-related biochemical regulation (Celi *et al.* 2015; Filiciotto *et al.* 2016) in crustaceans, and therefore may be similarly affecting *A. pedersoni.* For clients, cleaning symbioses improve fitness (Grutter 1999; Becker & Grutter 2004); therefore, SCUBA noise could lead to a negative impact on the reproductive success and longevity of clients that lose out on cleaning opportunities. Where cleaning stations fail altogether, reef communities can be affected in the form of reduced abundance and species richness, lower growth rates and survivorship, and diminished larval recruitment (Waldie *et al.* 2011).

Care is needed when extrapolating results from short-term noise experiments to fitness consequences, given that there can be increased tolerance and/or habituation, and compensation during quieter periods (Nedelec *et al.* 2016b; Radford *et al.* 2016b). However, popular dive sites can receive multiple visits per day, which may equally result in cumulative noise effects. Similar caution is advised about assuming lasting community-level impacts from short-term experiments, although longer-term terrestrial studies have revealed sustained changes in the composition and interactions of species in noisy areas (Francis *et al.* 2009; Slabbekoorn & Halfwerk 2009; Barber *et al.* 2010). Ultimately, extended experimental tests are needed in aquatic ecosystems if we are to understand the full impact of noise pollution.

While our study identifies SCUBA noise as a stressor to coral reef inhabitants, it also suggests a potential avenue for mitigating the impact of SCUBA diving. Managing acoustic disturbance has the potential to reduce the broad-ranging effects of divers on coral reef ecosystems (Lindfield *et al.* 2014; Titus *et al.* 2015a; Andradi-Brown *et al.* 2018; Benevides *et al.* 2019), without requiring a reduction or cessation of diving activity or the widespread uptake of expensive closed-circuit rebreathers. Instead, divers and the dive industry can adopt simple alterations to dive protocols that reduce the amount of noise exposure to coral reefs, which is a mitigation strategy that has been shown to negate biological responses to other sources of noise (Jain-Schlaepfer *et al.* 2018; McCormick *et al.* 2018, 2019; McCloskey *et al.* 2020). For example, increasing the distance between a source and the vulnerable site has been shown to be an effective means of reducing the amount of noise exposure to wildlife, alleviating noise-induced behavioural responses (MacLean *et al.* 2020; McCloskey *et al.* 2020). Furthermore, tourism and dive operators might consider rotating and/or including more dive sites to avoid concentrating noise exposure and disturbance to a few locations. This concept of managing noise exposure to protect wildlife has been successfully implemented and enforced to safeguard at-risk marine mammal populations, including the critically endangered southern resident killer whale *Orcinus orca* (Williams *et al.* 2019). We believe that similar practices can be, and should be, adopted to mitigate the negative impacts of anthropogenic noise on coral reef habitats, especially given that coral reefs are areas of high biodiversity (Roberts *et al.* 2002), provide nutrition and livelihoods for millions of people (Cinner 2014), and have high socio-economic importance and value (de Groot *et al.* 2012).

Chapter Four - Predicting the impacts of anthropogenic noise on fisheries for European sea bass *Dicentrarchus labrax* using a spatially explicit and bioenergetic individual-based model

Author contributions: K.P.M. was primarily responsible for establishing the collaboration, designing the research, updating the model code, carrying out simulations, analysing the data, and writing the manuscript.

Collaborator contributions: K.H. helped to develop the initial idea for the project and to setup the collaboration; N.M., R.S., K.H., A.N.R, and S.D.S assisted with designing the research; J.W., N.W., R.B., R.S., and K.H. developed previous versions of the model and provided model code and input files; A.F. and N.M. developed and provided the acoustic maps; J.W., N.W., and R.B. provided code for simulation and analysis and assisted with code writing; J.W., R.S., A.N.R, and S.D.S commented on drafts of the manuscript.

Acknowledgements: Thank you to Steven Railsback and Volker Grimm for providing feedback on the design concept, model testing, and documentation (TRACE) for this work, and for technical training. Thank you to Physalia Courses for hosting a training workshop, organised by K.P.M. This work was supported by funding from a University of Exeter Vice-Chancellor Scholarship for Postgraduate Research (to K.P.M.), and a Natural Environment Research Council Research Grant (NE/P001572/1 to S.D.S. and A.N.R.).

4.1. *Abstract*

Sublethal stressors that affect fish populations, such as anthropogenic noise, can have significant implications for fitness, but are often difficult to observe and quantify. Population modelling offers a complementary approach to empirical data collection, allowing further assessment of how the impacts of sublethal stressors on individuals may translate to population-level consequences for fishes. A population consequences of acoustic disturbance (PCAD) framework has enabled the assessment of how stressors influence ecologically relevant life processes of fish; while individual-based models (IBMs) are simulations of individual ‘agents’ of organisms that interact with each other and their environment and have been shown to be useful investigative tools for predicting changes to population dynamics and management. Here, we have successfully updated a spatially explicit and bioenergetic IBM for European sea bass *Dicentrarchus labrax* by incorporating realistic projections of anthropogenic noise levels in the Northeast Atlantic and pathways for the impacts of noise on individuals. In doing so, our model considers the impacts of noise to ecologically relevant life processes under a range of anthropogenic noise disturbance across a large geographic range. Essentially, we combine PCAD and IBM frameworks and can thus assess subsequent population-level changes of different noise scenarios. The model described is not intended to replace existing experimental approaches, but instead presents a simple, approachable method to assess the unknown impacts of anthropogenic noise to fish populations and may even be used to aid development of viable noise-mitigation approaches.

4.2. *Introduction*

Aquatic ecosystems and their fish populations face a multitude of threats and stressors that are ultimately driven by the growth of human populations (Gordon *et al.* 2018; Reid *et al.* 2019). Stressors that affect fishes can be direct (e.g., habitat loss and overexploitation), with impacts ranging from mortality through to life-history changes for populations, and/or indirect (e.g., chemical and noise pollution), whereby alterations in behaviour and physiology can have significant consequences for fitness (Gordon *et al.* 2018). The latter, also termed sublethal stressors, are often difficult to observe and quantify, especially when concerning impacts at the population level. For example, laboratory studies are often restricted by facility/tank capacity; while sample sizes in the field are similarly limited by the ability to recapture tagged individuals and usually require stressful handling/tagging procedures that may mask impacts of sublethal stressors. Population modelling offers a complementary approach to shed light on how sublethal stressors may translate to population-level consequences for fishes (Watson *et al.* 2020).

Anthropogenic noise is now recognised as a global pollutant that pervades almost all aquatic ecosystems (Duarte *et al.* 2021). Whether noise is generated intentionally or inadvertently, activities that contribute to elevated noise levels, including urbanisation, transportation, and resource extraction, are expected to increase along with human population growth (Jerem & Mathews 2020). Empirical evidence shows that noise, as a sublethal stressor, predominately impairs hearing, increases stress, reduces foraging ability, increases predation risk, impacts movement, and hinders reproductive success in fishes (Slabbekoorn *et al.* 2010; Shannon *et al.* 2016; Cox *et al.* 2018). However, while this growing body of research describes numerous consequences of noise exposure for individuals, it remains challenging to identify trends in response patterns (e.g., trends in reproductive responses to in fishes, as reviewed by de Jong *et al.* 2020), and even more difficult to translate effects on individuals into population-level consequences (Slabbekoorn *et al.* 2019; Mortensen *et al.* 2021). While modelling can be an important tool to bridge this gap between individual and population-level responses, there are only a few models dedicated to noise impacts, and even fewer concerning fishes (Mortensen *et al.* 2021).

The task of translating the effects of noise on individuals into consequences for populations has recently become more prominent due to the development of a population consequences of acoustic disturbance (PCAD) framework (National Research Council 2005). Originally established as an indicator of population decline in marine mammals, this stepwise approach translates behavioural and physiological responses of individuals into changes in vital rates, such as reproduction, mortality, and growth, to estimate the overall population-level dynamics (Pirotta *et al.* 2018;

Slabbekoorn *et al.* 2019). In marine mammals, PCAD has successfully been used to forecast population-level responses to noise pollution in a variety of contexts (King *et al.* 2015; Van Beest *et al.* 2017; Nabe-Nielsen *et al.* 2018). By contrast, only one application of PCAD has been carried out regarding fish; this showed that population growth rates were particularly sensitive to the effects of noise on energy expenditure and food intake (Soudijn *et al.* 2020). Consequently, the authors concluded that the sublethal effects of anthropogenic noise may affect fish populations more than lethal effects (Soudijn *et al.* 2020). While this study and other PCAD models are important tools for understanding changes to population-level dynamics, they lack spatial context that other modelling frameworks (e.g., individual-based modelling) can incorporate, which leaves a potential gap between changes in individual behaviour, population-level impacts, and the subsequent number of affected individuals (Mortensen *et al.* 2021).

The spatiotemporal components of individual-based modelling (IBM) can incorporate range and variation in noise disturbance experienced at the individual level, thus allowing for improved assessment of cumulative impact and population effects (Mortensen *et al.* 2021). Generally, IBM uses a bottom-up approach to simulate a population of discreet individuals where a combination of individual state and environmental variables change individual behaviour (DeAngelis & Grimm 2014). Therefore, individuals in an IBM react to stressors uniquely, and responses are dependent on, among many other things, their energy reserves, life stage, size, and proximity to the stressor. Subsequently, the proportion of individuals within a population that are affected, and the length and severity of those impacts on important life processes, determine the overall population-level impacts of a stressor (Grimm & Railsback 2005). Ultimately, population dynamics are not approached from a statistical interpretation of observations but emerge from simulated interactions between individuals and adapt to context and environment (Railsback & Grimm 2019). Thus, population-level predictions from IBM can be considered more realistic and are more likely to maintain predictive power in a variety of contexts and environments than population projections computed from more traditional modelling methods (Mortensen *et al.* 2021). While a handful of studies have successfully used IBM to explore the impacts of anthropogenic noise disturbance on marine organisms, only two studies are related to fish species (Rossington *et al.* 2013; Heinänen *et al.*

2018). A recent review, highlighting the similarities and differences of these previous IBM applications found spatial distribution and impacts on movement patterns to be the most common investigative drivers (Mortensen *et al.* 2021). Furthermore, the authors described spatial distributions and changes in movement characteristics and behaviour as the first stage of a combined PCAD/IBM framework (Mortensen *et al.* 2021). The subsequent stages of the combined model refer to the translation of affected life functions (second stage) into long-term age-specific vital rates (third stage), which have been quantified for marine mammals (Van Beest *et al.* 2017; Nabe-Nielsen *et al.* 2018) but not for fishes (Slabbekoorn *et al.* 2019; Mortensen *et al.* 2021).

Here, we present a combination of the PCAD and IBM frameworks in a single model intended to explore the population-level consequences of vessel noise in U.K. waters on a modelled population of European sea bass *Dicentrarchus labrax*. Our reason for developing this model is twofold. First, vessel traffic, and global shipping in particular, is thought to be a leading contributor of noise to our oceans (e.g., 32-fold increase in low-frequency noise along major shipping routes; Malakoff 2010; Duarte *et al.* 2021). The low-frequency sounds emanating from vessels propagate easily underwater and attenuate slowly over large distances (Urick 1975; Sertlek *et al.* 2019). Therefore, we can accurately project and map distributions of anthropogenic noise levels across large geographical ranges using validated satellite Automatic Identification System (sAIS) ship-tracking data, which has successfully been done for the Northeast Atlantic (Farcas *et al.* 2020). Second, European sea bass is an important target species, for both commercial and recreational fisheries, that is well-studied and known to respond behaviourally and physiologically to anthropogenic noise (Debusschere *et al.* 2014; Radford *et al.* 2016; Kastelein *et al.* 2017). Importantly, there exist spatially explicit models for sea bass that were developed to explore management strategies (Walker *et al.* 2020) and the impacts of sublethal stressors (Watson *et al.* 2020, 2022) on the northern stock population.

Specifically, we propose and evaluate a modelling approach where we have introduced validated projections of vessel-noise levels in the Northeast Atlantic (Farcas *et al.* 2020) to a spatially explicit, bioenergetic model of the northern stock of sea bass (Walker *et al.* 2020; Watson *et al.* 2022). To drive the responses of individuals to noise, we have imposed similar noise-effect pathways to those implemented by Soudijn *et al.* (2020) that were modelled after results from a meta-analysis by Cox *et al.* (2018). These four noise-effect pathways include changes in ingestion, energy use, mortality, and reproduction (Cox *et al.* 2018; Soudijn *et al.* 2020). Ultimately, this modelling application, which combines PCAD and IBM frameworks, will improve our understanding of the population-level responses of fishes to realistic range of anthropogenic noise levels and disturbance. While a handful of previous models have used PCAD/IBM to simulate responses to anthropogenic noise (Mortensen *et al.* 2021), our model is the first to simulate the complex process- and context-dependent consequences of noise for a population of fish in response to high-resolution, realistic noise maps across a large geographic range.

4.3. *Methods*

4.3.1. The model

We developed an IBM to evaluate the impact of noise on sea bass populations in the Northeast Atlantic. Here we provide a summary description of the IBM; a full description following the ODD (Overview, Design concepts, Details) protocol for individual- and agent-based models (Grimm *et al.* 2020) is provided in the TRACE (TRAnsparent and Comprehensive Ecological modelling documentation; Grimm *et al.* 2014) document (Appendix A). The model version presented here develops the approach of Walker *et al.* (2020) and Watson *et al.* (2022) to include validated noise maps for the Northeast Atlantic (Farcas *et al.* 2020) and noise-effect pathways for individual fish (Soudijn *et al.* 2020).

The IBM was implemented in *NetLogo 5.3.1* (Wilensky 1999). Subsequent simulations, support code and analysis were implemented in *RStudio V1.3.1093* using the *RNetLogo V1.0-4* extension and the *parallel V3.6.2* extension to improve task processing.

4.3.2. Overview

The model environment is composed of a grid landscape of 36 x 38 grid cells (hereto patches), which represent a geographical area from 9°E to 9°W and 48°N to 57.5°N (Fig. B.1). Patches consist of dynamic variables of sea surface temperature (SST; Fig. B.1a) and phytoplankton density (PHY; Fig. B.1b; Watson *et al.* 2022). Furthermore, patches are categorised depending on location and context. For example, 'coastal' patches are those that intersect with land and 'offshore' patches are all remaining sea patches. Moreover, between February and May, any offshore patches south of 54°N with an SST value between 9 and 15°C are designated as 'spawning' patches (Thompson & Harrop 1987), and 'nursery' patches are those south of 54°N that intersect with land (Kelley 1988; Beraud *et al.* 2018). Lastly, patches are assigned ICES designations, which are used for the gridding of data to make simplified analysis and visualisation (i.e., 4.b., 4.c., 7.a., 7.d., 7.e., or 7.f.; see https://www.ices.dk/data/maps/Pages/ICES-statistical-rectangles.aspx), and region (i.e., North Sea, English Channel, Celtic Sea, or Irish Sea). Consequently, ICES divisions and regions are mutually exclusive while patch types are not (i.e., all nursery patches are coastal, and all spawning patches are offshore).

To facilitate computing and reduce model run times, the sea bass population is modelled with super-individuals (hereafter termed individuals), each of which represents many fish—in this case, thousands—with identical state variables (Scheffer *et al.* 1995). These individual state variables include: the number of fish they represent, age, life stage, length, weight (including structural, gonadal and total masses), ingested energy, energy reserves, metabolic rate, location, swimming speed and daily directional changes, spawning trigger and counter (see section 4.3.4 of this chapter), mortality rates (natural, commercial, inshore/offshore fishing and recreational-fishing mortality) and the ICES division they have an affinity to feed in (Watson *et al.* 2022). After an initial spin up (1985–2004), the model runs in daily time steps from the 1st of January 2004 to the 31st of December 2014, just prior to emergency management measures in 2015, including restrictions on the amount of catch (i.e., daily bag limits on the number of fish taken per recreational fisher and monthly catch limits for commercial vessels), as well as spatial restrictions such as closed seasons and areas (Walker *et al.* 2020; ICES 2021). In each daily time step, individuals follow six main processes constructed from several sub-models: ingestion, metabolic rate, growth, reproduction, movement, and mortality. For simplicity, the population is closed to migration outside the model domain (Watson *et al.* 2022).

4.3.3. Initialisation and spin up

The model follows the same schedule and timespan as previous iterations (Walker *et al.* 2020; Watson *et al.* 2022), which includes initialisation on the 1st of January 1985 and daily time steps for a 19-year spin-up period. During the spin up, numbers-at-age data from the ICES stock assessment 2020 are used to condition the initialised population, as well as new agents introduced each subsequent year. The weekly remote sensing data for SST and PHY for 2004 are used on repeat for each year in the spin up, as they were unavailable prior to this date. Following the spin up, emergent model results are collected from the 1st of January 2004 until the 31st of December 2014, just prior to the implementation of emergency management measures in 2015 (Walker *et al.* 2020; ICES 2021; Watson *et al.* 2022).

4.3.4. Noise maps and responses by individuals to noise

Ocean noise maps were produced using data on noise sources (acoustic source spectrum level and location at each time increment) and the sound propagation properties of the environment, and predictions were validated against field measurements (Farcas *et al.* 2020; Fig. B.6). Specifically, annual median broadband (63–4000 Hz) noise levels (P50) were produced for the extent of available sAIS data for 2017 in the Northeast Atlantic (Farcas *et al.* 2020). These noise maps are implemented into the model as dynamic patch variables (Fig. B.1c) and are updated during each daily timestep following similar procedures to SST and PHY (updated every eight days). Lastly, the noise maps for 2017 are repeatedly used for each year of the emergent modelling period of 2004–2014 due to a lack of available noise predictions outside of this specific period.

Individual responses to noise are initiated by a Boolean response (hereafter referred to as noise-trigger) that is turned on when individuals are present at a patch with noise levels that exceed an imposed ‘noise-threshold’. During initialisation, each individual fish is introduced to the model with a noise-threshold that is fitted to the population using a normal distribution to reflect the known hearing range of European sea bass (Kastelein *et al.* 2008). Conversely, the noise-trigger is turned off when an individual moves or the patch it is in is updated to a noise level that is below that individual's designated noise-threshold. Individuals affected by noise (i.e., with noise-trigger on), initiate a set of four noise-effect pathways modelled after Soudijn *et al.* (2020) and Cox *et al.* (2018). Specifically, four main processes are adjusted using linear modifiers that reflect documented impacts of noise on individual fish: a reduction in food intake, an increase in energetic use, an increase in mortality, and a reduction in reproductive success (Cox *et al.* 2018; Soudijn *et al.* 2020). Lastly, the modelled impacts of noise are limited to larval, juvenile, and adult sea bass (except for *ingestion*; see section 4.3.5 of this chapter) due to a paucity of empirical evidence to support the application of these four noise-effect pathways to earlier life stages (eggs and yolk-sac larvae) (Fig. 4.1).

	Eggs		Larvae (exogenous)		Juvenile		Adult	
Foraging								
Foraging success	⬛	⬛	⬛	⬛	⬛	⬛	⬛	🟥 27, 35
Foraging behaviour	⬛	⬛	⬛	⬛	⬛	⬛	⬛	🟥 22, 29
Mortality								
Barotrauma	⬛	⬛	🟩 1, 3, 8*, 9*	⬛	🟩 8*, 9*, 10, 28*	⬛	⬛	🟥 12
Predation	⬛	⬛	⬛	🟥 22, 33	⬛	⬛	⬛	⬛
Anti-predator behaviour	⬛	⬛	⬛	🟥 20, 21, 33	⬛	🟥 4, 6, 32, 34*	🟩 36	🟥 26, 36
Energy								
Metabolic rate	⬛	🟥 17	⬛	🟥 9*, 33	⬛	🟥 4*, 6*, 7*, 9*, 28*, 32 , 37	🟩 5	🟥 5, 11, 13
Growth	⬛	⬛	🟩 3, 9*, 22, 28*	⬛	⬛	⬛	⬛	⬛
Stress-related behaviour	⬛	⬛	⬛	🟥 14, 20, 30, 31	⬛	🟥 4, 15*, 16*, 23*, 24*, 25*	⬛	🟥 27, 29, 35
Reproduction								
Reproductive success	⬛	⬛	⬛	⬛	⬛	⬛	⬛	🟥 22
Hatching success	🟩 3	⬛	⬛	⬛	⬛	⬛	⬛	⬛
Nesting behaviour	⬛	⬛	⬛	⬛	⬛	⬛	⬛	🟥 2*, 18, 19, 22, 26

1 = Bolle *et al.* 2012; 2 = Bruintjes & Radford 2013; 3 = Bruintjes & Radford 2014; 4 = Bruintjes *et al.* 2015; 5 = Bruintjes *et al.* 2016a; 6 = Bruintjes *et al.* 2016b; 7 = Buscaino *et al.* 2010; 8 = Debusschere *et al.* 2014; 9 = Debusschere *et al.* 2016; 10 = Casper *et al.* 2013; 11 = Celi *et al.* 2016; 12 = Halvorsen *et al.* 2012a; 13 = Harding *et al.* 2018; 14 = Holles *et al.* 2013; 15 = Kastelein *et al.* 2008; 16 = Kastelein *et al.* 2017; 17 = Jain-Schlaepfer *et al.* 2018; 18 = Maxwell *et al.* 2018; 19 = McCloskey *et al.* 2020; 20 = McCormick *et al.* 2018; 21 = McCormick *et al.* 2019; 22 = Nedelec *et al.* 2017; 23 = Neo *et al.* 2014; 24 = Neo *et al.* 2016; 25 = Neo *et al.* 2018; 26 = Picciulin *et al.* 2010; 27 = Purser & Radford 2011; 28 = Radford *et al.* 2016; 29 = Sabet *et al.* 2015; 30 = Simpson *et al.* 2005; 31 = Simpson *et al.* 2010; 32 = Simpson *et al.* 2014; 33 = Simpson *et al.* 2016; 34 = Spiga *et al.* 2017; 35 = Voellmy *et al.* 2014a; 36 = Voellmy *et al.* 2014b; 37 = Wysocki *et al.* 2006

KEY

🟥 Response
🟩 No response
⬛ No data

Figure 4.1. Summary table of the impacts of noise on fish from the literature. *Studies are divided by life-stages (eggs, larvae, juveniles, and adults), and impacts are sorted by biological response (refer to key). Some papers have multiple impacts that fill different response categories. '*' designates papers relating to European sea bass. Included studies are used to inform the implementation noise in the model; specific noise-related studies used for sensitivity analysis are discussed in section 4.3.7.2.*

4.3.5. Process overview, scheduling, and implementation of noise impacts

The majority of the submodels remain unchanged from the previous model iterations: Walker *et al.* (2020) and Watson *et al.* (2022). Here, we present a summary of the main processes/submodels; for further detail regarding submodels, parameters, input data and underlying assumptions, please refer to relevant TRACE sections (Appendix B). In the current modelling application, the effects of noise exposure to processes/submodels shown to be affected by noise were implemented (Fig. 4.2; Cox *et al.* 2018; Soudijn *et al.* 2020); specifically, four noise-modification parameters were added to the *ingestion, maintenance, natural mortality* and *spawning* submodels (bold text in this section). The model proceeds through all submodels in daily time steps, which reset every 365 days. During this schedule, agents age one day each time step, and the cohort age is increased every 365 time steps. The following submodels are executed in the order presented in this section. Lastly, individuals and patches are processed in a random order within each submodel.

Update-patches: New SST, PHY and noise data are assigned to patches, and offshore patches update their spawning patches.

Natural mortality: The number of fish in each individual N is subject to exponential decay that is determined by a natural mortality rate μ_n:

$$N = N * e^{(-\mu_n * (1 + \psi_M))}$$

Individuals affected by noise increase mortality rates proportionally with a linear ‘noise-mortality’ modification parameter ψ_M (Soudijn *et al.* 2020). Noise impacts on mortality apply to juveniles and mature sea bass only, as larval mortality is constant in the model (see sub-model section Appendix B.7)

Ingestion: Individuals that are capable of exogenous feeding (i.e., larvae, juveniles, and mature sea bass) are asked to calculate ingestion in the model. Eggs and yolk-sac larvae rely on their own, fixed energy sources rather than feeding (Pickett & Pawson 1994). For older life stages, the rates of ingestion I are calculated from the maximum consumption rate of food in relation to body size $Cmax$, energy available in the environment PHY, the half-saturation constant *H,* total mass M_t, conspecific density i, and the sum non-egg biomass in the same patch M_{nm}:

$$I = \left(\left(Cmax * (PHY/H + PHY)\right) * M_t{}^{2/3}\right) * \left(i * \left(1/M_{nm}{}^{2/3}\right)\right) * (1 - \psi_F)$$

Individuals affected by noise (noise-trigger turned on) decrease food ingestion rates proportionally with a linear ‘noise-feeding’ modification parameter ψ_F (Soudijn *et al.* 2020). Noise impacts on ingestion are restricted to juveniles and adults, as there is no evidence that noise would impair feeding in young, exogenous-feeding larvae (Fig. 4.1).

Assimilation: The assimilated energy is the energy available for energy budget processes (i.e., maintenance, growth, and reproduction). Ingested food is assimilated to energy with assimilation efficiency (i.e., proportion of energy absorbed from prey and tropic delay), and is dependent on temperature (i.e., Arrhenius function).

Maintenance**:** The assimilated energy is first used to cover metabolic maintenance requirements. Individuals that are capable of exogenous feeding (larvae, juveniles, and mature sea bass) are also asked to calculate metabolic rate and its energetic cost in the model. Thus, metabolic rates are calculated from metabolic rate normalisation Ao, total mass M_t, and an Arrhenius function Ah:

$$Mr = \left(\left(Ao * \left(M_t{}^{3/4} * 2\right)\right) * Ah\right) * (1 + \psi_E)$$

Individuals affected by noise increase metabolic rates proportionally with a linear ‘noise-energy’ modification parameter ψ_E (Soudijn *et al.* 2020). Noise impacts on metabolic rates are implemented across exogenous feeding life stages (larvae, juveniles, and mature sea bass), due to support from empirical evidence (Fig. 4.1).

Energy reserves: Once the energetic cost of maintenance/metabolic rate is established, it is either paid for directly from assimilated energy or, if this is insufficient (e.g., reduced feeding available in winter), then energy reserves are added to assimilated energy and metabolic costs are taken from this.

Growth: Individuals at all life stages (except eggs) calculate their total mass (mass of an individual, including, if any, fat reserves and gonad mass). Next, the maximum possible growth increment is calculated, and we assume individuals <70 days old have a constant maximum growth rate, while older individuals are assumed to follow a von Bertalanffy growth curve. After calculating the theoretical maximum size increase, the energetic cost of this maximum increase is calculated. Eggs do not grow, instead they develop and transform into yolk-sac larvae, which do not ingest energy and are thus assumed to have maximum energy available to grow maximally. However, once yolk-sac larvae have transformed to larvae, they begin to ingest energy. Subsequently, larvae, juveniles, and mature sea bass only grow maximally if there is adequate assimilated energy and individuals update length accordingly. If there is not enough assimilated energy, these older life stages grow at a suboptimal growth rate.

Calculate-speed: The swimming speed of each fish is calculated from its length and the SST of the patch.

Transform: If an individual meets the criterion (i.e., sufficient length; Fig. 4.2), then it transforms to the next life stage. The life stages are egg, yolk-sac larvae, larvae, juvenile, and mature sea bass.

Fishing-mortality: For fish that are over the minimum landing sizes, the number of fish represented by each super individual is discounted by fishing mortality rates from commercial offshore, commercial inshore and recreational fleets (data from ICES stock assessment 2020).

Spawn-migration: During the months October–May, if the SST is below the 9°C spawning trigger threshold, then mature sea bass move toward offshore spawning grounds.

Feeding-migration: When the spawning period is over at the end of May, each mature sea bass moves back towards/within its assigned coastal feeding ground.

Larval stages drift: Eggs, yolk-sac larvae, and larvae drift in the direction of their assigned coastal feeding ground.

Local-movement: Subsequently, juvenile sea bass move randomly with coastal patches; juveniles less than 32 cm long are further constrained to nursery coastal patches.

Reproduction and spawning**:** On the 17th of March (picked as the middle of the spawning period), mature sea bass calculate potential fecundity and the energy required to produce this number of eggs. If there is enough energy to meet calculated demands, a random sample of 10 mature sea bass individuals spawn one individual which represents as many eggs N_0 as determined by total realised fecundity F_r of the whole spawning stock divided by 10 N_c and the number of fish from the parent individual N_p:

$$N_0 = \left(\left(F_r * N_p\right)/N_c\right) * (1 - \psi_R)$$

With only 10 spawning individuals, the number of individuals per cohort and the spatial aspect of the fishery remain consistent. Individuals affected by noise reduce reproductive success proportionally with a linear ‘noise-reproduction’ modification parameter ψ_R (Soudijn *et al.* 2020).

4.3.6. Parameterisation

Parameters and their values are listed in the TRACE document and are based on available literature regarding European sea bass. Where absolute values of these parameters could not be directly sourced from the literature (mainly regarding energy budget parameters), Watson *et al.* (2022) used a version of Approximate Bayesian

Computation (ABC) called Simulated Annealing ABC (Albert *et al.* 2015) as implemented in the *Python* library *ABCpy* (Dutta *et al.* 2017). The data used for parameter calibration were from the sea bass assessment model (stock synthesis 3, SS3), which estimates annual outputs for spawning stock biomass (total mass of mature fish >42 cm; hereafter SSB), number/abundance of individuals (N), and numbers-at-age and subsequently calculates mass-at-age using the von Bertalanffy model; refer to Watson *et al.* (2022) for further details about calibration. Apart from the noise-related parameters, parameter values are as given in Watson *et al.* (2022).

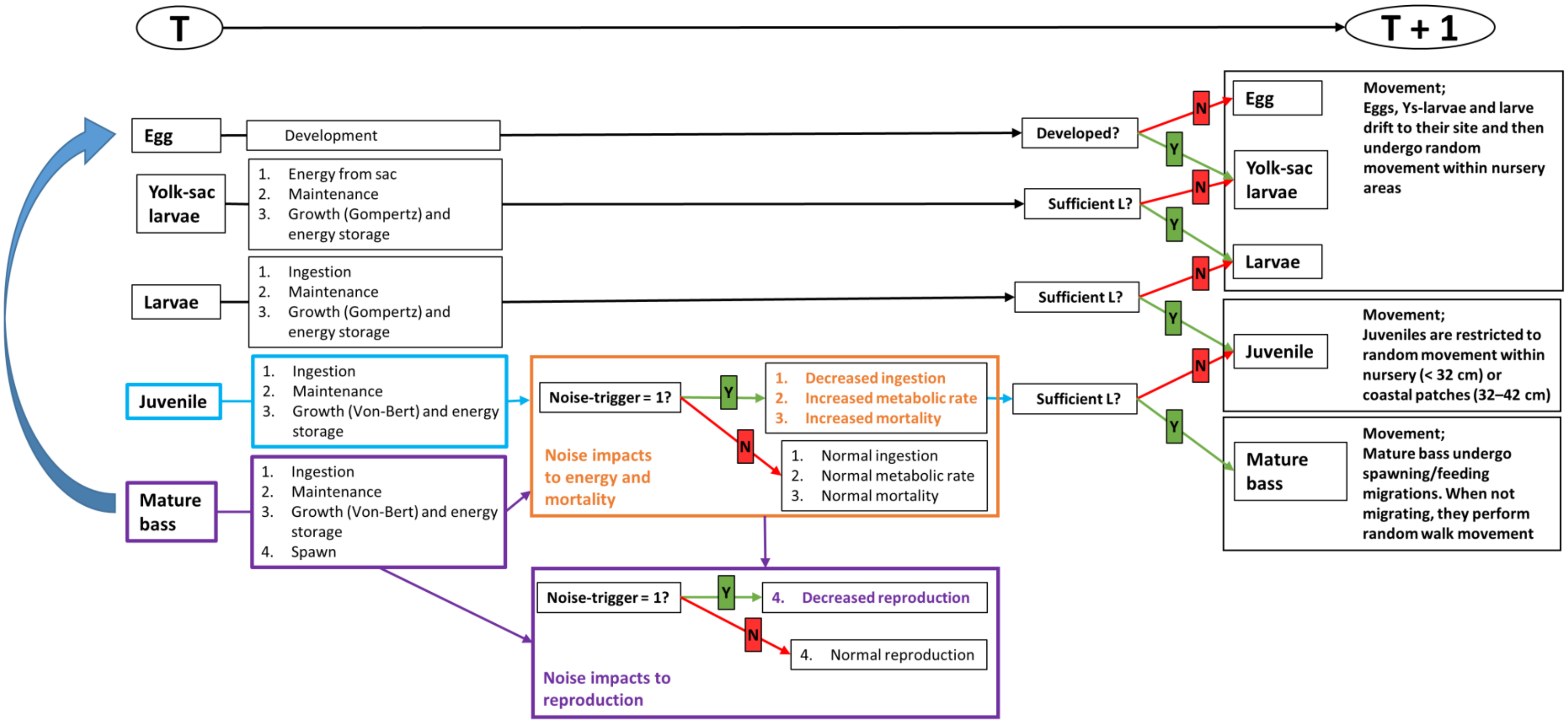

Figure 4.2. Model overview. *Each life stage (egg, yolk-sac larvae, larvae, juvenile, and mature sea bass) is outlined with the sub models applicable to each stage presented in the order of model execution. To transform to the next life stage, eggs develop after a specified time and from then on transformation is length-based. Each life stage gives details about their movement sub models. After spawning, the egg super-individuals then start the processes from the beginning again.*

4.3.7. Model testing

4.3.7.1. Conditioning and verification

To check conditioning of the population dynamics, SSB, abundance, mass-at-age and numbers-at-age from the IBM were compared to the same quantities from the SS3 from 2004 to 2014 (ICES 2020), which represents the best available knowledge on status of the stock. To account for stochasticity, the IBM was run 10 times and the differences between IBM output and the assessment quantified (Walker *et al.* 2020).

4.3.7.2. Sensitivity analysis

Local sensitivity analyses were conducted to explore how sensitive IBM outputs were to changes in model parameters and inputs. To assess temporal sensitivity, five simulations were performed for 10% increases and decreases in each model parameter, holding all other parameters at their baseline values, and compared to five baseline simulations (Walker *et al.* 2020). Median SSB, mass at age and numbers-at-age were averaged over the time-series with the result of each perturbation presented as a percentage of the baseline.

Values for the four noise-related parameters are extrapolated as percent changes from experimental studies on the impacts of noise in fishes. For feeding (NFm), noise was found to decrease foraging efficiency by 28% in three-spined sticklebacks *Gasterosteidae aculeatus* (Purser & Radford 2011) and reduce the proportion of prey consumed by 28% in European minnows *Phoxinus phoxinus* (Voellmy *et al.* 2014a). For energy use (NEm), noise was found to increase metabolic rates by 50% following 30 min of exposure to noise playback in wild-caught black seabream *Sparidae cantharus* (Bruintjes *et al.* 2016). For mortality (NMm), noise resulted in juvenile Ambon damselfish *Pomacentrus amboinensis* being three times as likely to be caught by predators in a controlled field experiment (Simpson *et al.* 2016). For reproduction (NRm), noise exposure resulted in a 30% decrease in offspring survival in both spiny chromis *Acanthochromis polyacanthus* (Nedelec *et al.* 2017) and painted gobies *Pomatoschistus pictus* (de Jong *et al.* 2018b).

4.3.7.3. Sensitivity scenarios for noise responses

To explore the degree and range that noise impacts the sea bass population within the model, each of the noise-affected processes (ingestion, metabolic rate, mortality, and reproduction) were tested by varying severity of impact (controlled by noise-modification parameters), and under a set of three noise scenarios: unmodified noise (+0 dB), increased noise (+10 dB) and decreased noise (-10 dB). For each scenario, a uniform adjustment was applied to the noise maps to achieve the desired change in noise levels. Subsequently, each of the noise-effect pathways (ingestion, energy use, mortality, and reproduction) was then tested in isolation against an incremental array (an increase of 10%; starting at 10% and ending at 90%) of response strength to noise that were implemented via the associated noise-modification parameters (see submodel section). This process was repeated three times to include variation of the results. Consequently, there was a total of 324 runs that were completed over these various scenarios.

For analysis, the model outputs (population biomass and abundance) for each run were averaged across the 10-year modelling period. Results were first compared to outputs from the acoustically undisturbed IBM runs previously used for verification. Subsequently, two-way ANOVAs were run, with noise scenario (either +0 dB, +10 dB or -10 dB) as a categorical, independent variable and percentage change in biological responses of the four noise-effect pathways as a continuous, independent variable. An interaction between the two independent terms was tested in each case.

4.4. *Results*

4.4.1. Conditioning and verification

The mean outputs following 10 IBM runs match well with the stock assessment, having significant, strong correlation and low root-mean square difference (Table 4.1; Fig. 4.3). The fit of SSB matches the shape and trends of the SS3 data, with slight overestimations, and follows a similar decline in SSB from 2010 (Fig. 4.3a). Similarly, abundance matches the trend of the SS3 data, with slight underestimations, but does have a deviation in trend trajectory from 2012 in comparison with the stock assessment (Fig. 4.3b). Mass-at-age estimations accurately match the trend and shape of the SS3 data, with only slight underestimations for ages older than about seven. Because of high abundances and significant mortality at early ages, the numbers-at-age distributions are highly skewed. To facilitate visualisation, estimations of numbers-at-age are shown on a logarithmic scale and demonstrate good fit with the SS3 data (Fig. 4.3c).

Table 4.1. Correlation and error of IBM outputs compared to SS3 verification data. *Shown are significance testing (p), correlation coefficient (r), normalised RMS difference (E), bias (E¯), and variability (E’).*

	p	*r*	*E* (%)	*E*¯ (%)	*E′* (%)
SSB	<0.001	0.95	16.82	13.93	9.43
Numbers	<0.001	0.96	16.50	-10.31	12.88
Mass at age	<0.001	0.99	11.40	-9.52	6.27
Numbers at age	<0.001	0.95	152.28	-57.92	140.83

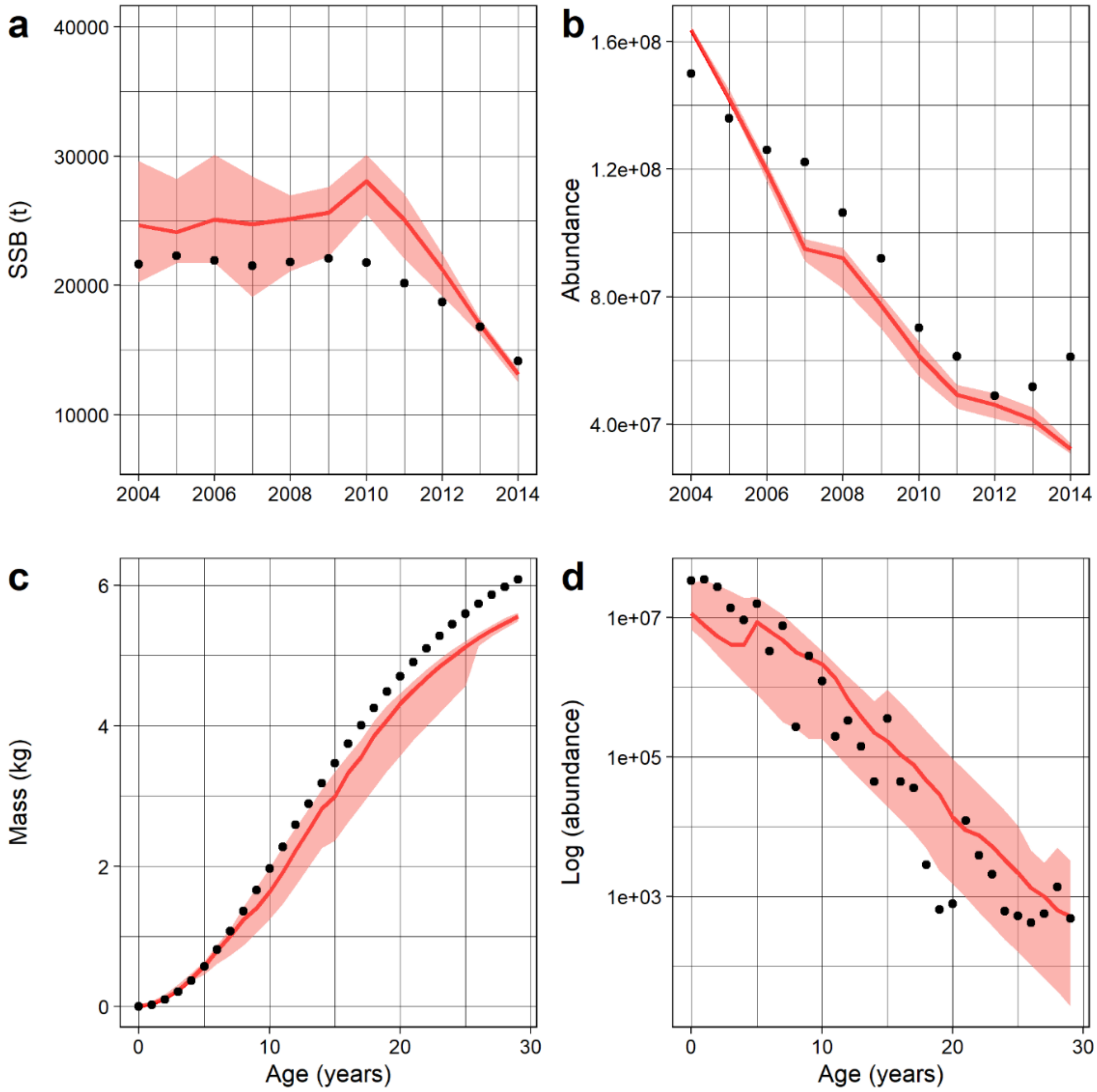

Figure 4.3. Model outputs averaged across 10 IBM runs compared to SS3 verification data *for: a) spawning stock biomass (SSB), b) abundance, c) mass-at-age and d) numbers-at-age. Plots a–c are true values, while plot d has been log-transformed for better visual comparison. Black dots represent outputs of SS3; red lines and ribbons represent means and 95% confidence intervals, respectively, from IBM outputs.*

4.4.2. Sensitivity analysis

Sensitivity of SSB, abundance, mass-at-age, and numbers-at-age to most parameter values and inputs was low, with 10% changes in these quantities mostly resulting in changes of <10% in model outputs (Table 4.2). Biomasses (SSB and mass-at-age) were most sensitive to changes in the length–weight parameter (*b_g*; Table 4.2), while abundances (N and numbers-at-age) were most sensitive to changes in the pelagic-mortality parameter (*PM*; Table 4.2). Of the noise-related parameters, SSB and mass-at-age outputs were most sensitive to changes in the noise-feeding modifier (*NFm;* Table 4.2), while abundance was most sensitive to changes in the noise-reproduction modifier (*NRm*; Table 4.2). Lastly, numbers-at-age outputs were most sensitive to decreases in the noise-mortality modifier (*NMm*; Table 4.2) and to increases in the noise-reproduction modifier (*NRm*; Table 4.2).

Table 4.2. Local sensitivity analysis outputs *following ± 10% changes in parameter values; input values rounded for presentation, for full values refer to TRACE document. Shown are spawning stock biomass (SSB), abundance (N), mass at age (MAA), and abundance at age (NAA).*

Parameter	Value	SSB-	SSB+	N-	N+	MAA-	MAA+	NAA-	NAA+
Asymptotic length (*linf*)	84.55	3.1	4.7	-2.7	2.8	[-22.5, 6.7]	[-4.4, 27.6]	[-15.2, 7.8]	[-2.7, 2.8]
Growth rate coefficient (*K*)	0.01	1.6	-4.9	-2.5	8.8	[-19.2, 4.7]	[-13.0, 26.0]	[-3.7, 3.3]	[-2.5, 8.8]
Age at length 0 (*t0*)	-0.73	1.3	-0.3	-3.2	19.5	[-10.2, 4.2]	[-12.4, 5.8]	[-2.9, 2.9]	[-3.2, 19.5]
Activation energy (*Ea*)	0.50	-1.1	9.3	-2.8	2.8	[-10.8, 1.7]	[-4.9, 11.2]	[-2.4, 32.6]	[-2.8, 2.8]
Activation energy for speed (*EaS*)	0.19	10.2	-0.9	-1.7	15.5	[-13.7, 7.8]	[-8.3, 10.5]	[-2.1, 10.9]	[-1.7, 15.5]
Max ingestion (*Cmax*)	0.54	0.9	3.6	-3.1	12.0	[-5.2, 8.8]	[-9.9, 9.1]	[-2.6, 2.0]	[-3.1, 12.0]
Phytoplankton energy content (*ep*)	6.02	-0.5	1.4	-2.5	22.1	[-10.4, 3.6]	[-5.3, 7.3]	[-2.5, 4.0]	[-2.5, 22.1]
Normalising constant (*A0*)	0.12	1.0	6.9	-2.9	3.7	[-13.5, 3.9]	[-10.7, 8.2]	[-3.5, 18.5]	[-2.9, 3.7]
Flesh energy content (*Ef*)	7.00	10.6	1.2	-7.8	6.1	[-5.8, 7.8]	[-7.5, 9.1]	[-3.0, 14.0]	[-7.8, 6.1]
Lipid energy content (*El*)	39.30	6.4	10.3	-2.8	14.3	[-10.7, 12.0]	[-15.3, 4.0]	[-12.6, 3.9]	[-2.8, 14.3]
Lipid-synthesis energy (*Ls*)	14.70	-8.3	0.8	-2.5	22.5	[-17.1, 10.8]	[-15.5, 11.8]	[-3.7, 8.0]	[-2.5, 22.5]
Flesh-synthesis energy (*Fs*)	3.60	0.8	-0.7	-14.0	9.9	[-10.4, 3.4]	[-9.9, 5.0]	[-2.6, 13.3]	[-14.0, 9.9]
Egg mass (*egg_mass*)	9.6x10^{-4}	7.7	-2.5	-6.0	29.4	[-11.1, 6.4]	[-7.6, 9.6]	[-2.3, 10.1]	[-6.0, 29.4]
Length-mass coefficient (*a_g*)	1.23x10^{-5}	-10.1	12.9	-2.8	8.9	[-16.6, 2.5]	[-1.6, 16.1]	[-2.3, 5.0]	[-2.8, 8.9]
Length-mass scaling exponent (*b_g*)	2.97	-57.4	180.3	-2.5	29.9	[-72.8, -40.3]	[23.2, 265.8]	[-44.1, 9.2]	[-2.5, 29.9]
Eggs per gram fish (*eggs_per_bass*)	3.75x10^{5}	4.0	7.8	-2.7	3.3	[-9.2, 10.3]	[-8.0, 10.8]	[-2.4, 9.3]	[-2.7, 3.3]
Larval growth coefficient (*Gl*)	0.03	3.7	1.1	-2.4	39.3	[-8.1, 3.7]	[-13.8, 6.4]	[-32.9, 9.8]	[-2.4, 39.3]
Half saturation constant (*H*)	4.87x10^{-1}	-1.4	2.3	-10.7	9.5	[-16.7, 4.1]	[-5.6, 12.8]	[-3.3, 11.8]	[-10.7, 9.5]
Natural mortality (juvenile–adult; *AM*)	4.71x10^{-4}	12.7	-8.3	-4.6	5.2	[-9.7, 8.9]	[-4.5, 3.2]	[-0.2, 22.0]	[-4.6, 5.2]
Absorption efficiency (*AE*)	1.64x10^{-3}	-0.4	-0.5	-2.2	11.9	[-10.1, 5.8]	[-16.2, 4.4]	[-2.1, 3.7]	[-2.2, 11.9]
Pelagic mortality (egg–larvae; *PM*)	8.01x10^{-2}	2.7	-7.5	-42.7	34.6	[-10.3, 5.4]	[-12.5, 5.5]	[-2.9, 77.2]	[-42.7, 34.6]
Density-dependent ingestion (*I*)	5.14x10^{13}	5.1	10.9	-3.3	7.0	[-18.4, 11.6]	[-13.0, 6.4]	[-2.6, 21.9]	[-3.3, 7.0]
Noise-feeding modifier (*NFm*)	0.28	-7.3	9.2	-3.0	5.6	[-15.5, 10.9]	[-6.1, 17.4]	[-1.6, 6.9]	[-3.0, 5.6]
Noise-energy modifier (*NEm*)	0.50	4.5	4.8	-4.8	8.8	[-7.9, 5.2]	[-13.5, 3.8]	[-9.2, 1.1]	[-4.8, 8.8]
Noise-mortality modifier (*NMm*)	0.33	-0.6	3.6	-3.3	4.1	[-10.1, 8.4]	[-6.1, 8.0]	[-2.9, 11.5]	[-3.3, 4.1]
Noise-reproduction modifier (*NRm*)	0.30	7.2	-0.7	-3.2	11.1	[-14.5, 5.7]	[-16.2, 6.0]	[-3.0, 2.5]	[-3.2, 11.1]

4.4.3. Sensitivity scenarios for noise responses

4.4.3.1. Spawning stock biomass (SSB)

The mean SSB averaged across 10 IBM runs without acoustic disturbance was found to be 23,082 ± 1312 (standard error of means) tonnes. When noise is distributed throughout the model and the noise-effect pathways are introduced in isolation, SSB decreases below the undisturbed average for three of the four noise pathways: ingestion, energy use, and mortality (Fig. 4.4a–c). Furthermore, there is an inverse relationship between SSB and the severity of impact for these three pathways (Fig. 4.4a–c). Conversely, SSB increases above the average when noise is affecting reproduction only (Fig. 4.4d).

There was a significant interaction of noise scenario (+0 dB, +10 dB, and -10 dB) and noise-impact severity on mean SSB output for ingestion ($F_{2, 75} = 19.79$, $p < 0.001$) and mortality ($F_{2, 75} = 14.35$, $p < 0.001$), but not energy use ($F_{2, 75} = 1.00$, $p = 0.37$) or reproduction ($F_{2, 75} = 0.06$, $p = 0.95$). Figure 4.4 shows that there is increasing separation between mean SSB output from the three noise scenarios as the severity impact for ingestion and mortality increases (Fig. 4.4a and c). There was however a significant difference between the three noise scenarios for SSB output resulting from noise-related changes in energy use ($F_{2, 75} = 11.32$, $p < 0.001$), as well as a significant effect of noise-impact severity on energy use ($F_{1, 75} = 33.19$, $p < 0.001$) and mortality ($F_{2, 75} = 44.99$, $p < 0.001$). When examining mean SSB outputs for tests when noise is impacting energy use, there is early separation of the quietest noise scenario from the comparatively two louder scenarios; however, this separation is less prominent as impact severity increases (Fig. 4.4b), consistent with a non-significant interaction term between noise scenario and impact severity. On the other hand, there was no significant difference between the three noise scenarios ($F_{2, 75} = 0.81$, $p = 0.45$) nor significant effect of noise-impact severity ($F_{1, 75} = 1.16$, $p = 0.29$) on mean SSB output because of noise-related changes in reproduction.

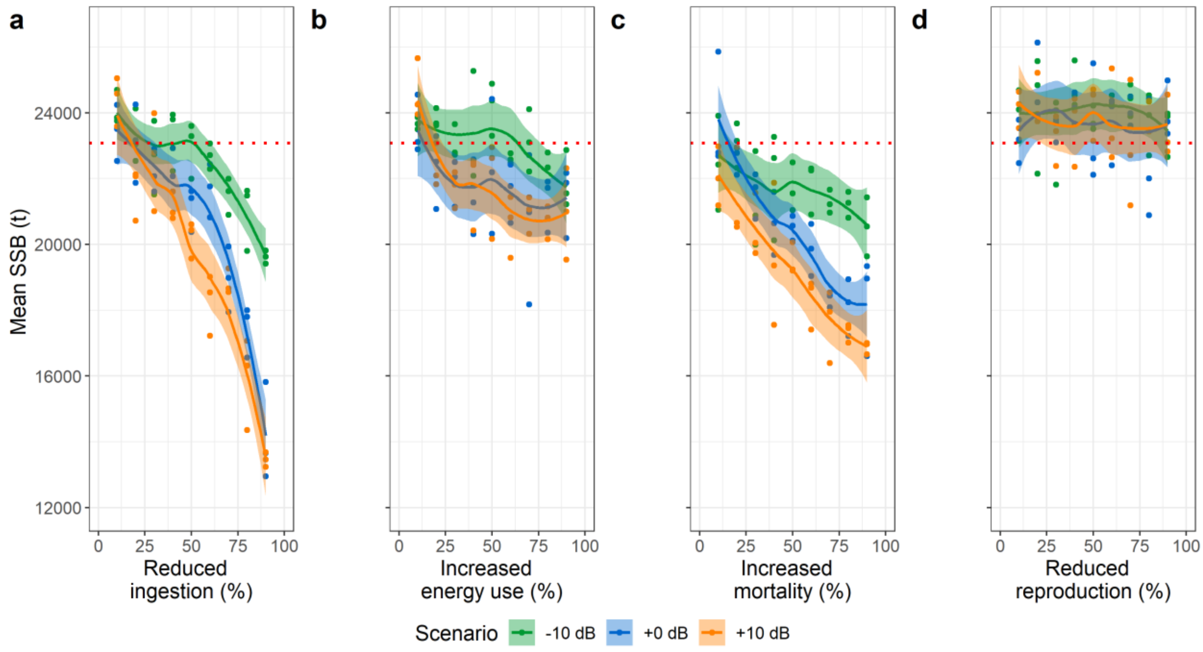

***Figure 4.4. Outputs of mean SSB from model runs with varying acoustic disturbance and noise-effect severity**; all outputs are averaged across the 10-year emergent modelling period. For a baseline comparison to acoustically undisturbed models, red dotted lines are comparable means from the verification results, averaged across 10 runs. Coloured dots represent SSB outputs from different noise scenarios for each of the four noise-effect pathways; coloured lines are linear-fitted curves; and shaded areas are 95% confidence intervals.*

4.4.3.2. Abundance

The mean abundance of modelled individuals averaged across 10 IBM runs without acoustic disturbance was found to be $8.36 \times 10^7 \pm 1.31 \times 10^7$. When acoustic disturbance and associated impacts are added to the model, abundance decreased compared to no-noise models across all four of the noise-effect pathways (ingestion, energy use, mortality, and reproduction; Fig. 4.5a–c). Similar to SSB, there is an inverse relationship between abundance and the severity of impact for the four pathways (Fig. 4.5a–c).

There was a significant interaction of noise scenario (+0 dB, +10 dB, and -10 dB) and noise-impact severity on abundance output for ingestion ($F_{2,\,75} = 33.99$, $p < 0.001$), mortality ($F_{2,\,75} = 71.48$, $p < 0.001$), and reproduction ($F_{2,\,75} = 16.58$, $p = 0.37$), but not energy use ($F_{2,\,75} = 1.29$, $p = 0.28$). Figure 4.5 shows that there is increasing separation between mean abundance output from the three noise scenarios as the severity impact for ingestion, mortality, and reproduction increases (Fig. 4.5a, c and d). There was however a significant difference between the three noise scenarios on mean abundance output for noise-related changes in energy use ($F_{2, 75}$ = 16.31, $p < 0.001$), as well as a significant effect of noise-impact severity ($F_{1, 75}$ = 87.44, $p < 0.001$). Similar to SSB outputs, there is early separation of the quietest noise scenario from the comparatively two louder scenarios when testing noise effects on energy use; again, this separation is less prominent as impact severity increases (Fig. 4.5b), consistent with a non-significant interaction term between noise scenario and impact severity.

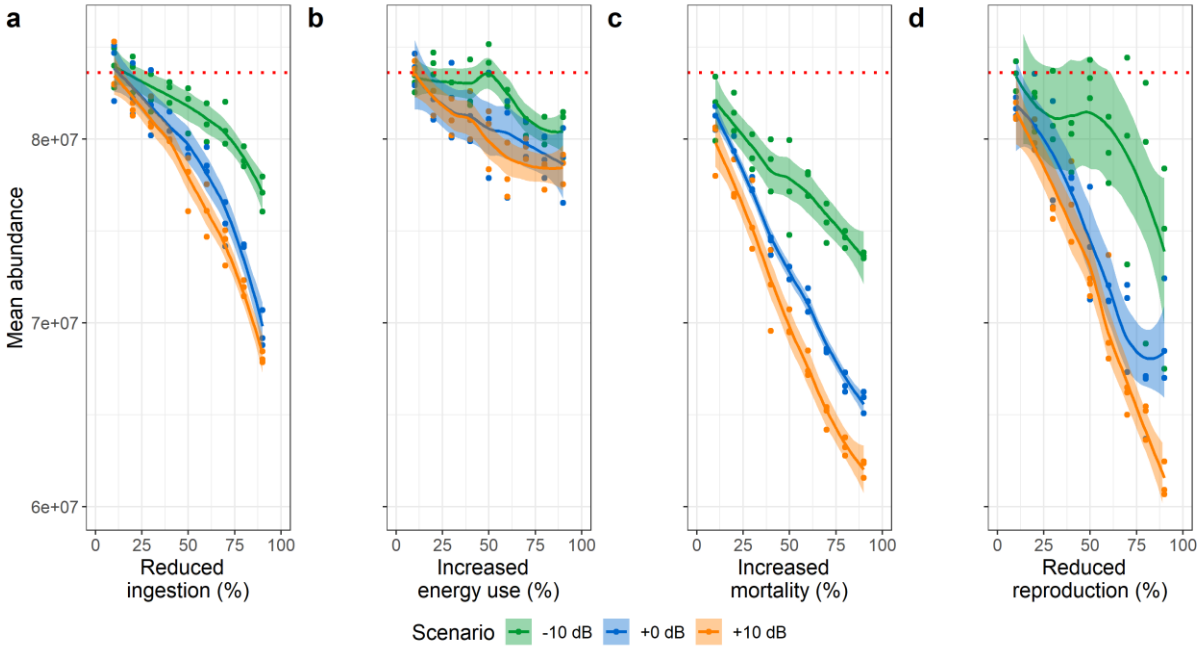

Figure 4.5. Outputs of mean abundance from model runs with varying acoustic disturbance and noise-effect severity*; all outputs are averaged across the 10-year emergent modelling period. For a baseline comparison to acoustically undisturbed models, red dotted lines are comparable means from the verification results, averaged across ten runs. Coloured dots represent abundance outputs from different noise scenarios for each of the four noise-effect pathways; coloured lines are linear-fitted curves; and shaded areas are 95% confidence intervals.*

4.5. *Discussion*

We present a spatially explicit and bioenergetic individual-based model of the northern stock of European sea bass that has been updated to include realistic projections of noise-pollution levels as well as scalable, biological responses to noise by individuals. Consistent with Walker *et al.* (2020), we used a ‘pattern-oriented approach’ (Grimm & Railsback 2005) to verify our model against SS3 stock assessment data (ICES 2020). Initial verification testing showed strong correlation between model outputs and verification data, with output data closely matching the shapes and trends of SS3 data. However, there were slight under- and over-estimations that were likely due to model output variability and might be addressed following more replicates/runs. The subsequent sensitivity analyses revealed a robust, well-calibrated model that was not overly sensitive to any one parameter (i.e., outputs changed <10% following ± 10% adjustments in parameter values). Lastly, our model demonstrated that noise has the potential to have a negative impact on fish population dynamics (e.g., biomass and abundance) through four noise-effect pathways (Soudijn *et al.* 2020), and that responses differed depending on the acoustic conditions (i.e., different noise-level scenarios) and which process was being affected by noise.

To develop our approach, we exposed the modelled fish population to a realistic range and degree of acoustic disturbance across a large geographic area using validated projections of noise pollution in the Northeast Atlantic (Farcas *et al.* 2020). We expanded on the PCAD framework used by Soudijn *et al.* by implementing similar noise-effect pathways to a spatially explicit IBM equipped with a calibrated energy budget. In developing a model that marries PCAD and IBM frameworks, we enable the consideration of important factors for the evaluation of noise impacts on fish populations, including spatial variation in species movement/distribution, noise-pollution levels, individual physiology and bioenergetics, density-dependent processes and life-history stages, environmental conditions, and variation and distribution of food availability (Mortensen *et al.* 2021). However, we do not claim that our model perfectly simulates real-world conditions. Rather, we strived to simplify and incorporate complex, but necessary, phenomena in the modelling process. For example, the validated noise maps produced by Farcas *et al.* (2020) are limited in temporal scale to one year and rely on certain assumptions, such as extrapolation to deep waters from measurements in coastal areas (Farcas *et al.* 2020). As these maps are further advanced, we can simultaneously update the modelling approach to include more accurate noise-level projections that span the same temporal period as our model. Similarly, responses by individuals to noise rely heavily on the importance of changes in four processes that are believed to be affected by exposure to noise (ingestion, energy use, mortality, and reproduction; Cox *et al.* 2018; Soudijn *et al.* 2020). Like Soudijn *et al.*

(2020), we decided to use this approach to compensate for the paucity of empirical information that directly links noise exposure to changes in life-history parameters. As relevant evidence emerges that accurately estimates/quantifies the effects of noise exposure on fish, especially in sea bass, we can begin to refine our approach to assess the population-level impacts of anthropogenic noise more accurately.

In our model, we found that noise influenced emergent outputs (biomass and abundance) through all four of the postulated noise-effect pathways. In most cases, these impacts were exacerbated by uniformly increased noise levels (+0 dB and +10 dB) and stronger changes in noise-affected processes. Population biomass and abundance were both sensitive to noise-driven changes in ingestion, corroborating similar results from Soudijn *et al.* (2020). In fishes, anthropogenic noise can directly impact foraging success in individuals through distraction (Purser & Radford 2011) or the masking of acoustic stimuli of prey (Sabet *et al.* 2015). Alternatively, noise might indirectly affect foraging through behavioural shifts (Voellmy *et al.* 2014a) or a reduction in appetite due to stress (Bernier 2006; Madison *et al.* 2015). In our model, individuals obtain energy from the environment (using phytoplankton as a proxy for energy distribution), which in turn provides the necessary energy for subsequent bioenergetic processes. Consequently, our results show that noise-reduced ingestion rates are likely to limit available energy for important processes, such as energy storage, growth, and reproduction, and thus have scalable consequences for populations. An empirical link between reduced foraging, energetic costs, and growth has been observed in fishes, but as a direct result of predation threat (Killen & Brown 2006). Therefore, we recommend that a similar link between noise, reduced foraging, and energetic costs and growth be a focus of future scientific investigations.

Additionally, we found that population abundance was particularly sensitive to noise-driven changes in mortality and reproduction, somewhat contrasting the PCAD model developed by Soudijn *et al.* (2020). With regards to mortality, this disparity could be attributed to different implementations of noise effects: we employ natural mortality using exponential decay rather than a linear probability of individual death. Fish mortality has been directly linked with exposure to loud, impulsive sounds (i.e., pile-driving noise), but only in cases where fish are in close proximity to the noise source (Halvorsen *et al.* 2012). Farther away from the source, noise may affect mortality through additional predation (Simpson *et al.* 2016), reduced anti-predator behaviour (Simpson *et al.* 2014; Voellmy *et al.* 2014b; Spiga *et al.* 2017), or altered risk assessment (McCormick *et al.* 2018). However, the overall links between anthropogenic noise and predation mortality remain contentious (Cox *et al.* 2018). With regards to reproduction, our model demonstrated compensation when individual reproduction was affected by noise disturbance that is consistent with known compensatory mechanisms of density-dependent processes (Rose *et al.* 2001). Specifically, our results show that population abundance is sensitive to changes in individual reproduction through reproductive failure and less recruitment. Consequently, noise-reduced recruitment corresponded with an increase in population biomass due to density-dependent compensation (i.e., reduced competition for resources subsequently leads to larger individuals). Reproductive output by individual fish has been shown to be affected by noise through a reduction in offspring survival (Nedelec *et al.* 2017), reduced spawning success (Sierra-flores *et al.* 2015; de Jong *et al.* 2018a), altered courtship behaviour and mating success (de Jong *et al.* 2018b; Blom *et al.* 2019), and disrupted nesting and parental behaviour (Bruintjes & Radford 2013; McCloskey *et al.* 2020).

In most cases, we found that uniformly increased noise levels exacerbated population-level responses by reducing biomass and abundance further, with noise-altered reproduction being an exception. This evaluation has presented an important area for investigation: the potential benefit of noise reduction and management. For example, uniformly reducing baseline noise levels by 10 dB increased average population biomass by 7.0% and average abundance by 4.8%. Conversely, increasing baseline noise levels by 10 dB reduced average population biomass by 3.5% and average abundance by 2.3%. Unfortunately, some scientists have warned that increased noise levels are a likely outcome if noise-reducing measures are not implemented (Duarte *et al.* 2021). However, there have been some recent, positive developments with regards to reducing anthropogenic noise in our oceans to benefit wildlife. For example, spatial management and speed restrictions have progressed as far as policy implementation and enforcement to bolster at-risk marine mammal populations, such as the critically endangered Southern Resident killer whales *Orcinus orca* (Williams *et al.* 2019). Similar concepts have been studied in coral reef fishes, where biological benefits were observed by switching to quieter engines (Jain-Schlaepfer *et al.* 2018; McCormick *et al.* 2018, 2019) or via the implementation of ‘acoustic buffer zones’ (McCloskey *et al.* 2020). Importantly, a strength of the IBM framework, and an important utility for fisheries management, is the ability to explore and predict the potential outcomes of various scenarios and/or management strategies (Boyd *et al.* 2020; Walker *et al.* 2020). Consequently, we believe our model could be similarly employed to evaluate the impacts of various noise pollution outcomes for fisheries in the Northeast Atlantic. Subsequently, we hope to explore the potential benefits of various noise-mitigation approaches to underpin the successful management of noise pollution to reduce/avoid unwanted consequences for important fish stock populations.

This first implementation of acoustic disturbance and associated biological impacts into a combined PCAD and IBM framework—for fishes—offers a useful tool to assess how anthropogenic noise impacts fish populations. By using an IBM framework, our model allows for variation in individual life-history, condition, environment, and response sensitivity to stressors (i.e., noise pollution) to better evaluate the cumulative impact of disturbance and associated population-level effects. We do recognise, however, that improvements will be needed as dose-dependent behavioural and physiological evidence for the impacts of noise on fishes becomes available. Furthermore, we do not consider this initial investigation as a replacement for experimental evidence, rather we strived to address the paucity of investigation for population-level consequences of noise in fishes by using an affordable and accessible complementary approach: computational modelling. Consequently, our model demonstrated how noise impacts at the individual level can have scalable consequences to population-level outcomes. We believe our model offers considerable scope for the evaluation of scenarios and changes in noise-pollution levels, as well as the potential benefits of noise-mitigation strategies for fisheries and fish populations.

Chapter Five – Potential consequences of anthropogenic noise and noise-mitigation scenarios for the northern fishery stock of European sea bass

Author contributions: K.P.M. was primarily responsible for designing the research, updating model and simulation code, carrying out simulations, analysing the data, and writing the manuscript.

Collaborator contributions: N.M., R.S., K.H., A.N.R, and S.D.S assisted with designing the research; J.W., N.W., R.B., R.S., and K.H. developed previous versions of the model and provided model code and input files; A.F. and N.M. developed and provided acoustic maps; J.W., N.W., and R.B. provided code for simulation and analysis; J.W., N.W., R.B., R.S., and K.H. advised on simulation and analysis; A.N.R and S.D.S. advised on noise-mitigation scenarios and testing; J.W., R.S., A.N.R, and S.D.S commented on drafts of the manuscript.

Acknowledgements: This work was supported by funding from a University of Exeter Vice-Chancellor Scholarship for Postgraduate Research (to K.P.M.), and a Natural Environment Research Council Research Grant (NE/P001572/1 to S.D.S. and A.N.R.).

5.1 Abstract

Anthropogenic noise is a global pollutant and stressor that has the potential to impact fishes at the population level. Understanding the population-level dynamics of fish populations is logistically challenging. Consequently, modelling scenarios and simulations have been a central part of fish stock assessment and fisheries management. More recently, fisheries models have been updated to assess threats from a wider range of stressors, including climate change and chemical pollution. Here, we use an ecological individual-based model (IBM) to assess how the northern stock of European sea bass *Dicentrarchus labrax* may be impacted by anthropogenic noise exposure. To do this, we have previously updated an existing spatially explicit and bioenergetic IBM to include realistic projections of noise-level distributions in the Northeast Atlantic along with pathways for the impacts of noise to affect life processes that are supported by experimental evidence. We take this investigation further by assessing how the northern stock may respond to two divergent scenarios of either increased or decreased noise, as well as scenarios of noise-mitigation strategies. Our results suggest that noise negatively affects population-level outputs of the northern sea bass stock, and we are able to simulate when and where impacts are happening in the Northeast Atlantic. We also found that increased noise is likely to exacerbate these effects. Conversely, decreased noise will improve population-level outputs, demonstrating the potential benefits of noise abatement. We then use this information to develop a targeted, practical noise-mitigation strategy that successfully improves population-level outputs.

5.2 Introduction

Fisheries resources are important sources of food, livelihoods, and income for millions of people globally (FAO 2020). However, increasing demand, overfishing and other sources of stress (e.g., pollution, habitat degradation, climate change, etc.) are likely to affect ecosystem integrity and compromise the provision of ecosystem services (Halouani *et al.* 2019). Successful fisheries management is often hindered by profound uncertainty and limitations of stock health evaluation (Memarzadeh *et al.* 2019). Consequently, models have come to play a key role in filling knowledge gaps of fisheries (Nielsen *et al.* 2018). Moreover, models can serve as ‘virtual laboratories’ for exploring casual hypotheses or potential consequences when real-life experiments are impracticable (Burgess *et al.* 2020). In recent years, the capabilities and scope of modelling frameworks have expanded, shifting from optimising single species yield to redefining sustainable fisheries management within the broader contexts of climate change, anthropogenic pressures, and ecosystem health (Curtin & Prellezo 2010; Lowerre-Barbieri *et al.* 2019). Consequently, the development of a suite of complex modelling approaches, for example individual-based models, have helped scientists and managers explore a wide range of issues threatening global fish populations (McLane *et al.* 2011; Weijerman *et al.* 2015; Lindkvist *et al.* 2020).

Individual-based models (IBMs) are a versatile tool that enable the synthesis of dynamic optimisation, movement, and management models. IBMs are a 'bottom-up' approach that simulate the actions of 'agents' (i.e., individuals or groups) using defined rules and behaviours that determine how individuals respond to one another and their environment (Railsback & Grimm 2019). Consequently, IBMs can accommodate individual behaviours, spatial systems, and dynamic changes in habitat, which allow for the emergence of population-level processes and patterns over space and time (McLane *et al.* 2011). Intrinsically, IBM embraces complexity and can be employed in cases of disparate or fragmented data, a serious weakness of fisheries surveillance (Lindkvist *et al.* 2020). Applications of IBM have been used to evaluate a broad range of issues related to fisheries management and health, including climate change (Boyd *et al.* 2020a), socio-economic pressures (Cenek & Franklin 2017), behaviour of fishers (Wijermans *et al.* 2020), MPA management and fishing strategies (Cabral *et al.* 2010), and fishing practices and policies (Lindkvist *et al.* 2020; Walker *et al.* 2020). Importantly, a key aspect of IBM is the ability to simulate and predict how animals may respond to changes in their environment, different management practices, and anthropogenic stressors (Watson *et al.* 2020; Mortensen *et al.* 2021).

One stressor in particular, anthropogenic noise, is ubiquitous to most aquatic environments and known to negatively affect a variety of fish species (Cox *et al.* 2018; Duarte *et al.* 2021). However, the majority of evidence for the impacts of noise on fishes relates to behavioural and physiological responses by individuals (Slabbekoorn *et al.* 2019; Mortensen *et al.* 2021). Quantifying the relationship between noise exposure and large-scale effects is complex due to extraneous factors that may affect populations and ecosystems, and methods for gathering direct evidence of large-scale effects remain impracticable (Merchant 2019). Consequently, Mortensen *et al.* (2021) postulate that a combined modelling framework of population consequences of acoustic disturbance (PCAD) models and IBMs may help bridge this gap by facilitating the translation of affected life functions into long-term age-specific vital rates (PCAD) across various spatiotemporal scales (IBM). Furthermore, the inclusion of stressor pathways through the modelling process (Soudijn *et al.* 2020) would allow for deeper evaluation for how stressors may be affecting animals, but also pinpoint plausible avenues for mitigation.

Mitigation of anthropogenic noise is still in the early stages of investigation and implementation. A recent review found few studies testing the effectiveness of mitigation measures, which precluded authors from providing confidence on their performance (Duarte *et al.* 2021). Additionally, another review of 10 major international agreements that address noise found that all but one, the European Union’s Marine Strategy Framework Directive (MSFD), are voluntary or noncommittal in nature (Lewandowski & Staaterman 2020). The only certain way to lower the risk of impact is noise abatement (i.e., reducing the amount of noise pollution entering the marine environment), either by reducing noise emitted at the source or by reducing the amount of noise-generating activity (Merchant 2019). For example, quieting vessels at the design stage could be achieved via economic incentives or mandated standards and would likely coincide with benefits to performance and reduced emissions. However, opportunities for noise abatement tend to be rare, and other forms of noise mitigation may be more accessible and easily implemented (Merchant 2019). For example, regulating speed and routes of ships can help reduce noise and/or divert impacts away from biologically sensitive areas, and has already been used to protect at-risk mammal populations (Williams *et al.* 2019; Duarte *et al.* 2021). Essentially, by controlling when, where or how we introduce noise into the environment, we may be able to reduce the detrimental impacts of anthropogenic noise to wildlife. However, these noise-reduction principles will require investigation to ensure the potential benefits of mitigation measures are validated scientifically.

In Chapter Four, I presented a spatially explicit, bioenergetic model of the northern stock of European sea bass *Dicentrarchus labrax* that uses projections of vessel-noise levels combined with stressor response pathways of noise impacts to explore population-level responses of fishes to noise disturbance over 10-year simulation periods (2004–2014). Here, I employ the same model to investigate the impacts of noise on the modelled northern stock population and evaluate potential strategies for mitigating anthropogenic noise at the population level. To do this, I used the model, along with inputs of noise impacts from the literature, to explore where and when noise impacts are occurring among the sea bass population and compare population-level responses under two possible absolute-level scenarios for noise pollution, either an increase or decrease of noise. Then, I compare three theoretical avenues for mitigating noise pollution in the marine environment: 1) universally reducing the absolute levels of noise (i.e., noise abatement), 2) changing the spatial distribution of noise, and 3) altering the temporal distribution of noise. Finally, using knowledge of sea bass ecology along with outputs of modelled noise impacts on the northern stock population, I will devise and present a possible targeted noise-mitigation strategy, and assess potential improvements of population-level outputs.

5.3 Methods

5.3.1 The model

Detailed descriptions of the IBM, including a model overview, initialisation and spin up, noise maps, responses by individuals to noise, processes, and scheduling, submodels, parameterisation, and conditioning, can be found in Methods section of Chapter Four and the TRACE (TRAnsparent and Comprehensive Ecological modelling documentation; Grimm *et al.* 2014) document (Appendix B). The current model was built from previous model versions developed by Walker *et al.* (2020) and Watson *et al.* (2022) and incorporates validated noise maps for the Northeast Atlantic (Farcas *et al.* 2020) and noise effect pathways for individual fish (Soudijn *et al.* 2020).

The IBM was implemented in *NetLogo 5.3.1* (Wilensky 1999). Subsequent simulations, support code and analysis were implemented in *RStudio V1.3.1093* using the *RNetLogo V1.0-4* extension and the *parallel V3.6.2* extension to facilitate with processing tasks.

5.3.2 Noise parameters and submodels

There is a paucity of quantitative empirical information available regarding the impacts of noise on life-history processes in sea bass that are transferrable to the IBM. Instead, relative changes observed in fishes (Cox *et al.* 2018; Soudijn *et al.* 2020) have been used to inform individual responses of sea bass to noise exposure. In Chapter Four, I explored a range of potential impacts via four noise-effect pathways (ingestion, energy use, mortality, and reproduction) (Cox *et al.* 2018; Soudijn *et al.* 2020) for the modelled sea bass population. Here, the same noise parameters/modifiers will be fixed based on empirical evidence for the impacts of anthropogenic noise observed of other fish species (Fig. 5.1). Specifically, percent changes related to the four noise-effect pathways have been referenced from the literature (Fig. 5.1; bold text) and input into the model as linear modifiers.

		Potential consequences			
Observed noise impacts	Sea bass	Energetic costs (increase costs)	Food intake (decrease food intake)	Mortality (increase death)	Reproduction (decrease reproduction)
Stress Higher levels of cortisol	4–5, 7, 23,27	🟧 Higher oxygen use when exposed to noise (seabass) [23, 27]; **50% increase in metabolic rates during noise treatment** (seabream) [4]; stress increases metabolic rates over short-term [1, 13] and long-term periods [12]	🟦 Cortisol suppresses appetite in teleost fish [2, 14]	🟦 Stress may impair behaviour and lead to mortality (salmon) [21]	🟧 Elevated cortisol decreases fertilisation rates [25]; Deformities in fish larvae [15]; **30% lower clutch survival** when exposed to noise (damselfish) [16]
Foraging behaviour Decrease of foraging behaviour: food consumption, foraging efficiency, and discrimination error	3–4	🟦 Higher energetic costs for same food intake (compensation)[11]; use of fat reserves and tradeoffs to account for effort [10]	🟧 **28% decrease in foraging efficiency** and feeding attempts when exposed to noise (stickleback) [22]; **28% decrease in proportion** of prey eaten (minnows) [28]	🟩	🟩
Movement behaviour Increase of movement: adjusted swimming depth, directional changes, schooling adjustments, swimming speed	3–5,7,9,17–20	🟨 Swim faster, tighter group cohesion, dive deeper [17–19]; swim away from the noise source (seabass) [19]; increased metabolic rate and responded less often and slower to simulated predatory attacks (damselfish) [26]	🟩	🟨 Increased turn angles when exposed to noise and predation risk [27]	🟩
Auditory system Changes in the auditory system: hering threshold	*	🟩	🟨 Possible that noise masked acoustic cues of *Daphnia* movement, contributing to decreased foraging (sticklebacks) [28] (zebrafish) [24]	🟧 **3x increased mortality** when exposed to noise (potentially related to predator detection; damselfish) [26]	🟧 Courtship vocalisations altered and **spawning success decreased by 30%** when exposed to noise (gobies) [8]

1 = Barton and Schreck 1987; 2 = Bernier *et al*. 2006; 3 = Bruintjes *et al*. 2014; 4 = Bruintjes *et al*. 2016; 5 = Buscaino *et al.* 2010; 6 = Debusschere *et al.* 2014; 7 = Debusschere *et al.* 2016; 8 = de Jong *et al*. 2018; 9 = Kastelein *et al.* 2017; 10 = Kemp *et al.* 2006; 11 = Killen *et al*. 2011; 12 = Lankford *et al.* 2005; 13 = Lawrence *et al.* 2019; 14 = Madison *et al.* 2015; 15 = Morgan *et al.* 1999; 16 = Nedelec *et al.* 2017; 17 = Neo *et al.* 2014; 18 = Neo *et al*. 2015; 19 = Neo *et al.* 2016; 20 = Neo *et al.* 2018; 21 = Olla et al. 1995; 22 = Purser and Radford 2011; 23 = Radford et al. 2016; 24 = Sabet et al. 2015; 25 = Sierra-Flores et al. 2015; 26 = Simpson et al. 2016; 27 = Spiga et al. 2017; 28 = Voellmy et al. 2014

KEY

🟧	Documented consequences of noise on modelled individual-level processes
🟨	Documented consequences of noise but not on modelled processes
🟦	Potential logical consequences but an absence of documented impacts
🟩	No short-term consequences for individual-level processes documented

***Figure 5.1. Potential consequences of anthropogenic noise for modelled individual-level processes** adapted from Soudjin et al. (2020). Observed noise impacts (left-hand column; Cox et al. 2018) have been cross-referenced with potential consquences to fishes in relation to modelled individual level processes of the IBM. Colours of the cells indicate quality of evidence (refer to key); bold text indicate direct evidence used to inform the impacts of noise in the IBM. The second column lists references with observed noise impacts (groups in the first column) on sea bass. Not all references included in the second column are related to modelled consequences (columns three to six), and no sea bass studies included evidence that can be directly input in the IBM. Therefore, modelled processes are driven by evidence for noise impacts on other fish species.*

Natural mortality: The number of fish in each individual N is subject to exponential decay that is determined by a natural mortality rate μ_n:

$$N = N * e^{(-\mu_n * (1 + \psi_M))}$$

Individuals affected by noise increase mortality rates proportionally with a linear 'noise-mortality' modification parameter ψ_M (Soudijn *et al.* 2020). Noise impacts on mortality apply to juveniles and mature sea bass only, as larval mortality is constant in the model (see sub-model section Appendix B.7). The best value from experimental evidence was found to be 0.33, based on the observed impacts of anthropogenic noise on morality in fishes (Simpson *et al.* 2016). In a controlled field experiment, exposure to noise resulted in prey being three times as likely to be caught by predators (Simpson *et al.* 2016).

Ingestion: All life stages calculate ingestion except for eggs and yolk-sac larvae, as these early life stages rely on their own energy sources rather than feeding (Pickett & Pawson 1994). For older life stages, the rates of ingestion I are calculated from the maximum consumption rate of food in relation to body size $Cmax$, energy available in the environment PHY, the half-saturation constant *H*, total mass M_t, conspecific density i, and the sum non-egg biomass in the same patch M_{nm}:

$$I = \left(\left(Cmax * (PHY/H + PHY)\right) * {M_t}^{2/3}\right) * \left(i * \left(1/{M_{nm}}^{2/3}\right)\right) * (1 - \psi_F)$$

Individuals affected by noise (noise-trigger turned on) decrease food ingestion rates proportionally with a linear 'noise-feeding' modification parameter ψ_F (Soudijn *et al.* 2020). Noise impacts on ingestion are restricted to juveniles and adults, as there is no evidence that noise would impair feeding in young, exogenous-feeding larvae (refer to Fig. 4.1 in Chapter Four). The best value from experimental evidence was found to be 0.28, based on the observed impacts of anthropogenic noise on foraging efficiency and behaviour in fishes (Purser & Radford 2011; Voellmy *et al.* 2014a). In the lab, noise was found to decrease foraging efficiency by 28% in sticklebacks

Gasterosteus aculeatus (Purser & Radford 2011) and reduce the proportion of prey consumed by 28% in minnows *Phoxinus phoxinus* (Voellmy *et al.* 2014a).

Maintenance: The assimilated energy is first used to cover metabolic maintenance requirements. Similarly, all life stages calculate metabolic rate and its energetic cost, except for eggs and yolk-sac larvae. Thus, metabolic rates are calculated from metabolic rate normalisation Ao, total mass M_t, and an Arrhenius function Ah:

$$Mr = \left(\left(Ao * \left(M_t^{3/4} * 2\right)\right) * Ah\right) * (1 + \psi_E)$$

Individuals affected by noise increase metabolic rates proportionally with a linear 'noise-energy' modification parameter ψ_E (Soudijn *et al.* 2020). Noise impacts on metabolic rates are implemented across exogenous feeding life stages (larvae, juveniles, and mature sea bass), due to support from empirical evidence (refer to Fig. 4.1 in Chapter Four). The best value from experimental evidence was found to be 0.5 (Bruintjes *et al.* 2016b). When exposed to noise in closed respirometry chambers, metabolic rates increased by 50% in wild-caught black seabream *Spondyliosoma cantharus* (Bruintjes *et al.* 2016b).

Reproduction and spawning: On the 17th of March (middle of the spawning period), a calculation is completed for mature sea bass to determine potential fecundity and the energy required to produce this number of eggs. If there is enough energy to meet calculated demands, a random sample of ten mature sea bass individuals spawn one individual which represents as many eggs N_0 as determined by total realised fecundity F_r of the whole spawning stock divided by ten N_c and the number of fish from the parent individual N_p:

$$N_0 = \left(\left(F_r * N_p\right)/N_c\right) * (1 - \psi_R)$$

With only ten spawning individuals, the number of individuals per cohort and the spatial aspect of the fishery remain consistent. Individuals affected by noise reduce reproductive success proportionally with a linear 'noise-reproduction' modification parameter ψ_R (Soudijn *et al.* 2020). The best value from experimental evidence was found to be 0.3 (Nedelec *et al.* 2017b; Jong *et al.* 2018). Noise exposure resulted in a 30% decrease in offspring survival in spiny chromis *Acanthochromis polyacanthus* (Nedelec *et al.* 2017b) and a 30% decrease in spawning success in painted gobies *Pomatoschistus pictus* (Jong *et al.* 2018).

5.3.3 Impacts of noise to sea bass

Population outputs (SSB and abundance) were compared between runs with and without added noise effects. Then, using fixed values for noise parameters based on the literature (Fig. 5.1), the impacts of noise on the modelled sea bass population were explored. To determine areas of highest impact percentages and numbers, model outputs were examined by regions and ICES designations and distributions of noise-affected individuals were mapped spatially.

Adult sea bass migrate to pre-spawning areas between October and December as females seek water warmer than 9°C. Subsequent spawning starts offshore in the Celtic Sea and western English Channel from February and spreads east as water temperature rises to the 9°C threshold (Thompson & Harrop 1987). After spawning, fish move to specific feeding grounds around April to May (Pickett & Pawson 1994). Importantly, movement between areas is thought to be rapid (Pontual *et al.* 2019), with most migrations being made along the coast (Pickett & Pawson 1994). Because of these migration patterns, monthly distributions of noise impacts were mapped to determine when and where noise effects are happening, and to help inform noise-management strategies/scenarios.

5.3.4 Scenario tests

For scenario tests, specific modifiers were coded and controlled via sliders/modifiers and choosers on the IBM interface. Specifically, scenarios were chosen using the ‘noise.management’ chooser on the interface, and noise levels were adjusted, in a manner dictated by the scenario, using the ‘absolute.mod’ slider/modifier. Simulations were run in *RStudio V1.3.1093* using *RNetLogo V1.0-4*; Parallel was used for simultaneous computation to reduce runtimes. To provide replication, the model was run 10 times for each set of conditions. Resulting SSB and abundances were compared to assess various scenarios.

5.3.4.1 Absolute levels of noise

Anthropogenic noise levels are predicted to increase along with human population and economic growth (Frisk 2012). However, solutions to mitigate anthropogenic noise, in terms of policy and technological measures, are becoming available and could be incorporated in internationally binding conventions to reduce unnecessary noise and support healthier ecosystems under a sustainable ocean economy (Merchant 2019; Duarte *et al.* 2021). Therefore, I have explored these two divergent scenarios of possible changes in absolute levels of noise (i.e., increased or decreased noise) in the Northeast Atlantic and the subsequent impacts on the northern stock population. To do this, two scenarios were evaluated and compared to contemporary noise levels of shipping (Farcas *et al.* 2020): a 6 dB increase or decrease in noise levels. This level was chosen based off calculated estimations of a 5–6 dB increase in global ambient noise levels by 2030 (Frisk 2012). In the model, the absolute levels of noise across the entire model were adjusted using the ‘absolute.mod’ modifier.

5.3.4.2 Scenarios of noise-reduction principles

Three noise-reduction scenarios were explored and compared using the model: a reduction in the absolute-level of noise throughout the model (i.e., noise abatement), changes in the spatial distribution of noise reduction and changes in the temporal distribution of noise reduction. Resultant changes in SSB and abundance were recorded and used for comparisons of population-level responses. Importantly, the spatial and temporal scenarios required noise levels to be adjusted using the ‘absolute.mod’, dependant on the scenario. Consequently, the absolute-level scenarios were tested first and used to inform the spatial and temporal scenarios.

To test changes to the absolute level of noise, noise levels were uniformly adjusted in the model in increments of 6 dB, using the ‘absolute.mod’ slider; range from -18 dB to +18 dB. For the spatial and temporal scenarios, noise levels of either the patches or for specific days were reduced by 6 dB, which is a plausible target for noise reduction that produced improved population-level outputs during the absolute-level scenario (Fig. 5.5a and d). To test the spatial distribution of noise reduction, the number of random patches with reduced noise levels of 6 dB was incrementally increased by 194 patches between 130 and 1295 patches using the ‘spatial.mod’ modifier. Lastly, to test the temporal distribution of noise reduction, random days were selected to receive a uniformly applied 6 dB reduction in noise. To implement this, a random float number (i.e., a random number between 0 and 1) was generated in *NetLogo* and tested against a probability threshold controlled by the ‘temporal.mod’ modifier. If the random float number was higher than the threshold, noise levels were uniformly reduced by 6 dB for that day and retested the next day. The temporal probability threshold was incrementally increased by 0.1 between 0.2 and 0.8. Each modification level was tested seven times for replication, therefore there was a total of 49 runs per noise-reduction scenario.

5.3.4.3 Targeted management scenarios

Using outputs from the impacts of noise on the northern stock population, a targeted set of spatial and temporal management strategies/scenarios was evaluated. First, spatial targeting of regions to receive 6 dB noise reductions was determined by the distribution of overall and monthly noise impacts (Table 5.1; Fig. 5.2 and 5.3). Population-level outputs of the various spatial management scenarios were compared to contemporary noise conditions without mitigation. Based on the distributions of noise impacts, the targeted regions to be evaluated were coastal, nursery, offshore, and English Channel areas (Fig. 5.2 and 5.3).

Temporal reductions were tested in the region that produced the highest SSB and abundance outputs following a 6 dB noise reduction. Similar to spatial management scenarios, population-level outputs of temporal management scenarios were tested against contemporary noise conditions without mitigation. To determine when to apply temporal reductions of noise, distributions of monthly noise impacts (Fig. 5.3) were used to gauge potential ‘quiet seasons’ for noise reduction with the aim of reducing noise when noise impacts are found to be highest in the target area.

For example, within the coastal regions, the highest distributions of monthly noise impacts were found from Summer to Winter, from June until January (Fig. 5.3).

5.3.5 Statistical analyses

We analysed differences in population-level outputs (SSB and abundance) between scenarios with and without implemented noise effects using independent t-tests. To determine whether population SSB and abundance differed based changes to the three noise-reduction principles (noise abatement, spatial distribution, and temporal distribution of noise reductions), linear regression was used; dependent variable ranges are described above under Section 5.3.4.2. Lastly, differences among remaining scenario tests (potential changes to absolute levels of noise and targeted management scenarios) were assessed using one-way ANOVAs (Chambers *et al.* 1992). *Post hoc* comparisons were conducted using Tukey Honest Significant Difference (HSD) (Yandell 1997).

All data were analysed using *R V4.1.2* (R Core Team 2021). Statistical tests were chosen after confirming that data met assumptions for parametric testing. Statistical significance was assumed where $p < 0.05$.

5.4 Results

5.4.1 Impacts of noise to sea bass

Without added noise effects, the mean SSB across 10 runs was found to be 23,979 ± 1,541 (standard error of means; SEM) tonnes and the mean abundance was $4.15 \times 10^{10} \pm 1.31 \times 10^{10}$. With fixed values for noise-effect parameters (i.e., noise effects turned on), there were noticeable differences in population SSB and abundance outputs. Added noise effects consistently produced lower SSB and abundance throughout the 10-year model period ($n = 10$; Fig. 5.1a and b), while maintaining a similar trend shape. Furthermore, mean SSBs averaged across years were significantly reduced by 20% (independent T-test: $t_{18} = 12.65$, $p < 0.001$; Fig. 5.2c), and mean abundances were significantly reduced by 19% ($t_{18} = 25.63$, $p < 0.001$; Fig. 5.2d) with the added impacts of noise.

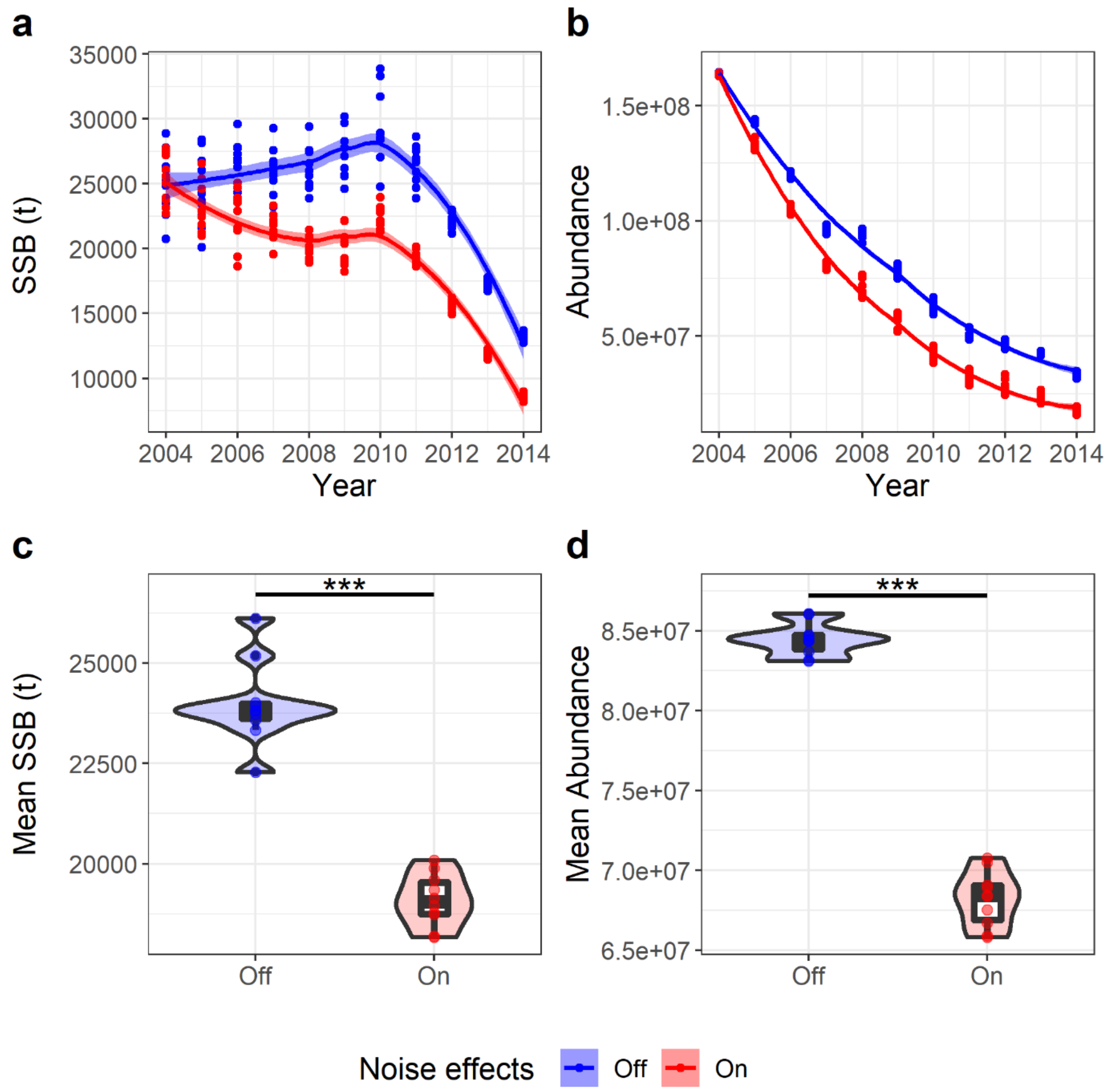

Figure 5.2. Population SSB and abundance outputs from simulations with noise effects turned off (blue) and on (red). *Plots a) and b) show total SSB and abundance per year. For plots a) and b), coloured points represent annual SSB outputs and abundance; solid-coloured lines represent a linear-fitted trendline; and shaded areas represent the 95% confidence intervals. Plots c) and d) show mean SSB and abundance averaged over years (2004–2014). For plots c) and d), coloured points show mean SSB and abundance per simulation run (averaged across years); boxes show median and interquartile ranges, violin plots show the kernel probability density of data at different values; and *** p > 0.05. N=20 simulation runs (10 runs per scenario).*

Model outputs from a single 10-year run show that most noise impacts are occurring near UK coastal areas and throughout the English Channel (Fig. 5.2b), which corresponds with the distribution of average noise levels throughout the Northeast Atlantic (Fig. 5.2a). Consequently, a high percentage of mature sea bass are being affected by noise on offshore patches (80.7%; Table 5.1), and in the English Channel (88.2%; Table 5.1). However, the highest total number of affected individuals were found on coast patches (ca. 4.76 x 106 super-individuals), which was roughly 66.9% of the coastal population. Therefore, while the highest levels of noise are found throughout the English Channel and some offshore areas (Fig. 5.2a), the higher distribution and movement of mature sea bass throughout the coastal areas means that moderate noise levels experienced in these regions are likely to affect a higher total number of fish (Fig. 5.2b and Table 5.1).

Table 5.1. Total noise impacts on mature sea bass across a single 10-year model run*, split among patch types (i.e., location and ICES designation).*

Patch type	Number affected (x 10^3)	Number unaffected (x 10^3)	Percent affected (%)	Mean individual mass (affected)	Mean individual mass (unaffected)
coast	475916	235434	66.9	3.51	3.53
nursery	175860	161988	52.1	3.53	3.52
offshore	162103	38828	80.7	3.51	3.54
Channel	84539	11358	88.2	3.62	3.72
IVb	12952	5593	69.8	4.54	4.24
IVc	43875	13764	76.1	3.80	3.66
VIIa	46928	52456	47.2	3.23	3.41
VIId	85223	38030	69.1	3.62	3.63
VIIe	184484	66989	73.4	3.44	3.65
VIIfg	102454	58602	63.6	3.43	3.33

Average monthly distributions of noise impacts corresponded with typical movement patterns of sea bass (Pickett & Pawson 1994; Walker *et al.* 2020). Between June and January, noise impacts mainly occurred in coastal areas (Fig. 5.3f–a). From February to May, noise impacts were high in offshore areas (e.g., English Channel and Celtic Sea), coinciding with offshore spawning in the warmer months (Fig. 5.3b–e). Furthermore, February and March appeared to have the highest densities of noise affected individuals in the English Channel (Fig. 5.3b and c).

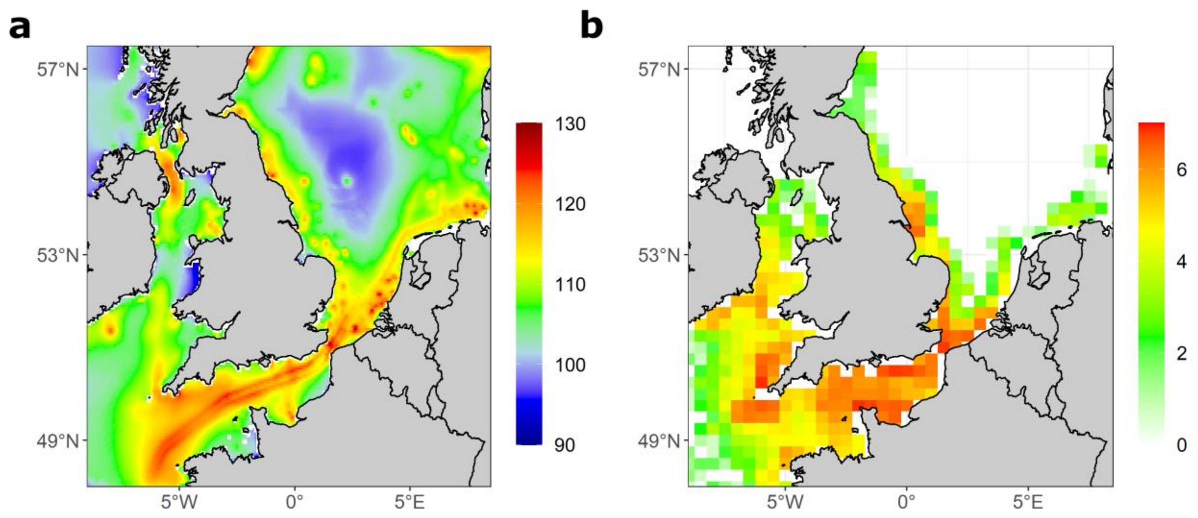

Figure 5.3. a) Projections of noise throughout, averaged across a single year (2017)*; which is used to input noise into the IBM each year,* ***and b) Total distribution of noise-impacted, mature sea bass over a single 10-year IBM run*** *shown on a log10 scale***.**

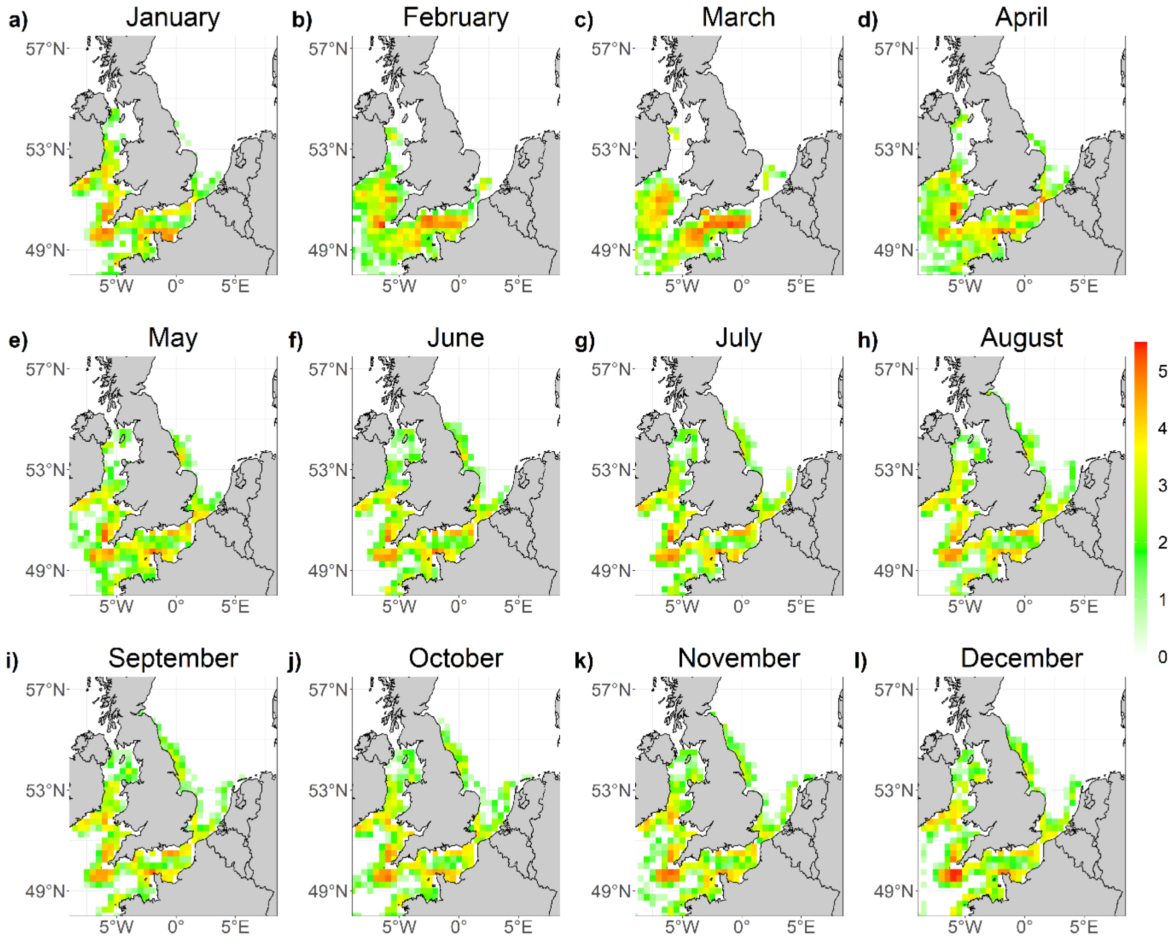

Figure 5.4. Monthly distribution of noise-impacted sea bass over a single 10-year IBM run shown on a log10 scale**.**

Based on these initial findings, peak impacts occur in the English Channel during offshore spawning. However, higher total numbers of affected individuals can be found in the coastal areas from June to January. Therefore, subsequent, targeted strategies for noise mitigation will focus on these main areas of activity.

5.4.1.1 Absolute levels of noise

The mean SSB averaged across ten IBM runs under contemporary noise conditions (+0 dB) and with fixed noise-impact parameter values was found to be 19,106 ± 1620 (SEM) tonnes. When absolute levels were adjusted based on scenarios of two possible noise pollution changes (either a reduction in noise by -6 dB or an increase of +6 dB), there were noticeable differences in population SSB and abundance outputs. Increased noise consistently produced lower SSB and abundance throughout the 10-year model period (n = 10; Fig. 5.5a and b), while maintaining a similar trend shape. Conversely, reduced noise levels consistently produced higher SSB and abundance throughout the 10-year model period (n = 10; Fig. 5.5a and b), while also maintaining a similar trend shape.

When averaged across years (2004–2015), modelled populations differed in outputs of mean SSB (one-way ANOVA: $F_{2,10}$ = 11.63, p < 0.001) and mean abundance ($F_{2,10}$ = 71.16, p < 0.001) between the three noise scenarios (-6 dB, +0 dB and +6 dB; Fig. 5.5c and d). Increasing absolute-noise levels by 6 dB compared to estimated current noise reduced SSB outputs by 8% (Tukey HSD: p = 0.03, 95% *CI* = [-2650.5, -136.1]) and abundance by 4% (p < 0.001, *95% CI* = [-4.0 x 106, -1.2 x 106]). Alternatively, reducing absolute-noise levels by 6 dB compared to current noise increased abundance by 6% (p < 0.001, *95% CI* = [-5.4 x 106, -2.6 x 106]). There was a non-significant trend of a 5% increase in SSB following a reduction of absolute-noise levels by 6 dB (p = 0.12).

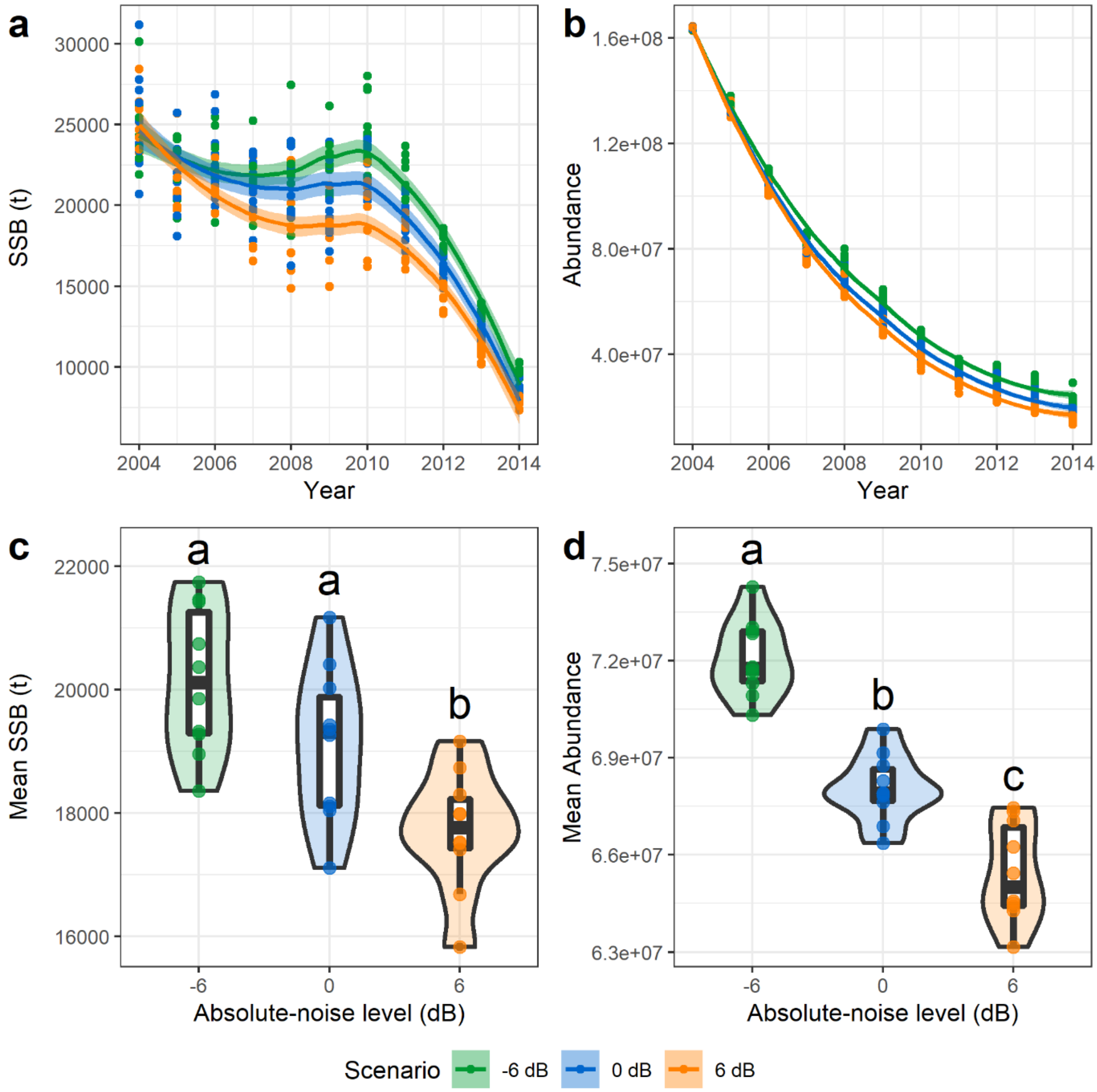

Figure 5.5. Population SSB and abundance outputs comparing current, unadjusted noise levels (+0 dB) to scenarios of either decreased (-6 dB) or increased noise (+6 dB). *Plots a) and b) show total SSB and abundance per year. For plots a) and b), coloured points represent annual SSB outputs and abundance; solid-coloured lines represent a linear-fitted trendline; and shaded areas represent the 95% confidence intervals. Plots c) and d) show mean SSB and abundance averaged over years (2004–2014). For plots c) and d), coloured points show mean SSB and abundance per simulation run (averaged across years); boxes show median and interquartile ranges, violin plots show the kernel probability density of data at different values; and letters (a, b, and c) above datapoints designate pairwise post-hoc analysis, where scenarios sharing the same letter are not statistically different (p > 0.05). N=30 simulation runs (10 runs per scenario).*

5.4.2 Noise-reduction principles

Noise abatement (i.e., adjusting absolute-noise levels), was found to have the strongest influence on population-level outputs (Fig. 5.6a and d). Across the distribution of tested noise levels, from -18 dB to + 18 dB relative to contemporary noise levels (+0 dB), average SSB changed by 27% and average abundance by 21%. Furthermore, changes in the absolute level of anthropogenic noise significantly affected both population-level SSB (linear regression: $F_{1,47} = 322.8$, $p < 0.001$, $r^2 = 0.87$) and abundance ($F_{1,47} = 449.7$, $p < 0.001$, $r^2 = 0.90$).

Comparatively, increasing the number of random areas of reduced noise (Fig. 5.6b and e) or the random number of days with reduced noise (Fig. 5.6c and f), both using 6 dB reductions, produced weaker changes in population-level outputs. Across the range of spatial distributions tested, from 130 to 1294 patches, average SSB changed by 6% and abundance by 5%. Importantly, changes in the spatial distribution of noise reductions significantly affected both population SSB (linear regression: $F_{1,47} = 15.36$, $p < 0.001$, $r^2 = 0.23$) and abundance ($F_{1,47} = 35.43$, $p < 0.001$, $r^2 = 0.42$). Across the range of temporal distributions tested, from a threshold of 0.2 to 0.8, average SSB changed by 4% and average abundance by 3%. Lastly, changes in the temporal distribution of noise reductions significantly affected population-level abundance ($F_{1,47} = 8.8$, $p = 0.005$, $r^2 = 0.14$) but did not significantly affect SSB ($F_{1,47} = 2.9$, $p = 0.10$, $r^2 = 0.04$).

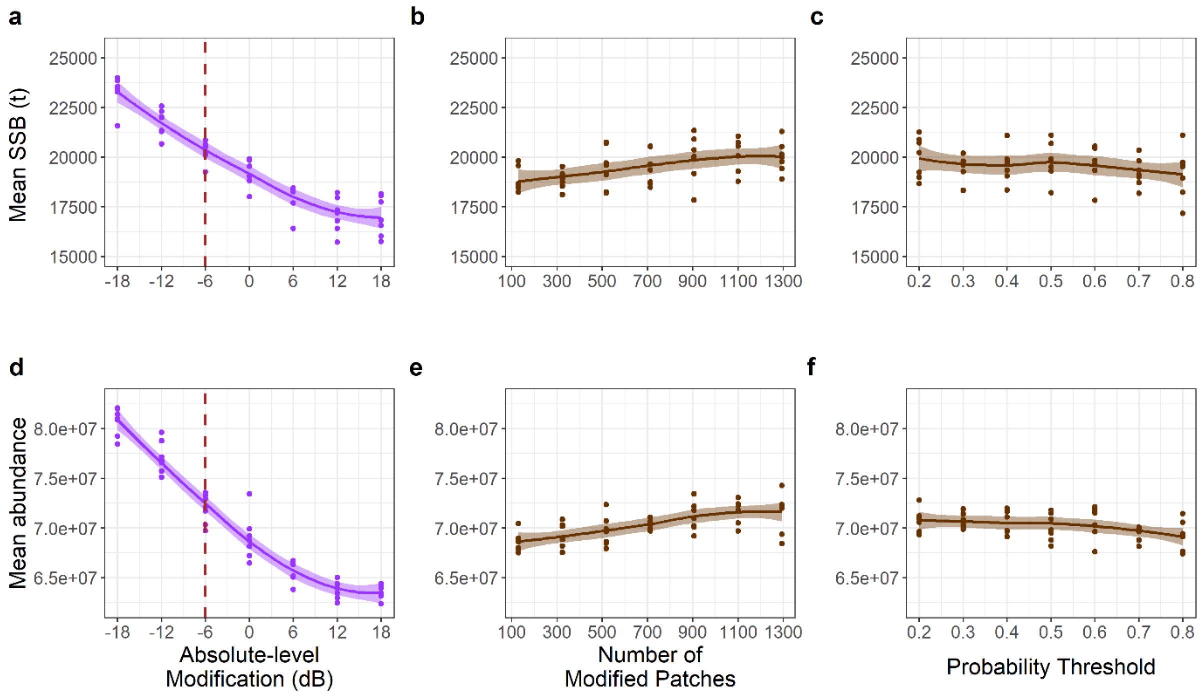

Figure 5.6. Mean SSB and abundance outputs averaged across years (2004–2014) from three management scenario tests*: a) and d) changes to absolute levels of noise, b) and e) changes to the spatial distribution of a 6 dB reduction of noise, and c) and f) changes in the amount of time noise levels are universally reduced by 6 dB. The outputs from absolute-level scenarios (plots a and d; purple points and lines) were used to inform input changes for the subsequent scenarios (plots b–c and e–f; brown points and lines). SSB and abundance outputs from the absolute-level scenarios identified 6 dB as a potential threshold point for noise reduction (vertical dashed line). Therefore, subsequent scenario tests (plots b–c and e–f) used 6 dB reductions for simulation experiments. Purple and brown dots represent SSB and abundance outputs from IBM runs; purple and brown solid lines represent a linear-fitted trendline; purple and brown shaded areas represent the 95% confidence intervals; and the brown vertical dashed line highlights the 6 dB threshold point identified following absolute-level scenarios. N=49 simulation runs (7 runs per modification level).*

5.4.3 Targeted management scenarios

When noise levels were reduced spatially per region, reductions to coastal areas had the highest population-level outputs of annual SSB across 10 simulations (Fig. 5.7c). Reductions to coastal areas produced the highest mean SSB, but there was no difference in mean SSB among the regional management scenarios and simulations without mitigation (one-way ANOVA: $F_{4,45}$ = 2.13, p = 0.10). There was a difference in mean abundance among the regional management and no-mitigation scenarios ($F_{4,45}$ = 6.88, p < 0.001). Upon further investigation, post-hoc analysis showed that 6 dB reductions to coastal regions produced 5% higher mean abundance compared to contemporary noise without mitigation (Tukey HSD: p < 0.001, *95% CI* = [-4.9 x 106, -1.2 x 106]). Noise reductions to coastal regions produced significantly higher mean abundances compared to reductions in the English Channel (3% change; p = 0.01, *95% CI* = [3.8 x 105, 4.1 x 106]) or nursery areas (3% change; p = 0.05, *95% CI* = [-3.7 x 106, -2.1 x 105]). Noise reductions to offshore areas also produced significantly higher mean abundances compared to no mitigation (3% change; p = 0.01, *95% CI* = [4.0x 105, 4.1 x 106]) and were not different to reductions in coastal areas (p = 0.70, *95% CI* = [-2.7x 106, 1.0 x 106]). Because reductions to coastal areas produced the highest mean SSB and abundance, coastal areas were further evaluated temporally through the addition of 'quiet seasons' from June until the end of November (Fig. 5.3).

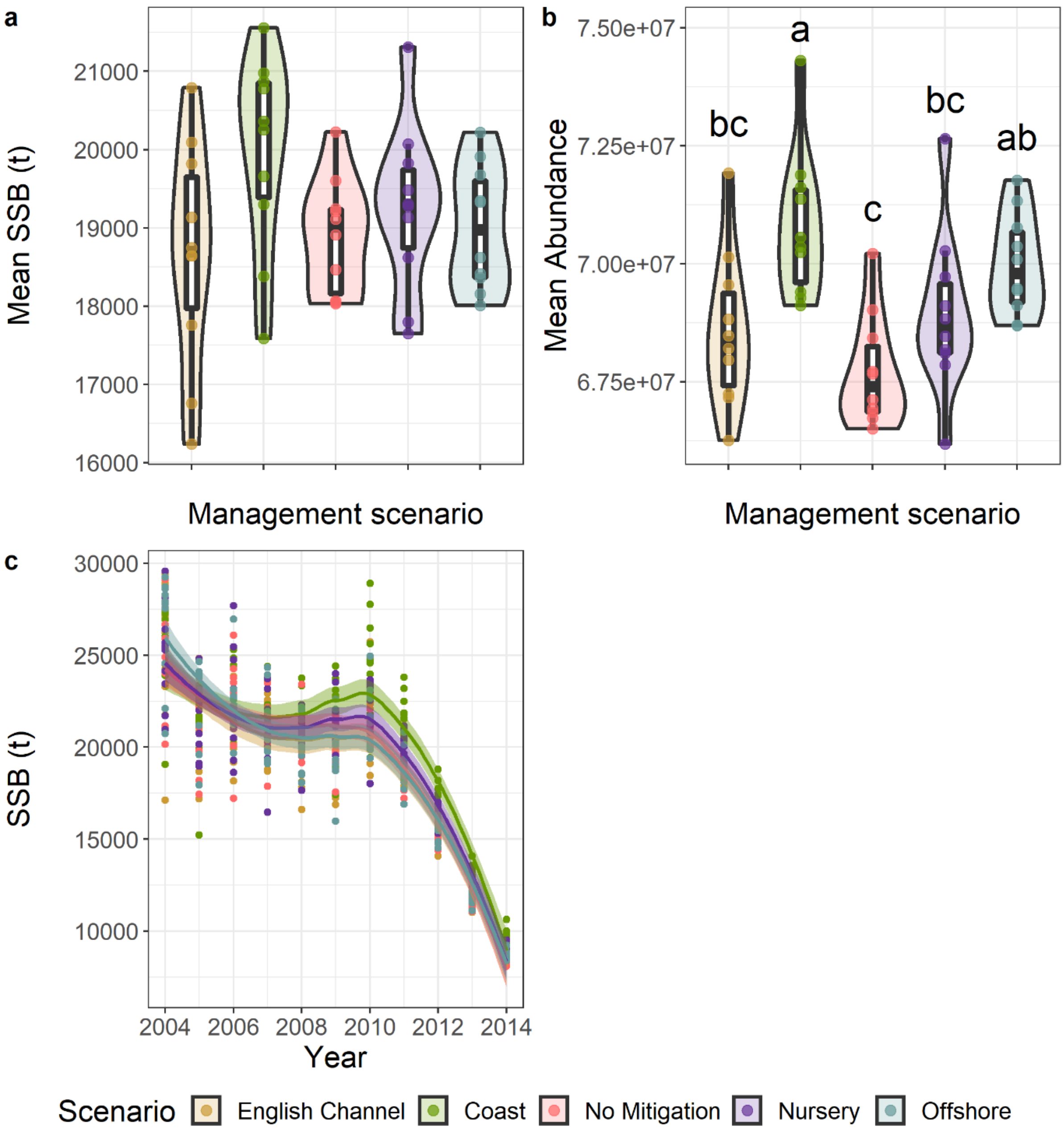

***Figure 5.7. Population SSB and abundance outputs from spatially targeted scenarios**, where regions are given a 6 dB noise reduction. Plots a) and b) show mean SSB and abundance averaged over years (2004–2014). For plots a) and b), coloured points show mean SSB and abundance per simulation run (averaged across years); boxes show median and interquartile ranges, violin plots show the kernel probability density of data at different values; and letters (a, b and c) above datapoints designate pairwise post-hoc analysis, where scenarios sharing the same letter are not statistically different ($p > 0.05$). Plot c) shows total SSB per year. For plot c), coloured points represent annual SSB outputs and abundance; solid-coloured lines represent a linear-fitted trendline; and shaded areas represent the 95% confidence intervals. N=50 simulation runs (10 runs per region).*

Noise reductions to coastal areas from June to the end of November produced the highest population-level outputs of annual SSB across 10 simulations

(Fig. 5.8c). Furthermore, 6 dB reductions to coastal areas from June to November produced the highest mean SSB, but there was no statistical difference in mean SSB among the temporal scenarios and the simulations without mitigation (one-way ANOVA: $F_{4,27} = 1.64$, $p = 0.21$). There was however a statistical difference in mean abundance among the temporal and no-mitigation scenarios ($F_{4,27} = 5.77$, $p = 0.008$). Post-hoc analysis showed that noise reductions to coastal areas from June to November produced 3% higher mean abundances than simulations without mitigation (Tukey HSD: $p = 0.008$, *95% CI* = [-3.0 x 106, -4.2 x 105]) and 2% higher mean abundances than reductions during remaining six months of the year, although the latter result was found to be a non-statistical trend ($p = 0.06$, *95% CI* = [-4.1 x 104, 2.5 x 106]).

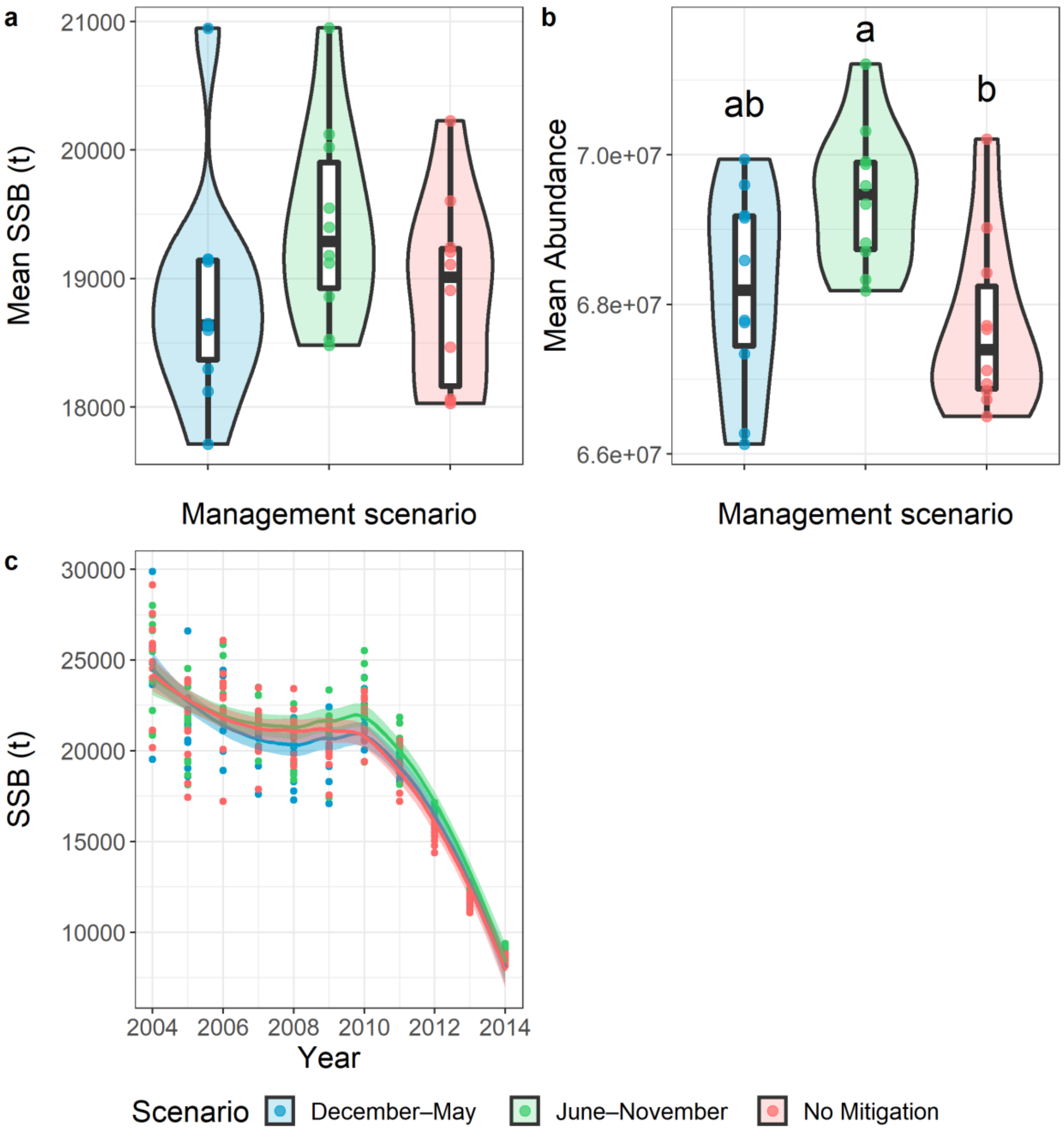

Figure 5.8. Population SSB and abundance outputs from temporally targeted scenarios within the coast region*, where specific time periods are given a 6 dB noise reduction. Plots a) and b) show mean SSB and abundance averaged over years (2004–2014). For plots a) and b), coloured points show mean SSB and abundance per simulation run (averaged across years); boxes show median and interquartile ranges, violin plots show the kernel probability density of data at different values; and letters (a, b and c) above datapoints designate pairwise post-hoc analysis, where scenarios sharing the same letter are not statistically different (p > 0.05). Plot c) shows total SSB per year. For plot c), coloured points represent annual SSB outputs and abundance; solid-coloured lines represent a linear-fitted trendline; and shaded areas represent the 95% confidence intervals. N=30 simulation runs (10 runs per time period).*

5.5 Discussion

Here, we employed a spatially explicit and bioenergetic individual-based model to explore the impacts of anthropogenic noise on the northern stock population of the European sea bass *D. labrax* and evaluated potential noise-mitigation approaches. We found that anthropogenic noise experienced by individuals may have significant consequences to overall population-level outputs. Furthermore, we used the model to pinpoint when and where modelled noise impacts are happening over time. Subsequently, we explored and compared absolute-level, theoretical and mitigation scenarios. Our results showed that less noise in the Northeast Atlantic might benefit sea bass compared to current, unadjusted noise conditions, and especially when compared to noisier conditions. Additionally, we found strong population-level improvements from reducing noise altogether (noise abatement via absolute-level reductions) and more moderate benefits from random spatial and temporal distributions of noise reductions. Using the modelled distributions of noise impacts along with the known ecology of sea bass, we devised a targeted noise-mitigation strategy and produced measurable benefits to population-level outputs. To our knowledge, this is the first use of an integrated PCAD and IBM framework to quantify the impacts of anthropogenic noise to a population of fish using realistic projections of noise levels across a large geographic range. Importantly, we have successfully demonstrated, from start to finish, how individual-based models may be used as an exercise to evaluate various aspects of sublethal stressor impacts and to explore and develop potential management strategies.

Our results showed that projected noise levels in the Northeast Atlantic resulted in a 20% reduction in SSB and a 19% reduction in population-level abundance of sea bass. By combining PCAD and IBM frameworks, we demonstrate how noise pollution experienced by individuals has the potential to scale up to measurable population-level consequences. In contrast to previous IBM investigations of noise impacts on fishes, we chose to exclude movement-related responses to noise, such as species distribution, avoidance, or changes to swimming speed. While sea bass have been shown to alter movement patterns in response to anthropogenic noise (Neo *et al.* 2015b), it remains uncertain whether fish will actively avoid noise (Neo *et al.* 2015a) and some species are unable to do so (e.g., site-attached or territorial species). Moreover, it is unlikely that avoidance would occur at the spatial scale of our model. Instead, we focus on vital rates and population consequences, which have not been evaluated using an IBM for fishes (Mortensen *et al.* 2021). Consequently, we believe we are able to demonstrate a more realistic scenario of how noise could be impacting fish populations through sublethal changes to important life-history processes rather than through changes to spatial distribution.

We used our model to explore important absolute-level, theoretical, and management scenarios of noise pollution levels in the Northeast Atlantic. We found that a 6 dB increase in noise levels, would reduce northern stock SSB by 8% and abundance by 4%. Alternatively, a 6 dB decrease in noise levels would bolster northern stock SSB by 5% and abundance by 6%, with even larger differences in comparison to noisier conditions. Of these absolute-level scenarios, it has been suggested that a 5–6 dB increase in noise levels is the most likely outcome for our oceans (Frisk 2012) unless actions to reduce noise pollution are taken (Duarte *et al.* 2021). Subsequently, we evaluated three main principles for reducing noise in our oceans: noise abatement (absolute-level reduction), spatial distribution, and temporal distribution (IMO 2014; Merchant 2019). Our results suggest that noise abatement is the most effective means of improving population-level outputs for fishes, followed by spatial distribution then temporal distribution. These results support the hypothesis outlined by Merchant (2019), which suggests that the only way to reduce risk of impact is noise abatement – reducing the quantity of noise pollution introduced into the marine environment. However, it is worth noting that experiments used to test population-level responses to the spatial and temporal distributions of noise were implemented randomly into the model. Therefore, reductions to unimpactful areas (i.e., where there are few to no fish) would have less benefits to the sea bass population. Consequently, the spatiotemporal experiments may have produced conservative results, and more targeted experiments (e.g., excluding areas where there are few/no fish) may help to tease apart differences and, more importantly, additional benefits. While there are clear benefits to noise abatement, the complete reduction of noise levels in the Northeast Atlantic is likely an unrealistic scenario from a management perspective.

We implemented a targeted spatiotemporal noise-management strategy based on the distribution of noise impacts produced by the model and the known ecology of sea bass. When comparing outputs from noise reductions to specific regions (spatially targeted scenarios), we found the most improvement following noise reductions to coastal and offshore areas compared to scenarios without noise reduction/mitigation. Moreover, coastal regions produced both the highest mean SSB and abundance of the northern stock. Importantly, coastal patches make up 35% of the total sea area in our model, while offshore patches make up the remaining 65%. Therefore, noise reductions to coastal regions might demonstrate maximum benefit to sea bass with minimal management effort. Implementing a ‘quiet season’ between June and the end of November to the coastal region (temporally targeted scenario) also produced noticeable differences in population-level outputs compared to modelled simulations without any mitigation measures. While the benefits from reducing noise to the coasts throughout the entire year might be greater, choosing a specific target period for noise reduction to coasts might be considered a more practical approach for management and enforcement. In fact, similar strategies have been successfully implemented in the Northwest Pacific, where noise reduction measures are implemented near coasts during ecologically important summer months to alleviate noise impacts and bolster resilience of the critically endangered southern resident killer whale *Orcinus orca* population (Williams *et al.* 2019).

From a management perspective, there are practical ways of reducing noise in the marine environment. With regards to vessel noise, the most widespread and persistent source of underwater noise, technological measures can be implemented to reduce the amount of underwater noise introduced into the environment by vessels (noise abatement), and would likely provide the most benefits (Merchant 2019). For example, noise from propeller cavitation might be reduced by modifying propellor and/or hull design, or by injecting air through propeller blades (IMO 2014; Merchant 2019). Additionally, underwater noise is generated by onboard machinery (e.g., engines and generators). On smaller vessels, changing engine types has been shown to reduce noise and negate negative biological responses in fishes (Jain-Schlaepfer *et al.* 2018; McCormick *et al.* 2018, 2019). Therefore, vessel noise might be reduced by implementing quieter machinery or by reducing noise transmission through the hull by vibrationally isolating machinery and optimising placement in the hull (IMO 2014). Furthermore, operational measures (e.g., speed and distance) can help affect ship noise emissions. For example, reducing speed near coral reefs was found to alleviate behavioural changes in nesting damselfish observed during high-speed boating (McCloskey *et al.* 2020). However, slower vessels take longer to transit, leading to a potential trade-off between duration and intensity of noise exposure, but this trade-off can be optimised (McKenna *et al.* 2013). Additionally, regularly enforced vessel inspection and maintenance of the propeller and hull may achieve modest noise reductions, as noise can be exacerbated by poor vessel maintenance (e.g., marine fouling or damage to the propeller/hull; WHOI 1952). Lastly, incentivising vessels to travel in convoy may reduce cumulative noise levels since quieter vessels within the convoy may be ‘masked’ by their noisier counterparts (Heise *et al.* 2017).

Our model demonstrates the potential for anthropogenic noise impacts to scale up from individuals to measurable population-level consequences. Forecasting the consequences of scenarios using models has been a long-standing, central component of fisheries management. Spatially explicit IBMs have been successfully used to simulate how fish communities may respond to the implementation of marine protected areas (Yemane *et al.* 2009; Brochier *et al.* 2013) and fisheries management (Boyd *et al.* 2020a; Walker *et al.* 2020). Here, we use our model as an exercise to demonstrate the application of IBM to investigate the overall impacts of noise exposure and the potential benefits of targeted spatiotemporal noise-mitigation strategies. Importantly, we are not, in this instance, attempting to pinpoint a specific mitigation approach, rather we are exploring the possibility of noise mitigation to benefit entire fish populations. Generally, our results suggest that targeted strategies aimed at reducing noise levels to ecologically relevant areas over specific periods of time have the potential to reduce anthropogenic noise impacts quantified at the population level. As field research methods for studying population-level responses in fishes (e.g., telemetry and mark-recapture studies) improve, our complementary model can help steer investigation of noise impacts on fish communities and populations.

Chapter Six – General Discussion

6.1 Overview

Anthropogenic noise is an established global pollutant with a broad range of effects on aquatic taxa (Duarte *et al.* 2021). Establishing anthropogenic noise as a stressor and pollutant has been an evolving process where research methods, techniques, and investigative scope continue to change and develop. As discussed in Chapter One, awareness of the negative impacts of noise began through observational evidence of physical injury to marine mammals following particularly loud and impulsive events (Parsons 2017). Subsequent laboratory investigation utilised species conducive to captivity and experimental study, such as fishes and invertebrates, which enabled researchers to focus on establishing physical, physiological, and behavioural responses to noise exposure in a controlled setting, further implicating noise as a stressor. However, there are certain limitations to laboratory research (e.g., unnatural behaviours and/or unrealistic acoustic conditions) that hinder extrapolation of findings to the natural environment. Consequently, carefully designed field experiments have enabled testing of anthropogenic noise impacts in the natural environment using real noise sources (e.g., motorboats). As study systems, model organisms, and methods continue to develop and broaden, so does the investigative scope of anthropogenic noise research. For example, identifying the appropriate study systems that enable observation and experimental study will help researchers explore logistically difficult questions, such as the impacts of anthropogenic noise on populations and communities. In parallel, there are complementary approaches, such as modelling, that can be used to explore the broader impacts of anthropogenic noise to these larger systems.

Following this pathway of innovation for anthropogenic noise research, I have employed an integrated approach to explore the impacts of noise at varying levels of biological organisation (Fig. 6.1). Importantly, I have strived to incorporate elements of mitigation in different aspects of this research. In this final chapter, I summarise the main findings from each study and suggest opportunities for further investigation.

More broadly, I provide possibilities for future work that would expand our understanding of the impacts of anthropogenic noise to wildlife. Lastly, I discuss and evaluate plausible strategies for reducing anthropogenic noise, and associated negative impacts, in aquatic ecosystems.

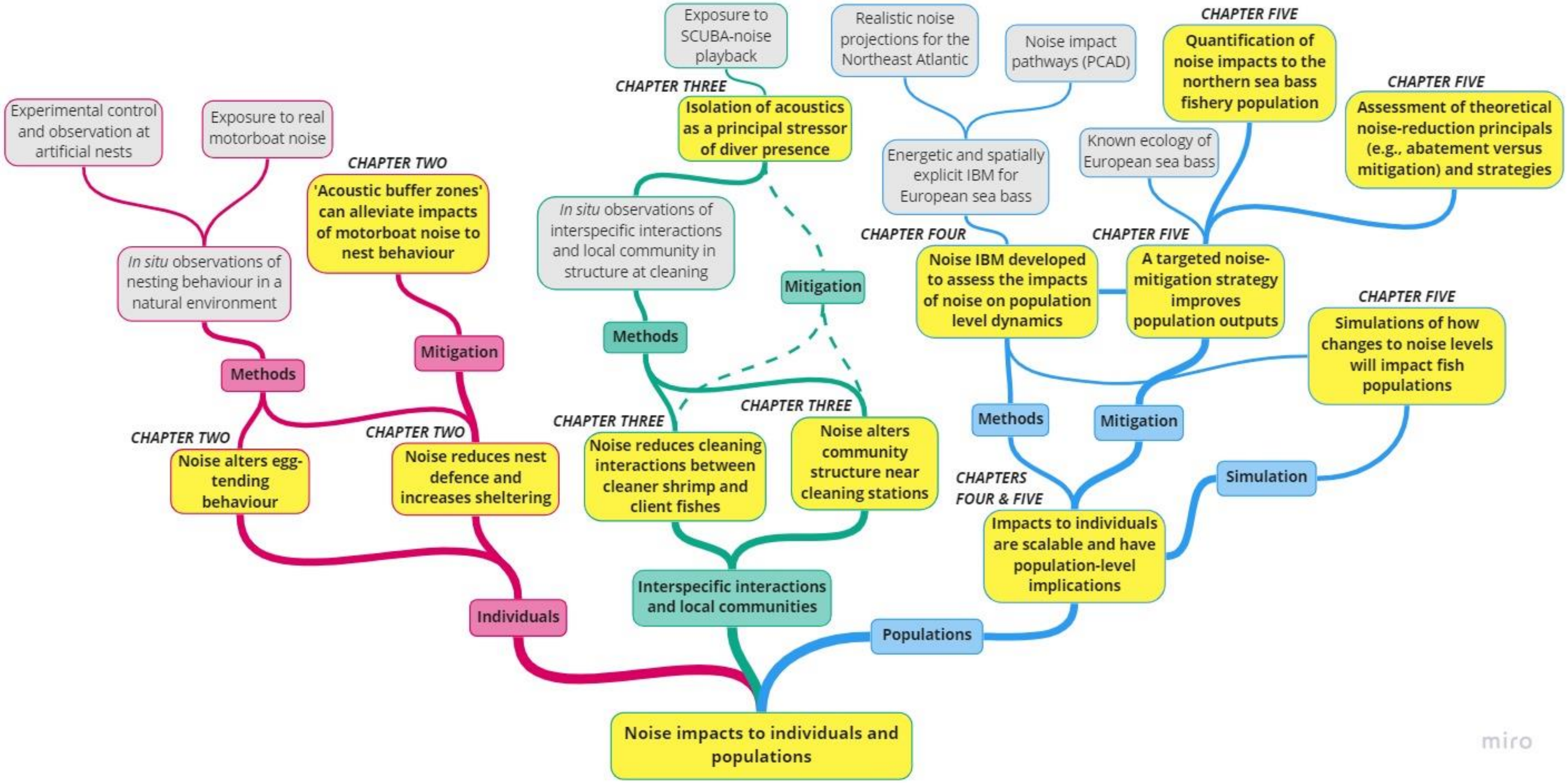

Figure 6.1. Conceptual mind map of the implementation the integrated approaches used in this thesis. *From top to bottom, methods were adapted to fit questions and scope to evaluate the impacts of anthropogenic noise on varying levels of biological organisation, including individuals, local communities, and populations. Considerations for mitigation were included at each level of biological organisation. Main study findings are shown in yellow boxes; coloured branches indicate levels of biological organisation; solid branches indicate implementation of methods or direct links supported by experimental evidence in this thesis; dashed branches are theoretical links that were not experimentally tested. Mind map created using miro.com.*

6.2 Chapter Summaries

My first data chapter (Chapter Two) focused on the impacts of *in situ* motorboat noise on egg-tending and nest-defence behaviour in nesting Ambon damselfish *Pomacentrus amboinensis*, and efficacy of a potential noise-mitigation strategy for motorboat driving. I found short-term impacts of noise on both egg-tending and nest defence in male *P. amboinensis*; I did not consider females, but future work should consider potential sex differences, as behaviourally induced stress negatively impacts female *P. amboinensis* and subsequent progeny (McCormick 1998). The employment of a noise-mitigation strategy designed to reduce noise levels experienced by nesting males—by slower/farther motoring from the reef—was effective in negating changes to nest-defence behaviours that were observed during nosier conditions. Consequently, I demonstrated the potential value of altering motoring practices near coral reef habitats to limit anthropogenic noise exposure to increasingly vulnerable wildlife.

In Chapter Three, I used an established study system to explore the impacts of anthropogenic noise on interspecific mutualisms and community structure near ecologically important cleaning stations of the Pederson's cleaner shrimp *Ancylomenes pedersoni*. Furthermore, I focused on an understudied source of anthropogenic noise, SCUBA noise. I found that playback of SCUBA noise reduced the overall occurrence of fishes and altered community structures near *A. pedersoni* cleaning stations. SCUBA-noise playback also prolonged initiation delays and reduced cleaning rates between *A. pedersoni* and fish clients. Because of the scarcity of evidence regarding anthropogenic noise impacts on communities, these results are an important step to understanding community-level responses to noise disturbance. Specifically, not all species responded the same to SCUBA-noise playback—whereas three species occurred less frequently during noisier conditions, one species occurred more frequently—corroborating complex community-level responses observed in terrestrial habitats (Francis *et al.* 2009). Importantly, these results shed new light on previous findings that the presence of divers affects cleaning rates observed at the same study location (Titus *et al.* 2015a), identifying acoustic disturbance as a causal mechanism for the impacts of SCUBA-diver presence on marine organisms. However, caution is advised when extrapolating short-term results to fitness or predicting lasting community-level impacts. Ultimately, extended experimental tests are needed.

Chapters Four and Five focused on the development and implementation of an individual-based model (IBM) to investigate the impacts of anthropogenic noise on fish stock populations. This was a collaborative project that I established and led: I brought together a network of experts to combine the necessary pieces for the model, including modelling experts at the University of Reading, who had previously developed an IBM for investigating the impacts of sublethal stressors to fish (Walker *et al.* 2020; Watson *et al.* 2022), and noise-mapping experts at Cefas, who had recently developed and released the most accurate and expansive noise projections for the Northeast Atlantic (Farcas *et al.* 2020). Furthermore, I organised an international workshop with expert authors and educators in IBM techniques when I found that there were no training opportunities on offer. Lastly, a recent application of the population consequences of acoustic disturbance framework (PCAD) by Soudijn *et al.* (2020) provided a conceptual basis for implementing the impacts of noise on fishes into the IBM. In Chapter Four, I integrated, tested, and evaluated these pieces within the IBM. Using the model, I found that noise has the potential to impact fish population dynamics (i.e., biomass and abundance) negatively through the four noise-effect pathways (feeding, energy use, mortality, and reproduction) presented by Soudijn *et al.* (2020), and that responses differed depending on acoustic conditions and which process was being affected by noise. I found that noise influenced population-level outputs (biomass and abundance) through all four of the postulated noise-effect pathways, and that biomass and abundance were both sensitive to noise-driven changes in ingestion, corroborating similar results from Soudijn *et al.* (2020). However, results also indicated that population abundance was particularly sensitive to noise-driven changes in mortality and reproduction, somewhat contrasting the PCAD model developed by Soudijn *et al.* Ultimately, further model evaluation and calibration will be required. As experimental evidence of noise impacts on life-history processes in European sea bass *Dicentrarchus labrax*, and other fish species, becomes more available, the model can be updated and fine-tuned.

In Chapter Five, I used the IBM developed in Chapter Four to examine the population-level impacts of noise on the northern stock of European sea bass and explore various scenarios for noise pollution (i.e., absolute-levels of noise, noise-mitigation theories, and targeted noise-mitigation strategies). First, I demonstrated how the model can be used to pinpoint when and where noise impacts are likely happening among the European sea bass population. I also showed that current noise levels in the Northeast Atlantic would likely reduce important population-level outputs (biomass and abundance). Next, I explored diverging changes to absolute-noise levels in the Atlantic (i.e., increased or decreased noise) and found that increased noise (the likeliest outcome for our oceans; Duarte *et al.* 2021) would further depreciate fish populations, while decreased noise would offer some benefit compared to current noise levels and significant benefit compared to noisier conditions. Subsequently, I used the model to explore theoretical approaches to reducing noise in the aquatic environment (i.e., noise abatement vs spatial/temporal distributions of noise reductions). Unsurprisingly, I found noise abatement to be the most effective way to improve population-level outputs. However, improvements were still observed following spatial/temporal noise reductions. Importantly, noise-mitigation measures, such as spatially or temporally imposed noise reductions, are likely to be the most practical noise-reduction approaches from a management perspective. Therefore, I concluded this investigation by tailoring and testing a noise-mitigation scheme designed to provide the most benefit to the population-level outputs using the most practical approach. Focusing on spatial implementation in specific regions first, I found that noise reductions in coastal regions provided the best population-level outcomes. Subsequently, I focused noise reductions to cover time periods with the highest amount of noise impacts and found that noise reductions in the summer and autumn months significantly improved population-level abundance compared to runs without management intervention. This model does not take the place of experimental evidence and should instead be viewed as a complementary tool. However, Chapters Four and Five demonstrate the practical application, from start to finish, of using IBMs for the exploration of anthropogenic noise impacts on fish populations. Additionally, Appendix B provides a standardised overview of the updated IBM that was previously developed by Walker *et al.* (2020) and updated by Watson *et al.* (2022). This TRACE document follows a general framework for documenting a model’s rationale, design, and testing, and is now considered a standard for good modelling practice (Grimm *et al.* 2014). Therefore, I focused on the implementation of noise maps and impacts within the model, the rationale behind specific decisions within the model, and provided testing of how the model performs when updated to include noise pollution and associated impacts.

6.3 Future Research

Chapters Two and Three concern the short-term impacts of anthropogenic noise on free-ranging marine organisms. However, potential changes in responses following long-term exposure to anthropogenic noise—as a result of, for example, habituation or sensitisation—remain unclear, especially in free-ranging animals (Chapter One, Section 1.5). Therefore, a growing number of noise studies are incorporating both short- and long-term responses to noise disturbances. For example, Kok *et al.* (2021) investigated both the short- and long-term impacts of motorboat-noise playback on antipredator behaviour in free-ranging sand gobies *Pomatoschistus minutus*. They found interacting short- and long-term levels of disturbance to noise playback, where absence/avoidance of the experimental area was significantly altered during both levels of noise exposure (short- and long-term), indicating a decreased magnitude of antipredator responses compared to silent control (Kok *et al.* 2021). Similarly, follow-up studies that build on the research presented in Chapters Two and Three would benefit from the incorporation of short- and long-term noise treatments.

Additionally, Chapters Two and Three focused on the impacts of anthropogenic noise to coral reef inhabitants, an area of research that is growing but may still be considered underexplored (Ferrier-Pages *et al.* 2021). In both chapters, I use study systems, namely nests and cleaning stations, where discrete locations can be revisited and retested to facilitate a matched experimental design. In particular, the static study system used in Chapter Three proved crucial for observing noise-induced changes to community structures near ecologically important *A. pedersoni* cleaning stations. However, to grasp fully the extent to which noise impacts coral reef taxa and communities, study systems that allow for experimental testing of impacts of noise on more mobile species are also needed. For example, recent advancements for measuring field metabolic rates (FMR) in teleost fish may offer a potential avenue for researchers to explore individual and population-level responses to environmental stressors, such as anthropogenic noise (Chung *et al.* 2019). Furthermore, *in vivo* electronic monitoring systems (e.g., implanted nanosensors) are novel and promising technologies for obtaining information about free-ranging aquatic animals (Lee *et al.* 2019; Yang *et al.* 2021). These implanted sensors can offer real-time monitoring of physiology (e.g., electrocardiogram, electromyogram), behaviour (e.g., telemetry, activity level, tail beat frequency), and the ambient environment (e.g., temperature, pressure, and potentially noise levels) (Yang *et al.* 2021). Consequently, these emerging technologies could facilitate studying the impacts of anthropogenic noise on mobile coral reef species and would also be particularly beneficial in examining impacts on entire communities.

In Chapter Two, I demonstrated that introducing an ‘acoustic buffer zone’ (i.e., speed and distance limitations) negated behavioural impacts observed in nesting male damselfish during noisier conditions. Consequently, further research is needed to tease apart and pinpoint the most important aspects of this noise-mitigation strategy, and noise reduction in general, that would provide the most benefits to aquatic organisms (e.g., speed, distance, and/or exposure time). Additionally, while not directly tested, lessons learned from Chapter Two could be applied in the context of Chapter Three, where acoustic disturbance was evidenced to be a potential mechanism for the negative impacts of diver presence on marine life. Consequently, decision-makers and managers within the diving industry may consider implementing distance and exposure limits aimed at reducing acoustic disturbance of divers to protect vulnerable coral reef communities and habitats. Ultimately, it is unlikely that general human presence and use of marine and coastal habitats will decrease in the future (Merchant 2019; Duarte *et al.* 2021). Therefore, noise-reduction technologies and solutions—that are proven scientifically to benefit wildlife—should be considered to be the most practical approach to managing noise pollution in our oceans.

While informed by evidence and supported by previous modelling applications (Soudijn *et al.* 2020), the IBM presented in Chapter Four relies on several assumptions due to knowledge gaps within the anthropogenic noise literature. For example, there exists a paucity of concrete evidence on the ultimate fitness consequences of noise (i.e., impacts on growth, survival, and reproduction) that translate easily to assessments of population viability and overall ecosystem functioning (Weilgart 2018). While an increasing number of studies have considered such vital rates over larger spatiotemporal scales, results thus far remain inconclusive and species-specific (Kunc *et al.* 2016; Duarte *et al.* 2021). Similar to considerations for sensitisation/habituation, future research should also consider the effects of short- and long-term sound exposure across different life-stages. Equally, the effects of seasonal and spatiotemporal variations on individual biological responses to noise remain unknown (Soudijn *et al.* 2020; Ferrier-Pages *et al.* 2021). A better understanding of these nuances regarding anthropogenic noise impacts would help fine-tune the model to evaluate population-level responses better.

In Chapter Five, I use the updated IBM to explore the population-level impacts of anthropogenic noise to the northern European sea bass stock, and also critically assess potential noise-mitigation approaches. The applications shown in this chapter demonstrate the significant contributions IBMs can make in the assessment and simulation of underwater noise impacts on marine animals (Mortensen *et al.* 2021). Outside of improvements to the model itself, the implications are extensive for future research and investigation using this, and similar, models to explore the broader impacts of anthropogenic noise to marine life. For example, this IBM only considers the impacts of one stressor to a population of a single species of fish. Multiple stressors may compound effects or interacting stocks may compete or predate on one another (Boyd *et al.* 2020a; Spence *et al.* 2021), limiting applicability of conventional single-species models. Therefore, multi-stressor (Boyd *et al.* 2020a) and multi-species (Spence *et al.* 2021) models are increasingly employed to consider and account for these factors, and future noise-related IBM iterations should strive to include these additional elements.

6.4 Managing noise pollution in our oceans

6.4.1 Public awareness and international governance

Compared to urban and terrestrial environments, there exists little public concern and corresponding legislation to address noise pollution in the marine environment, and regulations that do exist are voluntary or weakly enforced (Lewandowski & Staaterman 2020). This is perhaps due to a lack of ‘ocean literacy’ among the general public (Worm *et al.* 2021). However, in the last decade, environmental issues have become a major topic of public opinion and people have begun to develop increasing environmental awareness, this is especially apparent among younger generations (Calculli *et al.* 2021). Social and mass media have become powerful tools for spotlighting specific environmental issues, as was the case with single-use plastics following the release of the BBC *Blue Planet II* docuseries. In fact, a report by GlobalWebIndex found that 53% of people surveyed in the US and UK reduced single-use plastic consumption in the 12 months following the release of *Blue Planet II* (GlobalWebIndex 2019). However, it remains unclear whether *Blue Planet II* was proactive in influencing environmental preferences and choices made by individuals or whether reductions in single-use plastics were driven by changes made by businesses and governments that were pressured to act (Schnurr *et al.* 2018). Consequently, researchers fascinated by this phenomenon have yet to unpick the direct links between the series and environmental preferences by individuals, for example willingness to pay for marine conservation (Hynes *et al.* 2021) and plastic consumption (Dunn *et al.* 2020). Regardless, it is unlikely that underwater noise pollution will receive the same public outcry and media attention that was attributed to single-use plastics, thus more than increasing public awareness alone may be required to drive noise abatement in our oceans. Instead, positive outcomes are more likely to stem from carefully considered legislative action—underpinned by scientific evidence—and effective enforcement.

From an ocean governance perspective, a first line of action is investment into the research that underpins legislation (Ferrier-Pages *et al.* 2021). For instance, the 19th meeting of the United Nations encouraged studies on the impacts of ocean noise on marine living resources (UN 2018). In European waters, noise levels are a criterion used to determine the ecological status of habitats and certain anthropogenic underwater sounds are classified as noise pollution in the European Commission Marine Strategy Framework Directive (MSFD; Tasker *et al.* 2010). However, Lewandowski & Staaterman (2020) found that the MSFD was the only major international agreement (out of 10) that made firm commitments to addressing noise pollution; the rest were vague and voluntary in nature. In their review, the authors attempt to address this legislative inefficiency by identifying topical areas for collaboration and focusing on building collaborative processes that are designed to reach effective and lasting solutions (Lewandowski & Staaterman 2020). Ultimately, international cooperation on the issue of anthropogenic noise is complex and typically operates within an environment of conflict. Therefore, creative solutions and compromise will be needed to move forward with tractable changes.

6.4.2 Noise abatement via technology and design

As stated in Chapter One, and shown in Chapter Five, the most effective way of reducing the impacts of anthropogenic noise to wildlife is through noise abatement (i.e., lessening the amount of noise pollution entering the marine environment), either by reducing noise emitted at the source or by reducing the amount of noise-generating activity. Because marine-resource use and associated activity is likely to increase in the future, Merchant (2019) suggested that noise-abatement measures, such as technological/design augmentations, may be incentivised through existing management strategies, such as command and control (CAC; Cole & Grossman 1999) and market-based measures (MBM; Perman *et al.* 2011). The most appropriate and effective management policy option will vary according to industry-specific considerations. While it is possible that positive changes could be implemented via mandated standards (i.e., CAC) or market/economic incentives (i.e., MBM), such management measures to reduce noise pollution remain scarce (Merchant 2019).

Impulsive sounds, such as pile-driving and seismic air gun surveys for the oil and gas industry, pose a particularly dangerous threat to marine organisms (Carroll *et al.* 2017). There is evidence of benefits to noise-mitigation procedures specific to these practices, such as spatiotemporal restrictions (e.g., halting activity if a marine mammal is detected within a specified exclusion radius; JNCC 2017) or the introduction of additional, pre-emptive noise (e.g., acoustic deterrent devices (ADDs) or ‘ramp-up’ procedures prior to activities; Neo *et al.* 2016; JNCC 2017). However, these mitigation measures are targeted at protecting particular (protected) species or taxonomic groups, and therefore do not address effects on other taxa, nor the cumulative and long-term effects of repeated exposure from multiple sources (Merchant 2019). Instead, there are technological alternatives to both practices—for example, vibratory pile driving (vibropiling) and marine vibroseis survey systems—that produce less noise and support noise-abatement in the oceans. Although alternative methods have been successfully trialled and proven to provide the same desired outcomes, they are not presently in wide commercial use, likely due to a lack of requirement in current legislation (Merchant 2019).

With regards to vessel noise, which is the most widespread and persistent source of underwater noise (Hildebrand 2009; Frisk 2012), noise from propeller cavitation can be reduced by modifying propellor and/or hull design (IMO 2014). Three recent studies conducted on the Great Barrier Reef (Jain-Schlaepfer *et al.* 2018; McCormick *et al.* 2018, 2019) successfully reduced or negated biological responses to motorboat noise in embryonic and juvenile fish by switching to quieter engines. Consequently, vessel noise might be reduced by implementing quieter machinery or by reducing noise transmission through the hull (IMO 2014). Moreover, regularly enforced vessel inspection and maintenance of the propeller and hull may achieve modest noise reductions, as noise can be exacerbated by poor vessel maintenance (e.g., marine fouling or damage to the propeller/hull; WHOI 1952). However, retrofitting quieting technologies to existing vessels is more costly and less effective than quieting in the design stage (Spence & Fischer 2017), which could be achieved through mandated standards (CAC) or economic incentives (MBM).

6.4.3 Simple, accessible noise-mitigation approaches

In Chapter Two, I found that motorboat noise adversely affected parental behaviour of Ambon damselfish, and found release of negative effects by implementing simple speed and distance restrictions near reef edges (20–120 m; McCloskey *et al.* 2020). These results suggested that distance and speed could be used as potential avenues for the mitigation of noise impacts on coral reef organisms. In fact, the concept of adjusting distances and speed to limit damaging anthropogenic noise exposure has been successfully employed and enforced to protect at-risk marine mammal populations, such as the critically endangered southern resident killer whales *Orcinus orca* (Williams *et al.* 2019). However, slower vessels take longer to transit, leading to a potential trade-off between duration and intensity of noise exposure to wildlife, but this trade-off can potentially be optimised (McKenna *et al.* 2013). Along the same lines, incentivising vessels to travel in convoy may reduce cumulative noise levels since quieter vessels within the convoy may be ‘masked’ by their noisier counterparts (Heise *et al.* 2017). Ultimately, there is enough evidence that anthropogenic noise harms marine life to prompt action and management (Shannon *et al.* 2016; Kunc &

Schmidt 2019; Duarte *et al.* 2021), and the use of simple, accessible noise-mitigation measures that focus principally on reducing noise-exposure levels, present important opportunities to reduce the detrimental impacts of noise on wildlife.

6.4.4 Acoustic monitoring and spatial risk assessments

Generally, a broader understanding of baseline levels of ambient noise, both spatially and temporally, would help better regulate and protect marine habitats. The acoustic projections used in Chapters Four and Five are some of the more advanced spatiotemporal estimations of noise levels currently available (Farcas *et al.* 2020). These maps, developed by Cefas, use sAIS ship-tracking data along with sound-propagation characteristics of the environment to demonstrate the importance of including acoustic modelling into marine spatial planning. Furthermore, there are plans to extend these applications across longer time periods and at varying spatial scales to assess trends and develop a deeper understanding of noise pollution in the marine environment. Building on the success of this research, it would be beneficial for future applications to incorporate other types of noise sources (e.g., wind farms, construction, and seismic surveys) to develop a more comprehensive picture of marine noise. Additionally, the maps developed by Farcas *et al.* (2020) target large shipping vessels, and it would be beneficial if similar approaches were applied at local scales to monitor small motorboat activity. Smaller craft are particularly pervasive in coastal areas, typically accessing areas of high biodiversity for recreation and/or exploitation, thus exposing particular ecosystems (e.g., coral reefs) to anthropogenic noise. Therefore, it is important to monitor boating activities, and associated noise, in particularly sensitive areas (Venturini *et al.* 2021).

The maps provided by Farcas *et al.* (2020) also offer a unique opportunity for large-scale risk assessment and are therefore a first step towards determining areas that may require better noise protection. These maps, in conjunction with distribution maps of sensitive species, would benefit marine spatial planners in identifying areas to prioritise for mitigation and/or regulation (Erbe *et al.* 2014). This methodology could help assess cumulative and aggregate noise exposure in specific habitats and to associated wildlife. Furthermore, this may indicate sensitive time periods or high-risk habitats to prioritise monitoring, legislation, and protection. The identification of spatial and temporal risk could then help managers to employ tools discussed in this chapter (e.g., spatial exclusions or ‘acoustic buffer zones’). Similar risk-based management strategies have previously been suggested for commercial activities (Merchant *et al.* 2018). Already, noise features as a main consideration for the short-term planning of marine developments, such as the offshore construction of wind turbines, through environmental impact assessments (EIAs) (Oh *et al.* 2021). However, there is significantly less consideration of the long-term impacts of anthropogenic noise from windfarms and other major sources of underwater noise, such as vessels. Therefore, spatiotemporal maps, such as those created by Farcas *et al.* (2020), could help improve EIAs of noise for long-term development projects and maritime activity for the better protection of our marine environment.

6.5 Conclusions

As the human global population continues to rise, use of inshore and offshore waters will continue to increase. Consequently, it is imperative that we develop a comprehensive understanding of the impacts that anthropogenic noise can have on varying levels of biological organisation. In this thesis, I have explored the impacts of underwater noise to individuals, local communities, and populations using an integrated approach. Continued, holistic evaluation of anthropogenic noise impacts will greatly improve our understanding of how noise affects ecosystems and will help inform mitigation and management strategies used to safeguard marine fauna. Accordingly, I have endeavoured to incorporate and evaluate noise-mitigation methods and strategies, with the hope that these applications may provide managers and policymakers with the tools to underpin effective mitigation of noise and associated negative impacts on wildlife. Compared to other imposing threats to the marine environment (i.e., climate change and ocean acidification), underwater noise is a pollutant that we can realistically mitigate within the coming decades, given the right scientific evidence, management tools, and geopolitical will. Therefore, the current strides made towards mitigating underwater noise pollution are encouraging and will ultimately help alleviate some of the pressure and build resilience in increasingly threatened marine ecosystems.

References

Adams, S.M. (2003). Establishing causality between environmental stressors and effects on aquatic ecosystems. *Hum. Ecol. Risk Assess.*, 9, 17–35.

Aguilar de Soto, N., Gkikopoulou, K., Hooker, S., Isojunno, S., Johnson, M., Miller, P., Tyack, P., Wensveen, P., Donovan, C., Harris, C.M., Harris, D., Marshall, L., Oedekoven, C., Prieto, R. & Thomas, L. (2016). From physiology to policy: A review of physiological noise effects on marine fauna with implications for mitigation. *Proc. Meet. Acoust.*, 27, 040008

Albert, C., Künsch, H.R. & Scheidegger, A. (2015). A simulated annealing approach to approximate Bayes computations. *Stat. Comput.*, 25, 1217–1232.

Alves, D., Amorim, M.C.P. & Fonseca, P.J. (2017). Boat noise reduces acoustic active space in the lusitanian toadfish *Halobatrachus didactylus*. *Proc. Meet. Acoust.*, 27, 010033.

Amoser, S. & Ladich, F. (2003). Diversity in noise-induced temporary hearing loss in otophysine fishes. *J. Acoust. Soc. Am.*, 113, 2170–2179.

Andradi-Brown, D.A., Gress, E., Laverick, J.H., Monfared, M.A.A., Rogers, A.D. & Exton, D.A. (2018). Wariness of reef fish to passive diver presence with varying dive gear type across a coral reef depth gradient. *J. Mar. Biol. Assoc. U.K.*, 98, 1733–1743.

André, M., Solé, M., Lenoir, M., Durfort, M., Quero, C., Mas, A., Lombarte, A., Van Der Schaar, M., López-Bejar, M., Morell, M., Zaugg, S. & Houégnigan, L. (2011). Low-frequency sounds induce acoustic trauma in cephalopods. *Front. Ecol. Environ.*, 9, 489–493.

Annis, E.R., Houde, E.D., Harding, L.W., Mallonee, M.E. & Wilberg, M.J. (2011). Calibration of a bioenergetics model linking primary production to Atlantic menhaden *Brevoortia tyrannus* growth in Chesapeake Bay. *Mar. Ecol. Prog. Ser.*, 437, 253–267.

Armstrong, M. & Walmsley, S. (2012). *Life history estimates of natural mortality of sea bass around the UK*. Working Document IBP-NEW 2012 meeting. Cefas, Lowestoft, UK.

Au, W.W. & Hastings, M.C. (2008). *Principles of Marine Bioacoustics*. Springer, New York, NY, USA.

Balcomb, K.C. & Claridge, D.E. (2001). A mass stranding of cetaceans caused by naval sonar in the Bahamas. *Bahamas J. Sci.*, 8, 2–12.

Barber, J.R., Crooks, K.R. & Fristrup, K.M. (2010). The costs of chronic noise exposure for terrestrial organisms. *Trends Ecol. Evol.*, 25, 180–189.

Bates, D., Maechler, M., Bolker, B. & Walker, S. (2015). Fitting Linear Mixed-Effects Models Using lme4. *J. Stat. Softw.*, 1, 1–48.

Becker, J.H. & Grutter, A.S. (2004). Cleaner shrimp do clean. *Coral Reefs*, 23, 515–520.

van Beest, F.M., Kindt-Larsen, L., Bastardie, F., Bartolino, V. & Nabe-Nielsen, J. (2017). Predicting the population-level impact of mitigating harbor porpoise bycatch with pingers and time-area fishing closures. *Ecosphere*, 8, e01785.

Bejder, L., Samuels, A., Whitehead, H. & Gales, N. (2006). Interpreting short-term behavioural responses to disturbance within a longitudinal perspective. *Anim. Behav.*, 712, 1149–1158.

Benevides, L.J., Cardozo-Ferreira, G.C., Ferreira, C.E.L., Pereira, P.H.C., Pinto, T.K. & Sampaio, C.L.S. (2019). Fear-induced behavioural modifications in damselfishes can be diver-triggered. *J. Exp. Mar. Bio. Ecol.*, 514–515, 34–40.

Bennett, A.F. (1985). Temperature and muscle. *J. Exp. Biol.*, 115, 333–344.

Beraud, C., Van Der Molen, J., Armstrong, M., Hunter, E., Fonseca, L. & Hyder, K. (2018). The influence of oceanographic conditions and larval behaviour on settlement success—the European sea bass *Dicentrarchus labrax* (L.). *ICES J. Mar. Sci.*, 75, 455–470.

Bernier, N.J. (2006). The corticotropin-releasing factor system as a mediator of the appetite-suppressing effects of stress in fish. *Gen. Comp. Endocrinol.*, 146, 45–55.

Bhandiwad, A.A., Raible, D.W., Rubel, E.W. & Sisneros, J.A. (2018). Noise-induced hypersensitization of the acoustic startle response in larval zebrafish. *JARO - J. Assoc. Res. Otolaryngol.*, 19, 741–752.

Blom, E.L., Kvarnemo, C., Dekhla, I., Schöld, S., Andersson, M.H., Svensson, O. & Amorim, M.C.P. (2019). Continuous but not intermittent noise has a negative impact on mating success in a marine fish with paternal care. *Sci. Rep.*, 9, 1–9.

Blumer, L.S. (1982). A bibliography and categorization of bony fishes exhibiting parental care. *Zool. J. Linn. Soc.*, 76, 1–22.

Boyd, R., Thorpe, R., Hyder, K., Roy, S., Walker, N. & Sibly, R. (2020a). Potential Consequences of Climate and Management Scenarios for the Northeast Atlantic Mackerel Fishery. *Front. Mar. Sci.*, 7, 5494.

Boyd, R., Walker, N., Hyder, K., Thorpe, R., Roy, S. & Sibly, R. (2020b). SEASIM-NEAM: A spatially-Explicit Agent-based SIMulator of North East Atlantic Mackerel population dynamics. *MethodsX*, 7, 101044.

Branconi, R., Wong, M.Y.L. & Buston, P.M. (2019). Comparison of efficiency of direct observations by scuba diver and indirect observations via video camera for measuring reef-fish behaviour. *J. Fish Biol.*, 94, 490–498.

van Bree, P. & Kristensen, I. (1974). On the intriguing stranding of four Curvier’s beaked whales, *Ziphius cavirostris* G. Curvier, 1823, on the Lesser Antillean Island of Bonaire. *Bijdr. tot Dierkd.*, 44, 235–238.

Brochier, T., Ecoutin, J.M., De Morais, L.T., Kaplan, D.M. & Lae, R. (2013). A multi-agent ecosystem model for studying changes in a tropical estuarine fish assemblage within a marine protected area. *Aquat. Living Resour.*, 26, 147–158.

Bruintjes, R., Armstrong-smith, E., Jones, D., Renshaw, E., Rossington, K. & Simpson, S.D. (2014). A tool to predict the impact of anthropogenic noise on fish. *2nd International Conference on Environmental Interactions of Marine Renewable Energy Technologies*. Stornoway, Isle of Lewis, Outer Hebrides, Scotland.

Bruintjes, R., Purser, J., Everley, K.A., Mangan, S., Simpson, S.D. & Radford, A.N. (2016a). Rapid recovery following short-term acoustic disturbance in two fish species. *R. Soc. Open Sci.*, 3, 150686.

Bruintjes, R. & Radford, A.N. (2013). Context-dependent impacts of anthropogenic noise on individual andsocial behaviour in a cooperatively breeding fish. *Anim. Behav.*, 85, 1343–1349.

Bruintjes, R. & Radford, A.N. (2014). Chronic playback of boat noise does not impact hatching success or post-hatching larval growth and survival in a cichlid fish. *PeerJ*, 2, e594.

Bruintjes, R., Simpson, S.D., Harding, H., Bunce, T., Benson, T., Rossington, K., Bruintjes, R., Wallingford, H.R., Park, H., Simpson, S.D., Benson, T., Rossington, K. & Jones, D. (2016b). The impact of experimental impact pile driving on oxygen uptake in black seabream and plaice. *Proc. Meet. Acoust.*, 27, 010042.

Burgess, M.G., Carrella, E., Drexler, M., Axtell, R.L., Bailey, R.M., Watson, J.R., Cabral, R.B., Clemence, M., Costello, C., Dorsett, C., Gaines, S.D., Klein, E.S., Koralus, P., Leonard, G., Levin, S.A., Little, L.R., Lynham, J., Madsen, J.K., Merkl, A., *et al.* (2020). Opportunities for agent-based modelling in human dimensions of fisheries. *Fish Fish.*, 21, 570–587.

Buxton, R., McKenna, M., Mennitt, D., Fristrup, K., Crooks, K., Angeloni, L. & Wittemyer, G. (2017). Noise pollution is pervasive in U.S. protected areas. *Science*, 356, 531–533.

Cabral, R.B., Geronimo, R.C., Lim, M.T. & Aliño, P.M. (2010). Effect of variable fishing strategy on fisheries under changing effort and pressure: An agent-based model application. *Ecol. Modell.*, 221, 362–369.

Calculli, C., D'Uggento, A.M., Labarile, A. & Ribecco, N. (2021). Evaluating people's awareness about climate changes and environmental issues: A case study. *J. Clean. Prod.*, 324, 129244.

Campbell, J., Shafiei Sabet, S. & Slabbekoorn, H. (2019). Particle motion and sound pressure in fish tanks: A behavioural exploration of acoustic sensitivity in the zebrafish. *Behav. Processes*, 164, 38–47.

Carroll, A.G., Przeslawski, R., Duncan, A., Gunning, M. & Bruce, B. (2017). A critical review of the potential impacts of marine seismic surveys on fish & invertebrates. *Mar. Poll. Bull.*, 114, 9–24.

Casper, B.M., Halvorsen, M.B., Matthews, F., Carlson, T.J. & Popper, A.N. (2013). Recovery of barotrauma injuries resulting from exposure to pile driving sound in two sizes of hybrid striped bass. *PLoS One*, 8, e73844.

Casper, B.M., Popper, A.N., Matthews, F., Carlson, T.J. & Halvorsen, M.B. (2012). Recovery of barotrauma injuries in Chinook salmon, *Oncorhynchus tshawytscha* from exposure to pile driving sound. *PLoS One*, 7, e39593.

Caves, E.M., Green, P.A. & Johnsen, S. (2018). Mutual visual signalling between the cleaner shrimp *Ancylomenes pedersoni* and its client fish. *Proc. R. Soc. B Biol. Sci.*, 285, 20180800.

Celi, M., Filiciotto, F., Vazzana, M., Arizza, V., Maccarrone, V., Ceraulo, M., Mazzola,

S. & Buscaino, G. (2015). Shipping noise affecting immune responses of European spiny lobster (*Palinurus elephas*). *Can. J. Zool.*, 93, 113–121.

Celi, M., Filiciotto, F., Maricchiolo, G., Genovese, L., Quinci, E.M., Maccarrone, V., Mazzola, S., Vazzana, M. & Buscaino, G. (2016). Vessel noise pollution as a human threat to fish: assessment of the stress response in gilthead sea bream (*Sparus aurata*, Linnaeus 1758). *Fish Physiol. Biochem.*, 42, 631–641.

Cenek, M. & Franklin, M. (2017). An adaptable agent-based model for guiding multi-species Pacific salmon fisheries management within a SES framework. *Ecol. Modell.*, 360, 132–149.

Cerdá, J., Carrillo, M., Zanuy, S., Ramos, J. & de la Higuera, M. (1994). Influence of nutritional composition of diet on sea bass, *Dicentrarchus labrax* L., reproductive performance and egg and larval quality. *Aquaculture*, 128, 345–361.

Chambers, J., Hastie, T. & Hastie, T. (1992). *Statistical Models in S*. Wadsworth & Brooks/Cole Advanced Books & Software.

Chan, A.A.Y.H., Giraldo-Perez, P., Smith, S. & Blumstein, D.T. (2010). Anthropogenic noise affects risk assessment and attention: The distracted prey hypothesis. *Biol. Lett.*, 6, 458–461.

Chapuis, L. & Bshary, R. (2009). Strategic adjustment of service quality to client identity in the cleaner shrimp, *Periclimenes longicarpus*. *Anim. Behav.*, 78, 455–459.

Cheney, K.L. & Côté, I.M. (2001). Are Caribbean cleaning symbioses mutualistic? Costs and benefits of visiting cleaning stations to longfin damselfish. *Anim. Behav.*, 62, 927–933.

Chitre, M., Legg, M. & Koay, T. (2012). Snapping shrimp dominated natural soundscape in Singapore waters. *Contrib. to Mar. Sci.*, 127–134.

Chung, M.T., Trueman, C.N., Godiksen, J.A., Holmstrup, M.E. & Grønkjær, P. (2019). Field metabolic rates of teleost fishes are recorded in otolith carbonate. *Commun. Biol.*, 2, 24.

Cinner, J. (2014). Coral reef livelihoods. *Curr. Opin. Environ. Sustain.*, 7, 65–71.

Clack, J.A. (2002). Patterns and processes in the early evolution of the tetrapod ear. *J. Neurobiol.*, 53, 251–264.

Clague, G.E., Cheney, K.L., Goldizen, A.W., McCormick, M.I., Waldie, P.A. & Grutter, A.S. (2011). Long-term cleaner fish presence affects growth of a coral reef fish. *Biol. Lett.*, 7, 863–865.

Claireaux, G., Couturier, C. & Groison, A.L. (2006). Effect of temperature on maximum swimming speed and cost of transport in juvenile European sea bass (*Dicentrarchus labrax*). *J. Exp. Biol.*, 209, 3420–3428.

Cole, D.H. & Grossman, P.Z. (1999). When is command-and-control efficient? Institutions, technology, and the comparative efficiency of alternative regulatory regimes for environmental protection. *J. Econ. Issues*, 519, 887–938.

Cooke, S.C., Balmford, A., Donald, P.F., Newson, S.E. & Johnston, A. (2020a). Roads as a contributor to landscape-scale variation in bird communities. *Nat. Commun.*, 11, 3125.

Cooke, S.C., Balmford, A., Johnston, A., Newson, S.E. & Donald, P.F. (2020b). Variation in abundances of common bird species associated with roads. *J. Appl. Ecol.*, 57, 1271–1282.

Cox, K., Brennan, L.P., Gerwing, T.G., Dudas, S.E. & Juanes, F. (2018). Sound the alarm: A meta-analysis on the effect of aquatic noise on fish behavior and physiology. *Glob. Chang. Biol.*, 24, 3105–3116.

Curtin, R. & Prellezo, R. (2010). Understanding marine ecosystem based management: A literature review. *Mar. Policy*, 34, 821–830.

Curtin, S. & Garrod, B. (2008). Vulnerability of marine mammals to diving tourism activities. In: *New frontiers in marine tourism: Diving experiences, sustainability, management*. pp. 93–113.

Dahl, P.H. (2015). The underwater sound field from impact pile driving and its potential effects on marine life. *Acoust. Today*, 11, 18–25.

Davenport, J. & Davenport, J.L. (2006). The impact of tourism and personal leisure transport on coastal environments: A review. *Estuar. Coast. Shelf Sci.*, 67, 280–292.

DeAngelis, D.L. & Grimm, V. (2014). Individual-based models in ecology after four decades. *F1000Prime Rep.*, 6, 39.

Debusschere, E., Coensel, B. De, Bajek, A., Botteldooren, D., Hostens, K., Vanaverbeke, J., Vandendriessche, S., Ginderdeuren, K. Van, Vincx, M. & Degraer, S. (2014). *In situ* mortality experiments with juvenile sea bass (*Dicentrarchus labrax*) in relation to impulsive sound levels caused by pile driving of windmill foundations. *PLoS One*, 9, e109280.

Duarte, C.M., Chapuis, L., Collin, S.P., Costa, D.P., Devassy, R.P., Eguiluz, V.M., Erbe, C., Gordon, T.A.C., Halpern, B.S., Harding, H.R., Havlik, M.N., Meekan, M., Merchant, N.D., Miksis-Olds, J.L., Parsons, M., Predragovic, M., Radford, A.N., Radford, C.A., Simpson, S.D., Slabbekoorn, H., Staaterman, E., Van Opzeeland, I.C., Winderen, J., Zhang, X. & Juanes, H. (2021). The soundscape of the Anthropocene ocean. *Science*, 371, eaba4658.

Dunn, M.E., Mills, M. & Veríssimo, D. (2020). Evaluating the impact of the documentary series *Blue Planet II* on viewers' plastic consumption behaviors. *Conserv. Sci. Pract.*, 2, e280.

Dutta, R., Schoengens, M., Onnela, J.P. & Mira, A. (2017). ABCpy: A user-friendly, extensible, and parallel library for approximate Bayesian computation. In *Proceedings of PASC '17, Lugano, Switzerland, June 26-28, 2017,* 9 pages.

Emslie, M.J. & Jones, G.P. (2001). Patterns of embryo mortality in a demersally spawning coral reef fish and the role of predatory fishes. *Environ. Biol. Fishes*, 60, 363–373.

Erbe, C., Reichmuth, C., Cunningham, K., Lucke, K. & Dooling, R. (2016). Communication masking in marine mammals: A review and research strategy. *Mar. Pollut. Bull.*, 103, 15–38.

Erbe, C., Williams, R., Sandilands, D. & Ashe, E. (2014). Identifying modeled ship noise hotspots for marine mammals of Canada's Pacific region. *PLoS One*, 9, e89820.

Fakan, E.P. & McCormick, M.I. (2019). Boat noise affects the early life history of two damselfishes. *Mar. Pollut. Bull.*, 141, 493–500.

FAO. (2020). *The state of world fisheries and aquaculture 2020*. Sustainability in action. Food and Agricultural Organisation of the United Nations, Rome.

Farcas, A., Powell, C.F., Brookes, K.L. & Merchant, N.D. (2020). Validated shipping noise maps of the Northeast Atlantic. *Sci. Total Environ.*, 735, 139509.

Fay, R. (2009). Soundscapes and the sense of hearing of fishes. *Integr. Zool.*, 4, 26–32.

Fazio, F., Filiciotto, F., Marafioti, S., Di Stefano, V., Assenza, A., Placenti, F., Buscaino, G., Piccione, G. & Mazzola, S. (2012). Automatic analysis to assess haematological parameters in farmed gilthead sea bream (*Sparus aurata* Linnaeus, 1758). *Mar. Freshw. Behav. Physiol.*, 45, 63–73.

Ferrari, M.C.O., Mccormick, M.I., Meekan, M.G., Simpson, S.D., Nedelec, S.L. & Chivers, D.P. (2018). School is out on noisy reefs: the effect of boat noise on predator learning and survival of juvenile coral reef fishes. *Proc. R. Soc. B Biol. Sci.*, 285, 20180033.

Ferrier-Pages, C., Leal, M., Ricardo Calado, R., Schmid, D., Bertucci, F., Lecchini, D. & Allemand, D. (2021). Noise pollution on coral reefs? — A yet underestimated threat to coral reef communities. *Mar. Pollut. Bull*., 165, 112129.

Filiciotto, F., Vazzana, M., Celi, M., Maccarrone, V., Ceraulo, M., Buffa, G., Di Stefano, V., Mazzola, S. & Buscaino, G. (2014). Behavioural and biochemical stress responses of *Palinurus elephas* after exposure to boat noise pollution in tank. *Mar. Pollut. Bull.*, 84, 104–114.

Filiciotto, F., Vazzana, M., Celi, M., Maccarrone, V., Ceraulo, M., Buffa, G., Arizza, V., de Vincenzi, G., Grammauta, R., Mazzola, S. & Buscaino, G. (2016). Underwater noise from boats: Measurement of its influence on the behaviour and biochemistry of the common prawn (*Palaemon serratus*, Pennant 1777). *J. Exp. Mar. Biol. Ecol*., 478, 24–33.

Figueira, W.F. & Lyman, S.J. (2007). Context-dependent risk tolerance of the bicolour damselfish: courtship in the presence of fish and egg predators. *Anim. Behav.*, 74, 329–336.

Francis, C.D. & Barber, J.R. (2013). A framework for understanding noise impacts on wildlife: an urgent conservation priority. *Front. Ecol. Environ.*, 11, 305–313.

Francis, C.D., Ortega, C.P. & Cruz, A. (2009). Noise pollution changes avian communities and species interactions. *Curr. Biol.*, 19, 1415–1419.

Friard, O. & Gamba, M. (2016). BORIS: a free, versatile open-source event-logging software for video/audio coding and live observations. *Methods Ecol. Evol.*, 7, 1325–1330.

Frisk, G. V. (2012). Noiseonomics: The relationship between ambient noise levels in the sea and global economic trends. *Sci. Rep.*, 2, 437.

Froese, R. & Pauly, D. (2017). Fishbase. *World Wide Web Electron. Publ.*, 02/2017.

GBRMPA. (2014). *Great barrier reef outlook report 2014*. Great Barrier Reef Marine Park Authority, Townsville, Austrailia.

Giglio, V.J., Blumstein, D.T., Motta, F.S. & Pereira-Filho, G.H. (2022). Diver presence increases egg predation on a nesting damselfish. *J. Exp. Mar. Bio. Ecol.*, 549, 151694.

Gillooly, J.F., Allen, A.P., Savage, V.M., Charnov, E.L., West, G.B. & Brown, J.H. (2006). Response to Clarke and Fraser: effects of temperature on metabolic rate. *Funct. Ecol.*, 20, 400–404.

Gilpin, J.A. & Chadwick, N.E. (2017). Life-history traits and population structure of pederson cleaner shrimps *Ancylomenes pedersoni*. *Biol. Bull.*, 233, 190–205.

GlobalWebIndex. (2019). *Sustainable packaging unwrapped*. GWI, London, UK.

Gordon, T.A.C., Harding, H.R., Clever, F.K., Davidson, I.K., Davison, W., Montgomery, D.W., Weatherhead, R.C., Windsor, F.M., Armstrong, J.D., Bardonnet, A., Bergman, E., Britton, J.R., Côté, I.M., D’agostino, D., Greenberg, L.A., Harborne, A.R., Kahilainen, K.K., Metcalfe, N.B., Mills, S.C., Milner, N.J., Mittermayer, F.H., Montorio, L., Nedelec, S.L., Prokkola, J.M., Rutterford, L.A., Salvanes, A.G., Simpson, S.D., Vainikka, A., Pinnegar, J.K. & Santos, E.M. (2018). Fishes in a changing world: learning from the past to promote sustainability of fish populations. *J. Fish Biol.*, 92, 804–827.

Götz, T. & Janik, V.M. (2011). Repeated elicitation of the acoustic startle reflex leads to sensitisation in subsequent avoidance behaviour and induces fear conditioning. *BMC Neurosci.*, 12, 30.

Graham, A. & Cook, S. (2008). The effects of noise disturbance from various recreational boating activities common to inland waters on cardiac physiology of a freshwater fish, the largemouth bass (*Micropterus salmoides*). *Aquat. Conserv. Mar. Freshw. Ecosyst.*, 656, 636–656.

Green, B.S., Anthony, K.R.N. & McCormick, M.I. (2006). Position of egg within a clutch is linked to size at hatching in a demersal tropical fish. *J. Exp. Mar. Bio. Ecol.*, 329, 144–152.

Grimm, V., Augusiak, J., Focks, A., Frank, B.M., Gabsi, F., Johnston, A.S.A., Liu, C., Martin, B.T., Meli, M., Radchuk, V., Thorbek, P. & Railsback, S.F. (2014). Towards better modelling and decision support: Documenting model development, testing, and analysis using TRACE. *Ecol. Modell.*, 280, 129–139.

Grimm, V., Berger, U., Bastiansen, F., Eliassen, S., Ginot, V., Giske, J., Goss-Custard, J., Grand, T., Heinz, S.K., Huse, G., Huth, A., Jepsen, J.U., Jørgensen, C., Mooij, W.M., Pe, G., Piou, C., Railsback, S.F., Robbins, A.M., Robbins, M.M., Rossmanith, E., Rüger, N., Strand, E., Souissi, S., Stillman, R.A., Vabø, R., Visser, U. & DeAngelis, D.L. (2006). A standard protocol for describing individual-based and agent-based models. *Ecol. Modell.*, 198, 115–126

Grimm, V., Berger, U., DeAngelis, D.L., Polhill, J.G., Giske, J. & Railsback, S.F. (2010). The ODD protocol: A review and first update. *Ecol. Modell.*, 221, 2760–2768.

Grimm, V. & Railsback, S.F. (2005). *Individual-based Modeling and Ecology*. Princeton University Press. Princeton, New Jersey, USA.

Grimm, V., Railsback, S.F., Vincenot, C.E., Berger, U., Gallagher, C., Deangelis, D.L., Edmonds, B., Ge, J., Giske, J., Groeneveld, J., Johnston, A.S.A., Milles, A., Nabe-Nielsen, J., Polhill, J.G., Radchuk, V., Rohwäder, M.S., Stillman, R.A., Thiele, J.C. & Ayllón, D. (2020). The ODD protocol for describing agent-based and other simulation models: A second update to improve clarity, replication, and structural realism. *JASSS*, 23, 7.

de Groot, R., Brander, L., van der Ploeg, S., Costanza, R., Bernard, F., Braat, L., Christie, M., Crossman, N., Ghermandi, A., Hein, L., Hussain, S., Kumar, P., McVittie, A., Portela, R., Rodriguez, L.C., ten Brink, P. & van Beukering, P. (2012). Global estimates of the value of ecosystems and their services in monetary units. *Ecosyst. Serv.*, 1, 50–61.

Gross, M.R. & MacMillan, A.M. (1981). Predation and the evolution of colonial nesting in bluegill sunfish (*Lepomis macrochirus*). *Behav. Ecol. Sociobiol.*, 8, 163–174.

Gross, M.R. & Sargent, R.C. (1985). The evolution of male and female parental care in fishes. *Am. Zool.*, 25, 807–822.

Grutter, A.S. (1999). Cleaner fish really do clean. *Nature*, 398, 672–673.

Grutter, A.S., Murphy, J.M. & Choat, J.H. (2003). Cleaner fish drives local fish diversity on coral reefs. *Curr. Biol.*, 13, 64–67.

Hale, R. & Mary, C.M.S. (2007). Nest tending increases reproductive success, sometimes: environmental effects on paternal care and mate choice in flagfish. *Anim. Behav.*, 74, 577–588.

Haley, M.P. & Müller, C.R. (2002). Territorial behaviour of beaugregory damselfish (*Stegastes leucostictus*) in response to egg predators. *J. Exp. Mar. Bio. Ecol.*, 273, 151–159.

Halouani, G., Le Loc'h, F., Shin, Y.J., Velez, L., Hattab, T., Romdhane, M.S. & Ben Rais Lasram, F. (2019). An end-to-end model to evaluate the sensitivity of ecosystem indicators to track fishing impacts. *Ecol. Indic.*, 98, 121–130.

Halvorsen, M.B., Casper, B.M., Matthews, F., Carlson, T.J. & Popper, A.N. (2012a). Effects of exposure to pile-driving sounds on the lake sturgeon, Nile tilapia and hogchoker. *Proc. R. Soc. B Biol. Sci.*, 279, 4705–4714.

Halvorsen, M.B., Casper, B.M., Woodley, C.M., Carlson, T.J. & Popper, A.N. (2012b). Threshold for onset of injury in chinook salmon from exposure to impulsive pile driving sounds. *PLoS One*, 7, e38968.

Harding, H., Eastcott, E., Radford, A., Gordon, T. & Simpson, S. (2019). Causes and consequences of intraspecific variation in animal responses to anthropogenic noise. *Behav. Ecol.*, 30, 1501–1511.

Harding, H., Gordon, T., Havlik, M., Predragovic, M., Devassy, R., Radford, A., Simpson, S. & Duarte, C. (2021). A systematic literature assessment on the effects of human-altered soundscapes on marine life [Data set].

Harding, H.R., Gordon, T.A.C., Hsuan, R.E., Mackaness, A.C.E., Radford, A.N. & Simpson, S.D. (2018). Fish in habitats with higher motorboat disturbance show reduced sensitivity to motorboat noise. *Biol. Lett.*, 14, 20180441.

Hartman, E.J. & Abrahams, M. V. (2000). Sensory compensation and the detection of predators: the interaction between chemical and visual information. *Proc. R. Soc.*

B Biol. Sci., 267, 571–575.

Hastings, M.C., Popper, A.N., Finneran, J.J. & Lanford, P.J. (1996). Effects of low-frequency underwater sound on hair cells of the inner ear and lateral line of the teleost fish Astronotus ocellatus . *J. Acoust. Soc. Am.*, 99, 1759–1766.

Hawkins, A.D., Pembroke, A.E. & Popper, A.N. (2015). Information gaps in understanding the effects of noise on fishes and invertebrates. *Rev. Fish Biol. Fish.*, 25, 39–64.

Hawkins, A.D. & Popper, A.N. (2017). A sound approach to assessing the impact of underwater noise on marine fishes and invertebrates. *ICES J. Mar. Sci.*, 74, 635–651.

Hawkins, J.P. & Roberts, C.M. (1993). Effects of recreational scuba diving on coral reefs: trampling on reef-flat communities. *J. Appl. Ecol.*, 30, 25–30.

Heinänen, S., Chudzinska, M.E., Brandi Mortensen, J., Teo, T.Z.E., Rong Utne, K., Doksæter Sivle, L. & Thomsen, F. (2018). Integrated modelling of Atlantic mackerel distribution patterns and movements: A template for dynamic impact assessments. *Ecol. Modell.*, 387, 118–133.

Heise, K., Barrett-Lennard, L., Chapman, R., Dakin, T., Erbe, C., Hannay, D., Merchant, N., Pilkington, J., Thornton, S., Tollit, D., Vagle, S., Veirs, V., Vergara, V., Wood, J., Wright, B. & Yurk, H. (2017). *Proposed metrics for the management of underwater noise for southern resident killer whales*. Coastal Ocean Report Series, 2017/2. Coastal Ocean Research Institute, Vancouver, Canada.

Herrera-Montes, M.I. & Aide, T.M. (2011). Impacts of traffic noise on anuran and bird communities. *Urban Ecosyst.*, 14, 415–427.

Hildebrand, J.A. (2009). Anthropogenic and natural sources of ambient noise in the ocean. *Mar. Ecol. Prog. Ser.*, 395, 5–20.

Holles, S., Simpson, S.D., Radford, A.N., Berten, L. & Lecchini, D. (2013). Boat noise disrupts orientation behaviour in a coral reef fish. *Mar. Ecol. Prog. Ser.*, 485, 295–300.

Holmes, L.J., McWilliam, J., Ferrari, M.C.O. & McCormick, M.I. (2017). Juvenile damselfish are affected but desensitize to small motor boat noise. *J. Exp. Mar. Bio. Ecol.*, 494, 63–68.

Huebner, L.K. & Chadwick, N.E. (2012). Patterns of cleaning behaviour on coral reef fish by the anemoneshrimp *Ancylomenes pedersoni*. *J. Mar. Biol. Assoc.*, 92, 1557–1562.

Huebner, L.K., Shea, C.P., Schueller, P.M., Terrell, A.D., Ratchford, S.G. & Chadwick, N.E. (2019). Crustacean symbiosis with Caribbean sea anemones *Bartholomea annulata*: Occupancy modeling, habitat partitioning, and persistence. *Mar. Ecol. Prog. Ser.*, 631, 99–116.

Hynes, S., Ankamah-Yeboah, I., O’Neill, S., Needham, K., Xuan, B.B. & Armstrong, C. (2021). The impact of nature documentaries on public environmental preferences and willingness to pay: entropy balancing and the blue planet II effect. *J. Environ. Plan. Manag.*, 64, 1428–1456.

ICES. (2012). *Report of the Inter-Benchmark Protocol on New Species (Turbot and Sea bass; IBPNew 2012)*. ICES, Copenhagen, Denmark. ICES C. 2012/ACOM45.

ICES. (2018). *Report of the Working Group on Celtic Seas Ecoregion (WGCSE)*.. ICES, Copenhagen, Denmark. ICES C. 2018/ACOM13

ICES. (2020). *Sea bass (Dicentrarchus labrax) in divisions 4.b–c, 7.a, and 7.d–h (central and southern North Sea, Irish Sea, English Channel, Bristol Channel, and Celtic Sea).* ICES Advice on fishing opportunities, catch, and effort. ICES, Copenhagen, Demark

ICES. (2021). *Working group for the Celtic Seas ecoregion (WGCSE)*. ICES, Copenhagen, Denmark. ICES Scientific Reports, 2, 40.

IMO. (2014). *Guidelines for the Reduction of Underwater Noise from Commercial Shipping to Address Adverse Impacts on Marine Life*. International Maritime Organisation, London, UK. IMO MEPC.1/Circ.833.

Jain-Schlaepfer, S., Fakan, E., Rummer, J.L., Simpson, S.D. & McCormick, M.I. (2018). Impact of motorboats on fish embryos depends on engine type. *Conserv. Physiol.*, 6, coy014.

Jennings, S. & Ellis, J.R. (2015). *Fish atlas of the Celtic Sea, North Sea, and Baltic Sea*. *Fish atlas Celt. Sea, North Sea, Balt. Sea*. Wageningen Academic Publishers, The Netherlands.

Jennings, S., Jennings, S. & Pawson, M.G. (1992). The origin and recruitment of bass, *Dicentrarchus labrax*, larvae to nursery areas. *J. Mar. Biol. Assoc. U.K.*, 72, 199–212.

Jerem, P. & Mathews, F. (2020). Trends and knowledge gaps in field research investigating effects of anthropogenic noise. *Conserv. Biol.*, 0, 1–14.

JNCC. (2017). *JNCC guidelines for minimising the risk of injury and disturbance to marine mammals from seismic surveys*. Joint Nature Conservation Committee, Aberdeen, UK.

Johnson, M.W., Everest, F.A. & Young, R.W. (1947). The role of snapping in the production (Crangon and Synalpheus) in the production of underwater noise in the sea. *Biol. Bull.*, 93, 122–138.

de Jong, K., Amorim, M.C.P., Fonseca, P.J., Fox, C.J. & Heubel, K.U. (2018a). Noise can affect acoustic communication and subsequent spawning success in fish. *Environ. Pollut.*, 237, 814–823.

de Jong, K., Amorim, M.C.P., Fonseca, P.J. & Heubel, K.U. (2018b). Noise affects multimodal communication during courtship in a marine fish. *Front. Ecol. Evol.*, 6, 113.

de Jong, K., Forland, T.N., Amorim, M.C.P., Rieucau, G., Slabbekoorn, H. & Sivle, L.D. (2020). Predicting the effects of anthropogenic noise on fish reproduction. *Rev. Fish Biol. Fish.*, 30, 245–268.

Jourdan-Pineau, H., Dupont-Prinet, A., Claireaux, G. & McKenzie, D.J. (2010). An investigation of metabolic prioritization in the European sea bass, *Dicentrarchus labrax*. *Physiol. Biochem. Zool.*, 83, 68–77.

Kassambara, A. (2019). *Practical Statistics in R for Comparing Groups: Numerical Variables*. Independently published; Datanovia, Montpellier, France.

Kassambara, A. (2020). *rstatix: Pipe-Friendly Framework for Basic Statistical Tests*. [R Package version 0.6.0]; https://CRAN.R-project.org/package=rstatix.

Kastelein, R.A., Heul, S. van der, Verboom, W.C., Jennings, N., Veen, J. van der & Haan, D. de. (2008). Startle response of captive North Sea fish species to underwater tones between 0.1 and 64 kHz. *Mar. Environ. Res.*, 65, 369–377.

Kastelein, R.A., Jennings, N., Kommeren, A., Helder-Hoek, L. & Schop, J. (2017). Acoustic dose-behavioral response relationship in sea bass (*Dicentrarchus labrax*) exposed to playbacks of pile driving sounds. *Mar. Environ. Res.*, 130, 315–324.

Kelley, D.F. (1988). The importance of estuaries for sea-bass, *Dicentrarchus labrax* (L.). *J. Fish Biol.*, 33, 25–33.

Kelley, D.F. & Pickett, G.D. (1987). The distribution and migrations of bass, *Dicentrarchus labrax* L., in waters around England and Wales as shown by tagging. *J. Mar. Biol. Assoc. United Kingdom*, 67, 183–217.

Kenyon, T.N. (1996). Ontogenetic changes in the auditory sensitivity of damselfishes (pomacentridae). *J. Comp. Physiol. - A Sensory, Neural, Behav. Physiol.*, 179, 553–561.

Kerrigan, B.A. (1997). Variability in larval development of the tropical reef fish *Pomacentrus amboinensis* (Pomacentridae): the parental legacy. *Mar. Biol.*, 127, 395–402.

Killen, S.S. & Brown, J.A. (2006). Energetic cost of reduced foraging under predation threat in newly hatched ocean pout. *Mar. Ecol. Prog. Ser.*, 321, 255–266.

King, S.L., Schick, R.S., Donovan, C., Booth, C.G., Burgman, M., Thomas, L. & Harwood, J. (2015). An interim framework for assessing the population consequences of disturbance. *Methods Ecol. Evol.*, 6, 1150–1158.

Kok, A.C.M., Hulten, D. Van, Timmerman, K.H., Lankhorst, J., Visser, F. & Slabbekoorn, H. (2021). Interacting effects of short-term and long-term noise exposure on antipredator behaviour in sand gobies. *Anim. Behav.*, 172, 93–102.

Krahforst, C.S., Sprague, M.W. & Luczkovich, J.J. (2016). The impact of vessel noise on oyster toadfish (*Opsanus tau*) communication. *Proc. Meet. Acoust.*, 010031.

Krause, B.L. (2012). *The Great Animal Orchestra: Finding the Origins of Music in the World's Wild Places*. Little Brown & Co. New York, USA.

Krause J. & Godin J.G.J. (1996). Influence of prey foraging posture on flight behavior and predation risk: predators take advantage of unwary prey. *Behav. Ecol.*, 7, 264–271.

Kunc, H.P., McLaughlin, K.E. & Schmidt, R. (2016). Aquatic noise pollution: implications for individuals, populations, and ecosystems. *Proc. R. Soc. B Biol. Sci.*, 283, 1–8.

Kunc, H.P. & Schmidt, R. (2019). The effects of anthropogenic noise on animals: A meta-analysis. *Biol. Lett.*, 15, 20190649.

Ladich, F. & Schulz-Mirbach, T. (2016). Diversity in fish auditory systems: One of the riddles of sensory biology. *Front. Ecol. Environ.*, 4, 28.

Ladich, F. & Winkler, H. (2017). Acoustic communication in terrestrial and aquatic vertebrates. *J. Exp. Biol.*, 220, 2306–2317.

Lanari, D., D'Agaro, E. & Ballestrazzi, R. (2002). Growth parameters in European sea bass (*Dicentrarchus labrax* L.): Effects of live weight and water temperature. *Ital. J. Anim. Sci.*, 1, 181–185.

Lee, M.A., Nguyen, F.T., Scott, K., Chan, N.Y.L., Bakh, N.A., Jones, K.K., Pham, C., Garcia-Salinas, P., Garcia-Parraga, D., Fahlman, A., Marco, V., Koman, V.B., Oliver, R.J., Hopkins, L.W., Rubio, C., Wilson, R.P., Meekan, M.G., Duarte, C.M. & Strano, M.S. (2019). Implanted nanosensors in marine organisms for physiological biologging: Design, feasibility, and species variability. *ACS Sensors*, 4, 32–43.

Lema, S.C. & Kelly, J.T. (2002). The production of communication signals at the air-water and water-substrate boundaries. *J. Comp. Psychol.*, 116, 145–150.

Lewandowski, J. & Staaterman, E. (2020). International management of underwater noise: Transforming conflict into effective action. *J. Acoust. Soc. Am.*, 147, 3160–3168.

Lindfield, S.J., Harvey, E.S., Mcilwain, J.L. & Halford, A.R. (2014). Silent fish surveys: Bubble-free diving highlights inaccuracies associated with SCUBA-based surveys in heavily fished areas. *Methods Ecol. Evol.*, 5, 1061–1069.

Lindkvist, E., Wijermans, N., Daw, T.M., Gonzalez-Mon, B., Giron-Nava, A., Johnson, A.F., van Putten, I., Basurto, X. & Schlüter, M. (2020). Navigating complexities: Agent-based nodeling to support research, governance, and management in small-scale fisheries. *Front. Mar. Sci.*, 6, 1–12.

Link, J., Griswold, C., Methratta, E. & Gurnard, J. (2006). *Documentation for the Energy Modeling and Analysis eXercise (EMAX)*. Northeast Fisheries Science Center Reference Document 06-15.

Lissåker, M. & Kvarnemo, C. (2006). Ventilation or nest defense—parental care trade-offs in a fish with male care. *Behav. Ecol. Sociobiol.*, 60, 864–873.

Lobel, P.S. (2005). Scuba bubble noise and fish behavior: A rationale for silent diving technology. In: *Diving for Science: Proceedings of the American Academy of Underwater Sciences*. pp. 49–59.

Losey, G.S. (1972). The ecological importance of cleaning symbiosis. *Am. Soc. Ichthyol. Herpetol.*, 1972, 820–833.

Lowerre-Barbieri, S.K., Catalán, I.A., Frugård Opdal, A. & Jørgensen, C. (2019). Preparing for the future: Integrating spatial ecology into ecosystem-based management. *ICES J. Mar. Sci.*, 76, 467–476.

Lück, M. (2016). Scuba diving tourism. *Ann. Leis. Res.*, 19, 259–261.

Luczkovich, J.J., Krahforst, C.S., Kelly, K.E. & Sprague, M.W. (2017). The Lombard effect in fishes: How boat noise impacts oyster toadfish vocalization amplitudes in natural experiments. *Proc. Meet. Acoust.* 27, 010035.

Luna-Acosta, A., Lefrançois, C., Millot, S., Chatain, B. & Bégout, M.-L. (2011).

Physiological response in different strains of sea bass (Dicentrarchus labrax): Swimming and aerobic metabolic capacities. *Aquaculture*, 317, 162–167.

MacLean, K., Prystay, T.S., Lawrence, M.J., Zolderdo, A.J., Gutowsky, L.F.G., Staaterman, E., Gallagher, A.J. & Cooke, S.J. (2020). Going the distance: Influence of distance between boat noise and nest site on the behavior of paternal smallmouth bass. *Water. Air. Soil Pollut.*, 231, 151.

Madison, B.N., Tavakoli, S., Kramer, S. & Bernier, N.J. (2015). Chronic cortisol and the regulation of food intake and the endocrine growth axis in rainbow trout. *J. Endocrinol.*, 226, 103–119.

Magnhagen, C. & Vestergaard, K. (1991). Risk taking in relation to reproductive investments and future reproductive opportunities: field experiments on nest-guarding common gobies, *Pomatoschistus microps*. *Behav. Ecol.*, 2, 351–359.

Malakoff, D. (2010). A push for quieter ships. *Science*, 328, 1502–1503.

Manassa, R.P., McCormick, M.I., Chivers, D.P. & Ferrari, M.C.O. (2013). Social learning of predators in the dark: understanding the role of visual, chemical and mechanical information. *Proc. R. Soc. B Biol. Sci.*, 280, 20130720.

Mayer, I., Shackley, S.E. & Witthames, P.R. (1990). Aspects of the reproductive biology of the bass, *Dicentrarchus labrax* L. II. Fecundity and pattern of oocyte development. *J. Fish Biol.*, 36, 141–148.

McCammon, A., Sikkel, P.C. & Nemeth, D. (2010). Effects of three Caribbean cleaner shrimps on ectoparasitic monogeneans in a semi-natural environment. *Coral Reefs*, 29, 419–426.

McCauley, R.D., Fewtrell, J. & Popper, A.N. (2003). High intensity anthropogenic sound damages fish ears. *J. Acoust. Soc. Am.*, 113, 638–642.

McCloskey, K., Chapman, K., Chapuis, L., McCormick, M., Radford, A. & Simpson, S. (2020). Assessing and mitigating impacts of motorboat noise on nesting damselfish. *Environ. Pollut.*, 266, 115376.

McClure, C.J.W., Ware, H.E., Carlisle, J., Kaltenecker, G. & Barber, J.R. (2013). An experimental investigation into the effects of traffic noise on distributions of birds: Avoiding the phantom road. *Proc. R. Soc. B Biol. Sci.*, 280, 20132290.

McClure, C.J.W., Ware, H.E., Carlisle, J.D. & Barber, J.R. (2017). Noise from a phantom road experiment alters the age structure of a community of migrating birds. *Anim. Conserv.*, 20, 164–172.

Mccormick, M.I. (1998). Behaviorally induced maternal stress in a fish influences progeny quality by a hormonal mechanism. *Ecology*, 79, 1873–1883.

McCormick, M.I. (2016). Protogyny in a tropical damselfish: Females queue for future benefit. *PeerJ*, 2016, e2198.

McCormick, M.I., Allan, B.J.M., Harding, H. & Simpson, S.D. (2018). Boat noise impacts risk assessment in a coral reef fish but effects depend on engine type. *Sci. Rep.*, 8, 3847.

McCormick, M.I., Fakan, E.P., Nedelec, S.L. & Allan, B.J.M. (2019). Effects of boat noise on fish fast-start escape response depend on engine type. *Sci. Rep.*, 9, 6554.

McCormick, M.I. & Meekan, M.G. (2007). Social facilitation of selective mortality. *Ecology*, 88, 1562–1570.

McCormick, M.I. & Smith, S. (2004). Efficacy of passive integrated transponder tags to determine spawning-site visitations by a tropical fish. *Coral Reefs*, 23, 570–577.

McKenna, M.F., Wiggins, S.M. & Hildebrand, J.A. (2013). Relationship between container ship underwater noise levels and ship design, operational and oceanographic conditions. *Sci. Rep.* 3, 1760.

McLane, A.J., Semeniuk, C., McDermid, G.J. & Marceau, D.J. (2011). The role of agent-based models in wildlife ecology and management. *Ecol. Modell.*, 222, 1544–1556.

McLaughlin, K.E. & Kunc, H.P. (2015). Changes in the acoustic environment alter the foraging and sheltering behaviour of the cichlid *Amititlania nigrofasciata*. *Behav. Processes*, 116, 75–79.

Memarzadeh, M., Britten, G.L., Worm, B. & Boettiger, C. (2019). Rebuilding global fisheries under uncertainty. *Proc. Natl. Acad. Sci. U.S.A.*, 116, 15985–15990.

Merchant, N.D. (2019). Underwater noise abatement: Economic factors and policy options. *Environ. Sci. Policy*, 92, 116–123.

Merchant, N.D., Blondel, P., Dakin, D.T. & Dorocicz, J. (2016). Averaging underwater noise levels for environmental assessment of shipping. *J. Acoust. Soc. Am*, 132, 343–349.

Merchant, N.D., Faulkner, R.C. & Martinez, R. (2018). Marine noise budgets in practice. *Conserv. Lett.*, 11, 1–8.

Merchant, N.D., Fristrup, K.M., Johnson, M.P., Tyack, P.L., Witt, M.J., Blondel, P. & Parks, S.E. (2015). Measuring acoustic habitats. *Methods Ecol. Evol.*, 6, 257–265.

Methot, R.D. & Wetzel, C.R. (2013). Stock synthesis: A biological and statistical framework for fish stock assessment and fishery management. *Fish. Res.*, 142, 86–99.

Mills, S.C., Beldade, R., Henry, L., Laverty, D., Nedelec, S.L., Simpson, S.D. & Radford, A.N. (2020). Hormonal and behavioural effects of motorboat noise on wild coral reef fish. *Environ. Pollut.*, 262, 114250.

Monroe, J.D., Rajadinakaran, G. & Smith, M.E. (2015). Sensory hair cell death and regeneration in fishes. *Front. Cell. Neurosci.*, 9, 1–18.

Mortensen, L.O., Chudzinska, M.E., Slabbekoorn, H. & Thomsen, F. (2021). Agent-based models to investigate sound impact on marine animals: bridging the gap between effects on individual behaviour and population level consequences. *Oikos*, 130, 1074-1086.

Moyer, J.T. (1975). Reproductive behavior of the damselfish *Pomacentrus nagasakiensis* at Miyake-jima, Japan. *Japanse J. Ichthyol.*, 22, 151–163.

Nabe-Nielsen, J., van Beest, F.M., Grimm, V., Sibly, R.M., Teilmann, J. & Thompson, P.M. (2018). Predicting the impacts of anthropogenic disturbances on marine populations. *Conserv. Lett.*, 11, e12563.

Nakazono, A., Hamada, H. & Sakurai, M. (1989). Predation on eggs by conspecific males in two Japanese damselfishes, *Pomacentrus nagasakiensis* and *Chromis notatus notatus*, after removal of egg-guarding males. *J. Ethol.*, 7, 97–104.

Nanninga, G.B., Côté, I.M., Beldade, R. & Mills, S.C. (2017). Behavioural acclimation to cameras and observers in coral reef fishes. *Ethology*, 123, 705–711.

NASA OBPG. (2017). *Aqua Moderate Resolution Imaging Spectroradiometer (MODIS) chlor_a ocean color data*; 2018 Reprodcessing. NASA OB.DAAC, Greenbelt MD, USA.

NASA OBPG. (2017). Moderate-resolution Imaging Spectroradiometer (MODIS) Aqua Sea Surface Temperature (daytime) Data; 2014 reprocessing. NASA OB.DAAC, Greenbelt MD, USA.

National Research Council. (2005). *Marine mammal populations and ocean noise: Determining when noise causes biologically significant effects*. National Acadamies Press. Washington, DC, USA.

Nedelec, S.L., Campbell, J., Radford, A.N., Simpson, S.D. & Merchant, N.D. (2016a). Particle motion: the missing link in underwater acoustic ecology. *Methods Ecol. Evol.*, 7, 836-842.

Nedelec, S.L., Mills, S.C., Lecchini, D., Nedelec, B., Simpson, S.D. & Radford, A.N. (2016b). Repeated exposure to noise increases tolerance in a coral reef fish. *Environ. Pollut.*, 216, 428–436.

Nedelec, S.L., Mills, S.C., Radford, A.N., Beldade, R., Simpson, S.D., Nedelec, B. & Côté, I.M. (2017a). Motorboat noise disrupts co-operative interspecific interactions. *Sci. Rep.*, 7, 6987.

Nedelec, S.L., Radford, A.N., Pearl, L., Nedelec, B., Mccormick, M.I., Meekan, M.G. & Simpson, S.D. (2017b). Motorboat noise impacts parental behaviour and offspring survival in a reef fish. *Proc. R. Soc. B Biol. Sci.*, 284, 1–7.

Nedelec, S.L., Simpson, S.D., Radford, A.N. & Mills, S.C. (2014). Anthropogenic noise playback impairs embryonic development and increases mortality in a marine invertebrate. *Sci. Rep.*, 4, 5891.

Neo, Y.Y., Hubert, J., Bolle, L., Winter, H. V, Cate, C. & Slabbekoorn, H. (2016). Sound exposure changes European sea bass behaviour in a large outdoor floating pen: Effects of temporal structure and a ramp-up. *Environ. Pollut.*, 214, 26–34.

Neo, Y.Y., Hubert, J., Bolle, L.J., Winter, H. V. & Slabbekoorn, H. (2018). European sea bass respond more strongly to noise exposure at night and habituate over repeated trials of sound exposure. *Environ. Pollut.*, 239, 367–374.

Neo, Y.Y., Parie, L., Bakker, F., Snelderwaard, P., Tudorache, C., Schaaf, M. & Slabbekoorn, H. (2015a). Behavioral changes in response to sound exposure and no spatial avoidance of noisy conditions in captive zebrafish. *Front. Behav. Neurosci.*, 9, 28.

Neo, Y.Y., Ufkes, E., Kastelein, R.A., Winter, H. V, ten Cate, C. & Slabbekoorn, H. (2015b). Impulsive sounds change European sea bass swimming patterns: Influence of pulse repetition interval. *Mar. Pollut. Bull.*, 97, 111–117.

Nielsen, J.R., Thunberg, E., Holland, D.S., Schmidt, J.O., Fulton, E.A., Bastardie, F., Punt, A.E., Allen, I., Bartelings, H., Bertignac, M., Bethke, E., Bossier, S., Buckworth, R., Carpenter, G., Christensen, A., Christensen, V., Da-Rocha, J.M., Deng, R., Dichmont, C., *et al.* (2018). Integrated ecological–economic fisheries models—Evaluation, review and challenges for implementation. *Fish Fish.*, 19, 1–29.

NMMA. (2017). *U.S. Recreational Boating Statistical Abstract*. National Marine Manufacturers Association. Chicago, Illinois, USA.

Nousek-McGregor, A. E. & Mei, F. T. L. (2016). Does noise from shipping and boat traffic affect predator vigilance in the European common hermit crab? In: *The Effects of Noise on Aquatic Life II*, edited by N. A. Popper & A. Hawkins (Springer, New York), pp. 767-774.

Oh, H.T., Chung, Y., Jeon, G. & Shim, J. (2021). Review of the marine environmental impact assessment reports regarding offshore wind farm. *Fish. Aquat. Sci.*, 24, 341–350.

Oksanen, J., Blanchet, F.G., Friendly, M., Kindt, R., Legendre, P., McGlinn, D., Minchin, P.R., O'Hara, R.B., Simpson, G.L., Solymos, P., Stevens, M.H.M., Szoecs, E. & Wagner, H. (2020). *vegan: Community Ecology Package*. [R Packag. version 2.5-7]; https://CRAN.R-project.org/package=vegan.

PADI. (2021). *Worldwide corporate statistics*. PADI. Rancho Santa Margarita, California, USA.

Parsons, E.C.M. (2016). Why IUCN should replace "data deficient" conservation status with a precautionary "assume threatened" status—A cetacean case study. *Front. Mar. Sci.*, 3, 2015–2017.

Parsons, E.C.M. (2017). Impacts of Navy sonar on whales and dolphins: Now beyond a smoking gun? *Front. Mar. Sci.*, 4, 295.

Pawson, M.G. (1992). Climatic influences on the spawning success, growth, and recruitment of bass (*Dicentrarchus labrax* L.) in British waters. *ICES Mar. Sei. Symp.*, 195, 388–392.

Pawson, M.G., Brown, M., Leballeur, J. & Pickett, G.D. (2008). Will philopatry in sea bass, *Dicentrarchus labrax*, facilitate the use of catch-restricted areas for management of recreational fisheries? *Fish. Res.*, 93, 240–243.

Pawson, M.G., Pickett, G.D., Leballeur, J., Brown, M. & Fritsch, M. (2007). Migrations, fishery interactions, and management units of sea bass (*Dicentrarchus labrax*) in Northwest Europe. *ICES J. Mar. Sci.*, 64, 332–345.

Peixoto, M.J., Svendsen, J.C., Malte, H., Pereira, L.F., Carvalho, P., Pereira, R., Gonçalves, J.F.M. & Ozório, R.O.A. (2016). Diets supplemented with seaweed affect metabolic rate, innate immune, and antioxidant responses, but not individual growth rate in European sea bass (*Dicentrarchus labrax*). *J. Appl. Phycol.*, 28, 2061–2071.

Pereira, L.S., Agostinho, A.A. & Winemiller, K.O. (2017). Revisiting cannibalism in fishes. *Rev. Fish Biol. Fish.*, 27, 499–513.

Perman, R., Ma, Y., Common, M., Maddison, D. & McGilvray, J. (2011). *Natural Resource and Environmental Economics*. 4th ed. Pearson, UK.

Peters, R.H. (1986). *The Ecological Implications of Body Size*. Cambridge University Press.

Picciulin, M., Sebastianutto, L., Codarin, A. & Codarin, A. (2012). Brown meagre vocalization rate increases during repetitive boat noise exposures: A possible case of vocal compensation. *J. Acoust. Soc. Am.*, 132, 3118.

Picciulin, M., Sebastianutto, L., Codarin, A., Farina, A. & Ferrero, E.A. (2010). *In situ* behavioural responses to boat noise exposure of *Gobius cruentatus* (Gmelin, 1789; fam. Gobiidae) and *Chromis chromis* (Linnaeus, 1758; fam. Pomacentridae) living in a Marine Protected Area. *J. Exp. Mar. Bio. Ecol.*, 386, 125–132.

Pickett, G.D., Kelley, D.F. & Pawson, M.G. (2004). The patterns of recruitment of sea bass, *Dicentrarchus labrax* L. from nursery areas in England and Wales and implications for fisheries management. *Fish. Res.*, 68, 329–342.

Pickett, G.D. & Pawson, M.G. (1994). *S*ea bass: Biology, exploitation and conservation. In *Chapman & Hall; Fish and fisheries series 12*. pp. 643–644.

Pine, M.K., Jeffs, A.G., Wang, D. & Radford, C.A. (2016). The potential for vessel noise to mask biologically important sounds within ecologically significant embayments. *Ocean Coast. Manag.*, 127, 63–73.

Pirotta, E., Booth, C.G., Costa, D.P., Fleishman, E., Kraus, S.D., Lusseau, D., Moretti, D., New, L.F., Schick, R.S., Schwarz, L.K., Simmons, S.E., Thomas, L., Tyack, P.L., Weise, M.J., Wells, R.S. & Harwood, J. (2018). Understanding the population consequences of disturbance. *Ecol. Evol.*, 8, 9934–9946.

Pontual, H. de, Lalire, M., Fablet, R., Laspougeas, C., Garren, F., Martin, S., Drogou, M. & Woillez, M. (2019). New insights into behavioural ecology of European sea bass off the West Coast of France: Implications at local and population scales. *ICES J. Mar. Sci.*, 76, 501–515.

Popper, A.N. & Fay, R.R. (2011). Rethinking sound detection by fishes. *Hear. Res.*, 273, 25–36.

Popper, A.N. & Hawkins, A.D. (2019). An overview of fish bioacoustics and the impacts of anthropogenic sounds on fishes. *J. Fish Biol.*, 94, 692–713.

Pottinger, T.G. (2010). A multivariate comparison of the stress response in three salmonid and three cyprinid species: Evidence for inter-family differences. *J. Fish Biol.*, 76, 601–621.

Pullar, J. & Webster, A. (1977). The energy cost of fat and protein deposition in the rat. *Br. J. Nutr.*, 37, 355–363.

Purser, J. & Radford, A.N. (2011). Acoustic noise induces attention shifts and reduces foraging performance in three-spined sticklebacks (*Gasterosteus aculeatus*). *PLoS One*, 6, e17478.

Putland, R.L., Constantine, R. & Radford, C.A. (2017). Exploring spatial and temporal trends in the soundscape of an ecologically significant embayment. *Sci. Rep.*, 7, 1–12.

Radford, A.N., Kerridge, E. & Simpson, S.D. (2014). Acoustic communication in a noisy world: can fish compete with anthropogenic noise? *Behav. Ecol*, 25, 1022–

1030.

Radford, A.N., Lecaillon, G. & Simpson, S.D. (2016a). Repeated exposure reduces the response to impulsive noise in European sea bass. *Glob. Chang. Biol.*, 22, 3349–3360.

Radford, A.N., Purser, J., Bruintjes, R. & Voellmy, I.K. (2016b). Beyond a simple effect: Variable and changing responses to anthropogenic noise. In: *Advances in Experimental Medicine and Biology*. pp. 901–907

Radford, C.A., Tay, K. & Goeritz, M.L. (2022). Comparative sound detection abilities of four decapod crustaceans. *J. Exp. Biol.*, 225, jeb243314.

Radford, C.A., Jeffs, A.G., Tindle, C.T., Cole, R.G. & Montgomery, J.C. (2005). Bubbled waters: The noise generated by underwater breathing apparatus. *Mar. Freshw. Behav. Physiol.*, 38, 259–267.

Railsback, S.F. & Grimm, V. (2019). *Agent-Based and Individual-Based Modeling: A Practical Introduction*. 2nd Edition. Princeton University Press, Princeton, New Jersey, USA.

Read, J., Jones, G. & Radford, A.N. (2014). Fitness costs as well as benefits are important when considering responses to anthropogenic noise. *Behav. Ecol.*, 25, 4–7.

Regner, S. & Dulčić, J. (1994). Growth of sea bass, *Dicentrarchus labrax*, larval and juvenile stages and their otoliths under quasi-steady temperature conditions. *Mar. Biol.*, 119, 169–177.

Reid, A.J., Carlson, A.K., Creed, I.F., Eliason, E.J., Gell, P.A., Johnson, P.T.J., Kidd, K.A., MacCormack, T.J., Olden, J.D., Ormerod, S.J., Smol, J.P., Taylor, W.W., Tockner, K., Vermaire, J.C., Dudgeon, D. & Cooke, S.J. (2019). Emerging threats and persistent conservation challenges for freshwater biodiversity. *Biol. Rev.*, 94, 849–873.

Reijnen, R. & Foppen, R. (1994). The effects of car traffic on breeding bird populations in woodland. I. Evidence of reduced habitat quality for willow warblers (*Phylloscopus trochilus*) breeding close to a highway. *J. Appl. Ecol.*, 31, 85–94.

Reijnen, R., Foppen, R., Braak, C. Ter & Thissen, J. (1995). The effects of car traffic on breeding bird populations in woodland. III. Reduction of density in relation to the proximity of main roads. *J. Appl. Ecol.*, 32, 187–202.

Roberts, C.M., McClean, C.J., Veron, J.E.N., Hawkins, J.P., Allen, G.R., McAllister, D.E., Mittermeier, C.G., Schueler, F.W., Spalding, M., Wells, F., Vynne, C. & Werner, T.B. (2002). Marine biodiversity hotspots and conservation priorities for tropical reefs. *Science*, 295, 1280–1284.

Robertson, D.R. (1996). Interspecific competition controls abundance and habitat use of territorial caribbean damselfishes. *Ecology*, 77, 885–899.

Romero, L.M., Dickens, M.J. & Cyr, N.E. (2009). The reactive scope model – A new model integrating homeostasis, allostasis, and stress. *Horm. Behav.*, 55, 375–389.

Rose, K.A., Cowan, J.H., Winemiller, K.O., Myers, R.A. & Hilborn, R. (2001).

Compensatory density dependence in fish populations: Importance, controversy, understanding and prognosis. *Fish Fish.*, 2, 293–327.

Rosen, D.A.S. & Trites, A.W. (2007). *Marine Mammals in the Lab: Tools for Conservation & Science*. North Pacific Universities Marine Mammal Research Consortium, Workshop Preceedings, Sept. 10–11, 2007. Vancouver, Canada.

Rossington, K., Benson, T., Lepper, P. & Jones, D. (2013). Eco-hydro-acoustic modeling and its use as an EIA tool. *Mar. Pollut. Bull.*, 75, 235–243.

Sabat, A.M. (1994). Costs and benefits of parental effort in a brood-guarding fish (*Ambloplites rupestris*, centrarchidae). *Behav. Ecol.*, 5, 195–201.

Sabet, S., Neo, Y.Y. & Slabbekoorn, H. (2015). The effect of temporal variation in sound exposure on swimming and foraging behaviour of captive zebrafish. *Anim. Behav.*, 107, 49–60.

Sadoul, B. & Geffroy, B. (2019). Measuring cortisol, the major stress hormone in fishes. *J. Fish Biol.*, 94, 540–555.

Scheffer, M., Baveco, J.M., DeAngelis, D.L., Rose, K.A. & van Nes, E.H. (1995). Super-individuals a simple solution for modelling large populations on an individual basis. *Ecol. Modell.*, 80, 161–170.

Schmidt-Nielsen, K. (2013). *Animal physiology: Adaption and environment*. 5th edn. Cambridge University Press.

Schnurr, R.E.J., Alboiu, V., Chaudhary, M., Corbett, R.A., Quanz, M.E., Sankar, K., Srain, H.S., Thavarajah, V., Xanthos, D. & Walker, T.R. (2018). Reducing marine pollution from single-use plastics (SUPs): A review. *Mar. Pollut. Bull.*, 137, 157–171.

Scholik, A.R. & Yan, H.Y. (2001). Effects of underwater noise on auditory sensitivity of a cyprinid fish. *Hear. Res.*, 152, 17–24.

Scholik, A.R. & Yan, H.Y. (2002). Effects of boat engine noise on the auditory sensitivity of the fathead minnow, *Pimephales promelas*. *Environ. Biol. Fishes*, 63, 203–209.

Senzaki, M., Barber, J.R., Phillips, J.N., Carter, N.H., Cooper, C.B., Ditmer, M.A., Fristrup, K.M., McClure, C.J.W., Mennitt, D.J., Tyrrell, L.P., Vukomanovic, J., Wilson, A.A. & Francis, C.D. (2020). Sensory pollutants alter bird phenology and fitness across a continent. *Nature*, 587, 605–609.

Sertlek, H.Ö., Slabbekoorn, H., ten Cate, C. & Ainslie, M.A. (2019). Source specific sound mapping: Spatial, temporal and spectral distribution of sound in the Dutch North Sea. *Environ. Pollut.*, 247, 1143–1157.

Shannon, G., Mckenna, M.F., Angeloni, L.M., Crooks, K.R., Fristrup, K.M., Brown, E., Warner, K.A., Nelson, M.D., White, C., Briggs, J., Mcfarland, S. & Wittemyer, G. (2016). A synthesis of two decades of research documenting the effects of noise on wildlife. *Biol. Rev.*, 91, 982–1005.

Shin, Y. & Cury, P. (2001). Exploring fish community dynamics through size-dependent trophic interactions using a spatialized individual-based model. *Aquat. Living Resour.*, 14, 65–80.

Sibly, R.M. & Calow, P. (1986). *Physiological Ecology of Animals: An Evolutionary*

Approach. Wiley–Blackwell.

Sibly, R.M., Grimm, V., Martin, B.T., Johnston, A.S. a, Kulakowska, K., Topping, C.J., Calow, P., Nabe-Nielsen, J., Thorbek, P. & Deangelis, D.L. (2013). Representing the acquisition and use of energy by individuals in agent-based models of animal populations. *Methods Ecol. Evol.*, 4, 151–161.

Sierra-flores, R., Atack, T., Migaud, H. & Davie, A. (2015). Stress response to anthropogenic noise in Atlantic cod *Gadus morhua* L . *Aquac. Eng.*, 67, 67–76.

Simpson, S.D., Purser, J. & Radford, A.N. (2014). Anthropogenic noise compromises antipredator behaviour in European eels. *Glob. Chang. Biol.*, 21, 1–8.

Simpson, S.D., Radford, A.N., Nedelec, S.L., Ferrari, M.C.O., Chivers, D.P., Mccormick, M.I. & Meekan, M.G. (2016). Anthropogenic noise increases fish mortality by predation. *Nat. Commun.*, 7, 10544.

Slabbekoorn, H. (2015). Aiming for progress in understanding underwater noise impact on fish: Complementary need for indoor and outdoor studies. *Adv. Exp. Med. Biol.*, 875, 1057–1065.

Slabbekoorn, H., Bouton, N., Opzeeland, I. Van, Coers, A., Cate, C. & Popper, A.N. (2010). A noisy spring: the impact of globally rising underwater sound levels on fish. *Trends Ecol. Evol.*, 25, 419–427.

Slabbekoorn, H., Dalen, J., de Haan, D., Winter, H. V., Radford, C., Ainslie, M.A., Heaney, K.D., van Kooten, T., Thomas, L. & Harwood, J. (2019). Population-level consequences of seismic surveys on fishes: An interdisciplinary challenge. *Fish Fish.*, 20, 653–685.

Slabbekoorn, H. & Halfwerk, W. (2009). Behavioural ecology: Noise annoys at community level. *Curr. Biol.*, 19, R693–R695.

Smith, C. & Wootton, R.J. (1995). The costs of parental care in teleost fishes. *Rev. Fish Biol. Fish.*, 5, 7–22.

Smith, M.E., Kane, A.S. & Popper, A.N. (2004). Noise-induced stress response and hearing loss in goldfish (*Carassius auratus*). *J. Exp. Biol.*, 427–435.

Solan, M., Hauton, C., Godbold, J. A., Wood, C. L., Leighton, T. G. & White, P. (2016). Anthropogenic sources of underwater sound can modify how sediment-dwelling invertebrates mediate ecosystem properties. *Sci. Rep*., 6, 20540.

Soudijn, F.H., Kooten, T. Van, Slabbekoorn, H. & Roos, A.M. De. (2020). Population-level effects of acoustic disturbance in Atlantic cod: a size-structured analysis based on energy budgets. *Proc. R. Soc. B Biol. Sci.*, 287, 20200490.

Spence, J.H. & Fischer, R.W. (2017). Requirements for reducing underwater noise from ships. *IEEE J. Ocean. Eng.*, 42, 388–398.

Spence, M.A., Thorpe, R.B., Blackwell, P.G., Scott, F., Southwell, R. & Blanchard, J.L. (2021). Quantifying uncertainty and dynamical changes in multi-species fishing mortality rates, catches and biomass by combining state-space and size-based multi-species models. *Fish Fish.*, 22, 667–681.

Spiga, I., Aldred, N. & Caldwell, G.S. (2017). Anthropogenic noise compromises the anti-predator behaviour of the European sea bass, *Dicentrarchus labrax* (L.). *Mar. Pollut. Bull.*, 122, 297–305.

Tasker, M.L., Amundin, M., André, M., Hawkins, A., Lang, W., Merck, T., Scholik-Schlomer, A., Tellmann, J., Thomsen, F., Werner, S. & Zakharia, M. (2010). *Marine Strategy Framework Directive, Task Group 11 Report: Underwater noise and other forms of energy*. Office for Official Publications of the European Communities, Luxembourg.

Thompson, B.M. & Harrop, R.T. (1987). The distribution and abundance of bass (*Dicentrarchus labrax*) eggs and larvae in the English Channel and Southern North Sea. *J. Mar. Biol. Assoc. U.K.*, 67, 263–274.

Titus, B.M., Daly, M. & Exton, D.A. (2015a). Do reef fish habituate to diver presence? Evidence from two reef sites with contrasting historical levels of SCUBA intensity in the Bay Islands, Honduras. *PLoS One*, 10, e0119645.

Titus, B.M., Daly, M. & Exton, D.A. (2015b). Temporal patterns of Pederson shrimp (*Ancylomenes pedersoni* Chace 1958) cleaning interactions on Caribbean coral reefs. *Mar. Biol.*, 162, 1651–1664.

Titus, B.M., Daly, M., Vondriska, C., Hamilton, I. & Exton, D.A. (2019). Lack of strategic service provisioning by Pederson's cleaner shrimp (*Ancylomenes pedersoni*) highlights independent evolution of cleaning behaviors between ocean basins. *Sci. Rep.*, 9, 629.

Titus, B.M., Vondriska, C. & Titus, B.M. (2017). Comparative behavioural observations demonstrate the 'cleaner' shrimp *Periclimenes yucatanicus* engages in true symbiotic cleaning interactions. *R. Soc. open sci.* 4, 170078.

UN. (2018). *Nineteenth metting of the United Nations Open-ended Informative Consultaive Process on Oceans and the Law of the Sea: Anthropogenic underwater noise*. United Nations General Assebly, 9 July 2018, A/73/124.

Urick, R. (1975). *Principles of underwater sound*. New York: McGraw-Hill.

Vasconcelos, R.O., Amorim, M.C.P. & Ladich, F. (2007). Effects of ship noise on the detectability of communication signals in the Lusitanian toadfish. *J. Exp. Biol.*, 210, 2104–2112.

Vaughan, D.B., Grutter, A.S., Costello, M.J. & Hutson, K.S. (2017). Cleaner fishes and shrimp diversity and a re-evaluation of cleaning symbioses. *Fish Fish.*, 18, 698–716.

Vazzana, M., Celi, M., Arizza, V., Calandra, G., Buscaino, G., Ferrantelli, V., Bracciali, C. & Sarà, G. (2017). Noise elicits hematological stress parameters in Mediterranean damselfish (*Chromis chromis*, perciformes): A mesocosm study. *Fish Shellfish Immunol.*, 62, 147–152.

Venturini, S., Massa, F., Castellano, M., Fanciulli, G. & Povero, P. (2021). Recreational boating in the Portofino Marine Protected Area (MPA), Italy: Characterization and analysis in the last decade (2006–2016) and some considerations on management. *Mar. Policy*, 127, 103178.

Voellmy, I.K., Purser, J., Flynn, D., Kennedy, P., Simpson, S.D. & Radford, A.N. (2014a). Acoustic noise reduces foraging success in two sympatric fish species via different mechanisms. *Anim. Behav.*, 89, 191–198.

Voellmy, I.K., Purser, J., Simpson, S.D. & Radford, A.N. (2014b). Increased noise levels have different impacts on the anti-predator behaviour of two sympatric fish species. *PLoS One*, 9, e102946

Waldie, P.A., Blomberg, S.P., Cheney, K.L., Goldizen, A.W. & Grutter, A.S. (2011). Long-term effects of the cleaner fish labroides dimidiatus on coral reef fish communities. *PLoS One*, 6, e21201.

Wale, M.A., Radford, A.N. & Simpson, S.D. (2013). Size-dependent physiological responses of shore crabs to single and repeated playback of ship noise. *Biol. Lett.*, 9, 20121194.

Walker, N., Boyd, R., Watson, J., Radford, Z., Readdy, L., Sibly, R., Roy, S. & Hyder, K. (2020). A spatially explicit individual-based model to support management of commercial and recreational fisheries for European sea bass *Dicentrarchus labrax*. *Ecol. Modell.*, 44, 524450.

Ware, H.E., McClure, C.J.W., Carlisle, J.D., Barber, J.R. & Daily, G.C. (2015). A phantom road experiment reveals traffic noise is an invisible source of habitat degradation. *Proc. Natl. Acad. Sci. U. S. A.*, 112, 12105–12109.

Watson, J., Hyder, K., Boyd, R., Thorpe, R., Weltersbach, M.S., Ferter, K., Cooke, S.J., Roy, S. & Sibly, R. (2020). Assessing the sublethal impacts of anthropogenic stressors on fish: An energy-budget approach. *Fish Fish.*, 21, 1034–1045.

Watson, J.W., Boyd, R., Dutta, R., Vasdekis, G., Walker, N.D., Roy, S., Everitt, R., Hyder, K. & Sibly, R.M. (2022). Incorporating environmental variability in a spatially-explicit individual-based model of European sea bass. *Ecol. Modell.*, 466, 109878.

Weijerman, M., Fulton, E.A., Janssen, A.B.G., Kuiper, J.J., Leemans, R., Robson, B.J., van de Leemput, I.A. & Mooij, W.M. (2015). How models can support ecosystem-based management of coral reefs. *Prog. Oceanogr.*, 138, 559–570.

Weilgart, L.S. (2007). The impacts of anthropogenic ocean noise on cetaceans and implications for management. *Can. J. Zool.*, 85, 1091–1116.

Weilgart, L.S. (2018). *The impact of ocean noise pollution on fish and invertebrates*. Report for OceanCare, Switzerland*.*

Whiteman, E.A., Côté, I.M. & Reynolds, J.D. (2002). Do cleaning stations affect the distribution of territorial reef fishes? *Coral Reefs*, 21, 245–251.

Wijermans, N., Boonstra, W.J., Orach, K., Hentati-Sundberg, J. & Schlüter, M. (2020). Behavioural diversity in fishing—Towards a next generation of fishery models. *Fish Fish.*, 21, 872–890.

Wilensky, U. (1999). NetLogo.

Williams, R., Veirs, S., Veirs, V., Ashe, E. & Mastick, N. (2019). Approaches to reduce noise from ships operating in important killer whale habitats. *Mar. Pollut. Bull.*, 139, 459–469.

Williams, R., Wright, A.J., Ashe, E., Blight, L.K., Bruintjes, R., Canessa, R., Clark, C.W., Cullis-suzuki, S., Dakin, D.T., Erbe, C., Hammond, P.S., Merchant, N.D., Hara, P.D.O., Purser, J., Radford, A.N., Simpson, S.D., Thomas, L. & Wale, M.A. (2015). Impacts of anthropogenic noise on marine life: Publication patterns, new discoveries, and future directions in research and management. *Ocean Coast.*

Manag., 115, 17–24.

WHOI. (1952). The effects of fouling. In: *Marine fouling and its prevention.* pp. 1–19. Woods Hole Oceanographic Institution, Falmouth, MA, USA.

Worm, B., Elliff, C., Fonseca, J.G., Gell, F.R., Serra-Gonçalves, C., Helder, N.K., Murray, K., Peckham, H., Prelovec, L. & Sink, K. (2021). Making ocean literacy inclusive and accessible. *Ethics Sci. Environ. Polit.*, 21, 1–9.

Wright, K.J., Higgs, D.M. & Leis, J.M. (2011). Ontogenetic and interspecific variation in hearing ability in marine fish larvae. *Mar. Ecol. Prog. Ser.*, 424, 1–13.

Wright, L. & Nichols, C. (2018). Coastal Systems in the Anthropocene. In: *Tomorrow's Coasts: Complex and Impermanent*. pp. 85–99.

Yandell, B. (1997). *Practical Data Analysis for Designed Experiments (1st ed.)*. CRC Press. Boca Raton, Florida, USA.

Yang, Y., Lu, J., Pflugrath, B.D., Li, H., Martinez, J.J., Regmi, S., Wu, B., Xiao, J. & Deng, Z.D. (2021). Lab-on-a-fish: Wireless, miniaturized, fully integrated, implantable biotelemetric tag for real-time *in vivo* monitoring of aquatic animals. *IEEE Internet Things J.*

Yemane, D., Shin, Y.J. & Field, J.G. (2009). Exploring the effect of Marine Protected Areas on the dynamics of fish communities in the southern Benguela: An individual-based modelling approach. *ICES J. Mar. Sci.*, 66, 378–387.

Zakai, D. & Chadwick-Furman, N.E. (2002). Impacts of intensive recreational diving on reef corals at Eilat, northern Red Sea. *Biol. Conserv.*, 105, 179–187.

Zoran, M.J. & Ward, J.A. (1983). Parental egg care behavior and fanning activity for the orange chromide, *Etroplus maculatus*. *Environ. Biol. Fishes*, 8, 139–148.

Zupa, W., Carbonara, P., Spedicato, M.T. & Lembo, G. (2015). Modelling swimming activities and energetic costs in European sea bass (*Dicentrarchus labrax* L., 1758) during critical swimming tests. *Mar. Freshw. Behav. Physiol.*, 48, 341–357.

Appendices

Appendix A: Supplementary material for Chapter Two

Material in Appendix A presented as published in:
McCloskey KP, Chapman KE, Chapuis L, McCormick MI, Radford AN, Simpson SD. 2020. Assessing and mitigating impacts of motorboat noise on nesting damselfish. *Environ. Pollut.* 288, 115376.

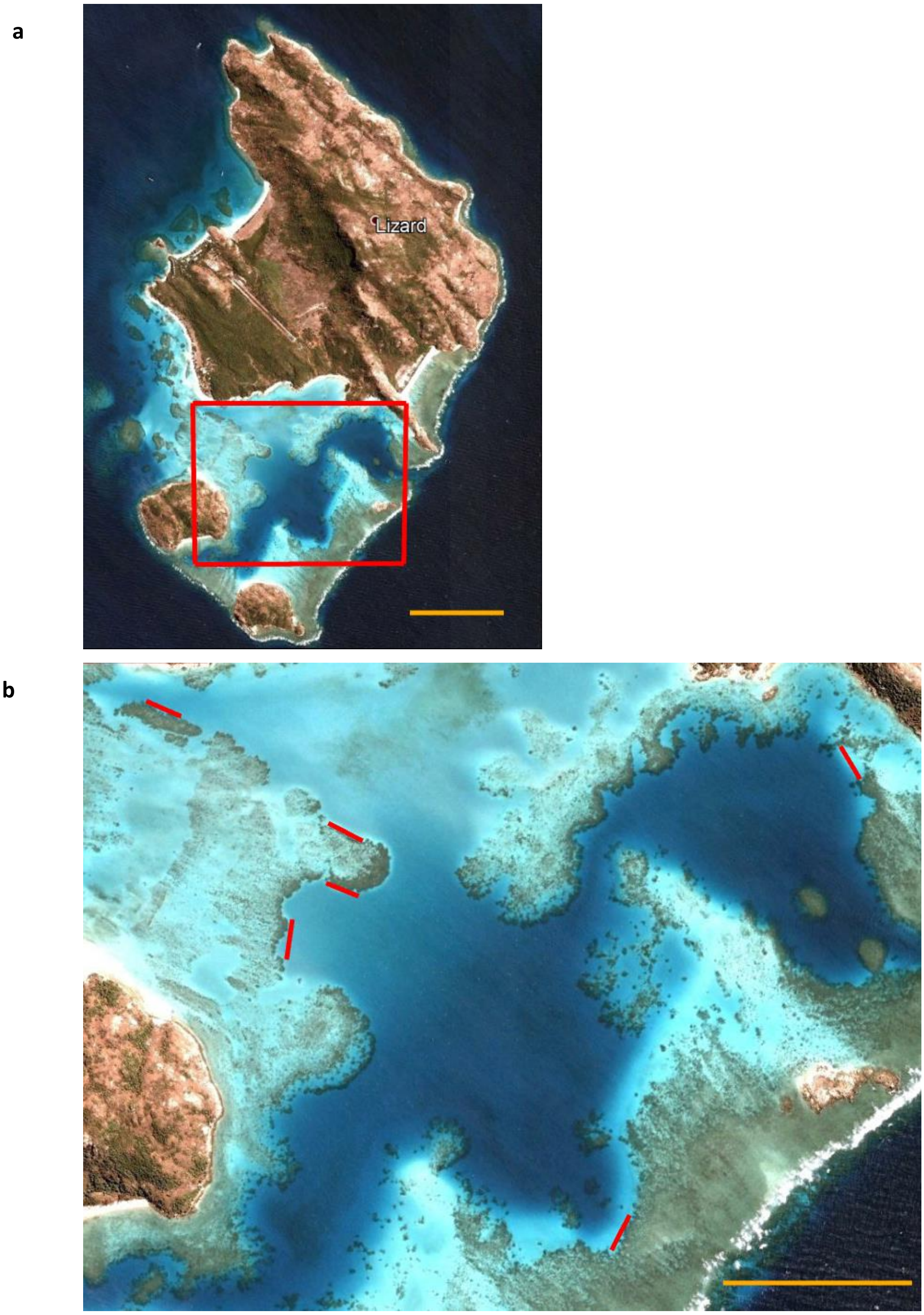

Figure A.1. Maps showing the locations of (a) the lagoon study area (red box) relative to Lizard Island, (b) the six study sites (red lines) within the lagoon. *Yellow lines show scales of (a) 1 km and (b) 0.5 km. Source: “Lizard Island.” 14°4’S 145° 28’E Google Earth. 22nd August, 2011. Accessed 9th March 2020.*

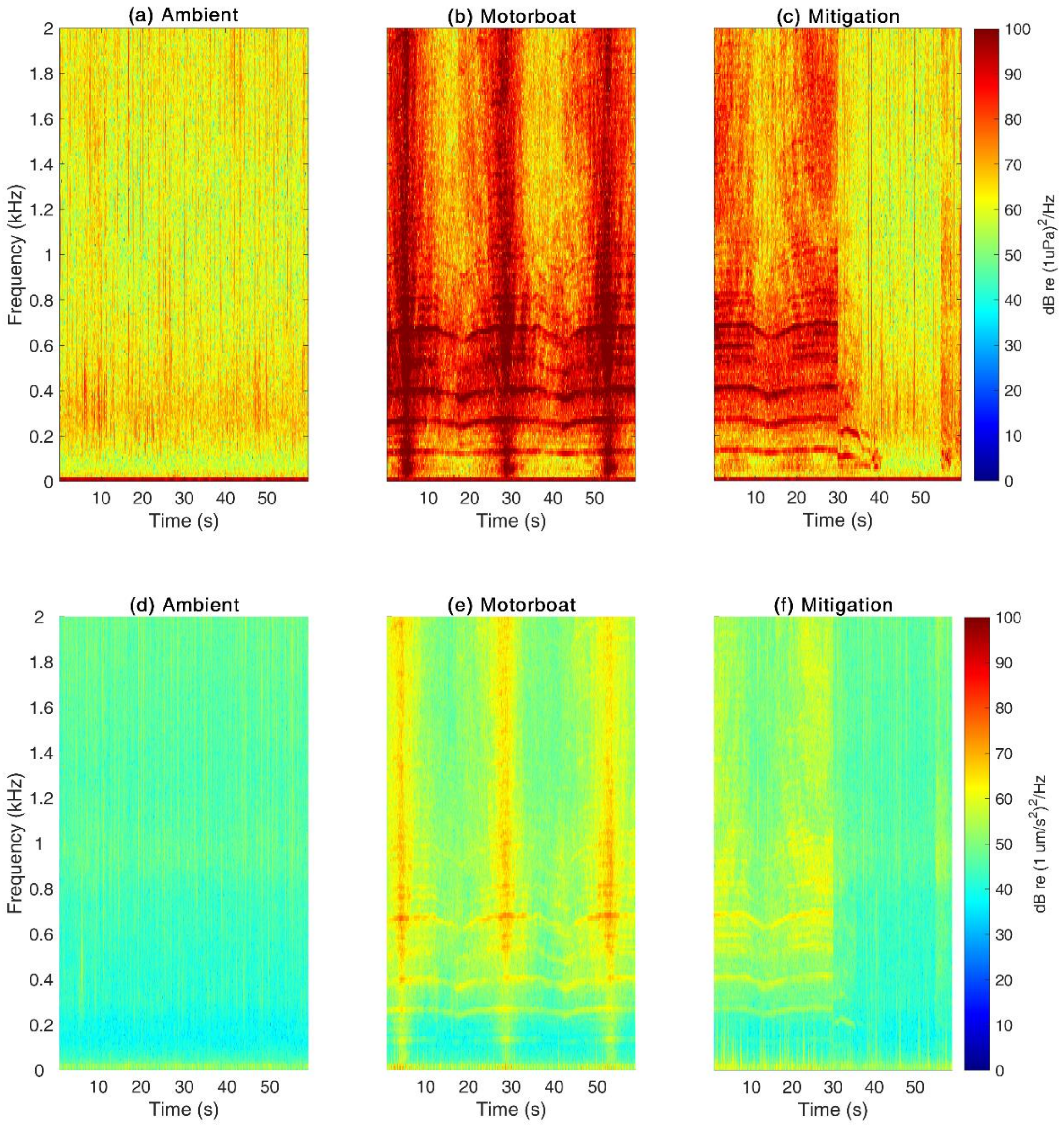

Figure A.2. Spectrograms of sound pressure (a–c) and triaxial particle acceleration levels (d–f) for ambient (a, d), motorboat (b, e), and mitigation (c, f) treatments*. For these comparisons, 1-min subsamples of one motorboat at one study site were analysed (fft window length = 4048, Hamming filter, 75% overlap, 0–2 kHz).*

Appendix B: TRACE document for Chapters Four and Five

This is a TRACE document ("TRAnsparent and Comprehensive model Evaludation") which provides supporting evidence that our model presented in:

Chapter Four:

Predicting the impacts of anthropogenic noise on fisheries for European sea bass *Dicentrarchus labrax* using a spatially explicit and bioenergetic individual-based model

and

Chapter Five:

Potential consequences of anthropogenic noise and noise-mitigation scenarios for the northern fishery stock of European sea bass

was thoughtfully designed, correctly implemented, thoroughly tested, well understood, and appropriately used for its intended purpose.

The rationale of this document follows:

> Schmolke A, Thorbek P, DeAngelis DL, Grimm V. 2010. Ecological modelling supporting environmental decision making: a strategy for the future. *Trends in Ecology and Evolution* 25: 479-486.

and uses the updated standard terminology and document structure in:

> Grimm V, Augusiak J, Focks A, Frank B, Gabsi F, Johnston ASA, Liu C, Martin BT, Meli M, Radchuk V, Thorbek P, Railsback SF. 2014. Towards better modelling and decision support: documenting model development, testing, and analysis using TRACE. *Ecological Modelling* 280:129-139.

and

> Augusiak J, Van den Brink PJ, Grimm V. 2014. Merging validation and evaluation of ecological models to 'evaludation': a review of terminology and a practical approach. *Ecological Modelling* 280:117-128.

B.1 Problem formulation

This TRACE element provides supporting information on: The decision-making context in which the model will be used; the types of model clients or stakeholders addressed; a precise specification of the question(s) that should be answered with the model, including a specification of necessary model outputs; and a statement of the domain of applicability of the model, including the extent of acceptable extrapolations.

B.1.1 Summary:

A spatially explicit individual-based model (IBM) was developed to simulate the population dynamics and geographical distribution of the northern sea bass stock. Life processes are driven by energy budget equations from sea surface temperature and phytoplankton density remote sensing inputs. Assumptions regarding movement relate to past observations.

The model is designed to model population dynamics and simulate spatial distribution of the European sea bass (*Dicentrarchus labrax)* in ICES divisions' 4.b–c, 7.a and 7.d–h. Sea bass are a large, slow growing, late maturing, high value fish that is exploited by both commercial and recreational fisheries (Pickett & Pawson 1994). Scientific assessments for the UK have shown a rapid decline in spawning stock biomass for eight years since 2010 which has been attributed to poor recruitment (driven by environmental factors) and high fishing mortality. The decline led to the implementation of emergency management measures in 2015, and has resulted in significant reductions in the harvest (ICES 2021).

The model described here builds upon the model of Walker *et al.* (2020) and Watson *et al.* (2022). In its initial implementation, the model by Walker *et al.* (2020) used the ICES stock assessment as a basis for population dynamics. Subsequently, Watson *et al.* (2022) updated the model so that population dynamics are now emergent from the model, based on an energy budget. In our update, we apply population-level patterns for the impacts of noise on energy budgets in fish (Soudijn *et al.* 2020) and use realistic noise-level projections for the Northeast Atlantic (Farcas *et al.* 2020) to investigate population-level responses of the stock to spatiotemporal variations of anthropogenic noise.

In the model, the energy budget is driven from remote sensing environmental data (sea surface temperatures [SST] and phytoplankton density [PHY]). In this way, environmental changes are linked to life processes and ultimately population dynamics. With emergent population dynamics, there is scope for model predictions in novel environmental conditions whilst improving reliability of predictions for management strategies for the spawning stock. The model output, spawning stock biomass (SSB), is an important metric of stock status currently used by scientists to provide advice on fishing opportunities for the stock. Therefore, we focus on statistics related to SSB to evaluate the impacts of anthropogenic noise and various management strategies on stock status. The IBM could also be used to assess other aspects of performance such as yield maximisation, risk reduction, and Total Allowable Catch (TAC) stability. In addition, the model could act as a tool to test the impact of:

- Behaviours of commercial and recreational fishers.
- Management approaches that limit catch and/or effort.
- Other environmental/anthropogenic stressors (e.g., catch and release fishing injuries).

The scope for a broad range of testing applications means stakeholders for this model include scientists and organisations advising on fishing opportunities for sea bass as well as decision makers.

The spatial component of the IBM retains the hardwired movement of Walker *et al.* (2020). However, the model remains a useful tool to complement the stock assessment through enhanced predictions of management scenarios and testing spatial strategies, which are not possible with a population-based assessment model. Important future additions to the model are steps to further elucidate the mechanisms underlying sea bass movement. This is suggested to be done with new mechanistic migration sub models that allow for spatial predictions in novel environmental conditions and improve reliability of predictions for strategies relating to the spawning stock.

B.2 Model description

This TRACE element provides supporting information on: The model and provides a detailed written model description. For individual/agent-based and other simulation models, the ODD protocol is recommended as standard format. For complex sub models it should include concise explanations of the underlying rationale. Model users should learn what the model is, how it works, and what guided its design.

B.2.1 Summary

Here, we provide an ODD (Overview, Design concepts and Details) description of the individual-based model for sea bass (Grimm *et al.* 2006, 2010, 2020)**.**

The model description follows the ODD (Overview, Design concepts, Details) protocol for describing individual- and agent-based models (Grimm *et al.* 2006, 2010, 2020). The model was implemented in *NetLogo 5.3.1* (Wilensky 1999), a free software platform for implementing individual-based models.

B.2.2 Purpose and patterns

The purpose of the model is to simulate the population dynamics and spatial distribution of the European sea bass (*Dicentrarchus labrax*) in the North Sea, Channel, Celtic & Irish seas (ICES divisions' 4.b–c, 7.a and 7.d–h). The use of emergent population dynamics offers scope to use the model as a tool to test the impacts of environmental/anthropogenic sublethal stressors (i.e., anthropogenic noise). Therefore, we apply population-level patterns for the impacts of noise on energy budgets in fish (Soudijn *et al.* 2020) and use realistic noise-level projections for the Northeast Atlantic (Farcas *et al.* 2020) to investigate population-level responses of the stock to spatiotemporal variations of anthropogenic noise.

Population-level patterns of anthropogenic noise:

The impacts of anthropogenic noise on populations are difficult to quantify. However, a recent population-level model was successful in using the known effects of anthropogenic noise on fish, based on a meta-analysis of sound exposure experiments (Cox *et al.* 2018), to evaluate how acoustic disturbances may affect individual-level processes and, consequentially, populations (Soudijn *et al.* 2020). Therefore, the model described by this ODD will use these population-level patterns to drive the impacts of noise on individual-level processes of agents, and evaluate how noise may be impacting the sea bass population in a spatiotemporal context.

Pattern one: *Anthropogenic noise has been shown to decrease food intake across different species* (Purser & Radford 2011; Voellmy *et al.* 2014a; Sabet *et al.* 2015). Therefore, individuals affected by noise will have lower ingestion rates, controlled by an acoustic disturbance foraging modifier.

Pattern two: *Anthropogenic noise has been shown to increase stress and movement behaviour, which likely lead to an increase in energy expenditure* (Bruintjes *et al.* 2014; Soudijn *et al.* 2020). Therefore, individuals affected by noise will expend more energy, controlled by an acoustic disturbance energy multiplier.

Pattern three: *Anthropogenic noise has been shown to increase short-term mortality through increased predation and impaired antipredator behaviour* (Simpson *et al.* 2016). Therefore, individuals affected by noise will have a higher mortality probability, controlled by an acoustic disturbance mortality multiplier.

Pattern four: *Anthropogenic noise has been shown to impact reproductive efficiency and success through changes to reproductive behaviours of parents and lower offspring survival* (Nedelec *et al.* 2017b; de Jong *et al.* 2018a)). Therefore, individuals affected by noise will have lower reproductive output, controlled by an acoustic disturbance reproductive failure modifier.

B.2.3 Entities, state variables and scales

The model has two types of entity: sea bass super-individuals and square patches which represent the local environment. Super-individuals (hereafter termed individuals) comprise many sea bass with identical state variables, and were employed to reduce run times while dealing with the large number of fish in the stock (Scheffer *et al.* 1995). Sea bass super-individuals are characterised by the variables: age (years), the number of fish represented, life stage (egg, yolk-sac larvae [ys-larvae], larvae, juvenile or mature [adult]), length (cm), weight (including structural mass, gonad mass and total mass [kg]), ingested energy, energy reserves, metabolic rate, location, swimming speed and daily direction changes, spawning trigger and counter, mortality rates (natural, commercial inshore/offshore fishing mortality and recreational-fishing mortality) and the division they have an affinity to feed in (site fidelity; 4.b, 4.c, 7.a, 7.d, 7.e or 7.fg). The temporal extent spans from 1st of January 2004 to 31st of December 2015 and the model proceeds in discrete daily time-steps. To implement responses to anthropogenic noise, a noise trigger is turned on when an individual experiences a noise level above a designated threshold (imposed based on known hearing ranges of *D. labrax* (Kastelein *et al.* 2008), and linear modifiers are applied to the variables that have been shown to be impacted by anthropogenic noise (Cox *et al.* 2018; Soudijn *et al.* 2020).

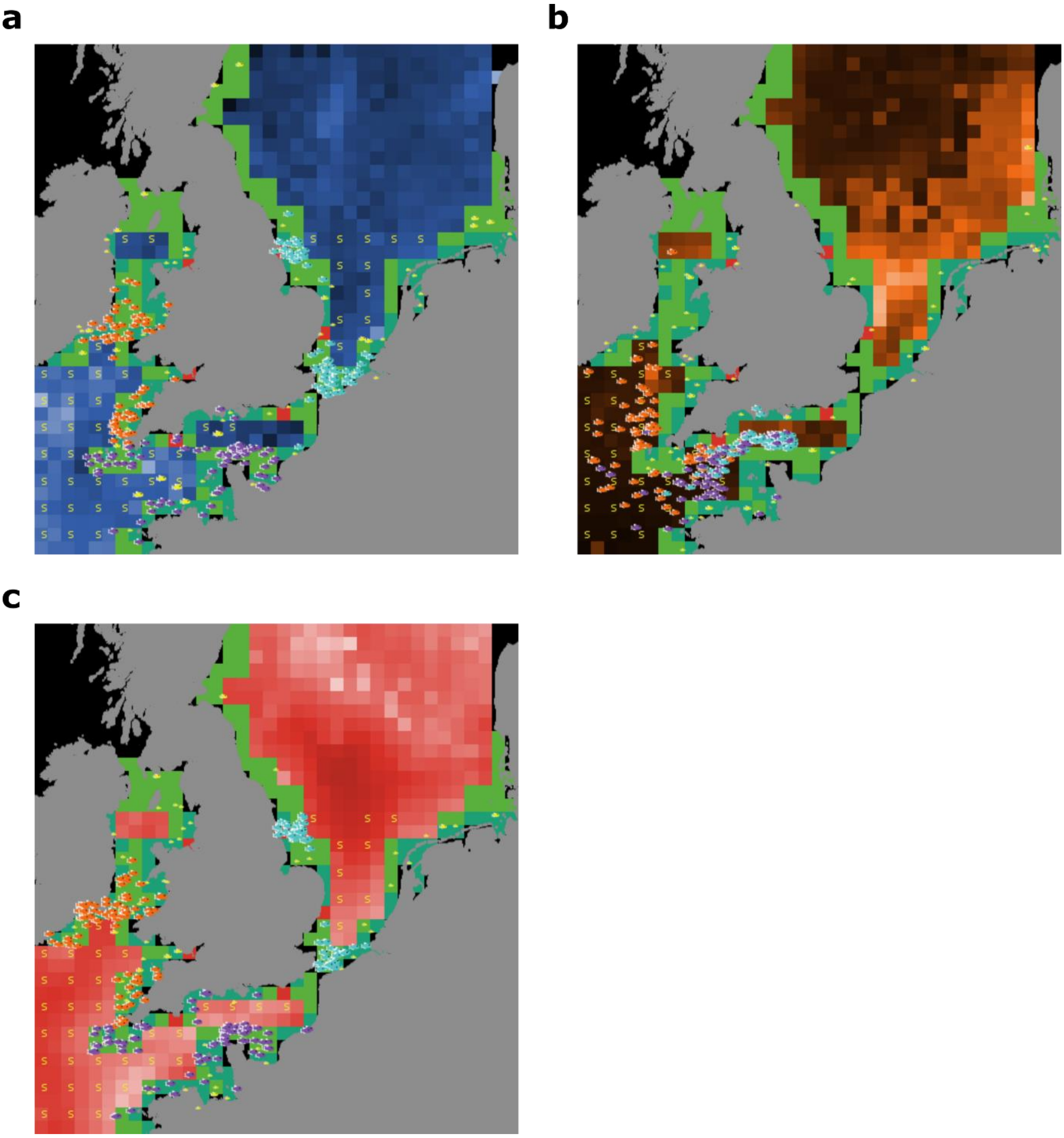

Figure B.1*. **The model interface; sea surface temperature (SST), phytoplankton concentration (PHY) and noise levels** cannot be shown simultaneously in the model interface so here; a) shows offshore patches as blue with dark to light representing increasing SST, b) shows offshore patches as orange with dark to light representing increasing PHY, and c) shows offshore patches as red with dark to light representing increasing anthropogenic noise levels. For a–c coastal patches represented in green, nursery patches (also coastal) are turquoise. Targets that eggs and larval stages drift towards (depending on ICES division affinity) are represented by red coastal patches. Agent colour represents life stage (white = eggs, black = ys-*

larvae and larvae, yellow = juvenile sea bass [not all life stages are shown here]). For mature sea bass colour represents affinity to a feeding ground. Spawning patches (which vary depending on time of year and environmental conditions) are shown with a yellow “S”. These remote sensing data are updated every 8 days and agents perform all sub models each day (see section below B.4.3.3).

The patches make up a grid landscape of 36 x 38 patches representing the area from 9° east to 9° west and 48° to 57.5° north (Fig. B.1). Sea patches are characterised by dynamic variables sea surface temperature (SST °C) (shown in blue for demonstration purposes in Fig. B.1a), phytoplankton density (shown in orange for demonstration purposes in Fig. B.1b) and mean projected noise level (dB) (shown in red for demonstration purposes in Fig. B.1c). The patches also have variables for area type (sea, coastal, offshore, spawning and nursery; see TRACE Section B.5), ICES division (4.b, 4.c, 7.a, 7.d, 7.e, or 7.fg) and spawning region (North Sea, Celtic Sea, Channel or Irish Sea). Each patch is approximately 30 x 30 km, although this distance varies by latitude due to the Earth's spheroid shape (29.9 x 27.8 km north of the domain, 37.2 x 27.8 km south of the domain). The model runs in discrete daily time steps (assuming 365 days in a year) from 2004 to 2015 (excluding a spin up from 1985 – 2004; see TRACE Section B.5). This time span covers 10 years of assessment period to a point when management measures were introduced.

Table B.1. Key state variables for the model entities.

State variable	**Description**	**Details**
Individuals		
Age	Non integer age of egg/larvae/fish.	years
Assimilation-energy	The energy that ends up assimilated by each individual fish within the super-individual.	kJ
Breed	Life stage of agent; Egg, yolk-sac larvae, larvae, juvenile or mature sea bass.	NA
Cohort	Integer age of year class.	years
Development	The number of days remaining before an egg hatches. Based on embryo-duration.	Days

Embryo-duration	The time for an egg to hatch. This is currently fixed at 5 days (range of 3-7.5 days in [Beraud *et al.* 2018]).	Days
Energy-reserve	The amount of energy a fish has stored based on the difference between ingested and expended energy.	kJ
Energy-reserve-max	The maximum amount of energy a fish can store, based on size.	kJ
ER	The energy reserve left after the energetic cost of maintenance is taken out.	kJ
Fci	Commercial inshore fishing mortality. Per day (fishing pressure limited to 214 days per year).	Daily
Fco	Commercial offshore fishing mortality. Per day (fishing pressure limited to 151 days per year).	Daily
Fri	Recreational offshore fishing mortality. Per day (fishing pressure is 365 days a year).	Daily
Func-response	Holling type II functional response adjusts ingestion rate based on phytoplankton density.	NA
Gonad-mass	Mass of gonads is calculated from the energy that went into producing eggs.	kg
Growth-costs	The energetic cost of adding new length and mass to larvae and fish.	kJ
Growth-rate	The realised amount of length added in a day if there is insufficient energy to grow maximally.	(cm)
Ingestion-rate	The maximum ingestion rate a fish	grams per day

	can achieve; based on size, temperature, availability of food, and conspecific density.	
IVbt	Affinity to division IVb. *	True or 0 for no affinity
IVct	Affinity to division IVc. *	True or 0 for no affinity
L	Length of egg, larvae or fish.	cm
Maintenance-energy	10% of energy reserves at the beginning of spawning is saved for maintenance costs while fasting on the spawning grounds.	kJ
Max-growth-rate	Maximum daily growth increment is calculated for different life stages. Mature and juvenile sea bass growth rate is calculated with the von Bertalanffy equation. Young life stages are calculated with the Gompertz growth equation.	cm
Max-R	The energetic costs of synthesising potential fecundity.	kJ
Migrating	A Boolean switch that prevents super-individuals "moving locally" if true.	True or 0 if False
MR	Metabolic rate equals SMR x2 (Peters, 1986) and is based on size and SST.	kJ
Number	Number of individual fish the super-individual represents.	Number
Potential-fecundity	The maximum potential number of eggs that can be produced based on size of fish.	Number
R	Movement repeats. Steps per day. This limits how far agents travel in one direction before turning.	Number

Realised-fecundity	Number of eggs that are produced from energy available.	Number
Spawn-count	Time in spawning ground.	days
Spawn-trigger	Migration switch.	0 = feeding; 1 = spawning
Speed	Swimming speed.	Patches per day
Standard-L	Standard length, the measure of head to base of tail fork.	cm
Std-mass	standard mass = mass as calculated from length using aL^b (see Table 2).	kg
Structural-mass	Structural mass is total mass minus lipid energy reserve and gonad mass.	kg
Total-mass	Total mass is the total of; structural, lipid energy reserve and gonad mass.	kg
VIIat	Affinity to division VIIa. *	True or 0 for no affinity
VIIdt	Affinity to division VIId. *	True or 0 for no affinity
VIIet	Affinity to division VIIe. *	True or 0 for no affinity
VIIfgt	Affinity to division VIIfg. *	True or 0 for no affinity
W	Body mass.	kg
noise-threshold	Minimum 50% hearing threshold imposed using normal distribution	Mean 105 dB ± 8 (SD)
noise-trigger	Noise impact switch	True or 0
NFm	Modifier to adjust feeding	0–1
NEm	Modifier to adjust energy use	0–1
NMm	Modifier to adjust mortality	0–1
NRm	Modifier to adjust reproductive output	0–1
Patches		
ArrS	Arrhenius multiplier calculated with specific parameters when calculating swimming speed.	
PHY	Phytoplankton density value from	gm^2

	remote sensing.	
Processed	For use in set up patches as a check that the distance from target patch is only calculated once.	True or 0
Spawn-patches	Marker for spawning patches, depending on time of year and SST.	True or 0 (dynamic)
SST	Sea surface temperature from remote sensing.	°C
noise-level	Acoustic projections for noise level	dB

*Affinity is the assigned ICES division that agents are given.

B.3 Process overview and scheduling

The model proceeds in daily time steps, resetting ticks every 365 days. The following sub models are executed in the order they are presented below. Within each sub model, super-individuals and patches are processed in a random order as there are no interactions among agents (an overview can be seen in Fig. B.2).

Sea check: Make sure super-individuals are in the sea, if not they move back to the sea and then continue with processes.

Update-patches: New SST and PHY data are assigned to patches, the Arrhenius rates for each patch recalculated (required to calculate speed), and offshore patches update their spawning patch status. Note this sub model is ran every tick but remote sensing data is only updated every 8 days due to limitations of the data

Calculate-catch: The catch taken by fishing fleets is calculated for each sea patch.

Noise-effect: If agents are found in a patch with a noise level that is above a set threshold (imposed hearing threshold; Kastelein *et al.* 2008), the switch *noise-trigger* is turned on to affect processes that are impacted by anthropogenic noise (Cox *et al.* 2018).

Natural mortality: The number of fish in each individual is discounted by its natural mortality rate. Individuals affected by noise increase mortality rates proportionally with a linear 'noise-mortality' modification parameter (Soudijn *et al.* 2020). Any super-individuals reaching the age of 30 or with less than one individual fish continue to represent a decimal number of fish.

Calc ingestion *larvae, juvenile and mature sea bass only*: Calculates the energy ingested from mass, energy available, temperature and density dependence. Individuals affected by noise (noise-trigger turned on) decrease food ingestion rates proportionally with a linear ‘noise-feeding’ modification parameter (Soudijn *et al.* 2020).

Calc assimilation *larvae, juvenile and mature sea bass only*: Calculates the energy assimilated and available for life processes.

Calc maintenance *larvae, juvenile and mature sea bass only*: The energy used for maintenance, adjusted by Arrhenius. Paid for either from assimilated energy or, if insufficient available food, paid from reserves. Individuals affected by noise increase metabolic rates proportionally with a linear ‘noise-energy’ modification parameter (Soudijn *et al.* 2020).

Calc-growth: The maximum daily growth rate is calculated. Agents under 70 days have a constant maximum growth rate (see TRACE Section B.8.3) for fish older than 70 days we use a von Bertalanffy curve. The maximum daily growth rate depends on fish length and SST.

Grow: Each fish increases its length as a fraction of the maximum growth increment, calculated above, dependent on SST and available energy.

Calc-total-mass: The mass of each fish is calculated from its length, with the addition of the mass of energy reserves and gonad mass.

Calculate-speed: The swimming speed of each fish is calculated from its length and SST of the patch.

Calculate-r: The number of ‘steps’ taken by each fish is calculated from its swimming speed.

Transform: If a super-individual meets the criteria (sufficient length; see Fig. B.2) then it transforms to the next life stage. The life stages are egg; yolk-sac larvae; larvae; juvenile; and mature. When juveniles graduate to mature sea bass (Length > 42 cm) they set their coastal feeding ground affinity as the ICES division in which they are in at the time of ticking over this length requirement (this could be a different division to the original ICES division target they would have drifted towards when they were in pelagic stages, see TRACE 8.7). Note that at the end of the first spawning migration there is an opportunity to change ICES division affinity which is altered with a probability defined by the site-fidelity slider on the model interface (GUI).

Fishing-mortality: The number of individuals each super individual represents is discounted by fishing mortality rates from the commercial offshore, commercial inshore and recreational fleets (data obtained from ICES stock assessment 2020).

Spawn-migration: If (ticks >= 274) or (ticks < 152) each mature sea bass with spawn-trigger equal to 1 moves towards offshore spawning grounds. This action can only be executed between ticks 274–151 corresponding to the months October–May.

Feeding-migration: Each mature sea bass with spawn-trigger equal to 0 moves towards or within its assigned coastal feeding ground.

Local-movement: Each juvenile sea bass moves randomly within coastal patches. Juveniles less than 32cm (not yet classed as “adolescent”) are further constrained to nursery coastal patches.

Drift eggs: Each egg moves one patch closer to its assigned coastal feeding ground.

Drift_ys-larvae: Each yolk-sac larva moves one patch closer to its assigned coastal feeding ground.

Drift_larvae: Each larva moves one patch closer to its assigned coastal feeding ground.

Age: Agents age a day each tick. The cohort age is increased by one at the end of tick 365.

Spawn: On the 60th tick every year (17th of March; picked as the middle of the spawning period) 10 mature sea bass super-individuals spawn, producing as many eggs as determined by total realised fecundity of the whole spawning stock (the number of eggs is based on cumulative available energy reserves and fish size, see TRACE Section B.8.7). Individuals affected by noise reduce reproductive success proportionally with a linear ‘noise-reproduction’ modification parameter (Soudijn *et al.* 2020).

Calc-egg-development: Eggs get one day older per tick until they hatch in correspondence with the embryo-duration.

Temperature effects

Throughout the model, temperature affects life processes via its effect on energy budgets. This is accomplished using the Arrhenius function. Biological rates increase exponentially with absolute temperature according to an Arrhenius function, A_T, as:

$$A_T = e^{-\left(\left[\frac{E_a}{boltz}\right]\left[\frac{1}{T} - \frac{1}{Tref}\right]\right)} \qquad (3)$$

where E_a is activation energy, *boltz* is the Boltzmann constant, T is absolute temperature and *Tref* is a reference temperature for the energy budget. The parameters used are different for calculating speed (see TRACE Section B.7 *calc speed*), where we use a specific activation energy (*EaS* = 0.1903656) and reference temperature (*TrefS* = 6^{o}C) (see TRACE Section B.8.4). For ease of understanding we write out the Arrhenius function where used throughout the document.

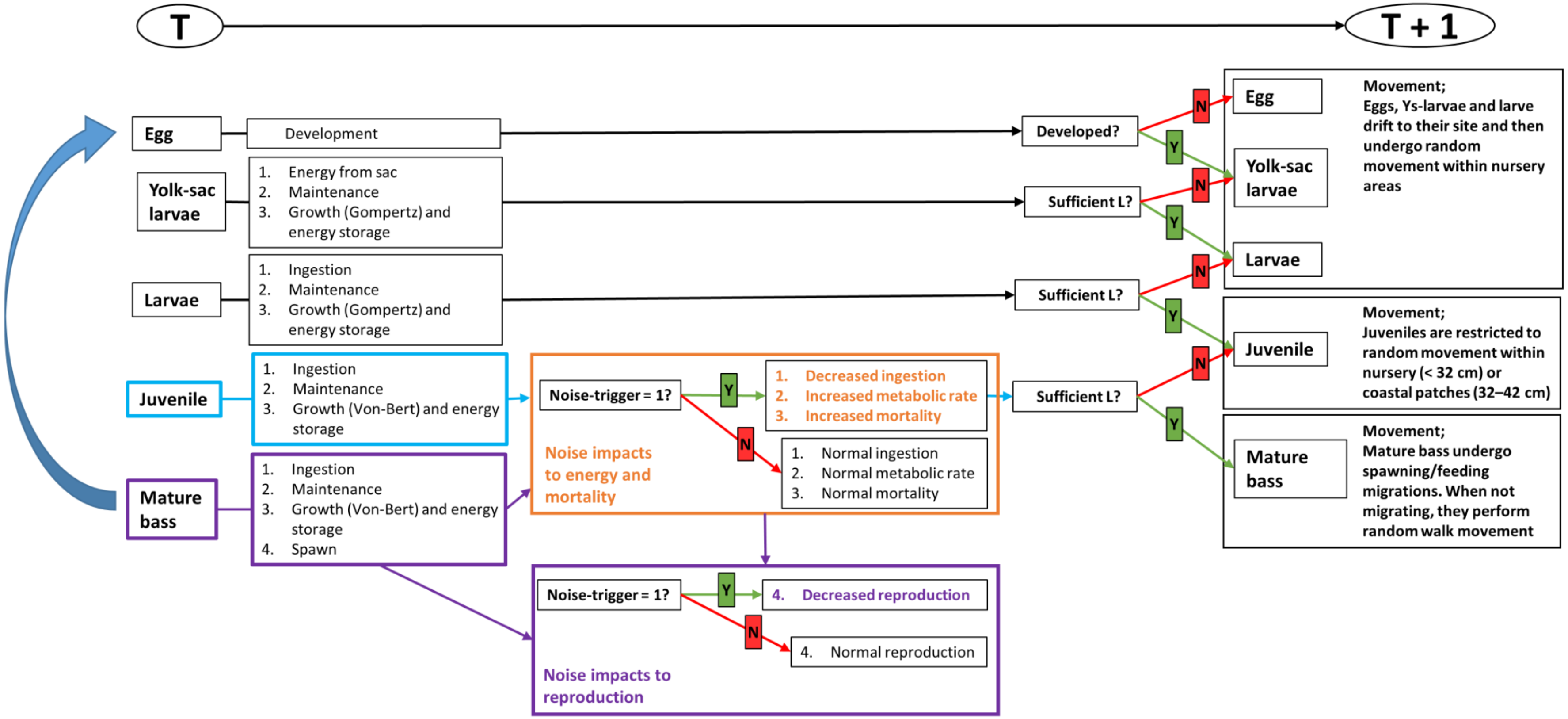

Figure B.2. Model overview. *Each life stage (egg, yolk-sac larvae, larvae, juvenile and mature sea bass) is outlined with the sub models applicable to each stage are presented in the order of model execution. To transform to the next life stage, eggs develop after a specified time and from then on transformation is length based. Each life stage gives details about their movement sub models. After spawning the egg super-individuals then start the processes from the beginning again.*

B.4 Design concepts

Basic principles: We aim to model the population dynamics and simulate spatial distribution of European sea bass in ICES divisions' 4.b–c, 7.a and 7.d–h. Life processes are driven by energy budget equations driven by sea surface temperature (SST) and phytoplankton density (PHY) remote sensing inputs to give emergent population dynamics. The spatial aspect of the model is not fully emergent and relies on assumptions relating to past observations. The visualisation of the large-scale migrations known to be undertaken by sea bass each year is not possible with a population model (for example the stock synthesis 3 model used for sea bass stock assessment) but is essential for simulating the spatial distribution of sea bass.

Emergence: The model's primary result – population dynamics – emerge from; the numbers at age 0, growth and mortality of sea bass.

Growth follows a fixed relationship adjusted by the effects of temperature and energy available.

Numbers at age 0 is dependent on energy ingested that is stored and then used to produce eggs as well as the environmental conditions that eggs and larvae experience.

Migrating adults follow a set of empirical rules triggered by an environmental cue while non-migrating adults and juvenile sea bass move randomly within an area type.

Adaptation: The movement and migratory behaviour of mature fish is an adaptive trait. The departure time and arrival in offshore spawning grounds is influenced by SST, while cessation of spawning is imposed after a fixed number of days.

All processes that are influenced by SST and energy availability are adaptive including ingestion, growth, spawning and numbers at age 0.

As the factors affecting navigation are otherwise unknown, fish follow a set of empirical rules that reproduce observed migratory patterns. Super individuals may choose to switch assigned feeding area after spawning; however, because the mechanisms of site fidelity are unknown, new allocations are assigned randomly with fixed probability defined by the *site-fidelity* slider on the model interface. Site fidelity was fixed at 100% in the current study.

Sensing: Individuals are assumed to know their length, location and the type of patch currently occupied so that they can apply the correct migratory rules. Mature sea bass are assumed to sense temperature so they may successfully arrive in suitable spawning grounds. To determine impacts on processes, individuals can sense noise levels above the set hearing thresholds. The model does not include *interaction* among sea bass.

Stochasticity: The main uses of stochasticity are to: (1) distribute and age super-individuals when they enter the model at initialisation; (2) simulate the movement and site fidelity of sea bass; (3) assign super-individuals to ICES division at initialisation; and (4) the random component of the movement sub models.

Collectives: Beyond the distinction of the different life stages (egg, yolk-sac larvae, larvae, juvenile or mature sea bass) there is no social grouping between the super-individuals. Using super-individuals to represent multiple individual fish could be representative of shoaling behaviour (e.g., Shin & Cury, 2001) although its introduction was for computational feasibility and reducing run times.

Observation: For model testing, the spatial distribution and migration patterns of the super-individuals were observed. The population variables spawning stock biomass (SSB), numbers at age and mass at age are recorded on the 1st of January (tick 1) and compared to ICES stock assessment values. For noise impacts, the percentage of noise-affected individuals is monitored, as well as the emergent SSB and abundance from noise-affected individuals which can subsequently be compared to unaffected individuals.

B.5 Initialisation

The model starts with a spin-up initiated in 1985 and then the model begins on 1st of January 2004 and continues till 2015. During the 19 years of spin up, we use the 2004 SST and PHY remote sensing data and read in yearly numbers-at-age data from the ICES stock assessment 2020. The spin up allows individual energy rates to settle before running the model for the years used for calibration and assessment of fits (2004-2015). The relevant SST and PHY data are loaded and assigned to patches within a shapefile of the UK and surrounding countries (Fig. B.1a and b). Patches with an SST value within the stock area (ICES divisions' 4.b–c, 7.a and 7.d–h) are set as sea patches. ICES rectangles (sets of four sea patches) intersecting land and patches (14, 34), (18, 24), (20, 20), and (16, 6) are set as coastal patches (green patches in Fig. B.1a and b), and all other sea patches are set as offshore (blue patches see Fig. B.1a). Coastal patches whose midpoint intersect land are assumed mostly land and set as non-sea patches, except for patches (28, 21), (15, 10), (13, 10) and (5, 22). Individual coastal patches intersecting land south of 54°N (y coordinate < 24) are assigned as nursery patches. The patches that eggs, ys-larvae and larvae drift towards are termed Target patches (shown as red patches in Fig. B.1 and used for ease of coding). We calculate how far away each patch is from each target patch for use in sub models Drift_eggs/ys_larvae/larvae (see TRACE 7 for details of sub models). All coastal patches are assigned to an ICES division (4.b, 4.c, 7.a, 7.d, 7.e or 7.fg) and all offshore patches south of 54° N to a spawning region (IS – Irish Sea, CS – Celtic Sea, C – Channel or NS – North Sea). Sea surface temperature (SST), phytoplankton concentration (PHY) and noise levels cannot be shown simultaneously in the model interface so for demonstration purposes Fig. B.1a shows offshore patches as blue with dark to light representing increasing SST and Fig. B.1b shows offshore patches as orange with dark to light representing increasing PHY.

Numbers-at-age data from the ICES stock assessment 2020 are used in spin up. 10 super-individuals are created per cohort, with the number of fish represented by an individual taken as the stock assessment numbers-at-age estimated for the year divided by 10. Juvenile super-individuals are distributed randomly amongst nursery patches if less than four years of age, and amongst all coastal patches if four to six years of age. Mature super-individuals are distributed randomly in pre-spawning areas (ICES divisions' 7.e–g) with *spawn-trigger* set equal to 1. Each mature individual is assigned a random ICES division (4.b, 4.c, 7.a, 7.d, 7.e, or 7.fg) for which it has an affinity to feed.

Initial *cohort* age of super-individuals is taken as the whole number stock assessment age, but actual *age* is incremented by a random number between 222 and 314 days to reflect mid-year spawning. From that *length* is calculated from the von Bertalanffy growth equation:

$$L_t = L_\infty\left(1 - e^{-K[t-t_0]}\right)$$

where L_∞ is the asymptotic length, K the growth rate coefficient and t_0 the hypothetical age at length 0 (Table 2). Note these calculations are at initialisation only, once running there are different processes for deciding ICES division affinity and growth of larval stages which use a different growth model (see TRACE sections 8.3.7 and 8.3.8.7).

Remaining energy budget variables starting values calculated and initialised as follows;

Calculate structural mass;

Structural-mass = a * (L ^ (b))

where *L* (cm) is the length and *a* and *b* are Length-mass coefficient values taken from the ICES stock assessment (Table 2) (parameter *a* is adjusted to account for the original values being used to calculate total mass, for details see TRACE Section B.8.3).

Calculate maximum energy reserve;

energy-reserve-max = ((Structural-mass * 0.01) * El)

where *El* is the energy content of lipid (Table 2).

Calculate energy reserve;

energy-reserve = (energy-reserve-max * 0.5)

Calculate total mass;

Total-mass = (structural-mass + (energy-reserve / El))

where *El* is the energy content of lipid (Table 2).

Calculate maintenance (the energy put aside to pay for maintenance during spawning);

Maintenance-energy = (energy-reserve * 0.1)

Calculate potential fecundity (number of eggs that could theoretically be produced by a fish that size);

Potential-fecundity = (std-mass / 1000) * (eggs_per_bass)

Calculate potential fecundity (the energy required to produce the potential fecundity);

Max-R = (potential-fecundity * egg-mass * (Ef + Fs))

where *Ef* is the energy content of flesh and *Fs* is the energy to synthesise flesh (Table 2).

Calculate-speed; See sub model Calc-speed.

Calculate-r; See sub model calc-r.

Table B.2. Parameter values used in the model.

Parameter	**Description**	**Value**	**Reference**
A	Aspect ratio of the caudal fin.	1.76	(Froese & Pauly 2017)
a	Length-mass coefficient (for details see TRACE Section B.8.3).	$1.296 \times 10^{-5} * 0.95$	(Pickett & Pawson 1994; ICES 2012)
b	Length mass scaling exponent.	2.969	(ICES 2012)
A0	Normalizing constant for relationship between Metabolic rate and fish size.	0.1227808	(Claireaux,2006 ; Jourdan-Pineau *et al.* 2010; Luna-Acosta *et al.* 2011; Zupa *et al.* 2015; Peixoto *et al.* 2016)
AE	Efficiency of energy from phytoplankton to fish.	1.64×10^{-3}	(Watson *et al.* 2022)
boltz	Boltzmann constant.	8.62 10×10^{-5} eV K^{-1}	
Cmax	Max ingestion.	0.54 grams per gram of fish	(Lanari *et al.* 2002)
Ea	Activation energy.	0.5 eV	(Gillooly *et al.* 2006)
EaS	Activation energy for speed Arrhenius function.	3.05×10^{-20} J	(Claireaux *et al.* 2006)
Ef	Energy content of flesh.	7 kJ g^{-1}	(Peters 1986)
egg-mass	Sea bass egg mass.	0.96×10^{-3} g	(Cerdá *et al.* 1994)
Eggs_per_bass	Potential egg production per gram of sea bass.	375,000	(Pickett & Pawson 1994) (reference states between 1/4 and 1/2 a million eggs per kg of sea bass)
El	Energy content of lipid.	39.3 kJ g^{-1}	(Schmidt-Nielsen 2013)
ep	Energy content of phytoplankton.	6.02 kJ g^{-1}	(Annis *et al.* 2011)

Fs	Energy to synthesise flesh.	3.6 kJ g^{-1}	(Sibly & Calow 1986; Sibly *et al.* 2013)
GL	Larval stages growth coefficient.	0.02485 cm d^{-1}	Jennings, Jennings and Pawson, 1992; Regner and Dulčić, 1994)
H	Half saturation constant.	4.87x10^{-1}	(Watson *et al.* 2022)
I	Importance of density on ingestion.	5.14x10^{+13}	(Watson *et al.* 2022)
k	Annual growth rate coefficient.	0.096699	(ICES 2012)
L^{∞}	Asymptotic length.	84.55 cm	(ICES 2012)
Ls	Energy to synthesise lipid.	14.7 kJ	(Pullar & Webster 1977)
μ_n	Natural mortality rate juvenile and mature sea bass.	4.71x10^{-4}	(Watson *et al.* 2022)
μ_p	Natural mortality rate eggs, ys-larvae and larvae.	8.01x10^{-2}	(Watson *et al.* 2022)
ncohort	Number in each super-individual.	10	
T_0	Age at length 0.	-0.73 years	(ICES 2012)
TrefS	Reference temperature at which swimming speed at the length used in the paper coincides with that from the model.	6 ^{o}C	(Claireaux *et al.* 2006)
Tref	Reference temperature for the energy budget.	285.15 K (12^{o}C)	
noise-threshold	Threshold level (dB) for noise impacts	Mean 105 dB ± 8 (SD); normal distribution	(Kastelein *et al.* 2008)
NFm, ψ_F	Acoustic disturbance feeding modifier	0–1	(Purser & Radford 2011; Voellmy *et al.* 2014a; Soudijn *et al.* 2020)
NEm, ψ_E	Acoustic disturbance energy expenditure multiplier	0–1	(Bruintjes *et al.* 2014; Soudijn *et al.* 2020)
NMm, ψ_M	Acoustic disturbance mortality multiplier	0–1	(Simpson *et al.* 2016; Soudijn *et al.* 2020)

NRm, ψ_R	Acoustic disturbance reproductive failure modifier	0–1	(Nedelec *et al.* 2017b; de Jong *et al.* 2018a; Soudijn *et al.* 2020)

B.6 Input data

Numbers-at-age, used to initialise the model and introduce recruits at setup come from the 2020 stock assessment. Environmental inputs comprise dynamic maps of chlorophyll-a concentration, SST and noise level. The satellite remote-sensing data were taken from NASA’s ocean colour portal in NetCDF format (NASA 2017; NASA OBPG 2017). Processing of the satellite data included: 1) cropping to the model extent (Fig. B.1) estimating missing values using linear temporal interpolation (e.g., NAs for a cell in one time period become the average of the last prior period with a value, and next subsequent period with a value); 3) fill in any further gaps with the annual average; 4) re-sampling the spatial resolution from 9km x 9km to 30km x 30km; and 5) convert chlorophyll to plankton biomass; Chlorophyll-a was converted to carbon mass using a C:Chl-a ratio of 75. Then, a wet mass:C ratio of 10 was used to obtain phytoplankton biomass (g wet mass m^{-2}) (Link *et al.* 2006). This gives phytoplankton biomass (g m^{-2}) = chl-a (mg m^{-2}) x 0.75 and 6) re-project on to lambert azimuthal equal area projection.

B.7 Sub models

The following sections provide full detail on how model processes are simulated. The equations in Netlogo code are shown in blue.

Seacheck: Super-individuals check if the patch they are on is sea if not then move to the closest sea patch within a radius of 2 patches before continuing processes.

Update-patches: Sea patches are assigned new SST data each tick. Between ticks 32–151 any offshore patches south of 54°N with a SST value between 9–15°C are set as *spawn-patches*.

Natural-mortality: The number of sea bass within each individual is discounted with a mortality constant.

Eggs, yolk-sac larvae and larvae have a greater mortality rate than older life stages. The quicker they grow through to a juvenile sea bass the higher the number of age 0 for that year. The growth of these is influenced by energy available [PHY] and sea surface temperature [SST].

We update the number of individuals each super-individual represents each tick with;

$$N = N * e^{(-\mu_p)}$$

Here N is the number of eggs, egg-sac larvae or larvae that the super-individual represents. μ_p is the daily natural mortality rate for these young life stages. The actual value of μ_p is unknown so is calibrated with ABC see TRACE Section B.9.

Juvenile and adult sea bass experience less mortality than egg, yolk-sac larvae and larvae life stages and we update the number of super-individuals each super-individual represents each tick with;

$$N = N * e^{(-\mu_n * (1+\psi_M))}$$

Here N is the number of individual fish the super individual represents and μ_n is the adult daily natural mortality rate calibrated with ABC see TRACE Section B.9 for details. Individuals affected by noise increase mortality rates proportionally with a linear ‘noise-mortality’ modification parameter ψ_M (Soudijn *et al.* 2020). Finally, in addition to daily natural mortality, any super-individuals reaching the age of 30 are removed from the simulation. If the super-individual represents less than one fish, then they become decimal. This is required to keep the number of super-individuals per cohort constant and avoid any erroneous knock-on distribution bias whilst making sure there is not misleading excess biomass.

Calculate-catch: Each patch calculates the catch, Ct, in tonnes taken by commercial and recreational fishing fleets during that time-step and adds it to a running total, resetting annually.

$$C_t = C_{t+1} + \frac{1}{1000}\sum_{a=0}^{30} w\left(\frac{\sum_f F_{a,f}}{\sum_f F_{a,f} + M}\right) N_t\left(1 - e^{-(M+\sum_f F_{a,f})}\right)$$

where Nt is the number of fish occupying the patch in time step t, Fa,f is the fishing mortality on cohort age; a, by fishing fleets; f (f = commercial inshore and recreational if the patch is coastal and commercial offshore if the patch is offshore; see TRACE Section B.8.9), M is natural mortality (see TRACE 7 *Natural-mortality*) and w is the mass of individual fish (see TRACE 7 *calc total mass*).

Fishing-mortality: The number of sea bass within each individual is discounted exponentially by fishing mortality *F*, partitioned and applied daily. Partial fishing mortality estimates by age and metier derived from the ICES stock assessment outputs (ICES 2018) were aggregated to give fishing mortality rates for three broad fishing fleets (see Trace Section B.8.9): commercial inshore (*Fci*), commercial offshore (*Fco*) and recreational (*Fri*). Fishing mortality is distributed by area type such that the commercial inshore and recreational fishing mortality rates are applied only to fish occupying coastal patches and the commercial offshore fishing mortality rate is applied only to fish occupying offshore patches. The annual commercial fishing mortality rates were raised inversely proportional to the number of days spent fishing, where the commercial offshore fleet is assumed to operate for 151 days between November and April (ICES 2012) and the commercial inshore fleet for 214 days during the remainder of the year (giving raising factors ~2.4 and ~1.7 respectively). Recreational fishing is assumed to occur all year and hence no raising factor is applied. The total *F* applied to super-individuals is then the sum of the fishing mortality from relevant fleets.

Catches taken by commercial fleets (commercial inshore and offshore) are summed across. Once the specified quota has been reached (if set), fishing mortality is switched off until the running total is reset according to the timescale specified.

Minimum conservation reference sizes (MCRS) for the commercial and recreational fleets can be specified via the com-net-hole-size and angler-min-size sliders on the models GUI. If set > 0 fishing mortality from the commercial and recreational fleets will apply only to the fish exceeding the specified lengths, which can be set up to 60cm / 80cm for the commercial / recreational fleets respectively. It is important to mention that any post-release/discard mortality is not included in the model.

Calc ingestion: The first life stages (Eggs and egg-sac larvae) do not feed until they transform into larvae. We calculate an ingestion rate for each life stage that is based on the energy available, the size of the larvae/fish and SST.

For older life stages, the rates of ingestion I are calculated from the maximum consumption rate of food in relation to body size $Cmax$, energy available in the environment PHY, total mass M_t, conspecific density i, and the sum non-egg biomass in the same patch M_{nm}:

$$I = \left(\left(Cmax * (PHY/H + PHY)\right) * M_t{}^{2/3}\right) * \left(i * \left(1/M_{nm}{}^{2/3}\right)\right) * (1 - \psi_F)$$

Individuals affected by noise (noise-trigger turned on) decrease food ingestion rates proportionally with a linear ‘noise-feeding’ modification parameter ψ_F (Soudijn *et al.* 2020). The remainder of the equation components relate to the Arrhenius function (Table 2).

Calc assimilation: We calculate the proportion of ingested energy available for energy budget processes (e.g., growth, maintenance and reproduction);

Assimilation-energy = ((Ingestion-rate * ep) * AE)

Ingestion rate is calculated as above and influenced by available food (PHY), fish size, SST and the density of agents competing for the same food. *Ep* is the energy in phytoplankton and *absorbed-energy* is the percentage of ingested energy that becomes available to the budget. *AE* is the product of assimilation efficiency (i.e., the proportion of energy that is absorbed from prey) and trophic delay (i.e., how long/how much energy from a phytoplankton bloom makes its way through the trophic levels to sea bass prey). For more details see TRACE Section B.10.3.

Calc maintenance: The assimilated energy is first used to cover metabolic maintenance requirements. Similarly, all life stages calculate metabolic rate and its energetic cost, except for eggs and yolk-sac larvae. Thus, metabolic rates are calculated from metabolic rate normalisation Ao, total mass M_t, and an Arrhenius function Ah:

$$Mr = \left(\left(Ao * \left(M_t{}^{3/4} * 2\right)\right) * Ah\right) * (1 + \psi_E)$$

Individuals affected by noise increase metabolic rates proportionally with a linear ‘noise-energy’ modification parameter ψ_E (Soudijn *et al.* 2020).

We calculate the field metabolic rate as twice the standard metabolic rate (Peters, 1986). Once we have calculated the cost of maintenance we check if it can be covered by the assimilated energy. If assimilated energy is sufficient to cover maintenance, we subtract this cost from the assimilated energy. If there is not enough assimilated energy (e.g., reduced feeding available in the winter) then energy reserves are added to assimilated energy and then metabolic costs are taken from this:

If there is sufficient assimilated energy to cover metabolic rate, then;

Assimilation-energy = assimilation-energy – MR

Otherwise, if there is insufficient assimilated energy to cover metabolic rate then pay out of reserves;

Energy-reserve = (energy-reserve + assimilation-energy) – MR

We then set assimilation energy to 0 as it has all been used.

Note that here we check that this does not create a negative energy reserve, if it does, we force the individual set energy reserves as 0.

Calc total mass: The structural mass (without reserves and gonad mass) of each fish is calculated from its length following the standard allometric equation:

Structural-mass = a L ^b

Where *a* and *b* are Length-mass coefficient values were taken from the ICES stock assessment (Table 2). Note ICES *a* and *b* coefficients are for calculating total mass (which includes energy reserves mass and gonad mass), to adjust this we adjust parameter *a*, reducing it by 5% for details see TRACE Section B.8.3.

To calculate the total mass (sum of structural, fat and gonad mass) we check if there are energy reserves then calculate the total mass of all reserves and gonads. If energy reserve is greater than 0 then:

Total-mass = structural-mass + (energy-reserve / El) + gonad-mass

where *El* is the energy content of lipid (Table 2).

However, if there are no energy reserves then:

Total-mass = structural-mass + gonad-mass

Calc growth: Calculate max daily growth rate. Agents under 70 days have a constant maximum growth rate (see TRACE Section B.8.3):

Max-growth-rate = GL * exp((- Ea / boltz) * ((1 / (SST + 273.15)) – (1 / Tref)))

where *GL* = 0.02485 and is the slope coefficient of a regression of larval length on age (see TRACE Section B.8.3). The remainder of the equation components relate to the Arrhenius function (Table 2).

Fish older than 70 days year are assumed to follow a von Bertalanffy growth curve:

Max-growth-rate = (linf – L) * (1 – exp(- k / 365)) * exp((- Ea / boltz) * ((1 / (SST + 273.15)) – (1 / Tref)))

where, *linf* is the asymptotic length of sea bass, *L* is fish length and *k* is the annual growth constant, divided by 365 to get daily growth. The remainder of the equation components account for the effects of temperature using the Arrhenius function (Table 2).

Now the max daily growth increment has been calculated we can apply this to agents.

We calculate what the potential new fish length could be and how much this will cost in energy.

Possible-L = (L + max-growth-rate)

Growth-costs = ((((a * (possible-L ^ b)) – structural-mass)) * (Fs + Ef))

where *L* is fish length, *a* and *b* are Length-mass coefficient values, *Fs* is the energy content of flesh and *Ef* the costs of synthesising flesh (Table 2).

Eggs; eggs do not grow, instead they develop (described later) and then transform into yolk-sac larvae.

Ys-larvae; yolk-sac larvae do not ingest energy and are nourished by the yolk sac thus are assumed to have maximum energy available to grow maximally;

Growth-rate = max-growth-rate

L = L + max-growth-rate

Structural-mass = a * (L ^ (b))

Total-mass = structural-mass

Larvae; once the egg-sac larvae have transformed to larvae they begin to ingest energy. We first check if there is adequate assimilated energy to grow maximally and update length accordingly (note this is a different measure of length specifically for calculating swimming speed). From the new length the new structural mass is calculated and because larvae do not store lipid their structural mass is equal to their total mass.

If larvae are assimilating enough energy, then they grow maximally:

L = L + max-growth-rate

```
Structural-mass = a * (L ^ b)
Total-mass = structural-mass
Assimilation-energy = assimilation-energy – growth-costs
```

If larvae don’t assimilate enough energy, they then grow sub-maximally:

```
Growth-rate = (max-growth-rate / growth-costs) * assimilation-energy
L= L + growth-rate
Structural-mass = a * (L ^ (b))
Assimilation-energy = 0
```

Juvenile and mature sea bass have to ingest energy so their growth will depend on the energy they have available.

If assimilated energy on a particular day is enough to cover growth, then they will grow maximally. Juvenile and mature sea bass allocate energy equally to growth in length and to fat reserves;

```
if (Assimilation-energy * 0.5) >= growth-costs
```

After checking available energy, sea bass with enough energy grow maximally;

```
L = L + max-growth-rate
Structural-mass = a * (L ^b)
Assimilation-energy = assimilation-energy – growth-costs
Calc-storage
```

If the sea bass don’t have enough energy, they grow at a suboptimal growth rate.

```
Growth-rate = (max-growth-rate / growth-costs) * (assimilation-energy * 0.5)
L = L + growth-rate
Structural-mass = a * (L ^ b)
Assimilation-energy = assimilation-energy * 0.5
Calc-storage
```

where *L* is length and *a*, *b* are Length-mass coefficient values were taken from the ICES stock assessment (Table 2). For both scenarios total mass is calculated later, after they have stored lipid a procedure *calc-storage* is called that converts remaining energy to lipid stores and accounts for the cost of synthesis.

<u>*Calc speed:*</u> The sustained swimming speed of each fish is calculated from its length and adjusted by the Arrhenius factor for the occupied patch to account for the effects of temperature on the chemical processes that contribute to swimming speed:

$$S = (10^{-0.828+0.6196(L_t)+0.3478(A)})\text{* Ks}$$

$$k_s = e^{\frac{EaS}{K}\left(\frac{1}{T}-\frac{1}{TrefS}\right)}$$

where A is the aspect ratio of the caudal fin (Froese & Pauly, 2017; Table 2). Note that the Arrhenius parameters are different for speed specific Arrhenius equations see table 2, and TRACE Section B.7 *update patches*. Values in kilometres per hour were converted to patches per day assuming 12 swimming hours spent per day in patches of 30 x 30 km.

<u>*Calculate-r:*</u> The speed of each fish is divided by a movement repeat variable r with fish moving r times per day. r is chosen as the smallest integer such that fish travel no more than 0.25 patches before changing direction. This allows fish to change direction whilst moving the correct distance and was introduced to reduce overlap with land.

<u>*Transform:*</u> If a super-individual meets the criteria (sufficient length [see Fig. B.2]) then it will transform to the next life stage and the necessary energy budget variables values will be calculated.

Eggs into yolk-sac larvae; after a development period of 5 days (a study by a Beraud *et al.* 2018 gave a range of 3 – 7.5 days):

Std-mass = 0.001

Energy-reserve-max = 0

Energy-reserve = energy-reserve-max

Larval-production = larval – production + number

Yolk-sac larvae into larvae: larvae do not store energy, they feed continuously to grow:

L >= 0.35 (study by Beraud *et al.* 2018 gives a range of 1.5 – 5.5mm) structural-mass = a * (L ^ b)

energy-reserve-max ((structural-mass * 0.01) * El)

Energy-reserve = energy-reserve-max

Larvae into juvenile sea bass:

L >= 1.425 (study by Beraud *et al.* 2018 gives a range of 10.5-18mm)

structural-mass = a * L ^ (b)

energy-reserve-max ((structural-mass * 0.01) * El)

Energy-reserve = energy-reserve-max * 0.5

Juvenile sea bass into mature sea bass:

L >= 42

Male and female sea bass mature at different rates which vary regionally within the stock (Pickett & Pawson 1994). However, for simplicity and to ensure the model remains precautionary with outputs of SSB we use the larger but generally accepted maturity length as 42cm for all adult sea bass (Pickett & Pawson 1994), note 42cm is also the minimum landing size for sea bass in northern stock legislation since 2015 [ICES, 2021]). When juveniles graduate to mature sea bass (Length > 42 cm) they set their coastal feeding ground affinity as the ICES division in which they are in at the time of ticking over this length requirement (this could be a different division to the original ICES division target they would have drifted towards when they were in pelagic stages, see TRACE Section B.8.7. At the end of the first spawning migration there is an opportunity to change ICES division affinity which is altered with a probability defined by the site-fidelity slider on the GUI.

Spawn-migration: This sub model is executed between ticks 274–151 corresponding to the months October–May. Between ticks 274–90, corresponding to the months October–March, any mature super-individuals not currently performing a spawning migration (spawn-trigger = 0) on a patch that either neighbours a spawning patch or is less than 9°C switches its spawning trigger to 1 (Fig. B.3). All super-individuals with spawn-trigger equal to 1 take r steps of distance S/r (see TRACE Section B.7 *calculate-speed* and *calculate-r*) according to the hierarchy presented in Fig. B.4.

Once a mature individual reaches a spawning patch its spawn-count increments by 1 each tick. When the spawn counter reaches 60 (indicating the agent has spent 60 ticks/days cumulatively on a spawning patch) or the end of the spawning period is reached (tick 152 corresponding to the 1st of June) both spawning trigger and counter are set to zero, and the individual no longer executes spawn-migration but defaults to feeding-migration (see TRACE Section B.7 *feeding-migration*). Before ending a spawning migration, each individual changes its affinity to a new coastal feeding area with fixed probability set by the site-fidelity slider on the model's interface. Each new assignment is random with equal probability between the six coastal feeding areas. Site fidelity was fixed at 100% in the reported results.

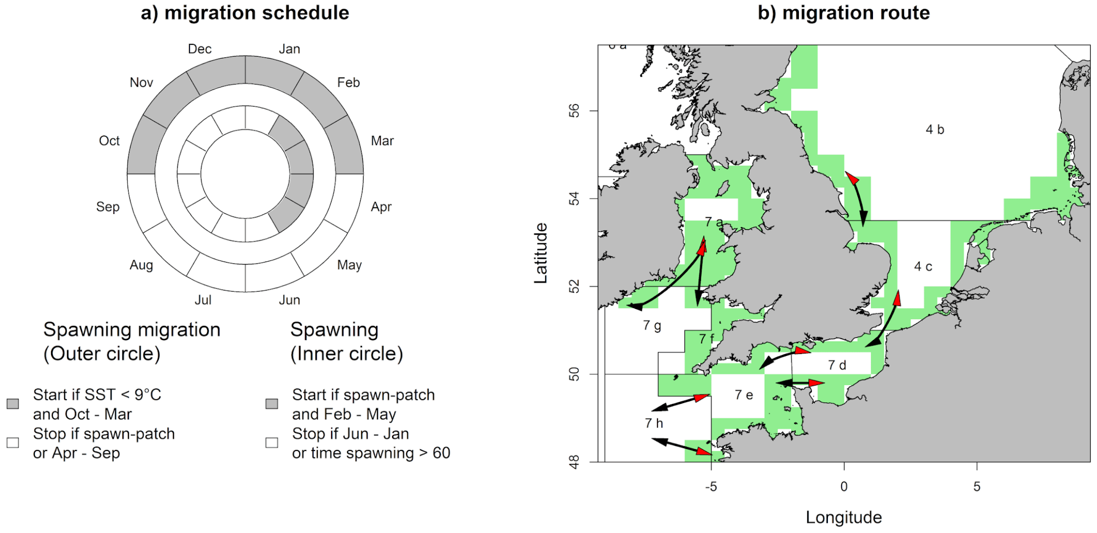

***Figure B.3. (a) Schedule for spawning migrations**. Outer circle: migration to (pre-) spawning areas is triggered by sea surface temperature and can take place between October and March. Inner circle: spawning takes place within offshore spawning patches in February–May. **B) Migrations of mature super-individuals** follow the hypotheses of Pawson et al. (1987, 2007). Arrows show movement around the coast to and from the Channel and Celtic Sea with black arrow heads representing the spawning migration and red arrow heads the feeding migration*.

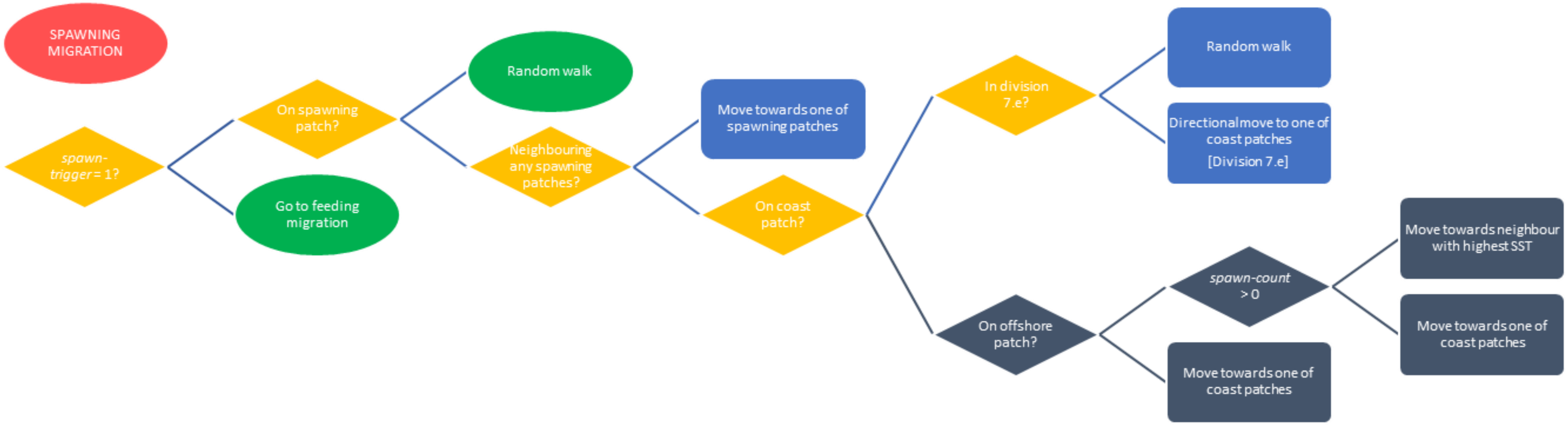

Figure B.4. Decision hierarchy for the spawning migration. *Diamonds represent decisions, green circles terminators and rectangles processes. Upward links are followed when the answer to a decision is 'yes' and downward links when the answer is 'no'. The hierarchy moves mature super-individuals towards offshore spawning patches where they are assumed to have reached their destination and move randomly (green 'Random walk' terminator). Blue processes show the action to take for a repeat in the current time-step, after which the hierarchy is followed from the beginning for the next repeat or time-step. Division 7.e. is a reported pre-spawning area; hence super-individuals take directed steps towards 7.e via coast patches, and then move randomly until spawning patches start to appear (see TRACE Section B.7 update-patches). The grey nodes represent troubleshooting decisions and actions. Given that migrations take place along the coast, any occupied offshore patch should be a spawning patch. If it is not then either (1) the offshore patch lost its spawning status during an update-patches, in which case the individual searches for a new spawning patch by moving to the offshore neighbour with the highest SST; or (2) the individual moved off the coast (either onto an offshore patch or land), as a consequence of allowing super-individuals to travel across square patches at any angle. In either of these two cases the individual is moved towards a neighbouring coastal patch.*

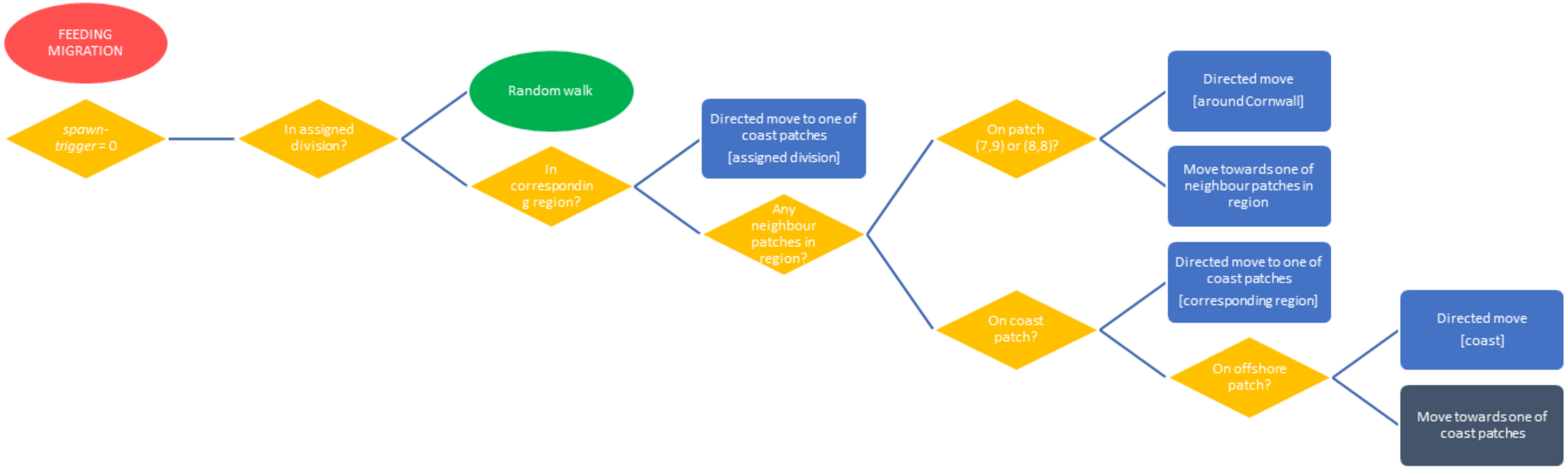

Figure B.5. Decision hierarchy for the feeding migration. *Diamonds represent decisions, green circles terminators and rectangles processes. Upward links are followed when the answer to a decision is 'yes' and downward links when the answer is 'no'. The hierarchy moves mature individuals towards their assigned feeding divisions where they are assumed to have reached their destination and move randomly (green 'Random walk' terminator). Blue processes show the action to take for a repeat in the current time-step, after which the hierarchy is followed from the beginning for the next repeat or time-step. The square brackets indicate the immediate target which, assuming the individual starts the feeding migration offshore following spawning, broadly follows (1) move to the coast, (2) move to the correct region and (3) move to assigned division. Additional rules are in place to move individuals around, rather than over, Cornwall. The grey node represents a troubleshooting action for individuals that move onto land as a result of individuals traveling across square patches at any angle. In this event the individual is moved towards a neighbouring coastal patch.*

Feeding-migration: This sub model is executed by mature individuals not on a spawning migration (spawn-trigger = 0). All individuals with spawn-trigger equal to 0 take r steps of distance S/r (see TRACE Section B.7 *calculate-speed* and *calculate-r*) according to the hierarchy in Fig. B.5.

Local-movement: All juvenile individuals follow a random walk process, taking r steps of distance S/r (see TRACE Section B.*7 calculate-speed* and *calculate-r*) in random directions. Juveniles that move off coastal patches turn 180° to move back to their last position on a coastal patch. Juveniles with length less than 32 cm are further constrained to nursery coastal patches.

Drift eggs: If the egg is on the target patch associated with is assigned affinity, then it moves at random around its target area. If not on the target patch it moves to the next patch with one less target distance, thus moving one patch closer to the target every tick. *

Drift_ys-larvae: If the ys-larvae is on the target patch associated with is assigned affinity then it moves at random around its target area. If not on target patch move to the next patch with one less target distance. Thus, moving one patch closer to target every tick. Once reached the target patch the ys-larvae undergoes random movement restricted to nursery patches. *

Drift larvae: If the larvae is on the target patch associated with is assigned affinity, then it moves at random around its target area. If not on target patch move to the next patch with one less target distance. Thus, moving one patch closer to target every tick. Once reached the target patch the larvae undergoes random movement restricted to nursery patches. *

* It is important to note that we use ICES affinity as a convenient way of ensuring new cohorts are split spatially across the model domain, and there is no evidence to our knowledge that larval stages inherit their affinity from their parents. Instead, once transformed through the life stages, a newly mature sea bass is leaving the coast for its first spawning migration, its fidelity is set to the ICES areas it is leaving. Thus, is more in-keeping with evidence from tagging studies reviewed by Pawson, Brown, Leballeur, & Pickett, 2008 (for more details see TRACE Section B.8.7).

Spawning: Initiate spawning on the 60th tick which is the 17th of March (picked as the middle of the spawning period). We first calculate potential fecundity and then the energy required to produce this number of eggs (*Max-R*) for all mature sea bass. We allow for maintenance costs whilst spawning by setting aside 10% of reserves:

Potential-fecundity = (std-mass / 1000) * (Eggs_per_bass)

Max-R = (potential-fecundity * (egg-mass * (Ef + Fs)))

Maintenance-energy = energy-reserve * 0.1

where we assume a female sea bass can produce 375,000 eggs per kg of sea bass (Pickett & Pawson, 1994 state between 0.25 and 0.5 million per kg). *Ef* is the energy in flesh and *Fs* is the cost of synthesising flesh (Table 2).

If there is enough energy to produce max fecundity, then the energy needed to produce the max number of eggs is taken from the energy reserve and we set the gonad mass and realised fecundity accordingly:

(Energy-reserve – maintenance-energy) >= max-R

Energy-reserve = energy-reserve – max-R

Gonad-mass = (max-R / (Ef + Fs))

Realised-fecundity = potential-fecundity

However, if there is not enough energy for max fecundity then energy reserve is set to whatever is left after subtracting maintenance costs. We then set the gonad mass and realised fecundity to what is achievable with the limited resources:

ER = energy-reserve – maintenance-energy

Gonad-mass = (ER) / (Ef + Fs)

Realised-fecundity = (ER / (max-R)) * potential-fecundity

where *Ef* is the energy in flesh and *Fs* is the cost of synthesising flesh (Table 2).

Once we have calculated how many eggs can be produced, we ask 10 mature super-individuals to spawn the total realised fecundity of the total SSB (all mature sea bass). The spawned individuals represent as many eggs N_0 as determined by total realised fecundity F_r of the whole spawning stock divided by ten N_c and the number of fish from the parent individual N_p:

$$N_0 = \left(\left(F_r * N_p\right)/N_c\right) * \left(1 - \psi_R\right)$$

Individuals affected by noise reduce reproductive success proportionally with a linear 'noise-reproduction' modification parameter ψ_R (Soudijn *et al.* 2020). We choose 10 to keep the number of super-individuals consistent for each cohort (see TRACE Section B.8.7). We split the 10 new super-individuals to represent the spatial aspect of the fishery (see TRACE Section B.8.7).

B.8 Data evaluation

This TRACE element provides supporting information on: The quality and sources of numerical and qualitative data used to design, parameterise (both directly and inversely via calibration), and run the model. This critical evaluation will allow model users to assess the scope and the uncertainty of the data and knowledge on which the model is based.

B.8.1 Summary

The population dynamics component of the IBM is emergent from the energy budget equations, while parameters and inputs were derived from the literature or public databases. The movement sub model was based on hypotheses drawn from tagging studies. Decisions for the effects of noise within the model are outlined at the end of the section; noise impacts are informed by a comprehensive meta-analysis (Cox *et al.* 2018) and implemented to affect life-history processes outlined by Soudijn *et al.* 2020.

B.8.2 Environmental inputs

<u>*SST and PHY*:</u> Environmental inputs comprise dynamic maps of chlorophyll-a concentration, and sea surface temperature. The satellite remote-sensing data were taken from NASA's ocean colour portal in NetCDF format (NASA 2017; NASA OBPG 2017). Processing of the satellite data included: 1) cropping to the model extent (Fig. B.1), 2) estimating missing values using linear temporal interpolation (e.g., NAs for a cell in one time period become the average of the last prior period with a value, and next subsequent period with a value), 3) fill in any further gaps with the annual average, 4) re-sampling the spatial resolution from 9km x 9km to 30km x 30km, 5) convert chlorophyll to plankton biomass. Chlorophyll-a was converted to carbon mass using a C:Chl-a ratio of 75, then, a wet mass:C ratio of 10 was used to obtain

phytoplankton biomass (g wet mass m^{-2}) (Link *et al.* 2006). This gives phytoplankton biomass (g m^{-2}) = chl-a (mg m^{-2}) x 0.75 and 6) re-project on to lambert azimuthal equal area projection.

Noise-level: Ocean noise maps were produced using data on noise sources (acoustic source spectrum level and location at each time increment) and the sound propagation properties of the environment, and predictions were validated against field measurements (Fig. B.6) (Farcas *et al.* 2020). Specifically, annual median broadband (63–4000 Hz) noise levels (P50) were produced for the extent of available sAIS data for 2017 in the Northeast Atlantic (Farcas *et al.* 2020). These noise maps were implemented into the model as dynamic patch variables and are updated during each daily timestep following similar procedures to SST and PHY (updated every eight days). Lastly, the noise maps for 2017 are repeatedly used for each year of the emergent modelling period of 2004–2014 due to a lack of available noise predictions outside of this specific period.

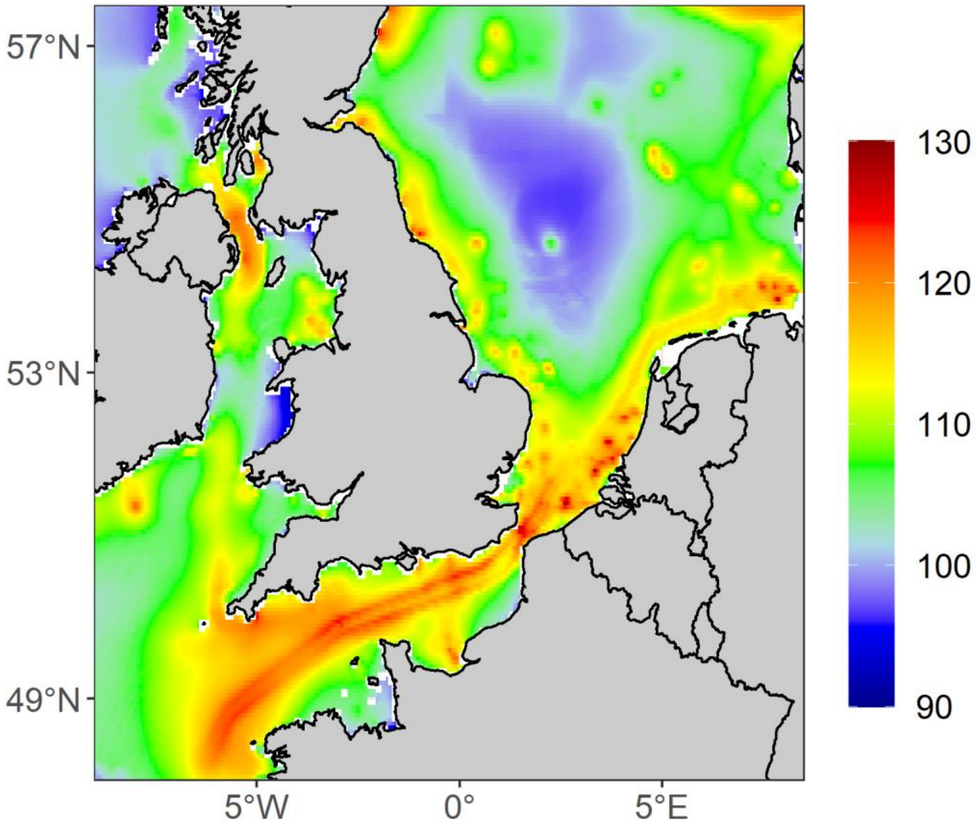

Figure B.6. Mean distribution of noise levels throughout the Northeast Atlantic*, averaged from daily maps across one year (2017; Farcas et al. 2020). Daily maps of* *total noise were created by Farcas et al. 2020 using sAIS ship-tracking data. Maps are implemented into the model daily and recycled for the 2004–2014 modelling period.*

B.8.3 Growth

Juvenile and mature sea bass von Bertalanffy L_∞, k: L_∞ is the maximum length a sea bass can reach, and *K* is annual growth constant. The IBM uses the same von Bertalanffy growth parameter values as used in the stock assessment (Table 2). These parameter values were estimated from data derived from sampling of UK fishery catches around England and Wales as well as from trawl surveys of young sea bass in the Solent and Thames estuary and consisted of over 90,000 fish sampled and aged between 1985–2011. All ageing was done from scales and the growth curve was fit in Excel solver using non-linear minimization. Standard deviations of length-at-age are also provided in (Armstrong & Walmsley 2012).

Length weight growth parameters *a, b*: Length weight parameters *a* and *b*, (used to convert calculated lengths from growth equations into estimates of mass are sourced from ICES, 2012). These parameters are originally used to calculate total mass from fish length, thus include the mass of gonads and fat reserves. In this model we require estimates of structural mass (the minimum weight of fish without gonad or fat reserve mass). To allow for this we have taken average figures of energy reserve mass (~1% of body weight [Pickett and Pawson, 1994]) and gonad somatic index (~4% of body weight [Pickett and Pawson, 1994]), to inform a reduction in parameter *a* by 5%.

Early life: We used sea bass larvae growth experimental data from Regner and Dulčić, 1994 to set the maximum growth rate during the first 70 days of growth after hatching (Fig. B.7). 70 days is also consistent with other studies of length of the pelagic stages of sea bass (Jennings & Ellis 2015; Beraud *et al.* 2018). For the first 70 days we calculate that larva grow at a constant rate which is affected by temperature. At the reference temperature of 14ºC this is 0.02485 cm/d (also consistent with daily growth value of 0.2mm in Jennings, Jennings and Pawson, 1992) We test the effect of extremes of observed SST on maximum growth rate. The highest observed SST (30°C) results in a greater maximum growth rate (0.07216844 cm/d) when compared to growth in the lowest observed SST (0°C, maximum growth = 0.008824422 cm/d).

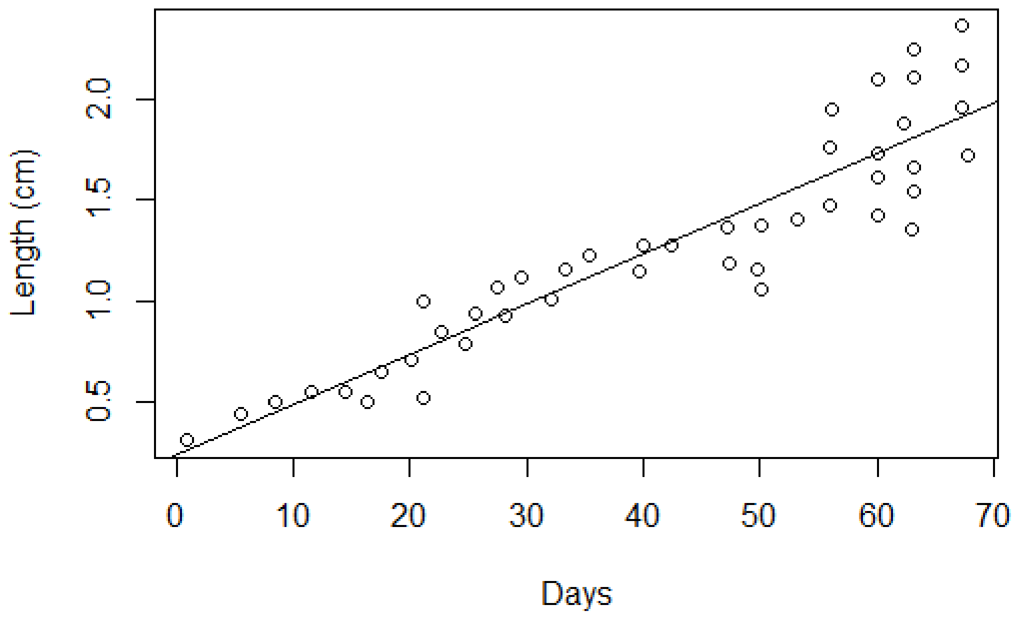

Figure B.7.Digitised larvae growth data *from* (Regner & Dulčić 1994). *The solid line represents the regression from which we use the slope coefficient (0.02485 cm/d) to represent maximum growth rate.*

Reference temperature: This is the temperature used in the Arrhenius functions throughout the model (except for the use with calc-speed). 12°C was chosen as the reference temperature following Walker *et al.* (2020).

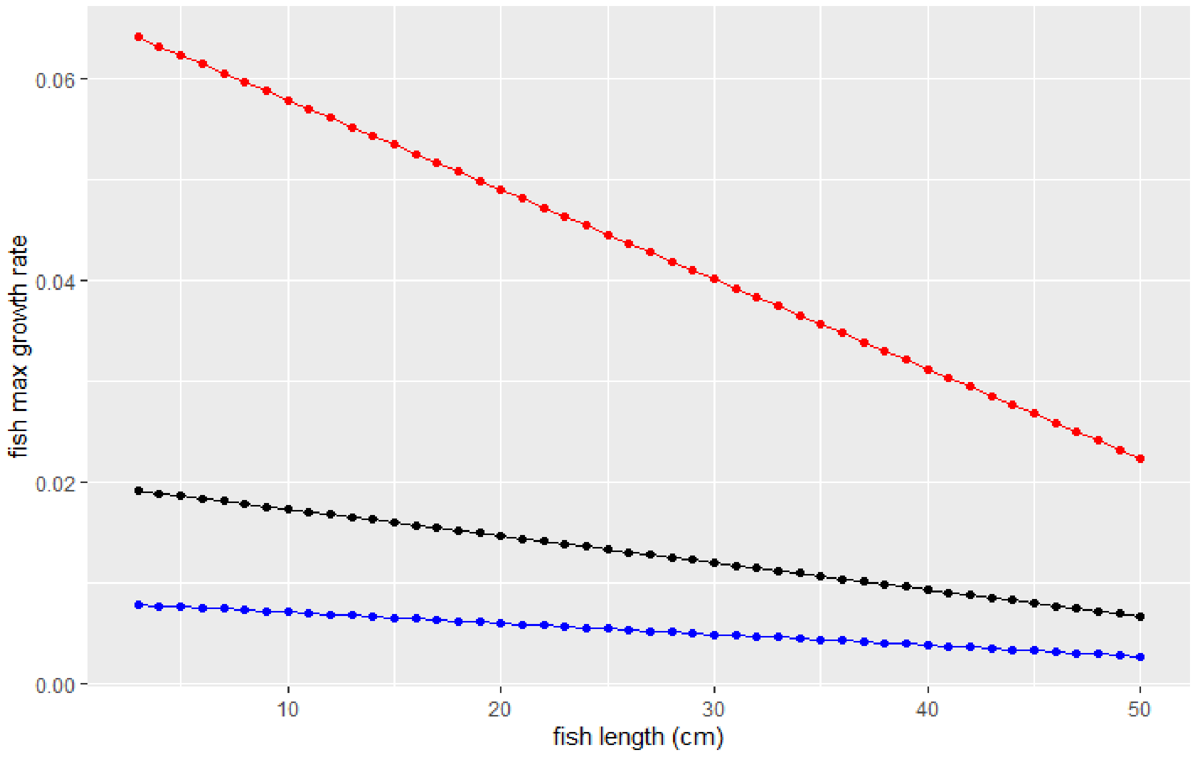

Figure B.8. Juvenile and mature max daily growth rate *using the von Bertalanffy growth equation for European sea bass. Red, black, and blue shows the extremes* *obtained if larvae were to continuously inhabit a patch at the highest (30°C), reference (14^{o}c) or lowest (0°C) observed SST.*

B.8.4 Swimming

Aspect ratio of the caudal fin A: The value of 1.76 was obtained from FishBase (Swim type) based on the value reported in a doctoral thesis (FishBase Ref No. 12676).

Activation energy E_S: The activation energy used in the Arrhenius equation used when calculating speed (see TRACE Section B.7 *calculate-speed*). The temperature dependences of biological processes are known to vary with activity levels, reducing as activity levels increase (Bennett 1985). This is why the activation energy for sea bass swimming fast is lower than the activation energy for sea bass at other times (Claireaux *et al.* 2006). The activation energy value used is 0.1903656 following (Walker *et al.* 2020).

Reference temperature T_S: The reference temperature used in the Arrhenius equation used when calculating speed (see TRACE Section B.7 *calculate-speed*) The reference temperature value used as 6^{o}C following rational in Walker *et al.* (2020). Fig. B.9 illustrates the potential effects of the Arrhenius multiplier on swimming speeds in the IBM.

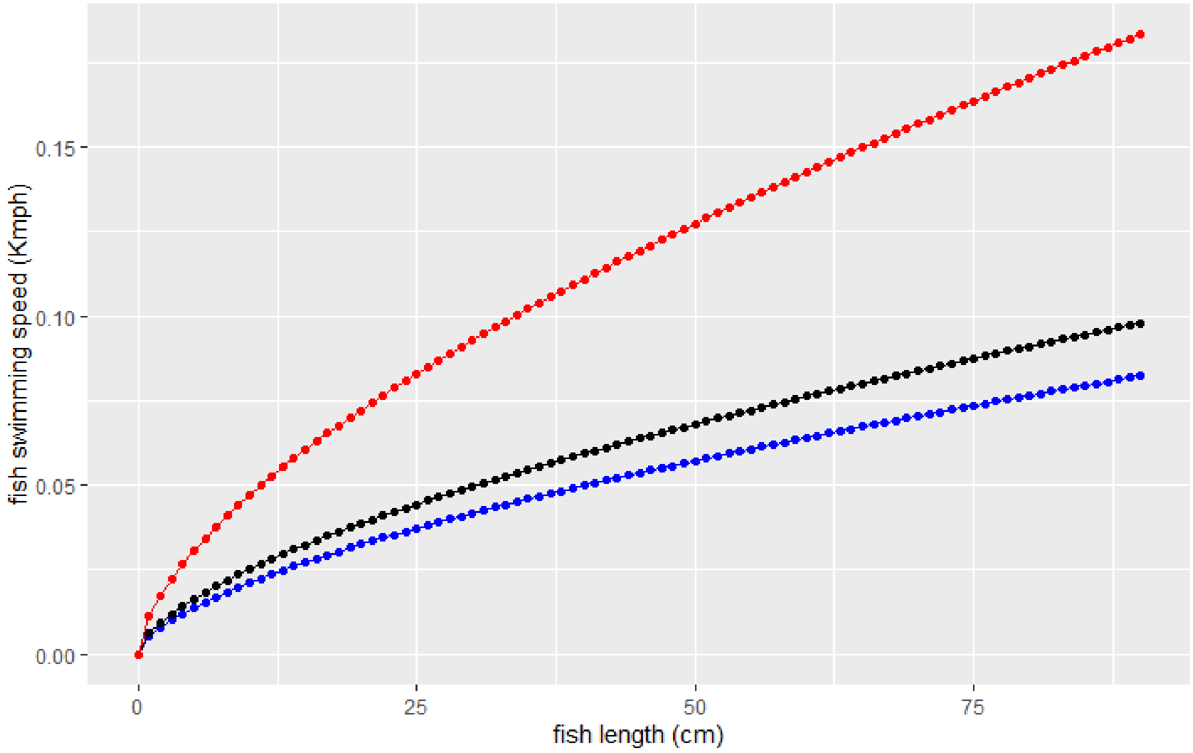

Figure B.9. The deterministic swimming speed of European sea bass *(kilometres per hour) at the reference temperature of 6^{o}C (black curve). Red, and blue which show the extremes obtained if larvae were to continuously inhabit a patch at the highest (30°C), or lowest (0°C) observed SST.*

Time spent swimming: 12 hours was chosen arbitrarily in the absence of further information.

Movement repeats: Fish move r times per day where r is the smallest integer is such that fish travel no more than 0.25 patches before changing direction. With no movement repeats ($r = 1$) fish sometimes overlap with land, while restricting movement to 0.1 patches before enforcing a direction change can prevent fish from reaching feeding grounds and results in tighter grouping at the divisional boundaries, particularly for fish with an affinity to feed in division 4.

B.8.5 Ingestion

Cmax: *Cmax* is the maximum ingestion rate in grams of food per day per gram of fish. Currently *Cmax* is set as Cmax = 0.54 grams per day per gram of fish. This value is used in Watson *et al.* (2020) which was based on extrapolation from data in Lanari, D'Agaro and Ballestrazzi, 2002. Lanari, D'Agaro and Ballestrazzi, 2002 used sea bass specimens weighing 60 - 250 grams but we assume this *Cmax* is appropriate for all agents in the model that feed (i.e., larvae, juvenile and mature fish).

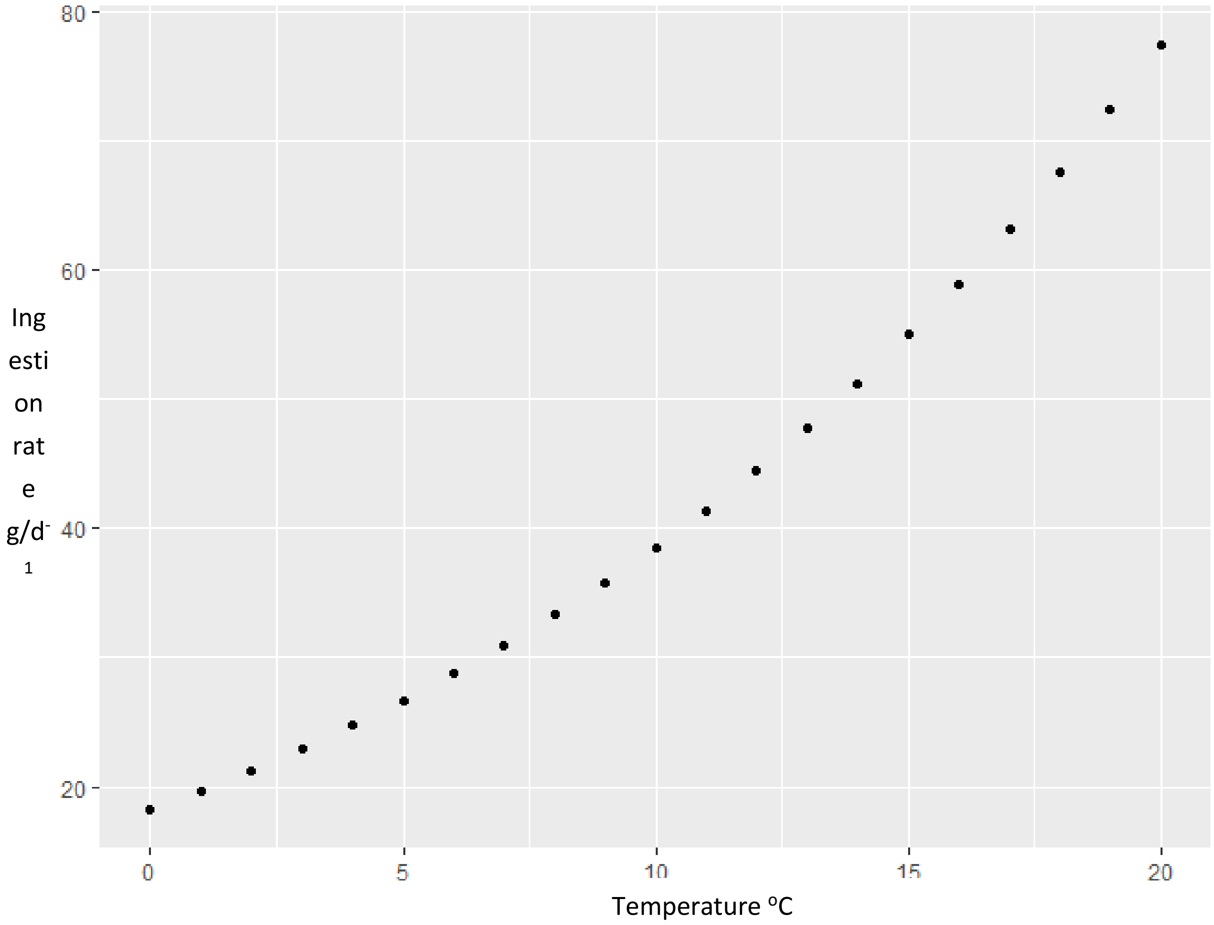

Figure B.10. Temperature effect on ingestion rate *(PHY = 2, h = 0.5, fish length = 42cm).*

Half saturation constant (*H*): Half saturation constant is the resource availability at which half of the maximum intake is reached. We show how *H* affects ingestion rate in Fig. B.11. This parameter is calibrated with ABC (see TRACE Section B.9)

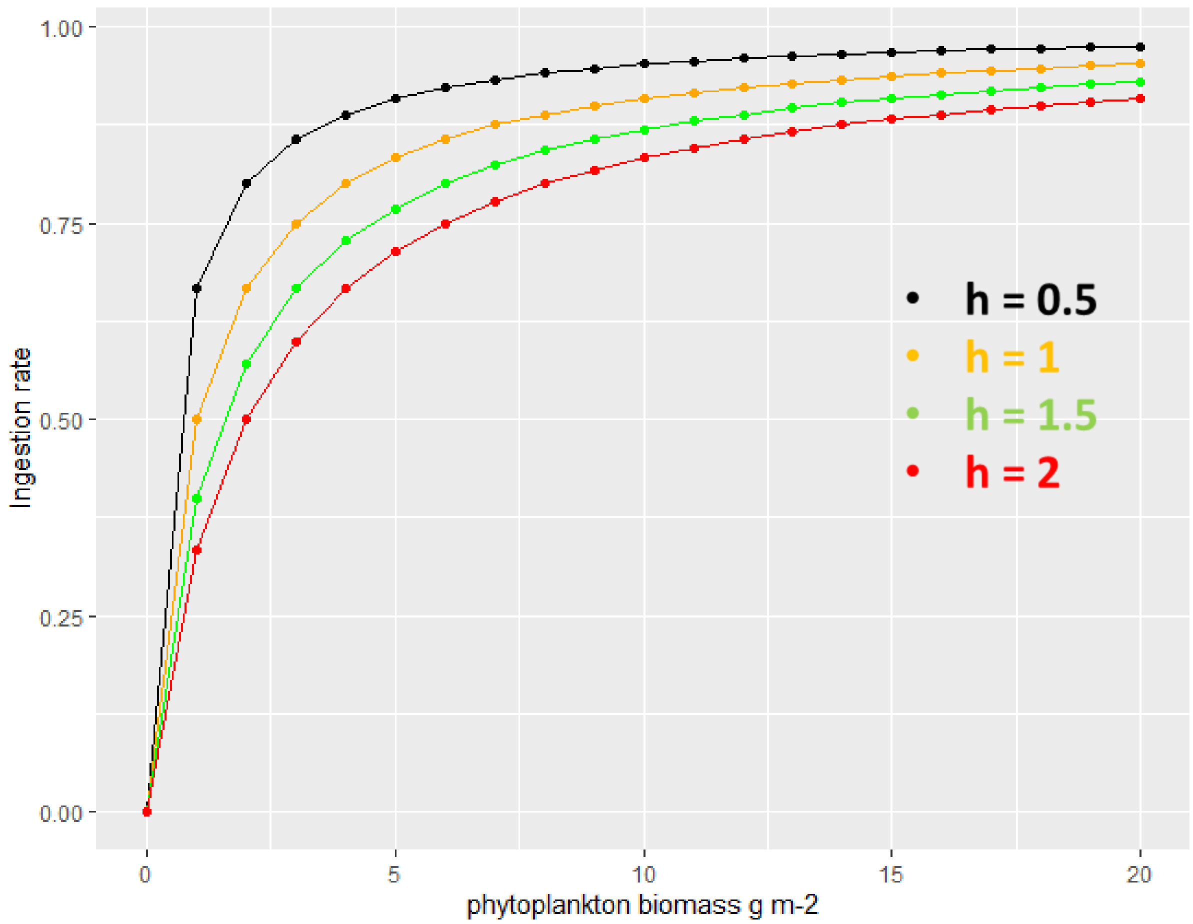

Figure B.11. Ingestion rate as a function of phytoplankton biomass *with half saturation constant values 0.5 (black), 1 (yellow), 1.5 (green) and 2 (red).*

Absorbed energy (*AE*): Absorbed energy is the fraction of energy in the environment (phytoplankton [PHY]) that is ingested and assimilated for use in life processes. To keep parameters to a minimum we combined the correlated parameters assimilation efficiency (which was set at 0.95 for mackerel in Boyd *et al.* 2020) and a trophic delay term. Trophic delay is needed as sea bass do not directly access the energy being read into the model in the form of PHY remote sensing data. The sea bass will only access a fraction of this due to inefficiencies as energy is passed through the trophic levels to the broad range of sea bass prey. This parameter is calibrated with ABC (see TRACE Section B.9)

Density dependence importance (*I*): Importance of density dependence is necessary to give a consequence of having an inflated population, for example a profitable area to feed becomes less optimal as the number of individuals there increases. This parameter is calibrated with ABC (see TRACE Section B.9).

B.8.6 Maintenance

Maintenance is assumed to be the same cost all year round and is assumed to be twice Standard Metabolic Rate to take account of activity in the field (Peters 1986).

Normalizing constant (*Ao*): *Ao* is the scaling coefficient between fish size and metabolic rate. We use the mean scale coefficient (*Ao* = 0.1227808) between fish size and metabolic rate from data used in Watson *et al.* (2020) (Fig. B.12).

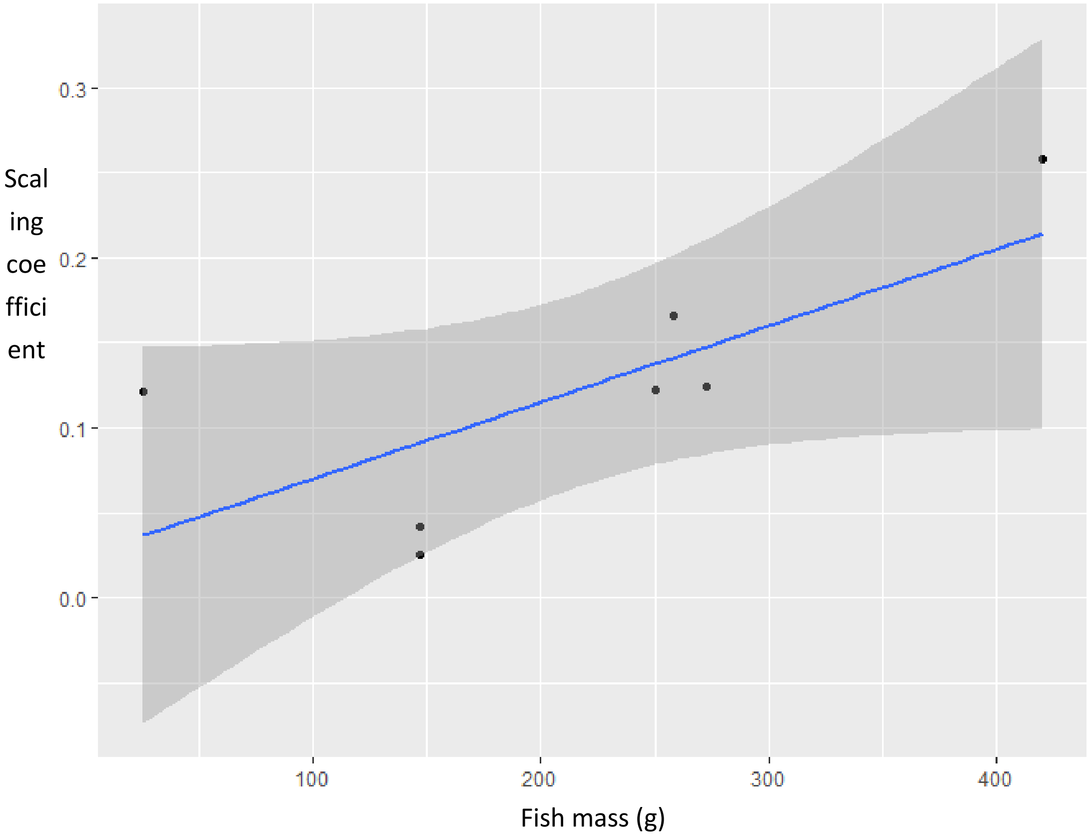

Figure B.12. The scale coefficient between fish mass and metabolic rate.

B.8.7 Spawning

Numbers eggs per sea bass: Pickett and Pawson, 1994 give a range of ¼ to ½ a million eggs per kg of sea bass so we use a value of $0.33x10^6$ eggs per kg of sea bass.

Representative spawning super-individuals: We maintain 10 super-individuals per cohort throughout the model simulation by introducing 10 new super-individuals each year. To ensure the new cohort are spatially representative we split the new 10 into; 3 super-individuals with affinity to Celtic/Irish Sea (VIIfg and VIIa), 5 with affinity to the Channel (VIId and VIIe) and 2 with affinity to the North Sea (IVb and Ivc). We have based this distribution on (Walker *et al.* 2020).

Although this fixes the number of super-individuals, note that each super individual can represent many fish. So, although there are only two super-individuals in the North Sea, they could in theory still represent more fish than the whole Channel if necessary. In this way we still can adequately spatially represent the fishery.

It is important to note that we use ICES affinity as a convenient way of ensuring new cohorts are split spatially across the model domain, and there is no evidence to our knowledge that larval stages inherit their affinity from their parents. Instead, once transformed through the life stages, a newly mature sea bass that is leaving the coast for its first spawning migration sets its fidelity to the ICES area it is leaving. Thus, is more in-keeping with evidence from tagging studies reviewed by (Pawson *et al.* 2008).

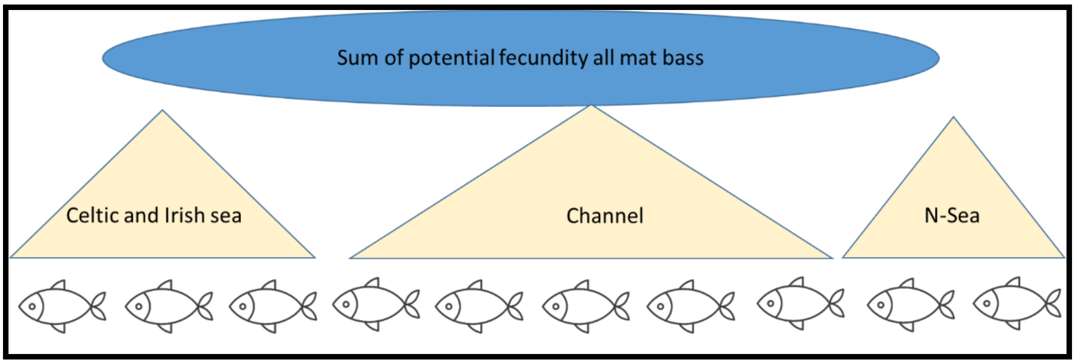

Figure B.13. Schematic showing how we represent the total spawning potential of all mature sea bass *with a new cohort consisting of 10 super-individuals split between the three main areas in the fishery.*

B.8.8 Natural mortality

Early life mortality (*PM*): *PM* is the young life stages daily natural mortality rate. Young life stages (eggs, egg-sac larvae, and larvae) are exposed to a much higher mortality rate than juvenile and mature sea bass. Early life mortality can be impacted by a multitude of factors including: SST, predation and weather, making it complex to model explicitly. Instead, *PM* is calibrated with ABC see TRACE Section B.9

Juvenile and mature mortality (*AM*): For juvenile and mature sea bass we do not follow the ICES assessment and *AM* is calibrated with ABC see TRACE Section B.9.

B.8.9 Fishing mortality

Fishing mortalities were taken as those estimated by the stock assessment (ICES 2018). Catch data for six fishing fleets (1. UK bottom trawls and nets; 2. UK lines; 3. UK midwater pair trawls; 4. French fleets (combined); 5. Other (other countries and UK fleets combined) and 6. Recreational fisheries) are taken as input to the SS3 assessment, and fishing mortalities estimated to match the observed catch (Methot & Wetzel 2013).

For the purposes of the IBM, fishing mortality was partitioned among the fleets modelled within SS3 by proportion of catch:

$$F_{a,y,f} = \frac{C_{a,y,f}}{\sum_f \quad C_{a,y,f}} F_{a,y}$$

Where $F_{a,y}$ is fishing mortality-at-age estimated by the assessment and $C_{a,y,f}$ catch-at-age by fleet *f*. Fishing mortalities for fleets 1–5 (UKOTB_Nets, Lines, UKMWT, French and Other) were summed to give overall commercial fishing mortality-at-age while fleet 6 (RecFish) gave recreational fishing mortality-at-age.

B.8.10 Numbers-at-age

Numbers-at-age data were used to set up the initial population of sea bass and introduce recruits into the IBM for the first year from the stock assessment. Thereafter the numbers at age are emergent from the energy budget equations and discounted by the appropriate fishing mortality.

B.8.11 Movement

Movements and migrations follow the Pawson *et al.* (1987) hypothesis. This hypothesis is based on data for 5959 tagged sea bass, with a follow-on exercise for 4959 sea bass confirming the validity of the hypothesis 20 years later (Pawson *et al.* 2007).

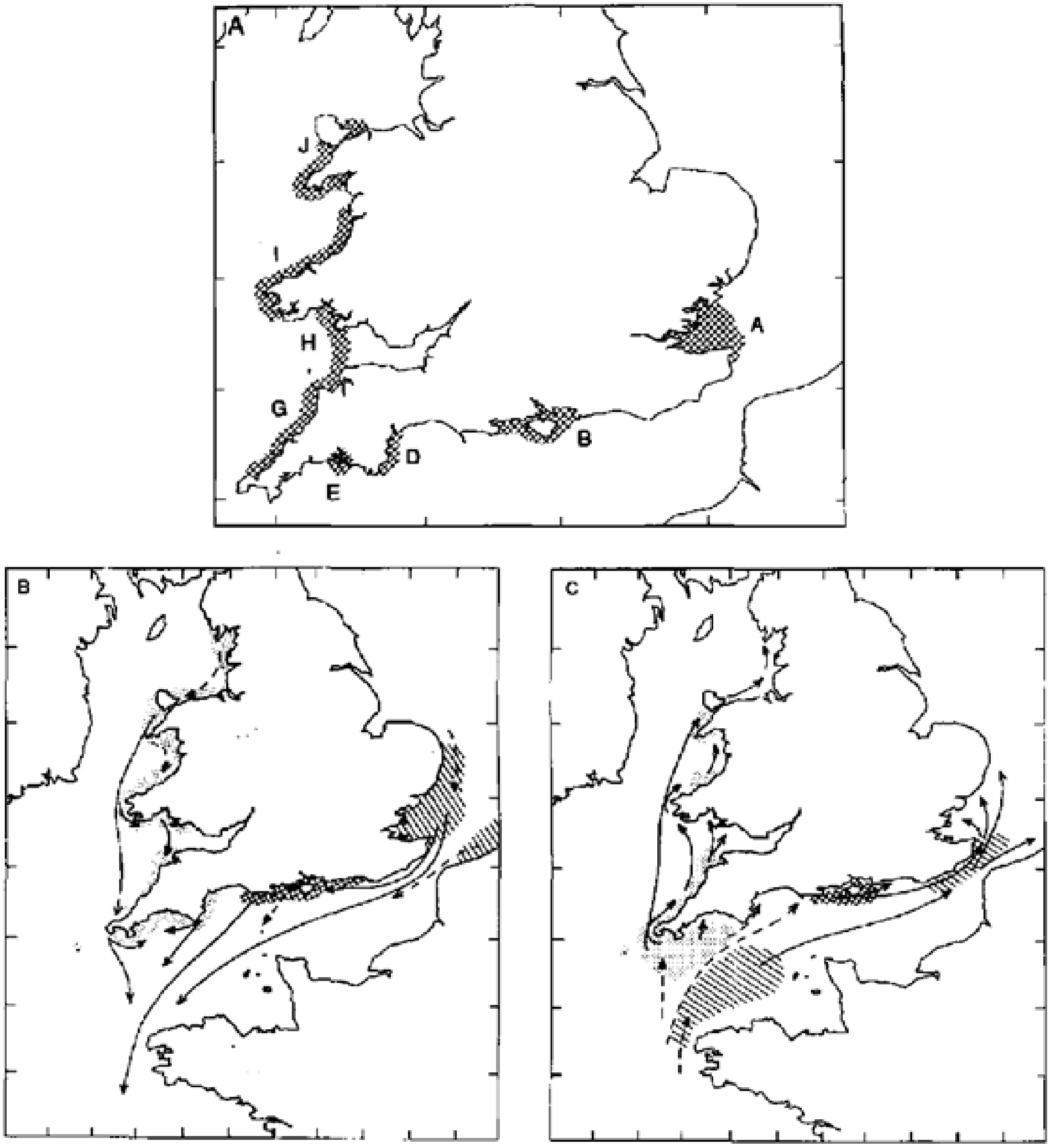

The typical distribution ranges of the tagged bass in populations around England and Wales.
(A) Juveniles throughout the year. (B) Adults in summer and their postulated autumn movements.
(C) Adults in winter and their postulated spring movements.

Figure B.14. Hypothesised distribution and movements of sea bass. *Figure from* (Kelley & Pickett 1987).

B.8.12 Responses by individuals to noise

B.8.12.1 Noise trigger

Individual responses to noise are initiated by a Boolean response (hereafter referred to as noise-trigger) that is turned on when individuals are present at a patch with noise levels that exceed an imposed ‘noise-threshold’. Conversely, the noise-trigger is turned off when an individual moves or the patch it is on is updated to a noise level that is below that individual’s designated noise-threshold.

B.8.12.2 Hearing thresholds

During initialisation, each individual fish is introduced to the model with a noise-threshold that is fitted to the population using a normal distribution to reflect the known hearing range of (Kastelein *et al.* 2008).

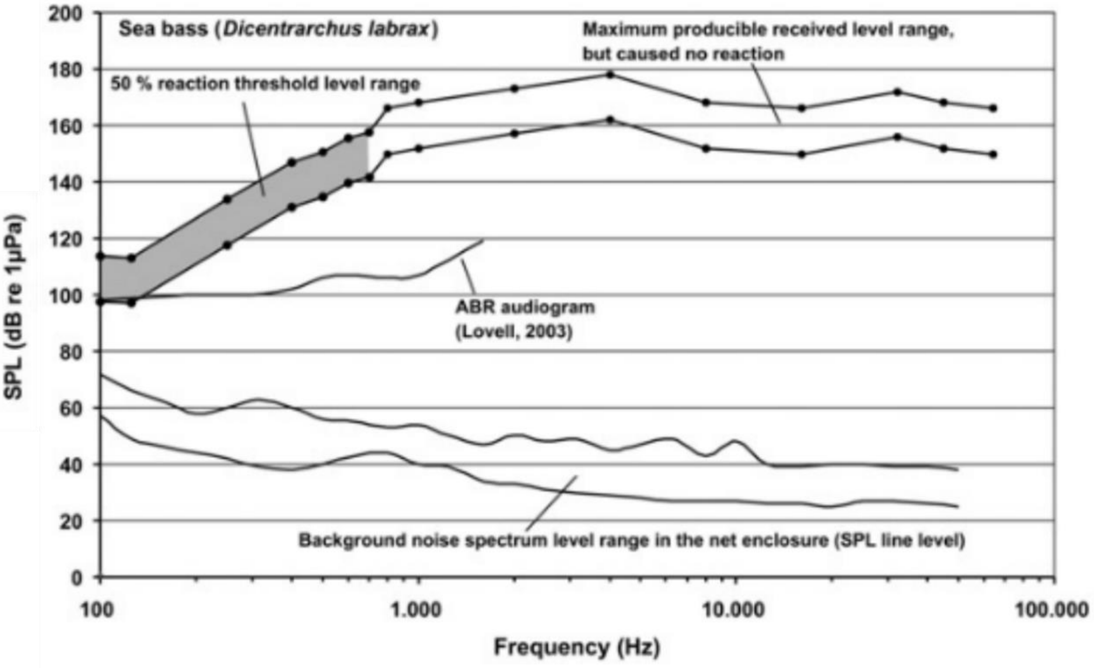

Figure B.15. Auditory brainstem response (ABR) audiogram of sea bass (Kastelein *et al.* 2008)*. Shown is the maximum received level range that could be produced in the tank for the test frequencies causing no reactions, and the 50% reaction SPL range (shaded areas represent ±8 dB of averaged received level). Frequency range tested was 0.1–0.7 kHz on a school size of 17 fish. Also shown is the background noise range in the net enclosure.*

B.9 Calibration

This TRACE element provides supporting information on: (1) Procedures for parameter calibration carried out by Watson *et al.* (2022), and (2) input data and prior and posterior distributions from calibration.

B.9.1 Summary

Where absolute values of parameters could not be directly sourced from the literature (mainly regarding energy budget parameters), Watson *et al.* (2022) used a version of Approximate Bayesian Computation (ABC) called Simulated Annealing ABC (SABC) to fit estimates using key population parameters.

B.9.2 Simulated Annealing ABC

Watson *et al.* (2022) used a version of Approximate Bayesian Computation (ABC) called Simulated Annealing ABC (SABC) (Albert *et al.* 2015), implemented in the Python library *ABCpy* (Dutta *et al.* 2017) to fit five parameters to calibrate the model. The five calibrated parameters were: *H*; half saturation constant, *AM*: adult natural mortality, *AE*; absorbed energy, *PM*: pelagic mortality, *I*; importance of density dependence. This method is highly parallelizable, making it an excellent algorithm for use by high-performance computers (Watson *et al.* 2022). In summary, ABC randomly drew values of calibrating parameters from uniform prior distributions and ran the IBM with these parameter values. Subsequent runs were then guided by performance compared to fitted data as indicated by the sum of weighted Euclidean distance between model outputs and data. Data used for parameter calibration was from the sea bass stock assessment model (stock synthesis 3, SS3). These outputs include annual time series of spawning stock biomass (SSB), numbers-at-age, and weight-at-age. SS3 outputs for SSB and numbers at age were estimated annually, however mass at age was taken as the stock assessment parameters of the bon Bertalanffy model. During calibration, mass at age produces a realistic population size structure in the absence of real data as a best available guide (Watson *et al.* 2022). The estimated posterior means for the five calibrated parameters are shown in Table 3 together with the prior distributions used by Watson *et al.* (2022).

Table B.3. Values for priors, posterior mean and 95% credible intervals from ABCpy runs *for parameters H; half saturation constant, AM: adult natural mortality, AE; absorbed energy, PM: pelagic mortality, I; importance of density dependence. For rationale for choice of priors see TRACE Section B.9.4.*

Parameter	**Priors**	**Posterior mean**	**95% credible intervals**
H	$2.5\text{x}10^{-1}$,$7.5\text{x}10^{-1}$	$4.87\text{x}10^{-1}$	$3.04\text{x}10^{-1}$, $7.26\ \text{x}10^{-1}$
AM	$2.8\text{x}10^{-4}$,$5.9\text{x}10^{-4}$	$4.71\text{x}10^{-4}$	$3.43\text{x}10^{-4}$, $5.87\ \text{x}10^{-4}$
Ae	0.0, $3\text{x}10^{-3}$	$1.64\text{x}10^{-3}$	$2.51\ \text{x}10^{-4}$, $2.88\ \text{x}10^{-3}$
PM	$4.5\text{x}10^{-2}$, $1.35\text{x}10^{-1}$	$8.01\text{x}10^{-2}$	$5.76\ \text{x}10^{-2}$, $1.02\ \text{x}10^{-1}$
I	$2.5\text{x}10^{+13}$,$7.5\text{x}10^{+13}$	$5.14\text{x}10^{+13}$	$2.72\ \text{x}10^{+13}$, $7.39\ \text{x}10^{+13}$

B.10 Conceptual model evaluation

This TRACE element provides supporting information on: The simplifying assumptions underlying a model's design, both with regard to empirical knowledge and general, basic principles. This critical evaluation allows model users to understand that model design was not ad hoc but based on carefully scrutinized considerations.

B.10.1 Summary

Here we provide rationale for our choice of temperature as a forcing variable and phytoplankton density as an energy input. We provide justification for our use and handling of super-individuals, life stages and describe the trade-offs associated with increasing the number of super-individuals in the IBM. We describe how we approached fishing pressure and summarise how observations and hypotheses in the literature have informed our movement sub models. Lastly, we discuss how responses to noise by individuals within the model affect population level outputs.

B.10.2 Temperature as a forcing variable

Temperature is a key driver of sea bass dynamics influencing several processes:

Spawning and numbers at age 0: Sea temperature influences distribution of the spawning population and the growth of eggs and larval stages. Larvae that grow faster are quicker to graduate to the lower mortality rate inflicted on the juvenile and adult/mature life stages. This means that faster growth in response to warmer SSTs will influence numbers at age 0 (Pawson 1992). To test this, we show a positive relationship between SST on spawning patches from the model and the numbers at age 0/SSB from ICES stock assessment figures for the years 1985.- 2017 (Fig. B.16 and Table B.4). Eggs are rarely found in SST of less than 8.5–9°C or above 15°C leading to the belief that spawning is bound by the 9°C isotherm (Thompson & Harrop 1987; Pickett & Pawson 1994), and this governs where spawning patches appear in the IBM (see TRACE Section B.2).

Growth: Water temperature affects growth of sea bass (Pickett & Pawson 1994) and is modelled through use of an Arrhenius multiplier.

Movement: Swimming speed is positively correlated with temperature (Pickett & Pawson 1994; Claireaux *et al.* 2006) and modelled through use of an Arrhenius multiplier. Temperature also provides an important cue to initiate spawning migrations (Kelley & Pickett 1987; Pickett & Pawson 1994) reflected in our migration sub models (TRACE Section B.7).

Ingestion: Water temperature affects ingestion rates of larvae , juvenile and mature sea bass (Pickett & Pawson 1994) and is modelled through use of an Arrhenius multiplier.

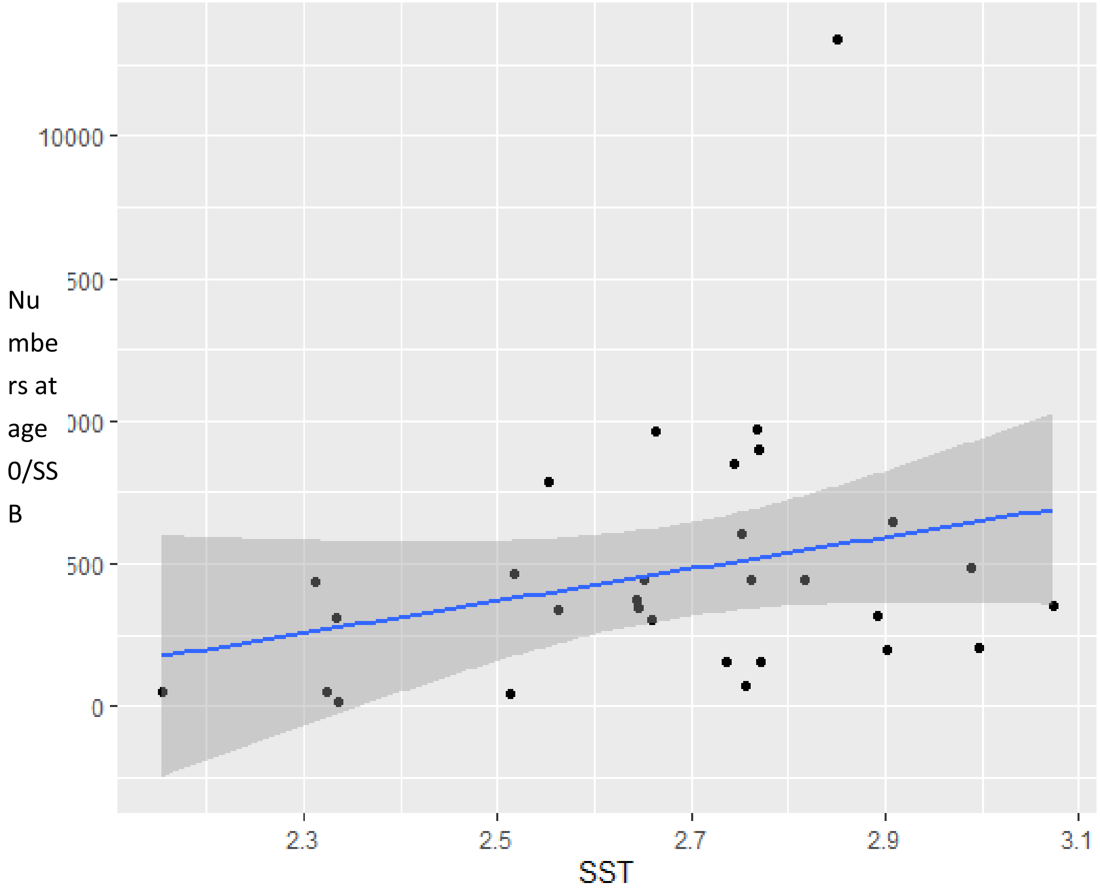

***Figure B.16. Numbers at age 0 over SSB data from ICES data plotted against the mean annual sea surface temperature** of the spawning patches from 1987 – 2017.*

***Table B.4. Analysis of Variance of a liner regression testing Numbers at age 0/SSB** as predicted by mean annual sea surface temperature of the spawning patches from 1987 – 2017.*

	Df	**Sum Sq**	**Mean Sq**	**F value**	**Pr(>F)**
SST	1	11563903	11563903	2.3994	0.1326
Residuals	28	134947308	4819547		

B.10.3 Using phytoplankton as driver of energy budgets

Sea bass are generalist predators, and their diet is opportunistic (Pickett & Pawson 1994), thus it is very difficult to predict what they will be eating at any particular time. In addition, the use of ecosystem model outputs was considered to introduce too much further uncertainty and calibration challenges. Instead, we use remote sensing data of phytoplankton blooms assuming this to be the base of the marine food web. This remote sensing data provides information on how much energy is being inputted to the marine ecosystem. With this method there are difficulties calculating explicitly how energy travels through trophic levels of the marine food web. We know energy is lost at each trophic interaction and many species in the marine environment (including much of sea bass prey) are highly mobile and may move around seeking energy in the form of their preferred prey. Modelling this complex phenomenon to calculate how much energy and how long it will take to get from a phytoplankton bloom to a sea bass is beyond the scope of this model and requires too many complex assumptions which we term trophic delay. *Trophic delay* is highly correlated with *assimilation efficiency* and so are combined as a single parameter termed *Absorbed energy (AE)*. *AE* is calibrated with ABC, for more details see TRACE Section B.9*.*

B.10.4 Super-individuals

Super-individuals comprise many sea bass with identical state variables and were employed to make simulation of the large population of European sea bass computationally feasible.

Grimm & Railsback (2005) list three approaches to handle the relationship between the number of super-individuals in an IBM and number of individuals per super-individual as population size decreases due to mortality:

1) Assume that mortality reduces the number of individuals per super-individual while the number of super-individuals remains constant.
2) Assume that mortality reduces the number of individuals per super-individual, but combine super-individuals as needed to keep the number of individuals relatively constant.

3) Assume that an entire super-individual either lives or dies.

Our approach is most similar to option 1, in that we fix the number of super-individuals per cohort and divide the population numbers-at-age accordingly (Shin & Cury 2001). This option reduces spatial artefacts by keeping the total number of super-individuals relatively constant and allows application of mortality in a way that is compatible with the stock assessment.

The fixed number of super-individuals chosen per cohort introduces a trade-off between spatial distributions, longevity and model run times: more super-individuals allow for more variability and better spatial age-structure, but the lower number of super-individuals within super-individuals may lead to truncation of cohorts before the maximum age of 30 years. Conversely, having fewer super-individuals containing more individual fish better preserves the overall age structure of the population and reduces model run times but may result in patchy age distributions at the divisional level.

B.10.5 Life stages

After the young life stages (eggs, ys-larvae, larvae) have drifted back to the coastline (see TRACE Section B.7 *drift_x sub models*) juvenile and adult/mature sea bass are the two life stages represented in the IBM. Juvenile and adult/mature sea bass are the two life stages which broadly relate to the two distinct movement patterns described in the literature (Kelley & Pickett 1987; Pickett & Pawson 1994; Pawson *et al.* 2007): (1) juvenile residency in nursery grounds and coastal areas and (2) large scale migrations between spawning and feeding grounds upon reaching maturity. Our choice of maturity of fish greater than 42 cm is consistent with observations in which maturity is based on length rather than age (Pickett & Pawson 1994).

B.10.6 Fishing fleets

Although sea bass are caught by a variety of gears, commercial fisheries operating in the northern management unit are considered to have two distinct components catching different subsets of the population throughout their life and migration-cycles (ICES 2012):

1) Offshore fisheries on pre-spawning and spawning sea bass, predominantly by pelagic trawlers from France and the UK, operating during November to April.

2) Small-scale inshore fisheries catching immature sea bass and mature sea bass returning to coastal areas following spawning. These fisheries include many small (10m and under) vessels employing a variety of gears and often take sea bass as by-catch with other species.

Sea bass are also a popular target for recreational fishing in European waters.

B.10.7 Movement and migrations

Although the mechanisms informing sea bass navigation are largely unknown, our empirical movement sub models were constructed to incorporate observations and hypotheses reported in the literature:

Egg, egg-sac larvae and larvae movement: The mechanism by which early life stages return to the coast after offshore spawning is understood to be driven by a complex combination of wind, currents and sea temperatures alongside some active vertical movement of larvae to utilize currents (Beraud *et al.* 2018). These enable the pelagic stages (eggs, yolk sac larvae and larvae) to reach nursery areas around the coast of the UK, made up of estuaries, harbours, backwaters, creeks and shallow bays (Pickett & Pawson 1994). It is not feasible to explicitly model this movement, instead for model simplicity the pelagic life stages drift the most direct route back to their target site. This is the forced distribution that ensures that each new 10 super individuals follow a spatial distribution as set out by (Walker *et al.* 2020) for more details see TRACE Section B.8.7.

Juvenile movement: The local movement of juveniles within the IBM is consistent with observations that juveniles remain within nursery grounds for the first few years of life and disperse primarily during the adolescent phase (Pickett & Pawson 1994; Pickett *et al.* 2004).

Spawning cues: Movement to pre-spawning and offshore spawning grounds takes place as the water cools between October and December, when mature females seek water warmer than 9°C (Kelley & Pickett 1987; Pickett & Pawson 1994) but may be delayed and take place over shorter distances during warmer winters. This is captured by using temperature as a trigger for the spawning migration: most mature sea bass will depart between October and December, but some will depart later in warmer years, which allows for spawning in the North and Irish Seas as spawning patches start appearing there. Triggering spawning migrations by appearance of spawning patches also encourages movement from the coastal Channel (divisions 7.de) to offshore in warmer years when patches there do not always drop below the 9°C temperature threshold. Use of a temperature-based cue also allows spawning to extend into April–May as super-individuals with a later departure complete their spawning cycle. Currently 10 mature sea bass spawn only once on the 60th tick (17th of March) assuming they are on a spawning patch. These 10 sea bass are representative of the entire SSB. We currently have only one spawning event (60th tick) for modelling simplicity, however we appreciate that there is evidence of sea bass as a fractional spawner (spawning 3-4 batches [Mayer, Shackley and Witthames, 1990]).

Cessation of spawning: Feeding migrations don't appear to be triggered by an environmental cue but occur when fish are spent at the end of spawning (Pawson *et al.* 2007). This is modelled with a 60-day spawning period once a mature fish locates a spawning patch, after which it is assumed spent and defaults to the feeding migration. Assumption of 60 days in spawning grounds was chosen for modelling reasons to prevent fish performing more than one spawning migration per year while ensuring that fish begin feeding migrations in the months April and May (Kelley & Pickett 1987; Pawson *et al.* 2007).

Migrations: Our empirical rules consist of choosing a suitable neighbouring patch based on destination direction and patch type, ensuring direct movement along the coast (Pickett & Pawson 1994) when migrating between spawning and feeding grounds.

Site fidelity: Sea bass have a high affinity for coastal feeding grounds (Kelley & Pickett 1987; Pawson *et al.* 2008), but the reason for this and its extent is unclear. Hence the probability that fish change affinity to a feeding area can be specified via the *site-fidelity?* Slider on the model's GUI. Site fidelity was fixed at 100% in the current study.

B.10.8 The effects of noise

B.10.8.1 Impacts on life history processes

Individuals affected by noise (i.e., with noise-trigger on), initiate a set of four noise-effect pathways modelled after Soudijn *et al.* 2020 and Cox *et al.* 2018. Specifically, four main processes are adjusted using linear modifiers that reflect documented impacts of noise on individual fish: a reduction in food intake, an increase in energetic use, an increase in mortality, and a reduction in reproductive success (Cox *et al.* 2018; Soudijn *et al.* 2020). Lastly, the modelled impacts of noise are limited to larval, juvenile and adult sea bass due to a paucity of empirical evidence to support the application of these four noise-effect pathways to earlier life stages (eggs and yolk-sac larvae) (Fig. B.13).

There is a paucity of quantitative empirical information available regarding the impacts of noise on life-history processes in sea bass that are transferrable to the IBM. Instead, relative changes observed in fishes (Cox *et al.* 2018; Soudijn *et al.* 2020) have been used to inform individual responses of *D. labrax* to noise exposure. For model applications, noise parameters/modifiers will be fixed based on empirical evidence for the impacts of anthropogenic noise observed in fishes (Fig. B.14). Specifically, percent changes related to the four noise-effect pathways have been referenced from the literature (Fig. B.14; bold text) and input into the model as linear modifiers.

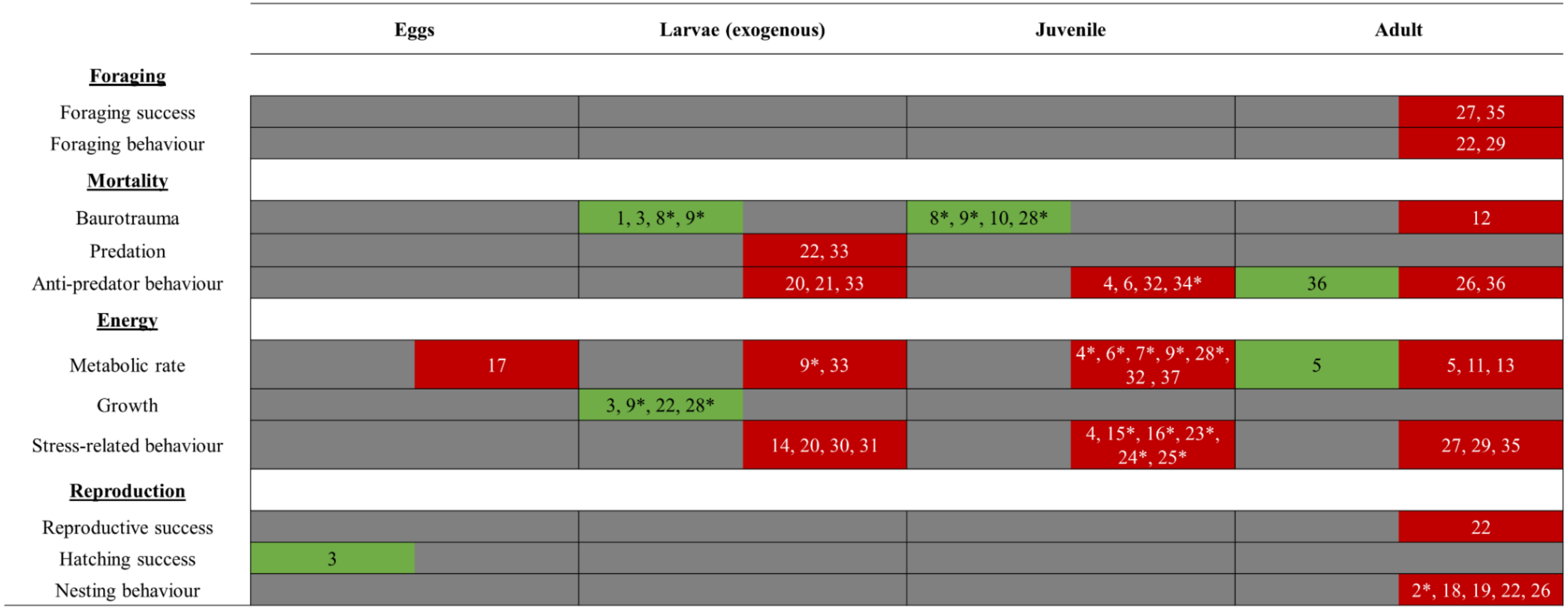

	Eggs		Larvae (exogenous)		Juvenile		Adult	
Foraging								
Foraging success	⬛	⬛	⬛	⬛	⬛	⬛	⬛	🟥 27, 35
Foraging behaviour	⬛	⬛	⬛	⬛	⬛	⬛	⬛	🟥 22, 29
Mortality								
Baurotrauma	⬛	⬛	🟩 1, 3, 8*, 9*	⬛	🟩 8*, 9*, 10, 28*	⬛	⬛	🟥 12
Predation	⬛	⬛	⬛	🟥 22, 33	⬛	⬛	⬛	⬛
Anti-predator behaviour	⬛	⬛	⬛	🟥 20, 21, 33	⬛	🟥 4, 6, 32, 34*	🟩 36	🟥 26, 36
Energy								
Metabolic rate	⬛	🟥 17	⬛	🟥 9*, 33	⬛	🟥 4*, 6*, 7*, 9*, 28*, 32 , 37	🟩 5	🟥 5, 11, 13
Growth	⬛	⬛	🟩 3, 9*, 22, 28*	⬛	⬛	⬛	⬛	⬛
Stress-related behaviour	⬛	⬛	⬛	🟥 14, 20, 30, 31	⬛	🟥 4, 15*, 16*, 23*, 24*, 25*	⬛	🟥 27, 29, 35
Reproduction								
Reproductive success	⬛	⬛	⬛	⬛	⬛	⬛	⬛	🟥 22
Hatching success	🟩 3	⬛	⬛	⬛	⬛	⬛	⬛	⬛
Nesting behaviour	⬛	⬛	⬛	⬛	⬛	⬛	⬛	🟥 2*, 18, 19, 22, 26

1 = Bolle et al. 2012; 2 = Bruintjes & Radford 2013; 3 = Bruintjes & Radford 2014; 4 = Bruintjes et al. 2015; 5 = Bruintjes et al. 2016a; 6 = Bruintjes et al. 2016b; 7 = Buscaino et al. 2010; 8 = Debusschere et al. 2014; 9 = Debusschere et al. 2016; 10 = Casper et al. 2013; 11 = Celi et al. 2016; 12 = Halvorsen et al. 2012a; 13 = Harding et al. 2018; 14 = Holles et al. 2013; 15 = Kastelein et al. 2008; 16 = Kastelein et al. 2017; 17 = Jain-Schlaepfer; 18 = Maxwell et al. 2018; 19 = McCloskey et al. 2020; 20 = McCormick et al. 2018; 21 = McCormick et al. 2019; 22 = Nedelec et al. 2017; 23 = Neo et al. 2014; 24 = Neo et al. 2016; 25 = Neo et al. 2018; 26 = Picciulin et al. 2010; 27 = Purser & Radford 2011; 28 = Radford et al. 2016; 29 = Sabet et al. 2015; 30 = Simpson et al. 2005; 31 = Simpson et al. 2010; 32 = Simpson et al. 2014; 33 = Simpson et al. 2016; 34 = Spiga et al. 2017; 35 = Voellmy et al. 2014a; 36 = Voellmy et al. 2014b; 37 = Wysocki et al. 2006

KEY

🟥	Response
🟩	No response
⬛	No data

Figure B.17. Summary table of the impacts of noise on fish from the literature. *Studies are divided by life-stages (eggs, larvae, juveniles, and adults), and impacts are sorted by biological response (refer to key). Some papers have multiple impacts that fill different response categories. '*' designates papers relating to D. labrax.*

		Potential consequences			
Observed noise impacts	Seabass	Energetic costs (increase costs)	Food intake (decrease food intake)	Mortality (increase death)	Reproduction (decrease reproduction)
Stress Higher levels of cortisol	4–5, 7, 23,27	🟧 Higher oxygen use when exposed to noise (seabass) [23, 27]; **50% increase in metabolic rates during noise treatment** (seabream) [4]; stress increases metabolic rates over short-term [1, 13] and long-term periods [12]	🟦 Cortisol suppresses appetite in teleost fish [2, 14]	🟦 Stress may impair behaviour and lead to mortality (salmon) [21]	🟧 Elevated cortisol decreases fertilisation rates [25]; Deformities in fish larvae [15]; **30% lower clutch survival** when exposed to noise (damselfish) [16]
Foraging behaviour Decrease of foraging behaviour: food consumption, foraging efficiency, and discrimination error	3–4	🟦 Higher energetic costs for same food intake (compensation)[11]; use of fat reserves and tradeoffs to account for effort [10]	🟧 **28% decrease in foraging efficiency** and feeding attempts when exposed to noise (stickleback) [22]; **28% decrease in proportion** of prey eaten (minnows) [28]	🟩	🟩
Movement behaviour Increase of movement: adjusted swimming depth, directional changes, schooling adjustments, swimming speed	3–5,7,9,17–20	🟨 Swim faster, tighter group cohesion, dive deeper [17–19]; swim away from the noise source (seabass) [19]; increased metabolic rate and responded less often and slower to simulated predatory attacks (damselfish) [26]	🟩	🟨 Increased turn angles when exposed to noise and predation risk [27]	🟩
Auditory system Changes in the auditory system: hering threshold	*	🟩	🟨 Possible that noise masked acoustic cues of *Daphnia* movement, contributing to decreased foraging (sticklebacks) [28] (zebrafish) [24]	🟧 **3x increased mortality** when exposed to noise (potentially related to predator detection; damselfish) [26]	🟧 Courtship vocalisations altered and **spawning success decreased by 30%** when exposed to noise (gobies) [8]

1 = Barton and Schreck 1987; 2 = Bernier *et al*. 2006; 3 = Bruintjes *et al*. 2014; 4 = Bruintjes *et al*. 2016; 5 = Buscaino *et al*. 2010; 6 = Debusschere *et al*. 2014; 7 = Debusschere *et al*. 2016; 8 = de Jong *et al*. 2018; 9 = Kastelein *et al*. 2017; 10 = Kemp *et al*. 2006; 11 = Killen *et al*. 2011; 12 = Lankford *et al*. 2005; 13 = Lawrence *et al*. 2019; 14 = Madison *et al*. 2015; 15 = Morgan *et al*. 1999; 16 = Nedelec *et al*. 2017; 17 = Neo *et al*. 2014; 18 = Neo *et al*. 2015; 19 = Neo *et al*. 2016; 20 = Neo *et al*. 2018; 21 = Olla et al. 1995; 22 = Purser and Radford 2011; 23 = Radford et al. 2016; 24 = Sabet et al. 2015; 25 = Sierra-Flores et al. 2015; 26 = Simpson et al. 2016; 27 = Spiga et al. 2017; 28 = Voellmy et al. 2014

KEY

🟧	Documented consequences of noise on modelled individual-level processes
🟨	Documented consequences of noise but not on modelled processes
🟦	Potential logical consequences but an absence of documented impacts
🟩	No short-term consequences for individual-level processes documented

Figure B.18. Potential consequences of anthropogenic noise for modelled individual-level processes *adapted from Soudijn et al. 2020. Observed noise impacts (left-hand column; Cox et al. 2018) have been cross-referenced with potential consequences to fishes in relation to modelled individual level processes of the IBM. Colours of the cells indicate quality of evidence (refer to key); bold text indicate direct evidence used to inform the impacts of noise in the IBM.*

B.11 Implementation verification

This TRACE element provides supporting information on: (1) whether the computer code implementing the model has been thoroughly tested for programming errors, (2) whether the implemented model performs as indicated by the model description, and (3) how the software has been designed and documented to provide necessary usability tools (interfaces, automation of experiments, etc.) and to facilitate future installation, modification, and maintenance.

B.11.1 Summary

A series of techniques were employed to test and debug the model code and check that it performs according to the ODD specification. These checks included syntax checking, visual testing, print and error statements, spot tests with agent monitors, test procedures and programs, independent reimplementation and testing of sub models in R.

The original model on which this model has developed from had extensive bug checking adding to the confidence in model behaviour (Walker *et al.* 2020). In addition to the bug testing on the original model we have performed a range of checks to ensure the model is behaving as expected. The NetLogo syntax checker and GUI interface was used to test and debug the code throughout all stages of model development. In the new model updates, we add dynamic maps of chlorophyll remote sensing data and realistic projections of noise-pollution levels. To check this is working correctly we visually checked the dynamic maps by representing the data as colours and plots in the model GUI. We performed extensive testing of energy budget sub models both through spot checks of individual agents and by re-coding the sub model in R and testing the outputs with a range of values. The model outputs we fit of number and mass at age also add to confidence in model performance allowing obscure results to be spotted and cohorts to be followed through the simulation. The model is coded in a modular fashion making it feasible for sub models to be updated by new users however modifications of the model will require knowledge of NetLogo. The model has been implemented in NetLogo version 5.3.1 (Wilensky 1999), a free software platform. The developers of NetLogo provide transition guides to new versions of NetLogo and keep old versions available for download.

B.11.2 Model output verification

This TRACE element provides supporting information on: (1) how well model output matches observations. (2) Non validated Spatial output from the model.

Summary: Here we compare model output to ICES SS3 stock assessment data without the addition of noise impacts. We also show spatial model outputs of sea bass biomass (tonnes), although note there is not adequate data to validate this.

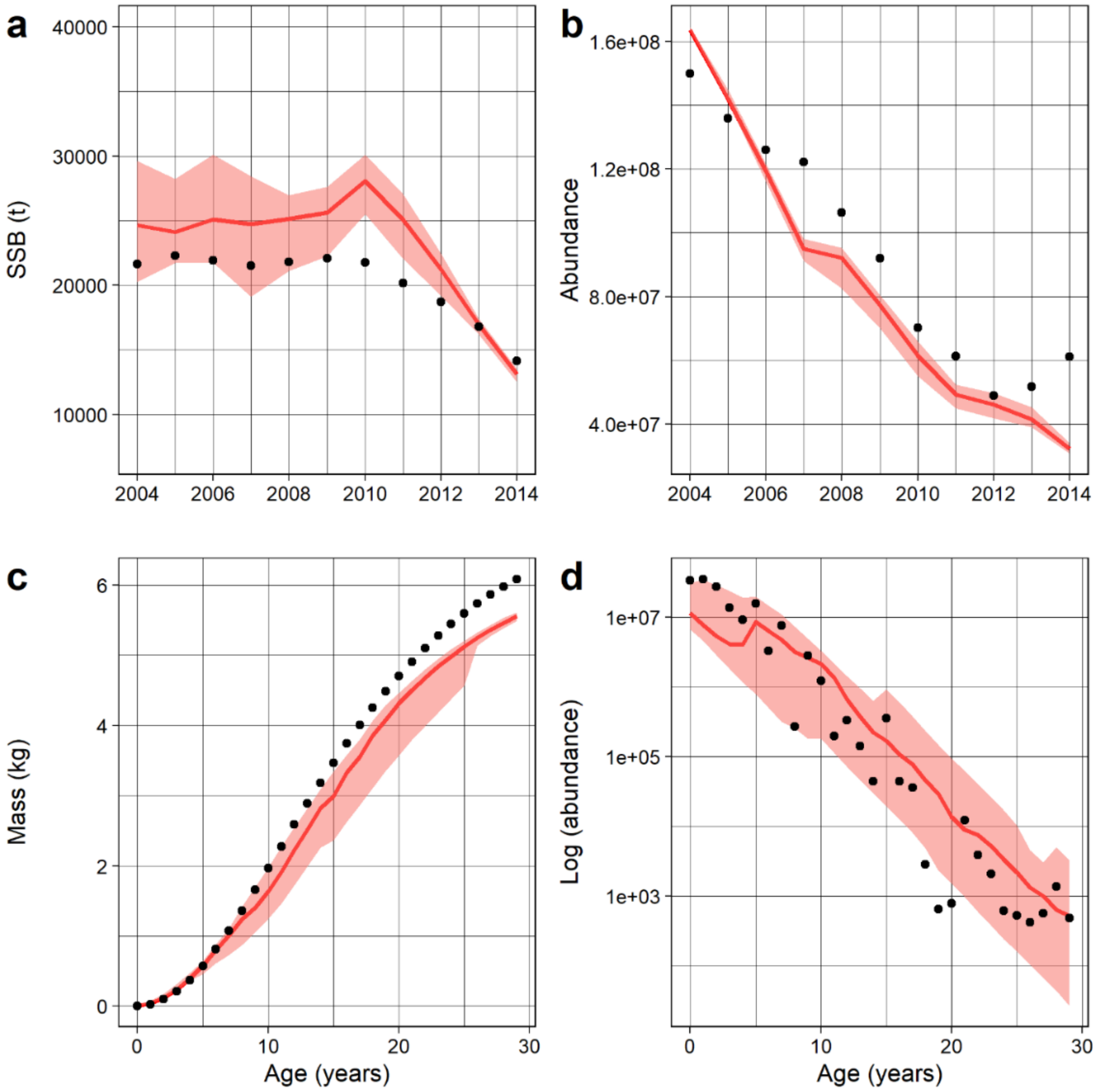

Figure B.19. Model outputs averaged across 10 IBM runs compared to SS3 verification data *for: a) spawning stock biomass (SSB), b) abundance, c) mass-at-age and d) numbers-at-age. Plots a–c are true values, while plot d has been log-transformed for better visual comparison. Black dots represent the outputs of SS3;*

red lines are the median of the IBM posterior predictive distribution; ribbon represents interquartile range.

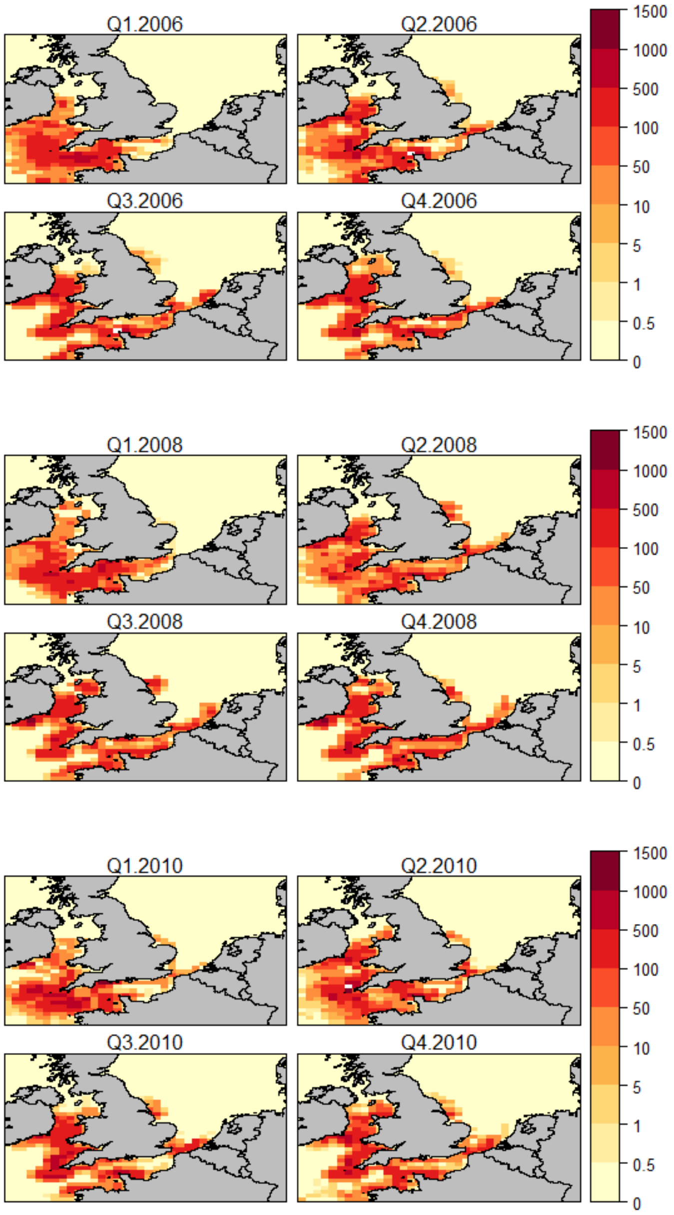

***Figure B.20. Mean daily biomass (tonnes) distribution per Quarter** for years 2006, 2008, 2010. Q1 = 1st January – 31st March, Q2 = 1st April – 30th June, Q3 = 1st July – 30th September, Q4 = 1st October, – 31st December. Note this data is not validated due to inadequate data options (Watson et al. 2022).*

B.12 Sensitivity analyses

This TRACE element provides supporting information on: (1) how sensitive model output is to changes in model parameters (sensitivity analysis), (2) how well the emergence of model output has been understood, and (3) how sensitivity scenarios were used to assess population-level responses to noise.

B.12.1 Sensitivity analysis of model parameters

The sensitivities of model outputs for SSB, mass at age and numbers at age are shown below as percentage change in output for a 10% increase and decrease in the model parameters. One parameter was tested at a time whilst keeping all other parameters at their base value. To keep run times achievable we repeat the test five times for each parameter and after the spin up (1985-2003) we take the results after one year of energy budget simulations (1st tick of 2005). A full table of results can be seen below in Table 6. The model is robust to most parameters with most sensitivities reported at less than 10% change in output for a 10% change in parameter value. Biomasses (SSB and mass-at-age) were most sensitive to changes in the length weight parameter (b_g; Table 6), while abundances (N and numbers-at-age) were most sensitive to changes in the pelagic mortality parameter (PM; Table 2). Of the noise-related parameters, SSB and mass-at-age outputs were most sensitive to changes in the noise-feeding modification parameter (NFm; Table 6), while abundance was most sensitive to changes in the noise-reproduction modification parameter (NRm; Table 6). Lastly, numbers-at-age outputs were most sensitive to decreases in the noise-mortality modification parameter (NMm; Table 6) and to increases in the noise-reproduction modification parameter (NRm; Table 6).

Table B.5. Sensitivities of SSB, mean mass at age, and numbers at age, to 10% changes in parameter values. *Results are presented as the change in relative output to a 10% decrease/increase in parameter value.*

Parameter	**Value**	**SSB.dec**	**SSB.inc**	**M0.dec.**	**M0.inc**	**M1.dec.**	**M1.inc**	**M2.dec.**	**M2.inc**	**M3.dec.**	**M3.inc**	**M4.dec.**	**M4.inc**	**M5.dec.**	**M5.inc**	**…**
linf	**84.55**	3.1	4.7	-22.5	27.6	-4.4	8.2	-13.9	9.5	-0.5	8.7	-0.1	7.6	0.6	2.2	…
K	**0.096699**	1.6	-4.9	-19.2	26.0	-8.8	9.9	-7.0	-7.0	-4.3	3.3	-3.7	-3.4	-14.1	-8.0	…
t0	**-0.73**	1.3	-0.2	2.0	1.4	-2.6	5.8	-3.8	-2.1	2.4	-3.7	-3.8	-12.4	-10.2	-8.5	…
Ea	**0.5**	-1.1	9.3	-1.8	4.4	-4.5	-4.9	-4.6	4.9	-7.4	4.0	-10.8	-2.1	-7.2	-4.5	…
EaS	**0.1903656**	10.2	-0.9	1.2	2.5	1.0	-8.3	-4.0	10.0	6.3	10.5	7.8	3.3	-13.7	-4.4	…
Cmax	**0.54**	0.9	3.6	-1.0	3.0	-1.3	2.7	-1.6	0.6	4.2	9.1	-1.8	1.2	-4.3	-3.3	…
ep	**6.02**	-0.5	1.4	3.0	3.8	-6.2	6.4	-7.4	7.3	-5.4	7.0	2.1	-2.0	-7.2	-5.3	…
A0	**0.1227808**	1.0	6.9	1.0	1.5	-4.7	0.4	3.9	-4.5	-11.7	8.2	-10.7	-4.7	-11.5	-10.7	…
Ef	**7**	10.6	1.1	-1.0	1.2	-0.5	2.9	-3.9	9.1	-4.0	2.0	-0.7	4.7	2.7	-5.1	…
El	**39.3**	6.4	10.3	-6.0	1.2	-3.3	-9.0	6.6	0.7	-4.9	-5.0	-1.4	-11.1	-10.7	-15.3	…
Ls	**14.7**	-8.3	0.8	-0.5	3.0	4.5	-0.2	-1.9	-2.9	10.8	11.8	-2.5	-3.4	-4.9	-15.5	…
Fs	**3.6**	0.8	-0.7	-1.4	-5.4	-2.1	-3.7	1.0	-5.4	3.4	5.0	-10.4	-5.6	-4.1	-6.3	…
egg_mass	**0.00096**	7.7	-2.5	1.4	0.2	-4.0	2.0	-0.5	-1.7	2.6	9.6	-0.8	-5.8	-11.1	-0.1	…
a_g	**1.231E-05**	-10.1	12.9	-7.3	9.7	-7.0	2.1	-10.0	14.4	2.5	16.1	-4.5	5.0	-16.6	0.9	…
b_g	**2.969**	-57.4	180.3	-43.0	23.2	-53.8	69.9	-55.4	84.7	-53.4	120.3	-60.1	118.2	-65.7	114.2	…
eggs_per_bass	**375000**	4.0	7.8	-4.3	0.2	-4.4	0.6	-0.2	2.1	1.9	1.0	-4.5	-5.9	-9.2	-8.0	…
Gl	**0.02485**	3.7	1.1	-2.1	5.8	-6.2	2.1	-4.2	-0.2	-0.9	3.9	-3.3	-13.6	-7.2	-13.8	…
H	**0.4866877**	-1.4	2.3	-1.0	2.4	4.1	2.2	1.4	3.3	4.0	2.2	-7.1	-1.3	-16.7	-5.6	…
AM	**0.0004709**	12.7	-8.3	0.0	1.4	0.3	1.1	-2.9	2.3	1.6	2.2	-8.0	-3.4	-9.7	-2.9	…
AE	**0.0016362**	-0.4	-0.5	1.1	2.1	-8.8	0.0	-7.3	-4.6	3.1	-8.0	5.8	-1.8	-0.4	-9.3	…
PM	**0.0800959**	2.7	-7.5	-1.8	2.0	1.5	-0.6	5.2	2.6	5.4	-2.6	-10.3	-2.4	-6.8	0.0	…
I	**5.142E+13**	5.1	10.9	1.0	1.6	-8.7	-5.2	4.5	2.4	-2.6	2.2	0.7	-13.0	-17.9	-0.6	…
NFm	**0.28**	-7.3	9.2	-2.1	0.4	-7.7	4.7	7.7	2.5	-4.9	9.6	10.9	-6.1	-12.3	-2.9	…
NEm	**0.5**	4.5	4.8	-1.7	-2.6	1.9	-1.3	-2.1	3.8	5.2	3.8	-2.2	-5.7	-1.6	-13.5	…
NMm	**0.33**	-0.6	3.6	1.2	0.8	-3.5	3.7	-6.8	1.7	3.9	3.7	4.2	-3.6	-10.1	-2.5	…
NRm	**0.3**	7.2	-0.7	1.1	-2.9	-2.3	-0.2	5.5	4.4	1.3	4.0	-9.1	-2.7	-4.0	-6.5	…

Parameter	Value	M6.dec.	M6.inc	M7.dec.	M7.inc	M8.dec.	M8.inc	M9.dec.	M9.inc	M10.dec.	M10.inc	M11.dec.	M11.inc	M12.dec.	M12.inc	…
linf	84.55	6.7	-1.8	2.6	-4.2	-4.2	5.4	-5.3	7.7	-6.6	-4.4	-9.7	-2.4	-4.9	-3.5	…
K	0.096699	-5.1	-4.1	4.7	0.9	-0.8	-2.1	-2.8	-3.4	-4.2	-5.1	-6.2	-13.0	-1.6	-0.7	…
t0	-0.73	-0.6	-6.5	1.5	5.1	-0.4	-3.3	4.2	2.7	-8.3	-2.6	-3.8	-0.8	-4.6	-0.2	…
Ea	0.5	1.2	11.2	-1.5	9.9	-9.4	3.0	-0.5	1.3	0.6	-1.6	-3.7	-3.6	0.0	-1.9	…
EaS	0.1903656	-2.0	1.1	-1.0	1.4	1.6	3.5	0.7	0.5	-5.0	-1.6	-4.7	-7.3	-3.9	-1.7	…
Cmax	0.54	-5.2	2.5	5.9	7.3	8.8	-9.9	-0.6	3.6	-3.5	-0.8	-4.7	-1.2	-2.3	-4.4	…
ep	6.02	-10.4	4.7	0.9	4.4	3.6	5.4	-0.8	4.6	-3.8	3.4	-1.8	-3.2	0.5	0.3	…
A0	0.1227808	-11.2	2.7	-6.2	3.1	-7.6	0.9	-3.4	1.9	-13.5	-4.6	-10.9	-3.7	-4.2	-0.4	…
Ef	7	-0.4	0.2	7.8	0.0	5.8	2.9	4.3	1.2	0.8	-2.3	-1.5	-7.5	-0.8	-1.3	…
El	39.3	12.0	-1.1	1.4	-4.5	0.3	-1.3	-1.3	1.1	-6.3	-6.7	-0.6	-2.5	-1.2	2.4	…
Ls	14.7	-3.8	0.0	2.7	0.8	-17.1	-12.9	2.5	2.5	-1.8	-1.4	-1.1	-0.8	-1.2	-5.7	…
Fs	3.6	1.6	3.9	-5.0	1.5	-2.9	-0.1	2.7	0.6	-7.0	-2.8	-5.3	-9.9	0.4	-1.3	…
egg_mass	0.00096	-10.2	7.8	2.6	3.5	6.4	1.7	2.1	1.9	0.5	-7.6	-2.1	-5.8	-1.3	-7.3	…
a_g	1.231E-05	-4.4	6.2	-8.9	15.1	-8.5	0.2	-10.0	14.6	-12.8	-1.6	-15.8	9.2	-10.4	5.6	…
b_g	2.969	-57.4	177.7	-62.8	178.3	-62.2	135.4	-69.6	210.6	-67.9	160.1	-69.7	182.9	-70.0	219.6	…
eggs_per_bass	375000	10.3	2.4	1.0	8.4	5.5	10.8	3.7	3.3	-1.7	-6.8	-3.5	-0.1	-0.8	-0.6	…
Gl	0.02485	-0.4	-1.7	3.7	6.4	2.7	-2.7	1.2	4.9	-5.5	-5.0	-8.1	-3.2	-0.3	-3.7	…
H	0.4866877	-3.6	12.8	2.0	8.6	2.3	5.8	2.3	-5.2	-3.8	-5.1	-6.2	-3.5	0.7	-3.5	…
AM	0.0004709	7.9	-2.0	8.9	-1.7	7.0	-2.3	0.2	-2.5	-3.7	-4.5	-7.4	-2.2	-2.8	-1.0	…
AE	0.0016362	5.1	4.4	4.0	-1.6	-0.7	-16.2	-4.1	-3.7	-10.1	-7.0	-5.4	-3.9	-0.3	-0.8	…
PM	0.0800959	4.5	1.0	0.0	0.4	4.5	-4.0	2.8	-1.1	-6.1	-7.5	-4.5	-12.5	-0.9	0.1	…
I	5.142E+13	11.6	2.2	-0.5	-3.2	-18.4	6.4	0.6	2.7	-0.8	0.8	-6.9	-3.5	-4.0	2.4	…
NFm	0.28	-15.5	17.4	-0.6	2.7	-5.5	4.6	0.7	-0.1	-7.2	-0.9	-3.4	-2.9	-0.1	-1.9	…
NEm	0.5	5.0	-8.2	1.3	-6.7	-4.2	-5.8	1.3	2.6	-6.2	0.0	-7.9	-1.9	0.7	-4.4	…
NMm	0.33	8.4	8.0	-0.3	7.0	-0.5	6.7	-2.1	-0.6	-1.4	-1.5	-6.0	-3.1	-1.5	-1.8	…
NRm	0.3	-0.7	-1.5	4.4	6.0	5.7	-3.9	2.7	-4.0	-14.5	-16.2	-3.5	-4.3	0.3	0.4	…

Parameter	**Value**	**M13.dec.**	**M13.inc**	**M14.dec.**	**M14.inc**	**M15.dec.**	**M15.inc**	**M16.dec.**	**M16.inc.**	**M17.dec.**	**M17.inc**	**M18.dec.**	**M18.inc**	**M19.dec.**	**M19.inc**	**…**
linf	**84.55**	-4.5	0.4	-5.0	0.5	-2.9	4.4	-3.6	5.2	-3.7	2.4	-3.0	2.5	-3.6	2.2	…
K	**0.096699**	-2.2	1.8	2.5	-0.1	1.5	2.5	-2.1	2.4	-0.5	0.9	0.2	0.1	-0.4	-0.1	…
t0	**-0.73**	-0.5	-1.2	0.6	0.2	1.7	3.7	1.1	-0.3	0.7	-0.1	-0.8	0.9	-0.4	0.5	…
Ea	**0.5**	0.8	-0.1	-0.2	1.2	0.3	-0.8	-1.3	-0.5	-0.9	-0.5	1.7	0.7	0.1	-0.1	…
EaS	**0.1903656**	-2.7	0.1	2.2	1.2	4.3	2.0	-1.9	-0.1	-3.4	-1.2	0.1	-0.5	-0.6	-0.3	…
Cmax	**0.54**	-1.4	-0.5	0.4	-1.4	1.0	-1.6	-0.4	-9.4	0.1	-1.3	-1.1	-0.3	0.4	0.3	…
ep	**6.02**	-1.0	1.5	1.3	1.1	0.5	3.5	0.7	-1.8	-0.5	1.3	0.3	1.3	-0.4	1.4	…
A0	**0.1227808**	1.3	1.0	0.2	0.0	-0.2	1.2	3.0	1.8	0.2	-1.6	0.6	1.4	-0.1	-0.3	…
Ef	**7**	0.4	-2.0	-5.8	-2.4	2.0	2.5	3.8	1.5	2.0	-1.0	0.5	0.5	-0.5	-0.7	…
El	**39.3**	2.7	2.7	0.6	1.0	2.7	4.0	3.5	2.5	-0.8	-2.5	0.9	0.1	-0.1	0.7	…
Ls	**14.7**	0.8	-5.7	1.0	-7.4	2.5	2.3	4.4	-5.3	-0.3	-0.1	-0.1	0.0	0.0	0.7	…
Fs	**3.6**	0.0	-3.1	1.6	1.3	3.3	1.0	-1.7	-0.1	-0.8	-2.5	-0.9	1.2	0.0	0.4	…
egg_mass	**0.00096**	1.0	0.2	0.8	-0.5	-1.1	1.0	0.8	-2.9	-0.7	-0.6	0.0	0.4	0.2	0.5	…
a_g	**1.231E-05**	-10.1	9.9	-9.1	12.1	-8.1	14.3	-12.5	7.6	-14.2	9.6	-9.8	11.3	-10.0	9.9	…
b_g	**2.969**	-70.7	224.5	-70.6	226.6	-70.1	252.1	-69.8	218.7	-71.3	251.5	-71.5	252.5	-72.0	253.0	…
eggs_per_bass	**375000**	-0.7	0.5	-1.1	0.5	2.0	4.3	-0.9	1.9	-2.8	-1.3	-0.7	0.4	0.5	-0.1	…
Gl	**0.02485**	-4.4	-0.3	0.9	-5.0	2.8	0.6	-1.0	1.2	0.7	1.0	0.7	0.5	-0.5	0.6	…
H	**0.4866877**	2.1	-5.1	1.3	0.3	2.1	2.6	0.2	-3.8	-1.9	-2.3	0.9	0.8	0.2	0.0	…
AM	**0.0004709**	-0.9	1.3	1.0	-1.1	2.1	3.2	0.2	1.6	-0.1	0.3	-0.7	0.1	0.2	0.5	…
AE	**0.0016362**	2.4	1.4	-1.4	0.9	2.7	0.5	2.9	2.0	-0.9	0.2	0.9	1.7	0.3	1.0	…
PM	**0.0800959**	-0.4	3.0	-2.1	0.7	2.1	5.5	2.8	-2.2	1.2	-1.3	1.3	-1.3	0.3	-0.6	…
I	**5.142E+13**	-1.0	1.4	-3.9	-0.8	-2.5	1.7	-1.3	-0.1	-0.7	-0.2	-0.3	0.3	-0.2	0.6	…
NFm	**0.28**	1.3	-0.9	1.3	-1.0	2.7	0.7	4.7	-0.1	1.4	1.2	0.3	1.0	0.2	0.3	…
NEm	**0.5**	1.7	0.9	0.2	-1.1	1.6	2.4	4.0	-0.7	0.3	-1.3	0.7	-0.3	0.1	-0.6	…
NMm	**0.33**	2.7	-2.3	-0.1	-3.1	1.8	-0.6	1.9	-6.1	-0.7	-1.5	0.6	0.9	0.6	-0.5	…
NRm	**0.3**	0.9	1.0	-0.4	0.1	1.1	2.5	1.3	-1.6	0.3	-1.2	0.4	0.8	-0.7	-0.2	…

Parameter	**Value**	**M20.dec.**	**M20.inc**	**M21.dec.**	**M21.inc**	**M22.dec.**	**M22.inc**	**M23.dec.**	**M23.inc**	**M24.dec.**	**M24.inc**	**M25.dec.**	**M25.inc**	**M26.dec.**	**M26.inc**	**…**
linf	**84.55**	-2.2	2.4	-2.3	2.3	-3.4	2.8	-2.5	3.1	-3.8	2.8	-3.4	2.7	-2.9	1.4	…
K	**0.096699**	-0.1	0.9	-0.1	1.1	-0.5	-0.2	-0.3	0.0	-1.1	-1.0	-0.1	0.0	-0.9	-1.8	…
t0	**-0.73**	0.2	-0.3	-0.4	-0.2	0.1	-1.3	0.0	-0.2	-0.6	-1.4	-0.6	-0.2	-0.8	-0.9	…
Ea	**0.5**	0.6	-0.7	-0.1	-0.7	0.5	-0.5	0.0	0.2	-0.2	-2.2	0.6	-0.7	-0.8	-0.5	…
EaS	**0.1903656**	0.2	0.2	-0.2	0.6	-0.1	-0.2	1.0	0.1	-0.7	-0.8	-0.4	-0.3	-0.2	-0.9	…
Cmax	**0.54**	-0.4	-0.1	-0.7	1.0	0.4	-0.5	0.0	0.3	-0.7	-1.0	0.1	-0.1	-1.3	-1.0	…
ep	**6.02**	0.0	0.0	0.6	0.5	0.0	0.5	0.5	-0.5	-0.4	0.0	-0.4	-0.9	0.2	-0.7	…
A0	**0.1227808**	0.7	0.6	-0.8	-0.1	0.5	-0.6	0.6	-0.6	-1.0	-1.4	0.8	0.3	-0.2	-0.3	…
Ef	**7**	-0.1	0.2	-0.6	-0.5	-0.5	-0.2	0.3	0.3	-0.4	-1.8	0.5	0.9	-0.1	-0.6	…
El	**39.3**	-0.8	0.8	0.0	-0.2	-0.9	0.4	0.2	0.3	-1.3	-0.7	0.3	0.2	-0.8	-0.4	…
Ls	**14.7**	0.5	0.2	-1.0	0.5	0.4	0.8	0.7	0.4	-1.0	-0.6	0.0	0.7	-0.1	-0.5	…
Fs	**3.6**	1.0	-0.4	-0.5	-0.3	-0.7	-0.1	0.1	0.9	-0.2	0.0	-0.4	-1.1	-0.9	-1.2	…
egg_mass	**0.00096**	1.0	0.9	0.3	0.6	0.0	-0.1	-0.1	0.3	-1.4	-1.1	-0.9	-0.4	-0.8	0.0	…
a_g	**1.231E-05**	-8.9	10.9	-9.0	10.7	-9.5	9.2	-9.4	10.0	-10.9	9.6	-10.0	9.6	-10.5	9.1	…
b_g	**2.969**	-71.9	254.4	-72.0	256.5	-72.2	255.8	-72.3	256.6	-72.5	258.2	-72.7	259.7	-72.8	260.0	…
eggs_per_bass	**375000**	1.3	0.8	0.4	-0.3	-0.7	0.3	0.9	0.0	-0.5	-0.6	-0.6	0.1	-0.6	-0.4	…
Gl	**0.02485**	-0.2	-0.1	0.1	0.3	0.1	0.3	0.5	-0.1	-1.0	-0.5	-0.7	-0.9	-1.5	-0.7	…
H	**0.4866877**	-0.2	-0.1	0.4	-0.3	0.6	-0.1	0.3	0.0	-0.7	-1.0	0.3	-0.1	-0.4	-1.2	…
AM	**0.0004709**	-0.1	-0.5	-0.7	-0.5	-1.3	-0.4	-0.2	0.2	0.2	-0.7	-0.1	-0.5	-1.0	-0.3	…
AE	**0.0016362**	0.2	0.5	0.2	-0.2	-1.4	0.6	0.5	-0.6	-0.6	-0.5	-0.2	-0.2	-0.7	-0.3	…
PM	**0.0800959**	0.1	-0.7	0.7	0.4	-0.4	0.7	-0.2	0.7	0.5	-1.1	0.2	-0.7	-0.4	-1.0	…
I	**5.142E+13**	-0.4	0.1	0.6	0.4	0.5	0.5	0.5	0.3	0.1	0.6	0.1	-0.5	-0.5	-0.8	…
NFm	**0.28**	0.7	0.5	-0.2	-0.4	0.3	-0.1	0.6	-0.3	-0.8	-0.6	0.5	-0.4	-0.9	-0.6	…
NEm	**0.5**	0.3	-0.3	0.5	-0.1	-0.1	0.0	-0.3	0.1	-1.0	-0.3	0.1	0.4	-0.7	-0.7	…
NMm	**0.33**	0.1	0.0	1.2	0.4	0.6	0.9	0.0	0.0	-0.5	-0.6	-0.8	-0.2	-0.4	-0.5	…
NRm	**0.3**	0.7	0.2	0.0	-1.1	-0.4	-0.4	-0.5	0.6	-1.3	-0.7	-0.6	-0.6	-1.3	-1.1	…

Parameter	**Value**	**M27.dec.**	**M27.inc.**	**M28.dec.**	**M28.inc.**	**M29.dec.**	**M29.inc.**	**N0.dec.**	**N0.inc**	**N1.dec.**	**N1.inc**	**N2.dec.**	**N2.inc**	**…**
linf	**84.55**	-2.7	2.7	-3.4	2.1	-3.2	2.5	-15.2	1.3	0.3	0.3	-0.1	0.1	…
K	**0.096699**	-0.2	0.4	-0.9	-0.4	-1.0	-0.5	-1.1	-0.4	0.2	0.7	0.3	0.0	…
t0	**-0.73**	-0.5	0.7	-0.6	-0.1	-0.3	-1.2	0.5	19.5	0.5	0.2	0.0	-0.1	…
Ea	**0.5**	0.0	-0.3	-0.7	-1.0	-0.2	-0.4	12.5	-2.7	0.1	0.0	0.1	-0.2	…
EaS	**0.1903656**	0.3	0.2	-0.8	-0.5	-0.2	-0.4	10.9	15.5	0.2	0.2	0.1	0.1	…
Cmax	**0.54**	-0.2	0.2	-0.7	0.2	-0.7	-0.1	-1.8	5.8	0.5	0.3	0.1	0.1	…
ep	**6.02**	0.4	-0.2	-0.1	-0.4	-0.4	-0.1	4.0	22.1	0.3	0.1	0.2	0.2	…
A0	**0.1227808**	-0.3	-0.2	-0.6	-0.5	-0.4	-0.7	5.2	1.4	0.4	0.3	0.2	-0.1	…
Ef	**7**	0.2	0.3	-0.3	0.4	-0.7	-0.3	14.0	-7.8	0.0	0.6	0.1	-0.4	…
El	**39.3**	0.4	0.1	-0.9	-0.2	-0.8	-0.3	-12.6	14.3	0.0	0.2	0.1	0.1	…
Ls	**14.7**	0.4	0.1	-0.6	-0.6	-0.7	-0.6	8.0	0.0	-0.1	0.3	0.1	-0.2	…
Fs	**3.6**	-0.3	-0.2	-0.6	-0.7	-0.1	-0.3	13.3	-14.0	0.3	0.6	0.1	0.0	…
egg_mass	**0.00096**	0.0	-0.3	-0.8	-0.1	-0.6	-0.6	7.1	-6.0	0.1	0.2	0.0	-0.1	…
a_g	**1.231E-05**	-10.1	10.3	-10.3	9.6	-10.4	9.2	5.0	8.9	0.7	0.0	0.2	0.0	…
b_g	**2.969**	-72.4	265.8	-72.7	263.8	-72.8	263.3	-44.1	29.9	0.4	0.8	0.2	0.3	…
eggs_per_bass	**375000**	0.0	0.2	-0.6	-0.5	-0.6	-1.0	9.3	3.3	0.1	0.4	-0.3	0.0	…
Gl	**0.02485**	0.3	0.2	-0.7	-0.4	-0.3	-0.6	-32.9	39.3	0.3	0.2	0.2	0.3	…
H	**0.4866877**	0.1	-0.1	-0.4	-0.4	-0.1	-0.7	11.8	-10.7	-0.1	0.3	-0.1	0.0	…
AM	**0.0004709**	0.3	0.1	-1.5	-0.5	-0.7	-0.4	22.0	5.2	2.3	-2.0	2.2	-2.0	…
AE	**0.0016362**	0.9	0.3	-1.0	-0.6	-0.8	-0.4	3.7	6.1	0.0	0.6	0.2	0.3	…
PM	**0.0800959**	-0.5	1.1	-0.1	-0.4	-0.8	-0.2	77.2	-42.7	0.9	0.3	-0.1	0.1	…
I	**5.142E+13**	0.1	0.1	-0.3	-0.6	-1.0	-0.5	-2.6	7.0	0.0	0.0	-0.2	0.0	…
NFm	**0.28**	-0.1	0.0	-0.2	-0.7	-0.8	-0.5	-1.5	5.6	0.2	0.4	-0.1	0.1	…
NEm	**0.5**	0.0	0.3	-0.3	-0.5	-0.2	-0.5	-9.2	-4.8	-0.3	0.4	-0.2	0.0	…
NMm	**0.33**	0.3	-0.5	-0.1	-0.7	-1.2	-1.4	11.5	0.0	0.6	-0.1	0.4	-0.4	…
NRm	**0.3**	-0.3	-0.3	-0.7	-1.2	-0.3	-1.8	1.6	1.1	0.1	-0.1	0.1	-0.1	…

Parameter	**Value**	**N3.dec.**	**N3.inc**	**N4.dec.**	**N4.inc**	**N5.dec.**	**N5.inc**	**N6.dec.**	**N6.inc**	**N7.dec.**	**N7.inc**	**N8.dec.**	**N8.inc**	**N9.dec.**	**N9.inc**	**…**
linf	**84.55**	0.2	0.0	-0.4	-0.3	0.5	0.3	0.8	-2.7	-2.9	-2.0	0.2	0.2	-1.2	-1.2	…
K	**0.096699**	0.2	0.2	0.0	0.0	0.2	-0.5	-0.6	-2.5	-3.7	-2.2	-2.0	4.7	-2.0	-1.9	…
t0	**-0.73**	-0.1	0.1	0.0	-0.1	0.4	-0.5	0.0	-0.7	-2.9	-3.2	-1.0	0.1	-1.2	-1.2	…
Ea	**0.5**	0.0	-0.1	-0.2	0.1	0.5	0.5	-0.5	-0.7	-1.5	-2.8	3.8	0.7	-0.9	-1.7	…
EaS	**0.1903656**	0.3	-0.1	-0.2	0.3	1.1	-0.2	0.6	-0.7	-1.4	-1.0	-0.6	2.3	-2.1	0.1	…
Cmax	**0.54**	0.1	0.1	-0.1	0.0	0.6	0.3	-1.5	-0.5	-1.3	-2.7	-1.4	1.5	-1.3	-0.1	…
ep	**6.02**	0.1	-0.1	0.1	0.2	1.5	0.0	-0.8	-2.0	-2.5	-1.5	1.3	-0.3	-2.1	-1.5	…
A0	**0.1227808**	0.4	0.3	-0.2	-0.2	0.5	-0.3	-1.1	1.1	-3.5	-2.9	2.9	-1.3	3.8	-1.4	…
Ef	**7**	0.1	0.3	-0.2	0.0	0.4	0.8	-1.7	-2.0	-3.0	-3.2	1.6	3.1	-1.4	-0.6	…
El	**39.3**	0.2	0.1	0.2	-0.3	1.0	0.1	-0.5	-1.2	-1.4	-2.3	3.9	3.1	-1.1	-1.7	…
Ls	**14.7**	0.1	-0.1	0.0	0.0	-0.1	0.5	-2.4	-2.5	-3.7	-1.7	-1.6	9.2	-1.2	-1.9	…
Fs	**3.6**	0.1	0.3	0.2	0.0	0.2	0.3	-1.9	-0.1	-2.6	-2.5	-0.2	5.0	-0.8	1.2	…
egg_mass	**0.00096**	0.1	0.1	0.1	-0.1	0.4	0.4	-1.4	-0.8	-2.3	-0.4	2.0	3.6	-2.0	-2.1	…
a_g	**1.231E-05**	0.5	0.3	0.0	-0.2	1.4	-0.2	-0.6	-1.7	-0.9	-1.0	1.4	0.6	-1.4	-0.8	…
b_g	**2.969**	0.0	0.3	-0.1	0.0	0.3	1.5	0.0	-0.4	-2.4	-1.5	2.4	1.6	-2.5	-1.4	…
eggs_per_bass	**375000**	0.2	0.0	-0.2	-0.2	0.2	0.3	-0.7	0.4	-1.8	-2.3	2.8	-0.8	-2.1	-1.6	…
Gl	**0.02485**	0.2	0.2	0.0	-0.7	-0.2	0.4	-1.5	-1.5	-0.6	-2.4	3.8	0.6	-2.2	-1.7	…
H	**0.4866877**	-0.1	0.3	0.0	-0.1	-0.3	0.2	-2.1	-1.8	-3.1	-1.8	-1.5	-0.6	-2.5	4.4	…
AM	**0.0004709**	2.1	-2.0	2.1	-2.4	2.0	-1.8	1.1	-3.0	-0.2	-2.6	2.4	-2.3	0.5	-3.5	…
AE	**0.0016362**	0.2	0.2	0.2	0.2	0.3	0.1	-1.7	-2.2	-2.1	0.2	-1.3	0.0	-1.1	-0.7	…
PM	**0.0800959**	0.4	0.1	0.0	0.0	0.0	-0.2	-0.6	-2.3	-2.9	-2.9	1.8	2.5	-0.9	-2.1	…
I	**5.142E+13**	-0.2	0.6	-0.1	-0.2	0.4	0.2	-0.4	-0.8	-2.5	-3.3	-0.9	2.8	-1.1	-1.7	…
NFm	**0.28**	0.2	0.5	0.0	0.1	0.3	0.3	-0.6	-0.8	-1.5	-3.0	-0.5	-0.2	-1.5	-0.8	…
NEm	**0.5**	0.1	0.2	0.2	0.1	0.2	-0.3	-0.4	-0.8	-2.4	-4.3	0.7	-1.5	-0.8	-1.4	…
NMm	**0.33**	0.8	-0.5	0.4	-0.5	0.2	0.1	-1.8	-1.9	-2.7	-1.3	5.9	-0.7	-1.0	0.6	…
NRm	**0.3**	0.3	-0.1	0.0	0.0	-0.1	0.2	-0.5	-1.2	-3.0	-3.2	1.9	-0.8	-0.5	-1.3	…

Parameter	**Value**	**N10.dec.**	**N10.inc**	**N11.dec.**	**N11.inc**	**N12.dec.**	**N12.inc**	**N13.dec.**	**N13.inc**	**N14.dec.**	**N14.inc**	**N15.dec.**	**N15.inc**	**N16.dec.**	**N16.inc.**	**…**
linf	**84.55**	-1.3	0.8	-1.7	1.7	1.1	0.0	2.4	-0.7	2.2	2.8	-1.1	0.1	7.8	-2.1	…
K	**0.096699**	3.3	8.8	-1.1	8.6	-0.4	0.6	-0.5	-0.5	1.4	1.3	-1.1	-0.5	-1.0	2.5	…
t0	**-0.73**	2.9	2.5	-0.1	-0.3	-0.3	0.4	0.8	1.4	1.0	1.7	-0.3	-0.3	-1.0	-1.2	…
Ea	**0.5**	0.7	2.8	3.5	-1.1	-1.8	-0.4	-0.2	-1.3	2.1	1.9	0.3	0.0	32.6	0.5	…
EaS	**0.1903656**	1.8	2.2	-1.6	2.8	-0.7	-0.6	7.4	-1.3	2.0	2.6	-1.5	-1.0	10.1	1.3	…
Cmax	**0.54**	0.0	0.8	-1.2	-0.5	0.1	0.9	-2.3	-0.4	2.0	2.7	-0.4	-1.4	1.4	12.0	…
ep	**6.02**	0.9	-0.9	-1.5	-1.8	0.0	-0.7	-1.5	-1.2	1.5	1.9	-2.0	-1.7	-2.3	0.5	…
A0	**0.1227808**	-1.6	-1.8	6.5	-0.6	9.2	0.1	-0.2	-0.7	1.6	3.7	-0.3	0.4	18.5	-1.9	…
Ef	**7**	0.6	-0.8	-1.1	-0.4	-1.1	0.4	-1.4	-2.0	7.6	2.1	-1.5	-0.5	11.9	6.1	…
El	**39.3**	-1.0	8.8	-0.1	-1.1	-0.3	0.4	-0.5	-0.6	2.5	2.1	0.7	1.0	-0.5	0.7	…
Ls	**14.7**	1.1	4.1	-1.9	-1.0	-1.4	-0.4	-1.0	-0.7	3.2	22.5	-1.5	-1.2	1.1	9.7	…
Fs	**3.6**	0.0	0.2	-0.9	-0.9	-1.0	-1.5	0.2	9.9	1.2	1.4	0.2	-0.8	7.7	0.4	…
egg_mass	**0.00096**	0.0	7.6	-0.2	4.2	-0.5	1.6	-2.2	-2.6	1.5	2.2	0.1	0.9	10.1	29.4	…
a_g	**1.231E-05**	0.1	-0.1	-1.9	-2.0	-0.8	-1.4	-0.2	-2.8	2.1	1.7	-2.3	-1.0	3.5	-0.6	…
b_g	**2.969**	0.1	2.4	-1.1	-1.3	-1.2	0.5	9.2	0.0	2.0	2.6	0.3	-0.5	5.6	-0.6	…
eggs_per_bass	**375000**	-2.2	0.1	-2.4	-0.8	0.6	-1.2	-1.8	-0.5	1.7	2.7	0.6	-1.9	-0.8	0.0	…
Gl	**0.02485**	0.9	1.7	-1.7	-1.3	-0.5	0.2	-2.5	-1.1	2.2	6.9	-0.7	-0.4	9.8	4.5	…
H	**0.4866877**	0.0	0.9	-0.2	-1.4	-0.2	0.1	-1.6	-1.5	2.0	2.0	-0.4	1.0	2.6	9.5	…
AM	**0.0004709**	2.6	-3.0	0.8	-2.3	1.8	-2.8	1.6	-4.6	3.4	2.0	1.2	-2.8	5.3	0.9	…
AE	**0.0016362**	0.3	1.3	-2.0	-0.6	0.0	0.2	-2.0	-1.6	1.3	2.8	-1.4	0.7	1.3	11.9	…
PM	**0.0800959**	-1.5	0.8	-1.4	-1.3	-0.8	-0.3	-0.6	0.0	2.5	1.6	-1.0	0.6	3.2	34.6	…
I	**5.142E+13**	3.4	-0.1	-1.7	-0.8	2.3	-0.1	-1.1	-1.7	5.4	2.3	-0.3	-1.3	21.9	6.5	…
NFm	**0.28**	6.9	1.2	-0.5	-1.5	-0.5	-0.1	0.0	-1.5	1.2	2.1	-0.8	-0.6	2.7	1.2	…
NEm	**0.5**	-0.5	1.1	-1.5	-1.0	-1.3	2.1	-2.3	1.2	0.8	1.3	-1.0	-1.4	-0.6	8.8	…
NMm	**0.33**	5.5	4.1	-1.5	1.1	0.7	-0.7	-1.1	-3.3	3.0	1.6	-0.3	-1.3	-1.3	-3.1	…
NRm	**0.3**	0.7	-1.0	-1.4	1.8	-0.9	-0.4	-0.9	-1.3	0.6	1.2	-0.6	0.1	-0.5	11.1	…

Parameter	**Value**	**N17.dec.**	**N17.inc**	**N18.dec.**	**N18.inc**	**N19.dec.**	**N19.inc**	**N20.dec.**	**N20.inc**	**N21.dec.**	**N21.inc**	**N22.dec.**	**N22.inc**	**N23.dec.**	**N23.inc**	**...**
linf	**84.55**	0.2	0.7	-2.2	-1.3	0.7	-0.4	0.2	-0.4	-1.3	-0.7	-0.1	0.3	-0.6	-0.5	...
K	**0.096699**	-1.6	0.3	-1.3	0.4	-0.5	-0.7	0.2	0.4	-0.5	0.8	0.3	0.1	-0.6	0.0	...
t0	**-0.73**	-0.5	0.1	-2.4	-2.0	-0.3	0.3	-0.1	-0.5	-1.6	-0.3	-0.1	1.6	0.3	0.1	...
Ea	**0.5**	1.4	-0.2	-2.4	-1.6	0.0	0.2	-0.1	-0.6	-0.9	0.2	0.1	0.8	-0.3	-0.6	...
EaS	**0.1903656**	0.5	-0.9	-1.2	-1.4	-2.1	-1.4	-1.0	1.1	-1.7	0.3	0.5	-1.7	1.0	1.2	...
Cmax	**0.54**	-0.5	0.1	-2.6	-3.1	0.4	-1.0	1.2	-1.8	0.3	-1.0	0.8	-0.4	-0.1	-0.2	...
ep	**6.02**	2.2	0.3	-1.5	-2.5	-1.1	-0.5	-0.4	0.6	-0.5	0.1	0.4	1.6	0.8	-0.7	...
A0	**0.1227808**	0.1	-0.6	-2.3	-2.7	-0.7	-1.6	1.3	-0.6	0.5	0.1	-1.1	0.5	-0.2	-0.6	...
Ef	**7**	-0.5	-1.3	-2.0	-1.4	-0.1	-0.7	-0.4	-0.2	-1.2	0.9	-0.6	-0.1	0.4	-0.6	...
El	**39.3**	-0.4	0.1	-1.8	-2.8	0.3	-1.6	0.5	-0.1	1.1	-1.1	0.3	0.9	1.0	-0.3	...
Ls	**14.7**	0.5	-1.1	-1.1	-0.5	-1.9	1.2	0.4	-0.4	-1.5	0.4	0.3	1.3	0.2	0.2	...
Fs	**3.6**	1.0	-1.7	-1.4	-2.5	0.7	-1.4	-1.8	-2.0	-1.1	-1.0	-1.3	0.7	0.7	-0.1	...
egg_mass	**0.00096**	0.5	-0.5	-0.8	-1.8	-1.0	0.4	-0.1	0.1	-1.3	-0.7	-0.6	-1.5	0.8	0.4	...
a_g	**1.231E-05**	-1.5	-0.6	-1.5	-1.2	-1.6	0.6	1.3	0.5	0.3	0.5	0.3	-1.3	0.8	-0.7	...
b_g	**2.969**	-0.2	0.1	-3.7	-2.5	-0.3	-0.6	-0.2	-1.8	0.2	-0.5	1.8	0.7	-0.2	-1.4	...
eggs_per_bass	**375000**	-0.1	-0.9	-2.3	-2.0	-0.3	-2.7	0.8	1.9	-0.3	0.4	-1.7	1.1	-0.1	-1.4	...
Gl	**0.02485**	0.2	0.0	-1.5	-1.6	1.1	0.0	-0.1	-1.5	0.0	-0.8	-1.0	0.6	-0.7	0.4	...
H	**0.4866877**	-0.2	-1.2	-3.3	-2.1	0.4	0.7	-0.7	1.4	-1.0	0.7	0.2	0.4	0.4	0.9	...
AM	**0.0004709**	3.6	-2.5	1.4	-3.8	0.3	-2.8	0.7	-2.8	2.2	-2.8	1.7	-0.7	3.4	-2.7	...
AE	**0.0016362**	-1.3	-0.9	-1.7	-1.6	-0.3	-1.0	-0.6	0.5	-0.7	-1.7	-0.7	-1.1	0.3	-1.2	...
PM	**0.0800959**	-0.9	-0.1	-2.4	5.1	-1.2	2.2	0.0	0.3	-0.8	-0.3	1.0	-0.8	0.9	1.7	...
I	**5.142E+13**	0.1	0.0	-1.2	-0.7	-1.1	-0.2	-0.9	-0.6	0.0	-1.9	1.1	0.4	1.0	-0.7	...
NFm	**0.28**	0.4	0.6	-1.1	-3.0	-1.5	-1.6	1.0	0.2	-0.3	1.0	-0.3	-0.6	-0.4	-1.1	...
NEm	**0.5**	-1.1	1.0	-2.6	-1.3	-0.7	-0.3	-0.4	-1.1	-1.6	0.5	0.7	1.4	0.1	2.0	...
NMm	**0.33**	-0.5	0.7	-2.9	-1.5	0.8	-0.7	1.4	-0.7	0.8	-0.3	-0.6	0.8	0.2	0.4	...
NRm	**0.3**	-0.5	0.3	-2.0	-0.3	-0.9	1.7	0.2	1.0	-0.2	-0.3	-0.3	0.5	2.5	1.2	...

Parameter	**Value**	**N24.dec.**	**N24.inc**	**N25.dec.**	**N25.inc**	**N26.dec.**	**N26.inc**	**N27.dec.**	**N27.inc**	**N28.dec.**	**N28.inc.**	**N29.dec.**	**N29.inc.**
linf	**84.55**	-1.2	0.9	0.8	0.6	0.2	-1.0	-0.2	0.5	-1.6	-0.2	0.1	1.3
K	**0.096699**	0.6	0.2	0.4	-0.6	0.8	-1.6	1.4	-0.4	-1.1	1.3	0.2	-0.3
t0	**-0.73**	0.2	-0.5	-1.4	-1.1	-0.5	-0.8	-0.3	2.0	-1.4	-1.4	0.6	1.4
Ea	**0.5**	0.0	-1.1	-0.2	-1.4	-0.1	-0.1	-0.2	-0.2	-1.1	0.3	0.1	1.1
EaS	**0.1903656**	-1.3	0.4	0.1	-1.0	-0.2	-0.3	0.2	1.0	-0.3	-0.8	0.4	0.2
Cmax	**0.54**	0.3	-0.6	-1.4	-0.8	-0.9	0.0	1.1	0.0	-1.5	-0.6	0.8	1.8
ep	**6.02**	-0.7	-0.8	-0.6	-2.1	2.4	-1.4	0.6	-0.1	-1.7	-0.3	0.5	1.1
A0	**0.1227808**	-0.5	0.7	-0.4	-1.5	0.5	-0.7	0.3	-0.2	-0.9	-0.4	2.0	0.5
Ef	**7**	0.2	-0.9	-0.7	-1.1	0.3	-2.0	0.2	-0.9	-0.4	0.3	0.6	1.5
El	**39.3**	0.4	-0.6	-1.4	-0.9	-0.1	0.6	0.5	-0.8	-2.3	-0.9	0.7	1.5
Ls	**14.7**	-0.5	0.0	0.2	-0.9	-0.3	-0.6	0.0	1.0	-1.1	-0.5	-0.3	0.6
Fs	**3.6**	0.9	2.0	-1.9	-0.2	-0.5	-0.9	0.7	-0.1	-1.5	-0.7	1.5	0.6
egg_mass	**0.00096**	-0.6	-0.8	-0.4	-1.4	0.2	0.7	-0.1	0.3	-0.4	0.0	1.7	0.3
a_g	**1.231E-05**	-0.8	-0.9	-1.7	0.4	-1.8	-0.9	-1.8	0.6	-0.1	0.1	0.4	0.5
b_g	**2.969**	-0.6	-0.3	-2.2	-1.0	-0.1	-1.0	0.5	0.8	-0.2	0.8	2.5	-0.2
eggs_per_bass	**375000**	-0.8	-0.6	-1.2	-1.1	-0.7	-0.1	1.0	1.1	0.2	-0.9	0.9	1.5
Gl	**0.02485**	0.4	-1.1	-2.3	-0.6	-1.6	-1.5	0.0	0.4	-0.7	2.0	1.4	1.1
H	**0.4866877**	0.3	-0.4	-0.3	0.0	0.4	0.0	-0.5	0.4	-0.2	0.6	1.8	-0.2
AM	**0.0004709**	3.3	-2.2	2.6	-2.5	0.7	-2.3	1.3	-2.0	0.6	-1.2	2.2	-1.7
AE	**0.0016362**	-0.1	-0.7	1.5	-0.8	-0.6	-0.2	0.5	0.5	-0.2	-1.7	0.8	0.9
PM	**0.0800959**	0.2	-0.8	1.0	-0.3	-1.5	-0.5	-0.4	0.4	-0.5	-1.0	0.3	2.8
I	**5.142E+13**	0.2	1.2	1.2	-0.7	-0.8	-0.6	0.3	2.0	-1.1	-1.5	1.6	1.5
NFm	**0.28**	1.0	0.6	-0.6	0.0	-1.6	0.7	0.4	-0.3	0.5	0.8	1.0	0.7
NEm	**0.5**	-1.6	-0.8	-0.1	-0.8	1.0	-2.5	0.1	0.9	-1.1	-1.2	1.1	0.1
NMm	**0.33**	-0.1	0.3	-0.2	-0.6	0.3	-1.4	-0.1	-0.9	-0.6	-1.6	0.4	0.2
NRm	**0.3**	-2.6	1.0	-1.0	-1.5	0.2	-1.6	-1.2	-0.1	-0.1	0.0	1.5	0.6

B.12.2 Sensitivity scenarios for noise responses

To explore the degree and range that noise impacts the D. labrax population within the model, each of the noise-affected processes (ingestion, metabolic rate, mortality and reproduction) were tested by varying severity of impact (controlled by noise modification parameters), and under a set of three noise conditions: unmodified noise (+0 dB), increased noise (+10 dB) and decreased noise (-10 dB). For each scenario, a uniform adjustment was applied to the noise maps to achieve the desired change in noise levels. Subsequently, each of the noise-effect pathways (ingestion, energy use, mortality and reproduction) was then tested in isolation against an incremental array (an increase of 10%; starting at 10% and ending at 90%) of response strength to noise that were implemented via the associated noise modification parameters (TRACE Section B.7, submodels). This process was repeated three times to include variation of the results. Consequently, there were a total of 324 runs that were completed over these various conditions and scenarios.

B.12.2.1 Spawning stock biomass (SSB)

The mean SSB averaged across ten IBM runs without acoustic disturbance was found to be 23,082 ± 1312 (standard error of means) tonnes. When noise is distributed throughout the model and the noise-effect pathways are introduced in isolation, SSB decreases below the undisturbed average for three of the four noise pathways: ingestion, energy use and mortality (Figures 8.3.21a–c). Furthermore, there is an inverse relationship between SSB and the severity of impact for these three pathways (Figures 8.3.21a–c). Conversely, SSB increases above the average when noise is affecting reproduction only (Figure B.21d).

Figure B.21 shows that there is increasing separation between mean SSB output from the three noise conditions as the severity impact for ingestion and mortality increases (Fig. B.21a and c). Furthermore, the reduced noise condition (-10 dB) results in SSB values that are closer to the mean SSB of acoustically undisturbed model runs (red-dotted lines in Fig. B.21), and the louder conditions (+0 dB and +10 dB) demonstrate little separation from one another. When examining mean SSB outputs for tests when noise is impacting energy use, there is early separation of the quietest noise condition from the comparatively two louder conditions; however, this separation is less prominent as impact severity increases (Fig. B.21b). Lastly, mean

SSB outputs for tests when noise is impacting reproduction show relatively no separation and complete overlap of the three noise conditions across the full range of severity impact (Fig. B.21d).

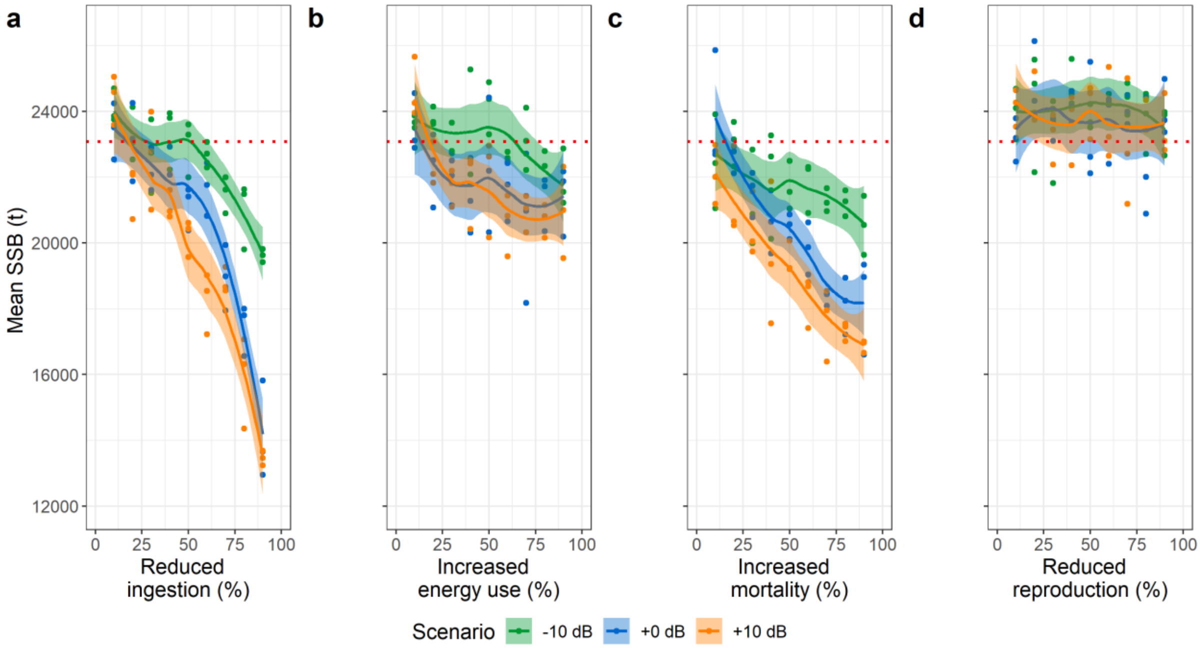

Figure B.21. Outputs of mean SSB from model runs with varying acoustic disturbance and noise-effect severity*; all outputs are averaged across the 10-year emergent modelling period. For a baseline comparison to acoustically undisturbed models, red dotted lines are comparable means from the verification results, averaged across ten runs. Coloured dots represent SSB outputs from runs with varying noise conditions and strength of response for each of the four noise-effect pathways; coloured lines are linear-fitted curves; and shaded areas are 0.95 confidence intervals.*

B.12.2.2 Abundance

The mean abundance of modelled individuals averaged across ten IBM runs without acoustic disturbance was found to be 8.36 x 10^7 ± 1.31 x 10^7. When acoustic disturbance and associated impacts are added to the model, abundance decreased compared to no-noise models across all four of the noise-effect pathways (ingestion, energy use, mortality and reproduction; Fig. B.22a–c). Similar to SSB, there is an inverse relationship between abundance and the severity of impact for the four pathways (Fig. B.22a–c).

Figure B.22 shows that there is increasing separation between mean abundance output from the three noise conditions as the severity impact for ingestion, mortality, and reproduction increases (Fig. B.22a, c, and d). Furthermore, the reduced noise condition (-10 dB) results in abundance values that are closer to the mean SSB of acoustically undisturbed model runs (red-dotted lines in Fig. B.22), and the louder conditions (+0 dB and +10 dB) demonstrate little separation from one another. Similar to SSB outputs, there is early separation of the quietest noise condition from the comparatively two louder conditions when testing noise effects on energy use; again, this separation is less prominent as impact severity increases (Fig. B.22b).

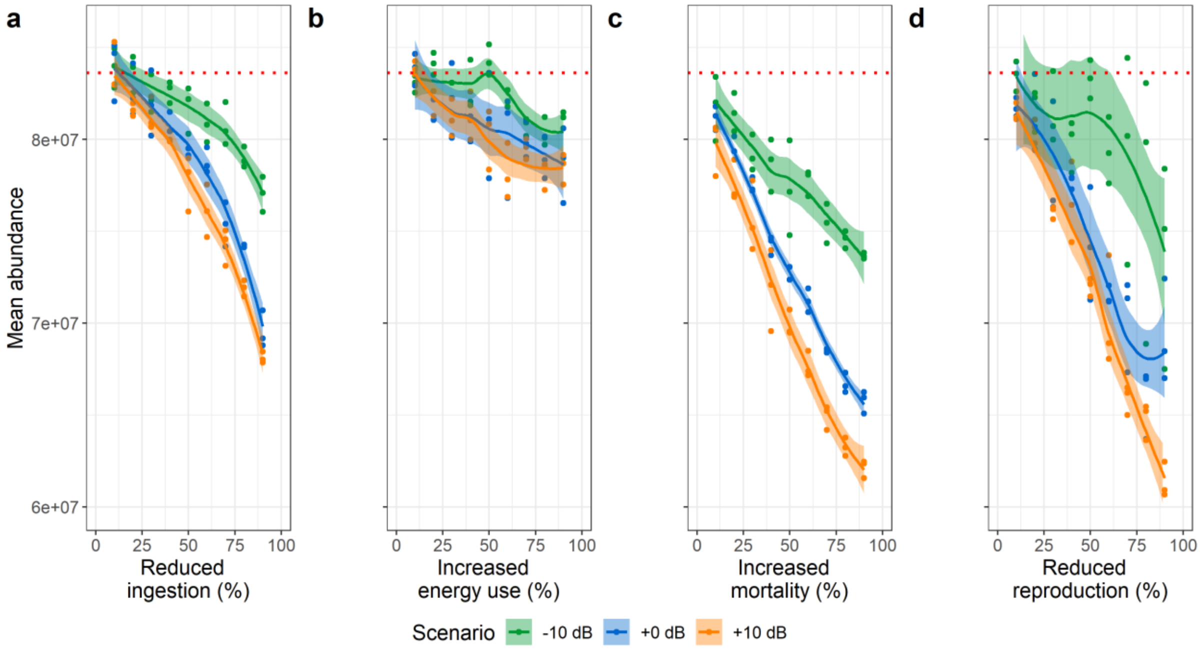

Figure B.22. Outputs of mean abundance from model runs with varying acoustic disturbance and noise-effect severity*; all outputs are averaged across the 10-year emergent modelling period. For a baseline comparison to acoustically undisturbed models, red dotted lines are comparable means from the verification results, averaged across ten runs. Coloured dots represent abundance outputs from runs with varying noise conditions and strength of response for each of the four noise-effect pathways; coloured lines are linear-fitted curves; and shaded areas are 0.95 confidence intervals.*

B.13 Model output corroboration

This TRACE element provides supporting information on: How model predictions compare to independent data and patterns that were not used, and preferably not even known, while the model was developed, parameterized, and verified. By documenting model output corroboration, model users learn about evidence which, in addition to model output verification, indicates that the model is structurally realistic so that its predictions can be trusted to some degree.

B.13.1 Summary

Tests from the original model by (Walker *et al.* 2020) **on the Spatial patterns of the IBM remain the same. In addition to these we compare estimations of egg production for the stock and maturity at age outputs from SS3.**

The IBM shows reasonable correlation between potential fecundity and predicted egg production in SS3 (Fig. B.23). Here the IBM output is the total combined potential egg production of the spawning stock, which is a function of the number and size of the individuals. When we compare realized fecundity with the egg predictions from SS3 we see poor fits (Fig. B.24). Here realized fecundity is a function of number, size, and condition of the individuals and one explanation for the poor fits may be that the data from the stock assessment we use for calibration and assessment of fits does not consider condition of individuals. An additional explanation for the poor fits may be an over estimation of the cost of producing eggs. We show a similar pattern to age at maturity in IBM outputs vs SS3 (Fig. B.25). Walker *et al.* (2020) compared IBM spatial outputs to catch data from the Scientific, Technical and Economic Committee for Fisheries (STECF) and showed reasonable correlation with some trends to overestimate catch in the Celtic and Irish Seas and underestimate catch in the North Sea. We did not re-run the spatial tests done by Walker *et al.* (2020) as the movement sub models for migration remain mostly unchanged (see TRACE sections 8.3.7 and 8.3.8.11 for more details on movement sub models).

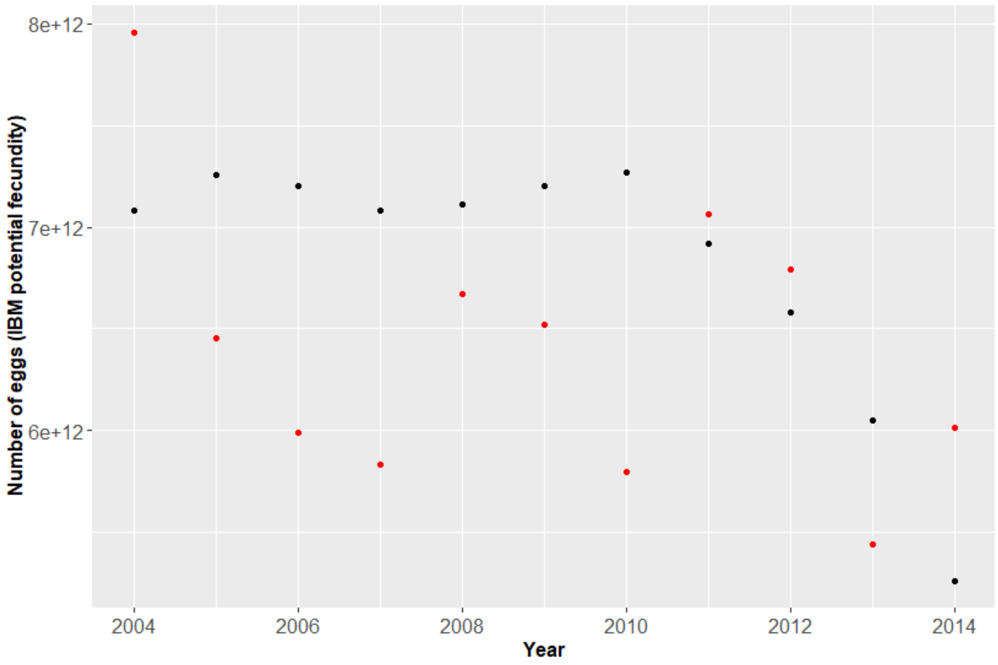

***Figure B.23. Combined potential fecundity IBM outputs vs number of egg predictions from the SS3 stock assessment** output for years 2004-2014. Black = SS3, Red = IBM outputs.*

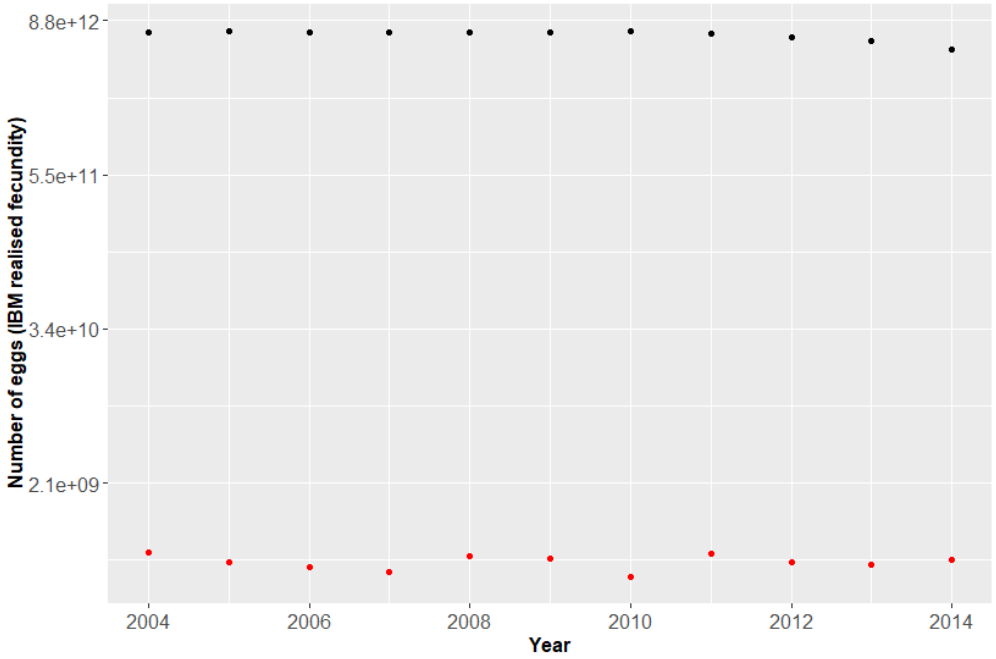

***Figure B.24. Combined realized fecundity IBM outputs vs number of egg predictions from the SS3 stock assessment** output for years 2004-2014. Black = SS3, Red = IBM outputs.*

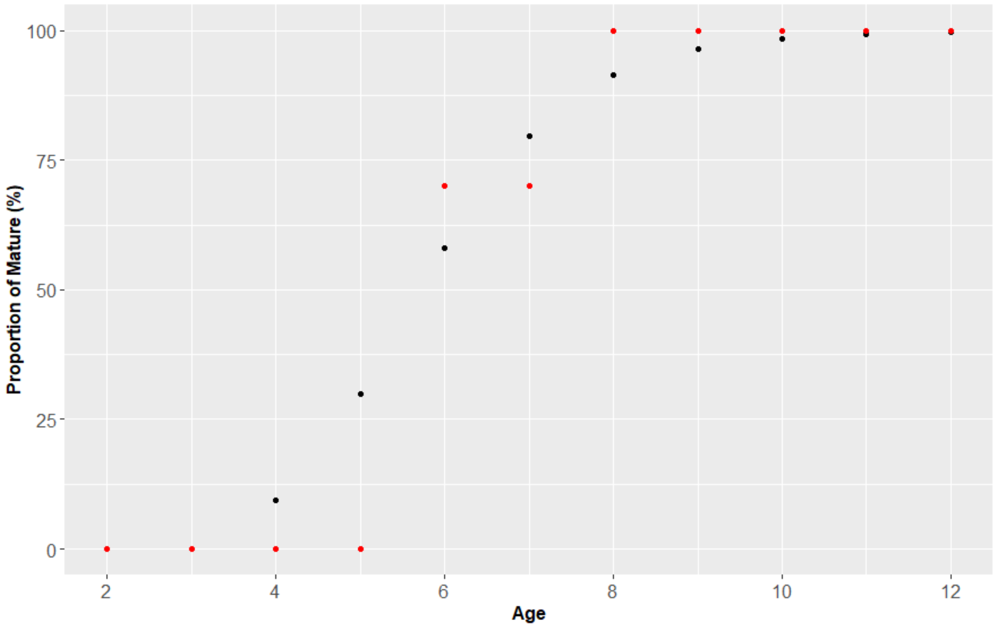

Figure B.25. Percentage of each age class (2- 12 years of age) that are mature (>42 cm L) IBM outputs vs proportion mature predictions from the SS3 stock assessment. *Black = SS3, Red = IBM outputs.*